

SYNTHESIS AND CHARACTERIZATION OF COPPER AND CUPROUS OXIDE NANOFLUIDS

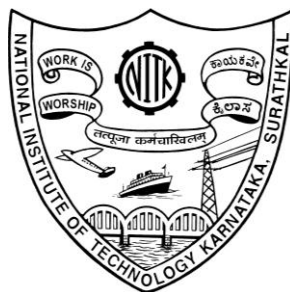
Thesis

Submitted in partial fulfillment of the requirements for the degree of

DOCTOR OF PHILOSOPHY

by

SANDHYA SHENOY U

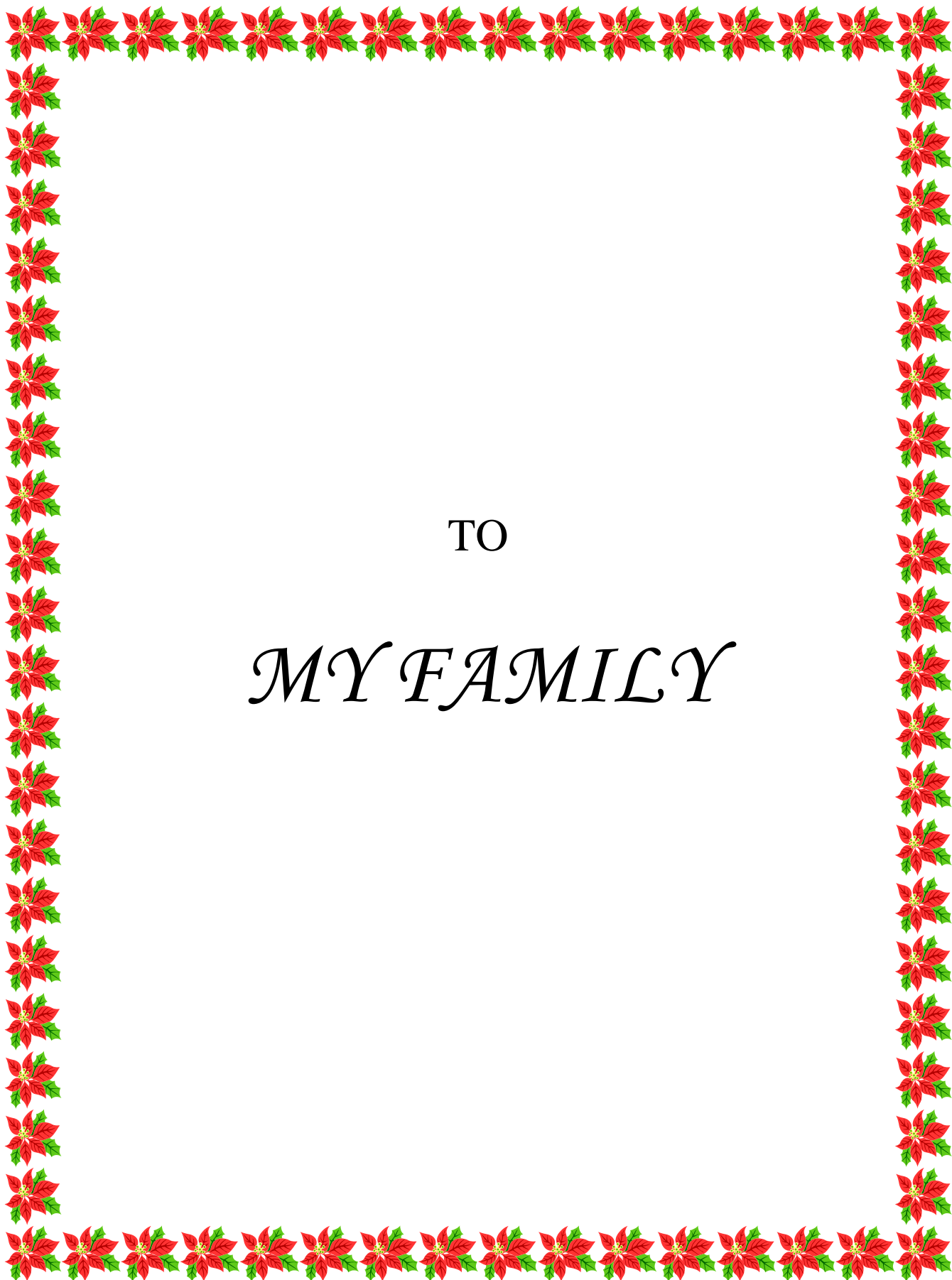


DEPARTMENT OF CHEMISTRY

NATIONAL INSTITUTE OF TECHNOLOGY KARNATAKA,

SURATHKAL, MANGALORE - 575 025

FEBRUARY, 2013



TO

MY FAMILY

DECLARATION

I hereby *declare* that the Research Thesis entitled “SYNTHESIS AND CHARACTERIZATION OF COPPER AND CUPROUS OXIDE NANOFUIDS” Which is being submitted to the **National Institute of Technology Karnataka, Surathkal** in partial fulfillment of the requirements for the award of the Degree of **Doctor of Philosophy** in Chemistry is a *bonafide report of the research work carried out by me*. The material contained in this Research Thesis has not been submitted to any University or Institution for the award of any degree.

Sandhya Shenoy U

Register Number: 090718CY09F03,

Department of Chemistry

Place: NITK, Surathkal

Date: 25-02-2013

CERTIFICATE

This is to *certify* that the Research Thesis entitled “SYNTHESIS AND CHARACTERIZATION OF COPPER AND CUPROUS OXIDE NANOFUIDS” submitted by Sandhya Shenoy U (Register Number: 090718CY09F03) as the record of the research work carried out by her, is accepted as the *Research Thesis submission* in partial fulfillment of the requirements for the award of degree of **Doctor of Philosophy**.

Research Guide

Chairman- DRPC

ACKNOWLEDGEMENT

It is my pleasure to acknowledge the assistance of a number of people without whose help this work would not have been possible.

First and foremost I would like to express my sincere gratitude to my esteemed guide, Dr. A. Nityananda Shetty for introducing me to this interesting problem. I place on record my profound sense of gratitude for his keen interest, methodical approach, timely suggestions, enthusiastic guidance and faith in me. His painstaking efforts in training students as well as his thoroughness in the field have helped me in completing this work. I deem it my privilege to have carried out my research work under his able guidance.

I am greatly indebted to Dr. A. Chitharanjan Hegde, Head, Department of Chemistry for his support and encouragement provided in completion of the work. I am thankful to Dr. Subba Rao and Dr. Udaya Kumar D. for being the RPAC members and providing excellent suggestions. I am extremely grateful to Dr. A. Vasudeva Adhikari, Dr. B. Ramachandra Bhat, Dr. D. Krishna Bhat, Dr. A. M. Isloor and Dr. Darshak R. Trivedi of Department of Chemistry for their encouragement.

Thanks are also due to my fellow research scholars, M.Sc. students and non teaching staff of Department of Chemistry for their valuable assistance. I also acknowledge Department of Physics and Department of Metallurgy and Material Science, NITK, Surathkal for their lab facilities. I also acknowledge SAIF, IIT Bombay and IIT Kanpur for extending their lab facilities for TEM and FESEM analysis.

Sandhya Shenoy U

ABSTRACT

This Research work entitled, '**Synthesis and Characterization of Copper and Cuprous Oxide Nanofluids**' deals with the single step chemical synthesis of nanofluids, involving simultaneous in situ synthesis of nanoparticles and their dispersion in the base fluid. Nanofluids have been synthesized by a reliable, versatile and well controlled solution phase approach using mixture of water and ethylene glycol as base fluids. Copper nitrate, copper sulfate and copper acetate have been used as precursors for the synthesis. Copper salts have been reduced using ascorbic acid and glucose. Sodium lauryl sulfate, cetyl trimethyl ammonium bromide and poly vinyl pyrrolidone have been used for the stabilization of the nanofluids. By varying the synthetic conditions precise control on the size of the particles has been established. The as prepared nanofluids have been characterized by X ray diffraction and selected area electron diffraction technique for the phase structure; electron diffraction X ray analysis for chemical composition, transmission electron microscopy and field emission scanning electron microscopy for the morphology; fourier transform infrared spectroscopy and ultra violet - visible spectroscopy for analysis of ingredients of the solution. Thermal conductivity, sedimentation and rheological measurements have also been carried out. Interesting copper and cuprous oxide structures with octahedral, cuboctahedral, truncated cube, whorled leaf like, flower like, hexagonal disc like and star like shapes have been prepared. It has been found that the reaction parameters have considerable influence on the size of the particle formed and rate of the reaction. The as synthesized nanofluids have been found to exhibit Newtonian behavior. The sedimentation measurements showed that the nanofluids have very high stability. Uniform dispersion of the nanoparticles in the base fluid led to promising increase in its thermal conductivity. The reported methods have been found to be facile, expeditious and cost effective for preparing heat transfer fluids with higher stability and enhanced thermal conductivity.

Key words: Copper, cuprous oxide, nanofluids, thermal conductivity, viscosity.

CONTENTS

DECLARATION	
CERTIFICATE	
ACKNOWLEDGEMENT	
ABSTRACT	
CONTENTS	i
LIST OF FIGURES	v
LIST OF TABLES	xviii
NOMENCLATURE	xxii
CHAPTER 1 INTRODUCTION AND A REVIEW OF THE LITERATURE	1
1.1 NANOTECHNOLOGY	2
1.2 NANOFUIDS	3
1.3 SYNTHESIS OF NANOFUIDS	6
1.4 APPLICATIONS OF NANOFUIDS	11
1.4.1 Cooling Applications	12
<i>1.4.1.1 Crystal silicon mirror cooling</i>	12
<i>1.4.1.2 Transportation</i>	12
<i>1.4.1.3 Electronics cooling</i>	13
<i>1.4.1.4 Space and nuclear systems cooling</i>	13
<i>1.4.1.5 Defense applications</i>	14
1.4.2 Mechanical Applications	14

1.4.2.1 Tribological applications	14
1.4.2.2 Magnetic sealing	15
1.4.3 Biomedical Applications	16
1.4.4 Other Applications	16
1.5 COPPER AND CUPROUS OXIDE NANOFLUIDS	17
1.6 LITERATURE REVIEW	18
1.7 SCOPE	36
1.8 OBJECTIVES	37
CHAPTER 2 EXPERIMENTAL	39
2.1 MATERIALS	40
2.1.1 Copper Salts	40
2.1.2 Reducing Agents	41
2.1.3 Stabilizing Agents	43
2.2 SYNTHESIS OF NANOFLUIDS	45
2.2.1 Synthesis of Copper Nanofluids	46
2.2.1.1 Synthesis of copper nanofluids in the presence of SLS	46
2.2.1.2 Synthesis of copper nanofluids in the presence of CTAB	48
2.2.1.3 Synthesis of copper nanofluids in the presence of PVP	50
2.2.2 Synthesis of Cuprous Oxide Nanofluids	51
2.2.2.1 Synthesis of cuprous oxide nanofluids in the presence of SLS using copper acetate and glucose	51
2.2.2.2 Synthesis of cuprous oxide nanofluids in the presence of CTAB	52

2.2.2.3 <i>Synthesis of cuprous oxide nanofluids in the presence of PVP</i>	54
2.3 CHARACTERIZATION	55
2.3.1 XRD Studies	55
2.3.2 TEM Analysis	57
2.3.3 FESEM Analysis	57
2.3.4 FTIR and UV-Vis Spectroscopic Analysis	58
2.3.5 Thermal Conductivity Measurements	58
2.3.6 Viscosity Measurements	59
CHAPTER 3 RESULTS AND DISCUSSION	60
3.1 COPPER NANOFLUIDS	61
3.1.1 Copper Nanofluids Synthesized in the Presence of SLS	69
3.1.1.1 <i>Nanofluids synthesized using copper nitrate and ascorbic acid</i>	69
3.1.1.2 <i>Nanofluids synthesized using copper nitrate and glucose</i>	79
3.1.1.3 <i>Nanofluids synthesized using copper sulphate and ascorbic acid</i>	86
3.1.1.4 <i>Nanofluids synthesized using copper sulphate and glucose</i>	90
3.1.1.5 <i>Nanofluids synthesized using copper acetate and ascorbic acid</i>	95
3.1.2 Copper Nanofluids Synthesized in the Presence of CTAB	99
3.1.2.1 <i>Nanofluids synthesized using copper nitrate and ascorbic acid</i>	99
3.1.2.2 <i>Nanofluids synthesized using copper sulfate and ascorbic acid</i>	105
3.1.2.3 <i>Nanofluids synthesized using copper acetate and ascorbic acid</i>	109
3.1.3 Copper Nanofluids Synthesized in the Presence of PVP	113
3.1.3.1 <i>Nanofluids synthesized using copper nitrate and ascorbic acid</i>	113

3.1.3.2 <i>Nanofluids synthesized using copper sulfate and ascorbic acid</i>	117
3.1.3.3 <i>Nanofluids synthesized using copper acetate and ascorbic acid</i>	122
3.2 CUPROUS OXIDE NANOFLUIDS	126
3.2.1 Cuprous Oxide Nanofluids Synthesized in the Presence of SLS	
Using Copper Acetate and Glucose	135
3.2.2 Cuprous Oxide Nanofluids Synthesized in the Presence of CTAB	141
3.2.2.1 <i>Nanofluids synthesized using copper nitrate and glucose</i>	141
3.2.2.2 <i>Nanofluids synthesized using copper sulfate and glucose</i>	146
3.2.2.3 <i>Nanofluids synthesized using copper acetate and glucose</i>	150
3.2.3 Cuprous Oxide Nanofluids Synthesized in the Presence of PVP	155
3.2.3.1 <i>Nanofluids synthesized using copper nitrate and glucose</i>	155
3.2.3.2 <i>Nanofluids synthesized using copper sulfate and glucose</i>	159
3.2.3.3 <i>Nanofluids synthesized using copper acetate and glucose</i>	163
CHAPTER 4 SUMMARY AND CONCLUSIONS	169
4.1 SUMMARY	170
4.2 CONCLUSIONS	172
4.3 SCOPE FOR FURTHER WORK	173
REFERENCES	174
BIODATA	190

LIST OF FIGURES

3.1	Powder XRD pattern of copper nanoparticles prepared by the reduction of copper nitrate by ascorbic acid in the presence of CTAB	61
3.2	Powder XRD pattern of copper nanoparticles prepared by the reduction of copper sulfate by ascorbic acid in the presence of CTAB	62
3.3	Powder XRD pattern of copper nanoparticles prepared by the reduction of copper acetate by ascorbic acid in the presence of CTAB	62
3.4	EDX spectrum of copper nanoparticles prepared by the reduction of copper nitrate by ascorbic acid in the presence of CTAB	63
3.5	EDX spectrum of copper nanoparticles prepared by the reduction of copper sulfate by ascorbic acid in the presence of CTAB	63
3.6	EDX spectrum of copper nanoparticles prepared by the reduction of copper acetate by ascorbic acid in the presence of CTAB	64
3.7	SAED pattern of copper nanoparticles prepared by the reduction of copper nitrate by ascorbic acid in the presence of CTAB	64
3.8	SAED pattern of copper nanoparticles prepared by the reduction of copper sulfate by ascorbic acid in the presence of CTAB	65
3.9	SAED pattern of copper nanoparticles prepared by the reduction of copper acetate by ascorbic acid in the presence of CTAB	65
3.10	FTIR spectra of (A) ethylene glycol and (B) copper nanofluid prepared by the reduction of copper nitrate by ascorbic acid in the presence of CTAB	66

3.11	FTIR spectra of (A) ethylene glycol and (C) copper nanofluid prepared by the reduction of copper sulfate by ascorbic acid in the presence of CTAB	66
3.12	FTIR spectra of (A) ethylene glycol and (D) copper nanofluid prepared by the reduction of copper acetate by ascorbic acid in the presence of CTAB	67
3.13	UV-Vis spectrum of copper nanofluid prepared by the reduction of copper nitrate by ascorbic acid in the presence of CTAB	68
3.14	UV-Vis spectrum of copper nanofluid prepared by the reduction of copper sulfate by ascorbic acid in the presence of CTAB	68
3.15	UV-Vis spectrum of copper nanofluid prepared by the reduction of copper acetate by ascorbic acid in the presence of CTAB	69
3.16	Schematic representation of influence of rate of reduction on the sizes of the particles formed	70
3.17	Schematic representation of influence of concentration of SLS on the sizes of the particles formed	73
3.18	TEM image of copper nanofluid prepared by the reduction of copper nitrate by ascorbic acid in the presence of SLS (A) under microwave irradiation and (B) by conventional heating	75
3.19	Variation of thermal conductivity ratio with particle weight fraction for copper nanofluid prepared by the reduction of copper nitrate by ascorbic acid in the presence of SLS	76

3.20	Shear stress verses shear rate for copper nanofluid prepared by the reduction of copper nitrate by ascorbic acid in the presence of SLS	77
3.21	Viscosity as a function of shear rate at different temperatures for copper nanofluid prepared by the reduction of copper nitrate by ascorbic acid in the presence of SLS	78
3.22	Variation of relative viscosity with particle weight fraction for copper nanofluid prepared by the reduction of copper nitrate by ascorbic acid in the presence of SLS	78
3.23	Viscosity as a function of temperature for copper nanofluid prepared by the reduction of copper nitrate by ascorbic acid in the presence of SLS	79
3.24	(A) TEM image and (B) FESEM image of copper nanoparticles prepared by the reduction of copper nitrate by glucose in the presence of SLS	83
3.25	Variation of thermal conductivity ratio with particle weight fraction for copper nanofluid prepared by the reduction of copper nitrate by glucose in the presence of SLS	84
3.26	Viscosity measurements of copper nanofluid prepared by the reduction of copper nitrate by glucose in the presence of SLS. (A) Shear stress verses shear rate; (B) Viscosity as a function of shear rate at different temperatures; (C) Variation of relative viscosity with particle weight fraction; (D) Viscosity as a function of temperature	85
3.27	(A) TEM image and (B) FESEM image of copper nanoparticles prepared by the reduction of copper sulfated by ascorbic acid in the presence of SLS	88

3.28	Variation of thermal conductivity ratio with particle weight fraction for copper nanofluid prepared by the reduction of copper sulfate by ascorbic acid in the presence of SLS	89
3.29	Viscosity measurements of copper nanofluid prepared by the reduction of copper sulfate by ascorbic acid in the presence of SLS. (A) Shear stress verses shear rate; (B) Viscosity as a function of shear rate at different temperatures; (C) Variation of relative viscosity with particle weight fraction; (D) Viscosity as a function of temperature	90
3.30	(A) TEM image and (B) FESEM image of copper nanoparticles prepared by the reduction of copper sulfate by glucose in the presence of SLS	93
3.31	Variation of thermal conductivity ratio with particle weight fraction for copper nanofluid prepared by the reduction of copper sulfate by glucose in the presence of SLS	93
3.32	Viscosity measurements of copper nanofluid prepared by the reduction of copper sulfate by glucose in the presence of SLS. (A) Shear stress verses shear rate; (B) Viscosity as a function of shear rate at different temperatures; (C) Variation of relative viscosity with particle weight fraction; (D) Viscosity as a function of temperature	94
3.33	TEM image of copper nanofluid prepared by the reduction of copper acetate by ascorbic acid in the presence of SLS	97
3.34	Variation of thermal conductivity ratio with particle weight fraction for copper nanofluid prepared by the reduction of copper acetate by ascorbic acid in the presence of SLS	98

3.35	Viscosity measurements of copper nanofluid prepared by the reduction of copper acetate by ascorbic acid in the presence of SLS. (A) Shear stress verses shear rate; (B) Viscosity as a function of shear rate at different temperatures; (C) Variation of relative viscosity with particle weight fraction; (D) Viscosity as a function of temperature	99
3.36	(A) TEM image and (B) FESEM image of copper nanoparticles prepared by the reduction of copper nitrate by ascorbic acid in the presence of CTAB	103
3.37	Variation of thermal conductivity ratio with particle weight fraction for copper nanofluid prepared by the reduction of copper nitrate by ascorbic acid in the presence of CTAB	103
3.38	Viscosity measurements of copper nanofluid prepared by the reduction of copper nitrate by ascorbic acid in the presence of CTAB. (A) Shear stress verses shear rate; (B) Viscosity as a function of shear rate at different temperatures; (C) Variation of relative viscosity with particle weight fraction; (D) Viscosity as a function of temperature	104
3.39	(A) TEM image and (B) FESEM image of copper nanoparticles prepared by the reduction of copper sulfate by ascorbic acid in the presence of CTAB	107
3.40	Variation of thermal conductivity ratio with particle weight fraction for copper nanofluid prepared by the reduction of copper sulfate by ascorbic acid in the presence of CTAB	107

3.41	Viscosity measurements of copper nanofluid prepared by the reduction of copper sulfate by ascorbic acid in the presence of CTAB. (A) Shear stress verses shear rate; (B) Viscosity as a function of shear rate at different temperatures; (C) Variation of relative viscosity with particle weight fraction; (D) Viscosity as a function of temperature	108
3.42	(A) TEM image and (B) FESEM image of copper nanoparticles prepared by the reduction of copper acetate by ascorbic acid in the presence of CTAB	111
3.43	Variation of thermal conductivity ratio with particle weight fraction for copper nanofluid prepared by the reduction of copper acetate by ascorbic acid in the presence of CTAB	111
3.44	Viscosity measurements of copper nanofluid prepared by the reduction of copper acetate by ascorbic acid in the presence of CTAB. (A) Shear stress verses shear rate; (B) Viscosity as a function of shear rate at different temperatures; (C) Variation of relative viscosity with particle weight fraction; (D) Viscosity as a function of temperature	112
3.45	(A) TEM image and (B) FESEM image of copper nanoparticles prepared by the reduction of copper nitrate by ascorbic acid in the presence of PVP	115
3.46	Variation of thermal conductivity ratio with particle weight fraction for copper nanofluid prepared by the reduction of copper nitrate by ascorbic acid in the presence of PVP	116

3.47	Viscosity measurements of copper nanofluid prepared by the reduction of copper nitrate by ascorbic acid in the presence of PVP. (A) Shear stress verses shear rate; (B) Viscosity as a function of shear rate at different temperatures; (C) Variation of relative viscosity with particle weight fraction; (D) Viscosity as a function of temperature	117
3.48	(A) TEM image and (B) FESEM image of copper nanoparticles prepared by the reduction of copper sulfate by ascorbic acid in the presence of PVP	120
3.49	Variation of thermal conductivity ratio with particle weight fraction for copper nanofluid prepared by the reduction of copper sulfate by ascorbic acid in the presence of PVP	121
3.50	Viscosity measurements of copper nanofluid prepared by the reduction of copper sulfate by ascorbic acid in the presence of PVP. (A) Shear stress verses shear rate; (B) Viscosity as a function of shear rate at different temperatures; (C) Variation of relative viscosity with particle weight fraction; (D) Viscosity as a function of temperature	121
3.51	(A) TEM image and (B) FESEM image of copper nanoparticles prepared by the reduction of copper acetate by ascorbic acid in the presence of PVP	124
3.52	Variation of thermal conductivity ratio with particle weight fraction for copper nanofluid prepared by the reduction of copper acetate by ascorbic acid in the presence of PVP	125

3.53	Viscosity measurements of copper nanofluid prepared by the reduction of copper acetate by ascorbic acid in the presence of PVP. (A) Shear stress verses shear rate; (B) Viscosity as a function of shear rate at different temperatures; (C) Variation of relative viscosity with particle weight fraction; (D) Viscosity as a function of temperature	126
3.54	Powder XRD pattern of cuprous oxide nanoparticles prepared by the reduction of copper nitrate by glucose in the presence of CTAB	127
3.55	Powder XRD pattern of cuprous oxide nanoparticles prepared by the reduction of copper sulfate by glucose in the presence of CTAB	127
3.56	Powder XRD pattern of cuprous oxide nanoparticles prepared by the reduction of copper acetate by glucose in the presence of CTAB	128
3.57	EDX spectrum of cuprous oxide nanoparticles prepared by the reduction of copper nitrate by glucose in the presence of CTAB	129
3.58	EDX spectrum of cuprous oxide nanoparticles prepared by the reduction of copper sulfate by glucose in the presence of CTAB	129
3.59	EDX spectrum of cuprous oxide nanoparticles prepared by the reduction of copper acetate by glucose in the presence of CTAB	130
3.60	SAED pattern of cuprous oxide nanoparticles prepared by the reduction of copper nitrate by glucose in the presence of CTAB	130
3.61	SAED pattern of cuprous oxide nanoparticles prepared by the reduction of copper sulfate by glucose in the presence of CTAB	131
3.62	SAED pattern of cuprous oxide nanoparticles prepared by the reduction of copper acetate by glucose in the presence of CTAB	131

3.63	FTIR spectra of (A) ethylene glycol and (E) cuprous oxide nanofluid prepared by the reduction of copper nitrate by glucose in the presence of CTAB	132
3.64	FTIR spectra of (A) ethylene glycol and (F) cuprous oxide nanofluid prepared by the reduction of copper sulfate by glucose in the presence of CTAB	132
3.65	FTIR spectra of (A) ethylene glycol and (G) cuprous oxide nanofluid prepared by the reduction of copper acetate by glucose in the presence of CTAB	133
3.66	UV-Vis spectrum of cuprous oxide nanofluid prepared by the reduction of copper nitrate by glucose in the presence of CTAB	133
3.67	UV-Vis spectrum of cuprous oxide nanofluid prepared by the reduction of copper sulfate by glucose in the presence of CTAB	134
3.68	UV-Vis spectrum of cuprous oxide nanofluid prepared by the reduction of copper acetate by glucose in the presence of CTAB	134
3.69	TEM image of cuprous oxide nanofluid prepared by conventional heating by the reduction of copper acetate by glucose in the presence of SLS	139
3.70	FESEM image of cuprous oxide nanoparticles prepared by (A) 7 minutes and (B) 10 minutes microwave irradiation by the reduction of copper acetate by glucose in the presence of SLS	139
3.71	Variation of thermal conductivity ratio with particle weight fraction for cuprous oxide nanofluid prepared by the reduction of copper acetate by glucose in the presence of SLS	140

3.72	Viscosity measurements of cuprous oxide nanofluid prepared by the reduction of copper acetate by glucose in the presence of SLS. (A) Shear stress verses shear rate; (B) Viscosity as a function of shear rate at different temperatures; (C) Variation of relative viscosity with particle weight fraction; (D) Viscosity as a function of temperature	141
3.73	(A) Low magnification and (B) high magnification FESEM images of cuprous oxide nanoparticles prepared by the reduction of copper nitrate by glucose in the presence of CTAB	144
3.74	Variation of thermal conductivity ratio with particle weight fraction for cuprous oxide nanofluid prepared by the reduction of copper nitrate by glucose in the presence of CTAB	144
3.75	Viscosity measurements of cuprous oxide nanofluid prepared by the reduction of copper nitrate by glucose in the presence of CTAB. (A) Shear stress verses shear rate; (B) Viscosity as a function of shear rate at different temperatures; (C) Variation of relative viscosity with particle weight fraction; (D) Viscosity as a function of temperature	145
3.76	(A) Low magnification and (B) high magnification FESEM images of cuprous oxide nanoparticles prepared by the reduction of copper sulfate by glucose in the presence of CTAB	148
3.77	Variation of thermal conductivity ratio with particle weight fraction for cuprous oxide nanofluid prepared by the reduction of copper sulfate by glucose in the presence of CTAB	149

3.78	Viscosity measurements of cuprous oxide nanofluid prepared by the reduction of copper sulfate by glucose in the presence of CTAB. (A) Shear stress verses shear rate; (B) Viscosity as a function of shear rate at different temperatures; (C) Variation of relative viscosity with particle weight fraction; (D) Viscosity as a function of temperature	150
3.79	FESEM image of cuprous oxide nanoparticles prepared by the reduction of copper acetate by glucose in the presence of CTAB (A) under microwave irradiation and (B) by conventional heating	153
3.80	Variation of thermal conductivity ratio with particle weight fraction for cuprous oxide nanofluid prepared by the reduction of copper acetate by glucose in the presence of CTAB	153
3.81	Viscosity measurements of cuprous oxide nanofluid prepared by the reduction of copper acetate by glucose in the presence of CTAB. (A) Shear stress verses shear rate; (B) Viscosity as a function of shear rate at different temperatures; (C) Variation of relative viscosity with particle weight fraction; (D) Viscosity as a function of temperature	154
3.82	(A) TEM image and (B) FESEM image of cuprous oxide nanoparticles prepared by the reduction of copper nitrate by glucose in the presence of PVP	157
3.83	Variation of thermal conductivity ratio with particle weight fraction for cuprous oxide nanofluid prepared by the reduction of copper nitrate by glucose in the presence of PVP	157

3.84	Viscosity measurements of cuprous oxide nanofluid prepared by the reduction of copper nitrate by glucose in the presence of PVP. (A) Shear stress verses shear rate; (B) Viscosity as a function of shear rate at different temperatures; (C) Variation of relative viscosity with particle weight fraction; (D) Viscosity as a function of temperature	158
3.85	(A) TEM image and (B) FESEM image of cuprous oxide nanoparticles prepared by the reduction of copper sulfate by glucose in the presence of PVP	161
3.86	Variation of thermal conductivity ratio with particle weight fraction for cuprous oxide nanofluid prepared by the reduction of copper sulfate by glucose in the presence of PVP	162
3.87	Viscosity measurements of cuprous oxide nanofluid prepared by the reduction of copper sulfate by glucose in the presence of PVP. (A) Shear stress verses shear rate; (B) Viscosity as a function of shear rate at different temperatures; (C) Variation of relative viscosity with particle weight fraction; (D) Viscosity as a function of temperature	163
3.88	(A) TEM image and (B) FESEM image of cuprous oxide nanoparticles prepared by the reduction of copper acetate by glucose in the presence of PVP	166
3.89	Variation of thermal conductivity ratio with particle weight fraction for cuprous oxide nanofluid prepared by the reduction of copper acetate by glucose in the presence of PVP	166

3.90 Viscosity measurements of cuprous oxide nanofluid prepared by the reduction of copper acetate by glucose in the presence of PVP. (A) Shear stress verses shear rate; (B) Viscosity as a function of shear rate at different temperatures; (C) Variation of relative viscosity with particle weight fraction; (D) Viscosity as a function of temperature

167

LIST OF TABLES

1.1	Review on two step synthetic methods	18
3.1	Effect of concentration of SLS on the size of copper particles prepared by the reduction of copper nitrate by ascorbic acid	72
3.2	Effect of concentration of SLS on the size of copper particles prepared by the reduction of copper nitrate by glucose	82
3.3	Effect of irradiation duration on the size of copper particles prepared by the reduction of copper nitrate by glucose in the presence of SLS	83
3.4	Effect of dilution on the size of copper particles prepared by the reduction of copper sulfate by ascorbic acid in the presence of SLS	86
3.5	Effect of concentration of SLS on the size of copper particles prepared by the reduction of copper sulfate by ascorbic acid	87
3.6	Effect of irradiation duration on the size of copper particles prepared by the reduction of copper sulfate by ascorbic acid in the presence of SLS	88
3.7	Effect of ratio of reactants on the size of copper particles prepared by the reduction of copper sulfate by glucose in the presence of SLS	91
3.8	Effect of concentration of SLS on the size of copper particles prepared by the reduction of copper sulfate by glucose	92
3.9	Effect of dilution on the size of copper particles prepared by the reduction of copper acetate by ascorbic acid in the presence of SLS	96

3.10	Effect of concentration of SLS on the size of copper particles prepared by the reduction of copper acetate by ascorbic acid	96
3.11	Effect of dilution on the size of copper particles prepared by the reduction of copper nitrate by ascorbic acid in the presence of CTAB	101
3.12	Effect of concentration of CTAB on the size of copper particles prepared by the reduction of copper nitrate by ascorbic acid	101
3.13	Effect of concentration of CTAB on the size of copper particles prepared by the reduction of copper sulfate by ascorbic acid	106
3.14	Effect of dilution on the size of copper particles prepared by the reduction of copper acetate by ascorbic acid in the presence of CTAB	109
3.15	Effect of concentration of CTAB on the size of copper particles prepared by the reduction of copper acetate by ascorbic acid	110
3.16	Effect of concentration of PVP on the size of copper particles prepared by the reduction of copper nitrate by ascorbic acid	114
3.17	Effect of concentration of PVP on the size of copper particles prepared by the reduction of copper sulfate by ascorbic acid	119
3.18	Effect of dilution on the size of copper particles prepared by the reduction of copper acetate by ascorbic acid in the presence of PVP	123
3.19	Effect of concentration of PVP on the size of copper particles prepared by the reduction of copper acetate by ascorbic acid	123
3.20	Effect of concentration of SLS on the size of cuprous oxide particles prepared by the reduction of copper acetate by glucose	137

3.21	Effect of concentration of CTAB on the size of cuprous oxide particles prepared by the reduction of copper nitrate by glucose	143
3.22	Effect of ratio of reactants on the size of cuprous oxide particles prepared by the reduction of copper sulfate by glucose in the presence of CTAB	146
3.23	Effect of dilution on the size of cuprous oxide particles prepared by the reduction of copper sulfate by glucose in the presence of CTAB	147
3.24	Effect of concentration of CTAB on the size of cuprous oxide particles prepared by the reduction of copper sulfate by glucose	147
3.25	Effect of dilution on the size of cuprous oxide particles prepared by the reduction of copper acetate by glucose in the presence of CTAB	151
3.26	Effect of concentration of CTAB on the size of cuprous oxide particles prepared by the reduction of copper acetate by glucose	152
3.27	Effect of concentration of PVP on the size of cuprous oxide particles prepared by the reduction of copper nitrate by glucose	156
3.28	Effect of ratio of reactants on the size of cuprous oxide particles prepared by the reduction of copper sulfate by glucose in the presence of PVP	159
3.29	Effect of dilution on the size of cuprous oxide particles prepared by the reduction of copper sulfate by glucose in the presence of PVP	160
3.30	Effect of concentration of PVP on the size of cuprous oxide particles prepared by the reduction of copper sulfate by glucose	160

3.31	Effect of dilution on the size of cuprous oxide particles prepared by the reduction of copper acetate by glucose in the presence of PVP	164
3.32	Effect of concentration of PVP on the size of cuprous oxide particles prepared by the reduction of copper acetate by glucose	165
3.33	Comparison of particle sizes and thermal conductivities of synthesized nanofluids	168

NOMENCLATURE

ABBREVIATIONS

ASNSS	Arc Spray Nanofluid Synthesis System
CBN	Copper oxide Brake Nanofluid
CMC	Critical Micelle Concentration
CNSL	Cashew Nut Shell Liquid
CSCS	Chloride Solution Combustion Synthesis
CTAB	Cetyl Trimethyl Ammonium Bromide
CVD	Chemical Vapor Deposition
DSC	Differential Scanning Calorimetry
EDXA	Energy Dispersion X- ray Analysis
EG	Ethylene Glycol
ESCA	Electron Spectroscopy for Chemical Analysis
FESEM	Field Emission Scanning Electron Microscopy
Fig.	Figure
FTIR	Fourier Transform Infra-Red
JCPDS	Joint Committee on Powder Diffraction Standards
MUA	Mercapto Undecanoic Acid
NMR	Nuclear Magnetic Resonance
PEG	Poly Ethylene Glycol
PPy	Poly Pyrrole
PVD	Physical Vapor Deposition
PVP	Poly Vinyl Pyrrolidone

SAED	Selected Area Electron Diffraction
SANSS	Submerged Arc Nanoparticle Synthesis System
SDBS	Sodium Dodecyl Benzene Sulfonate
SLS	Sodium Lauryl Sulfate
TEM	Transmission Electron Microscopy
UV-Vis	Ultra Violet-Visible
XPS	X-ray Photoelectron Spectroscopy
XRD	X-Ray Diffraction

SYMBOLS & UNIT

α	Alpha
A	ampere
Å	angstrom
β	Beta
cm	Centi meter
°C	Degree Celsius
emu	Electromagnetic unit
eV	Electron volt
γ	Gamma
g	Gram
Hz	hertz
h	Hour
⁻¹	Inverse
J	joule

K	kelvin
k	Kilo
λ	Lamda
<	Less than
L	Liter
μ s	Micro second
m	Milli
min	Minute
μ	Mu
M	Molar
mol	Mole
nm	Nano meter
Pa	pascal
ppm	Parts per million
%	Percent
\pm	Plus-minus
rpm	Revolutions per minute
s	Second
/	Solidus
τ	Tau
θ	Theta
~	Tilde
V	volt
W	watt



CHAPTER 1

**INTRODUCTION AND A
REVIEW OF THE LITERATURE**

Chapter 1 gives a general introduction to nanotechnology and nanofluids, chemical and physical methods of synthesis of nanofluids and its applications. It provides an overview of the literature on synthesis and properties of metal and metal oxide nanofluids. Scope and objectives of the work has also been included in this chapter.

1.1 NANOTECHNOLOGY

Nanotechnology is a broad term that encompasses many application specific technologies and research into objects that are nanometer or smaller. In nanoscience and technology, a particle is defined as a small object that behaves as a whole unit in terms of its transport and properties. It is further classified according to size, in terms of diameter, fine particles cover a range between 100 nm and 2500 nm, while ultrafine particles, on the other hand, are sized between 1 nm and 100 nm. Similar to ultrafine particles, nanoparticles are sized between 1 nm and 100 nm, though the size limitation can be restricted to one or two dimensions. In general, nano structures are defined as those having at least one of the dimensions between 1 nm and 100 nm.

Nanotechnology is considered by many to be one of the significant forces that would drive the next major industrial revolution of this century that can significantly improve device performance, communication technology, sensor applications, drug delivery and several areas of practical importance (Manna 2009). It represents the most relevant technological cutting edge currently being explored.

Nanoparticles are of great scientific interest as they are effectively a bridge between bulk materials and atomic or molecular structures. The primary approach of nanotechnology is to manipulate the structure at the molecular or atomic aggregate level with the goal of achieving desired change in property with unprecedented precision and also innovation in virtually every industry and public endeavor including biological sciences, physical sciences, electronics cooling, transportation, environment and national security.

A bulk material should have constant physical properties regardless of its size, but at the nano-scale this is often not the case. The properties of materials change as their size approaches the nanoscale and as the percentage of atoms at the surface of a material becomes significant. For bulk materials larger than one micrometer the percentage of atoms at the surface is minuscule relative to the total number of atoms of the material. The interesting and sometimes unexpected properties of nanoparticles are partly due to the aspects of the surface of the material dominating the properties in lieu of the bulk properties.

1.2 NANOFUIDS

Nanofluids are a relatively new class of fluids which consists of a base fluid with nano sized particles suspended within them, developed with the specific aim of increasing the thermal conductivity of heat transfer fluids. Though exploits of nanotechnology mostly concerns engineering solids either for functional (electronic, magnetic, optical, catalytic, etc.) or structural (strength, hardness, wear/abrasion resistance, etc.) applications, the concept of nanofluid is rather new (Manna 2009). This term was first introduced by Choi in 1995 at the Argonne National Laboratory.

Ultra high performance cooling has become one of the most crucial technical challenges faced with advancement of device miniaturization and escalating need for improvement of heat transfer. Heat dissipation could be increased by increasing the area available for heat exchange to the surrounding but this will lead to the increase in the device size as well as the cost of production. Alternative would be to increase the effective thermal conductivity of the conventional base fluids, which basically have a lower magnitude, by the addition of particles with higher thermal conductivity (Eastman et al. 2001).

It is well known that crystalline solids have higher thermal conductivities than traditional fluids (such as water, ethylene glycol, and oil) by 1-3 orders of magnitude (Zhu et al. 2004a; Wang and Mujumdar 2008a; Li et al. 2009b). Therefore, an innovative

way in improving thermal conductivities of a fluid is to suspend solid particles within it. Since nanoparticles offer extremely large total surface areas, the nanofluid is expected to exhibit reasonably superior thermal properties relative to conventional heat transfer fluids and fluids containing micrometer-sized particles. Hence addition of metal and metal oxide nanoparticles would be a proficient way to bring about dramatic improvements in the heat transfer characteristics of the base fluid.

Suspensions of nanoparticles are possible because the interaction of the particle surface with the solvent is strong enough to overcome differences in density, which usually result in a material either sinking or floating in a liquid. The resulting mixture is referred to as a nanofluid and the presence of the nanoparticles increases appreciably the effective thermal conductivity of the fluid and consequently enhances the heat transfer characteristics.

Nanofluids have a distinctive characteristic, which is quite different from those of traditional solid–liquid mixtures in which millimeter and/or micrometer- sized particles are involved (Das et al. 2008). Such particles can clog equipment and can increase pressure drop due to settling effects. Moreover, they settle rapidly, creating substantial additional pressure drop. However, nanofluids exhibit little or no penalty in pressure drop when flowing through the passages (Li et al. 2009b). The minimum pressure drop can be attributed to several factors such as nanoparticle clustering, ballistic phonon transport, layering at the solid/liquid interface, the interaction and collision among particles and surface area enhancement. Moreover, they flow smoothly through microchannels without clogging them. Thus, nanofluids are best for applications in which fluid flows through small passages because nanoparticles are small enough to behave similar to liquid molecules. In addition, the suspended particles increase the surface area and the heat capacity of the fluid. That is, a significant improvement in the effective thermal conductivity is achieved as a result of decreasing the size of the suspended particles (nano-sized particle) rather than using larger particles (micro-sized particle). Since heat

transfer occurs on the surface of a solid, this feature greatly enhances the heat conduction contribution of the fluid.

When the particles are properly dispersed, these features of nanofluids are expected to yield several benefits like: higher heat conduction due to large specific surface area and greater mobility (micro-convection) of tiny particles (Manna 2009). It is found that:

1. The thermal conductivity of nanofluids increases significantly with a rise in temperature, which may be attributed to the above reasons.
2. Greater stability against sedimentation due to smaller size and weight.
3. More efficient heat transfer in microchannels.
4. Negligible friction and erosion of conduit surfaces.

Increasing interest in the transport of thermal energy at nanometer length scales is accompanying the miniaturization of devices and emerging applications for new nanocomposite materials and heat transfer fluids (Li et al. 2009b). Nanofluids represent the cutting edge technology of liquid coolants where in the heat transfer properties of the conventional base fluids are enhanced by the addition of nanoparticles in them to form stable dispersions. Higher thermal conductivity of the heat transfer fluids transmutes into higher efficiency, better performance, significant energy savings and reduced costs.

However, the increases in thermal conductivities are different for different types of nanofluids. The thermal conductivity of nanofluids varies with the size, shape, and material of nanoparticles. For example, nanofluids with metallic nanoparticles were found to have a higher thermal conductivity than nanofluids with nonmetallic (oxide) nanoparticles. The smaller the particle size, the higher the thermal conductivities of nanofluids. Furthermore, nanofluids with spherical shape nanoparticles exhibit a smaller increase in thermal conductivity compared with the nanofluids having cylindrical (nanorod or tube) nanoparticles.

Although liquid molecules close to a solid surface are known to form layered structures, little is known about the connection between this nanolayer and the thermal properties of solid/liquid suspensions. The solid-like nanolayer acts as a thermal bridge between a solid nanoparticle and a bulk liquid and so is the key to enhance thermal conductivity. From this thermally bridging nanolayer idea, a structural model of nanofluids that consists of solid nanoparticles, bulk liquid and solid-like nanolayers is reported in literature. Conventional pictures of the solid/liquid suspensions do not have this nanolayer. The thermal conductivity of the nanolayer on the surface of the nanoparticle is not known. However, because the layered molecules are in an intermediate physical state between a bulk liquid and a solid, the solid-like nanolayer of liquid molecules would be expected to lead to a substantially higher thermal conductivity than that of the bulk liquid.

1.3 SYNTHESIS OF NANOFLUIDS

Preparation of nanofluids is the first key step in experimental studies with nanofluids (Li et al. 2009b). Nanofluids are not just dispersion of solid particles in a fluid. The essential requirements that a nanofluid must fulfill are even and stable suspension, adequate durability, negligible agglomeration of particles, no chemical change of the particles or fluid, etc. Nanofluids are produced by dispersing nanometer scale solid particles into base liquids such as water, ethylene glycol, oil, etc.

Depending on the requirements of a particular application, many combinations of particle materials and fluids are of potential interest. For example, nanoparticles of pure metals, nonmetals; their oxides, nitrides, sulfides and carbides with or without surfactant molecules can be dispersed into fluids such as water, ethylene glycol, or oils (Kao et al. 2007; Phuoc et al. 2007; Chang et al. 2008; Choi et al. 2008; Chen et al. 2009; Zheng et al. 2010; Zhang et al. 2012).

Studies to date have used one or more of several possible methods for nanoparticle production and dispersion. There are mainly two techniques used to produce

nanofluids: the single-step and the two-step method. In either case, a well-mixed and uniformly dispersed nanofluid is needed for successful production or reproduction of enhanced properties and interpretation of experimental data.

Several studies, including the earliest investigations of nanofluids, used a two-step process in which nanoparticles are first produced as a dry powder, often by inert gas condensation, chemical vapor deposition (CVD), physical vapor deposition (PVD) mechanical alloying or other techniques (Das et al. 2003a; Hong et al. 2005; Chopkar et al. 2006; Li et al. 2009b). CVD has been used to produce materials for use in nanofluids, particularly multiwalled carbon nanotubes. The CVD technique appears to offer advantages in terms of control of particle size, ease of scalability, and the possibility of producing novel core-shell nanostructures. The nanoparticles or nanotubes are then dispersed into a fluid in a second processing step. Simple techniques such as ultrasonic agitation, control of pH or the addition of surfactants to the fluids are sometimes used to minimize particle aggregation and improve dispersion behavior (Li and Chang 2004; Das et al. 2008; Li et al. 2008; Murshed et al. 2008; Beck et al. 2010). These methods change the surface properties of the suspended particles and thus suppress the tendency to form particle clusters. It should be noted that the selection of surfactants depend mainly on the properties of the solutions and particles.

Such a two-step process works well in some cases, such as nanofluids consisting of oxide nanoparticles dispersed in deionized water. Less success has been found when producing nanofluids containing heavier metallic nanoparticles. The two-step method is extensively used in the synthesis of nanofluids considering the available commercial nanopowders supplied by several companies. Since nanopowder synthetic techniques have already been scaled up to industrial production levels by several companies, there are potential economic advantages in using two-step synthetic methods that rely on the use of such powders (Li et al. 2009b).

The single-step method simultaneously makes and disperses nanoparticles directly into base fluids. An example for one step physical method of synthesis is synthesis of nanofluids containing dispersed metal nanoparticles by a 'direct evaporation' technique, which involves direct condensation of metallic vapor into nanoparticles by contact with a flowing low vapor pressure liquid (Eastman et al. 2001). An advantage of this technique is that nanoparticle agglomeration is minimized, while a disadvantage is that only low vapor pressure fluids are compatible with the process. Vacuum evaporation on running oil substrate is a similar method in which the metals evaporated by electron beam heating, deposits on the surface of running oil. This method is used to produce both metal and metal oxide nanofluids (Akoh et al. 1978).

Submerged arc nano particle synthesis and arc spray nano particle synthesis, involves the vaporization of source material submerged in the dielectric liquid in a vacuum chamber (Chang et al. 2004; Chang et al. 2005; Lo et al. 2005a; Lo et al. 2005b; Lo et al. 2005c; Chang and Liu 2007; Chein and Chuang 2007). The applied electrical power on heating source generates an arc of high temperature to heat the metal and vaporize it along with the surrounding liquid. The vaporized metal expands and creates an inertial force around the dielectric liquid. The vaporized metal is then rapidly quenched by a low temperature dielectric liquid to suppress the growth of nanoparticles. The concentration of nanoparticles within the resulting nanofluids can be controlled by optimizing the nucleation process. High nucleation can be achieved when the metal is vaporized at high temperature and condensed rapidly at low temperature.

Laser ablation in liquid has been considered as an attractive technique for the preparation of nanoparticles and nanomaterial fabrications free from counter ions (Phuoc et al. 2007; Kim et al. 2009). It has been demonstrated that the technique can generate stable colloids containing nano-sized particles without the use of any dispersants or surface reactive reagents by ablating metals and metal oxides in deionized water and solvents. Laser ablation in liquid occurs when a high-power laser beam is focused for an appropriate time onto a solid target that is submerged in a liquid. Conversely, laser

ablation in liquid can be used to control the compositions, particle size, production rate and morphology of the ablated product by tailored selection of liquid medium, surfactants and other additives. This is because the liquid phase not only provides confinement for the plasma expansion and particle kinetic growth processes but also an environment for various chemical reactions between the generated solid clusters and the molecules of the liquid medium.

Dual plasma synthesis which is a single step physical synthetic method, uses a combination of low-pressure pulsed cathodic arc erosion to generate metal nanoparticles and in-flight radio-frequency glow discharge plasma functionalization for surface stabilization (Tavares and Coulombe 2011). The surface-stabilized nanoparticles are collected in situ by a falling film of base fluid, the vapors of which are used for plasma functionalization. Little to no agglomeration is observed in the suspension, although this process is shown to occur when the produced suspensions are heated to temperatures well beyond the range of effectiveness of typical surfactants. The thermally induced agglomeration if occurs is fully reversible in this method.

Pulsed wire evaporation is yet another one step physical method used to synthesize nanofluids (Lee et al. 2012a). In this technique a pulsed high voltage is driven through a thin metal wire. The non equilibrium overheating induced in the wire makes the wire to evaporate into plasma. The high temperature plasma is then cooled by interaction with argon-oxygen mixed gas and condensed into small sized particles. These particles come in direct contact with the base fluid and hence nanofluids containing nanoparticles without any surface contamination is obtained. The advantage of this method is that the concentration of the nanofluid can be controlled by the wire explosion number.

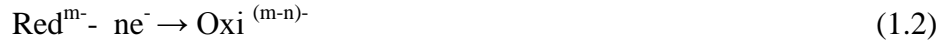
Various single-step chemical synthetic techniques can also be employed to produce nanofluids. For example, a technique for producing metallic nanoparticles by the reduction of metal salts has been used to produce colloidal suspensions in various

solvents for a wide range of applications, including studies of thermal transport (Liu et al. 2006a; Wang and Mujumdar 2008a; Wang and Mujumdar 2008b; Kumar et al. 2009). Excellent control of size and very narrow size distributions can be obtained by using such methods.

One of the chemical reduction methods is through the solution phase route. Reduction of metal ions leads to the metal atom, which upon aggregation forms nanoparticles (Das et al. 2008). The growth of the aggregate is arrested at some stage of its growth by stabilizing or protecting agents. The reduction reaction can be represented as



The electron is not supplied as an electron per se but as a reducing agent, which gets oxidized in the process:



where the reducing species (reductant) of finite charge gets oxidized, losing a certain charge. Both the metal and the reductant may not contain any distinct charge, and those mentioned are only nominal. The feasibility of the net reaction



depends on the thermodynamics of the process, which in turn is represented by the electrochemical potentials of the corresponding half-cell reactions called the standard electrode potentials. If the electrode potentials corresponding to reactions (1.1) and (1.2) are added (with their signs), and if we get a net positive value, the process is thermodynamically feasible. This corresponds to a net negative free-energy change $\Delta G = -nFE$, where ΔG is the free-energy change of reaction (1.3), n the number of electrons involved, F the Faraday constant, and E the electrochemical potential of the reaction

(1.3). It is written E not E° as the potential has to be taken at the appropriate conditions. The process is thermodynamically feasible if ΔG is negative.

Microwaves are electromagnetic waves containing electric and magnetic components. Recently, microwave irradiation has been widely applied to material science due to its thermal and non thermal effects (Habibzadeh et al. 2009). It is well known that the interaction of dielectric materials, liquids or solids, with microwaves leads to dielectric heating. As a heating method, compared with the conventional methods, it has the properties of being fast, simple, and energy-saving. Due to the intense friction and collision of the molecules created by microwave irradiation, microwave irradiation not only provides the energy for the heating, but also greatly accelerates the nucleation of particles and depresses the straightforward growth of newly born particles. With microwave irradiation of the reactant solution, temperature and concentration gradients can be avoided, leading to uniform nucleation (Wang et al. 2002). Consequently, the as-prepared nanoparticles are of small size, narrow particle size distribution and the obtained nanofluids have good stabilization.

1.4 APPLICATIONS OF NANOFUIDS

Nanofluids as a new innovative class of heat transfer fluids represent a rapidly emerging field of great scientific interest where nanoscale science and thermal engineering meet (Murshed et al. 2009). Research on a variety of nanofluids applications is under way because the thermal transport phenomena of these fluids are unprecedented and surpass the fundamental limits of conventional macroscopic theories of suspensions. Nanofluids find most of their applications in thermal management since efficient cooling are vital in realizing the functions and long-term reliability of a variety of industrial and consumer products. Nanofluids have a plethora of potential tribological and biomedical applications. Recent studies have demonstrated the ability of nanofluids to improve the performance of real-world devices and systems.

1.4.1 Cooling Applications

1.4.1.1 Crystal silicon mirror cooling

One of the first applications of research in the field of nanofluids is for developing an advanced cooling technology to cool crystal silicon mirrors used in high-intensity X ray sources (Lee and Choi 1996). Because an X-ray beam creates tremendous heat as it bounces off a mirror, cooling rates of 2000 W cm^{-2} to 3000 W cm^{-2} should be achievable with the advanced cooling technology. Comparison of performance of a nanofluid-cooled microchannel heat exchanger with water-cooled and liquid-nitrogen-cooled microchannel heat exchangers shows that nanofluids can remarkably reduce the thermal resistances and increase the power densities, establishing the superiority of a nanofluid-cooled silicon microchannel heat exchanger. Furthermore, the possibility of thermal distortion and flow-induced vibration will be eliminated by passing the nanofluids through microchannels within the silicon mirror itself. The advanced cooling technology could provide more efficient cooling than that of other cooling technologies because the microchannels increase the effective heat transfer area and the metallic nanoparticles increase the effective thermal conductivity of coolants.

1.4.1.2 Transportation

An ethylene glycol and water mixture, the nearly universally used automotive coolant, is a relatively poor heat transfer fluid compared to water alone. The addition of nanoparticles to the standard engine coolant has the potential to improve automotive and heavy-duty engine cooling rates (Choi et al. 2008). Such improvement can be used to remove engine heat with a reduced-size coolant system which results in smaller and lighter radiators, which in turn benefit performance and lead to increased fuel economy. A promising nanofluid engine coolant is pure ethylene glycol with nanoparticles (Yu et al. 2009b). Pure ethylene glycol is a poor heat transfer fluid compared to a 50/50 mixture of ethylene glycol and water, but the addition of nanoparticles will improve the situation. If the resulting heat transfer rate can approach the 50/50 mixture rate, there are important

advantages. Perhaps one of the most prominent is the low pressure operation of an ethylene glycol based nanofluid compared with a 50/50 mixture of ethylene glycol and water. An atmospheric pressure coolant system has lower potential capital cost. This nanofluid also has a high boiling point, which is desirable for maintaining single-phase coolant flow. In addition, a higher boiling point coolant can be used to increase the normal coolant operating temperature and then reject more heat through the existing coolant system. More heat rejection allows a variety of design enhancements including engines with higher horsepower. The results of nanofluids research are being applied to the cooling of automatic transmissions (Tzeng et al. 2005).

1.4.1.3 Electronics cooling

The power density of integrated circuits and microprocessors has increased dramatically in recent years. Future processors for high-performance computers and servers have been projected to dissipate higher power, in the range of 100 W cm^{-2} – 300 W cm^{-2} . Existing aircooling techniques for removing this heat are already reaching their limits, and liquid cooling technologies are being, and have been, developed for replacing them. Single-phase fluids, two-phase fluids, and nanofluids are candidate replacements for air. All have increased heat transfer capabilities over air systems, and all are being investigated. Nanofluids have been considered as the working fluids for heat pipes in electronic cooling applications (Tsai et al. 2004; Kang et al. 2006b; Chein and Chuang 2007). The positive results are promoting the continued research and development of nanofluids for such applications.

1.4.1.4 Space and nuclear systems cooling

Due to restriction of space, energy and weight in space stations and aircrafts, there is a strong demand for highly efficient cooling system with smaller size. Cooling devices that incorporate nanofluids for ultra high heat flux electronic systems present the possibility of raising chip power in electronic components or simplifying cooling requirements for space applications. Nuclear applications of nanofluids appear to be very

promising perhaps the most promising of currently envisaged uses (Das et al. 2008). Nanofluids could be used in primary systems, emergency safety systems, and severe accident management systems, with resulting benefits such as power uprates in commercial pressurized water reactors and enhanced safety margins during design basis events and severe accidents. They have a potential as a coolant for safer and smaller nuclear generators.

1.4.1.5 Defense applications

A number of military devices and systems require high-heat-flux cooling to the level of tens of $MW m^{-2}$. At this level, cooling with conventional fluids is challenging. Examples of military applications include cooling of power electronics and directed energy weapons. Nanofluids have the potential to provide the required cooling in military vehicles, submarines, and high-power laser diodes (Wang and Mujumdar 2008b). In some cases, nanofluid research for defense applications includes multifunctional nanofluids with added thermal energy storage or energy harvesting through chemical reactions. Transformer cooling is important to the navy as well as the power generation industry with the objective of reducing transformer size and weight. A potential alternative in many cases is the replacement of conventional transformer oil with a nanofluid. Such retrofits can represent considerable cost savings. It has been demonstrated that the heat transfer properties of transformer oils can be significantly improved by using nanoparticle additives.

1.4.2 Mechanical Applications

1.4.2.1 Tribological applications

Nanofluids are also used to enhance tribological properties such as load-carrying capacity, anti wear, and friction reduction between moving mechanical components (Zhang et al. 1997). Such results are encouraging for improving heat transfer rates in automotive systems through the use of nanofluids. In lubrication application, surface

modified nanoparticles stably dispersed in base fluids are very effective in reducing wear and friction; enhancing the load-carrying capacity. The antifriction behavior of the nanoparticles on the wear surfaces can be attributed to third body and tribo-sinterization mechanisms (Battaz et al. 2010). Nanoparticles suspended in nanofluids can easily penetrate into the rubbing surfaces. During the frictional process, the thin physical tribofilm of the nanoparticles is formed between rubbing surfaces. The tribofilm can, not only bear the load but also separate the rubbing faces. The nanoparticles can roll between the rubbing faces during sliding friction and hence the originally pure sliding friction combines with the rolling friction. Therefore the friction co-efficient declines markedly and then remains constant (Peng et al. 2010).

1.4.2.2 Magnetic sealing

Magnetic fluids are nanofluids containing magnetic nanoparticles, whose properties can be tailored by varying their size and adapting their surface coating in order to meet the requirements of colloidal stability of nanofluids with non polar and polar carrier liquids (Vekas et al. 2007). Compared to the mechanical sealing, magnetic sealing offers a cost effective solution to environmental and hazardous gas sealing in a wide variety of industrial rotation equipment with high speed capability, low friction power losses, long life and high reliability (Rosensweig 1987). A ring magnet forms a part of a magnetic circuit in which an intense magnetic field is established in the gaps between the teeth on a magnetically permeable shaft and the surface of an opposing pole block. Magnetic fluid introduced into the gaps forms discrete liquid rings capable of supporting a pressure difference while maintaining zero leakage. The seals operate without wear as the shaft rotates because the mechanical moving parts do not touch. With these unique characteristics, sealing liquids with magnetic nanofluids can be applied in many areas like sealing for rotary blood pumps, oil sealing, rotating shafts, reciprocating seal, high vacuum seals (Ochonski 1989; Kim et al. 1999; Kim and Kim 2003; Li et al. 2005; Mitamura et al. 2008). Magnetic sealing is reversible and reversible sealing allows a

device to be dismountable so that the device can be cleaned when needed and also offers reusability and portability (Anwar et al. 2011).

1.4.3 Biomedical Applications

Nanofluids and nanoparticles have many applications in the biomedical industry. For example, to circumvent some side effects of traditional cancer treatment methods, iron based nanoparticles could be used as delivery vehicles for drugs or radiation without damaging nearby healthy tissue. Such particles could be guided in the bloodstream to a tumor using magnets external to the body. Nanofluids could also be used for safer surgery by producing effective cooling around the surgical region and thereby enhancing the patient's chance of survival and reducing the risk of organ damage. In a contrasting application to cooling, nanofluids could be used to produce a higher temperature around tumors to kill cancerous cells without affecting nearby healthy cells (Jordan et. al. 1999; Sharifi et al. 2012).

Nanofluids such as those of ZnO show antibacterial activity due to the photocatalytic properties of ZnO (Zhang et al. 2007; Zhang et al. 2008). The nanofluid showed higher efficiency of antibacterial activities with longer storage period. This is likely due to the production of more amounts of active oxygen species with time, which are toxic to bacterial cells because of their oxidizing action.

1.4.4 Other Applications

There are unending situations where an increase in heat transfer effectiveness can be beneficial to the quality, quantity, and/or cost of a product or process. In many of these situations, nanofluids are good candidates for accomplishing the enhancement in heat transfer performance. For example, nanofluids have potential application in building where increase in energy efficiency could be realized without increased pumping power. Such an application would save energy in heating, ventilating, and air conditioning system while providing environmental benefits (Wang and Mujumdar 2008b).

In the renewable energy industry, nanofluids could be employed to enhance heat transfer from solar collectors to storage tanks and to increase the energy density. Hence a novel approach is to introduce nanofluids in solar water heater instead of conventional heat transfer fluids (Saidur et al. 2011). Nanofluid coolants also have potential applications in major process industries, such as materials, chemical, food and drink, oil and gas, paper and printing, and textiles.

1.5 COPPER AND CUPROUS OXIDE NANOFLUIDS

Copper and cuprous oxide nanoparticles have received considerable attention in the past two decades due to their unusual properties and potential applications in nanomaterials, thermal conduction, lubrication, nanofluids and catalysis (Eastman et al. 2001; Kumar et al. 2009; Lee et al. 2009; Yu et al. 2010; Li et al.2011). Copper nanofluids prepared using two step method generally makes use of commercially available nano powders. Two step methods involving synthesis of copper nanofluids basically use water as base fluid while one step methods mostly use water and ethylene glycol as base fluid. Instances of using dielectric liquids and cashew nut shell liquid (CNSL) as base fluids are also present (Bonnemann et al. 2005; Lo et al. 2005a).

Copper and cuprous oxide nanofluids have been prepared using one step physical methods like direct condensation and evaporation technique, submerged arc nano synthesis and dual plasma process (Eastman et al. 2001; Lo et al. 2005a; Tavares and Coulombe 2011). Chemical methods like reductive stabilization, solution phase synthesis and microwave synthesis have also been applied for the synthesis of copper and cuprous oxide nanofluids (Zhu et al. 2004a; Bonnemann et al. 2005; Kumar et al. 2009; Wei et al. 2009).

Copper nanofluids have been used as coolants in small flat capillary pumped loops, as heat transfer agents in high temperature evacuated tubular solar collectors, in rotary blade coupling of four wheel drive vehicles and in open loop pulsating heat pipes (Tzeng et al. 2005; Lu et al. 2011a; Lu et al. 2011b; Riehl and Santos 2012).

1.6 LITERATURE REVIEW

The research topic of nanofluids has been receiving increased attention worldwide. Research and engineering practice in nanofluids are aimed at enhancing fluid macro scale and system scale properties through the manipulation of micro scale physics (structure, property and activity). The recent growth of work in this rapidly emerging area of nanofluids is most evident from the exponentially increasing number of publications.

The developments in research in the synthesis of nanofluids of metals, metal oxides and non metal oxides and its properties that took place in the recent past have been briefly reviewed here.

Search in the literature reveals that the synthesis of nanofluids mostly involves two step processes, with the preparation of nanoparticles as the first step and dispersion of the nanoparticles in the liquid medium as the second step. A few important papers on synthetic methods involving two steps are listed in Table 1.1. In these reports nanofluids were synthesized by dispersing nanoparticles in appropriate base fluids and their properties were studied.

Table 1.1 Review on two step synthetic methods

Particle Type	Base Fluid	Particle Size (nm)	Properties Studied	Author (Year)
Cu Cu	Water Transformer oil	100 100	Heat transfer enhancement	Xuan and Li (2000)
Ag Au Au	Water Water Toluene	60-70 10-20 3-4	Temperature effect on enhancement of thermal conductivity	Patel et al. (2003)
Au	Water	2-75	Structural character effect	Tsai et al. (2004)
Fe	Ethylene glycol	10	Thermal conductivity and sonication time effect	Hong et al. (2005)

Particle Type	Base Fluid	Particle Size (nm)	Properties Studied	Author (Year)
Fe	Ethylene glycol	10	Thermal conductivity and cluster size effect	Hong et al. (2006)
Au	Water	35	Thermal performance	Kang et al. (2006a)
Ag	Water	8-15	Thermal conductivity	Kang et al. (2006b)
Au Au	Ethanol Toluene	4 2	Thermal conductivity	Putnam et al. (2006)
Cu	Water	1-100	Dispersion and stability	Li et al. (2007)
Cu	Water	25	pH effect Surfactant effect	Li et al. (2008)
Ag	Water	20	Thermal performance	Lin et al. (2008)
Cu	Water	100	Heat transfer augmentation	Santra et al. (2008)
Au	Water	7-12	Stability	Kim et al. (2009)
Cu	Water	100	Heat transfer	Santra et al. (2009)
Ag Ag Ag	Kerosene n-Hexane Chloroform	5 5 5	Stability and thermal conductivity	Li et al. (2010)
Al-Cu	Water	200-300	Dispersion stability	Samal et al. (2010)
Ag	Diethylene glycol	40	Rheology and colloidal structure	Tamjid and Guenther (2010)
Au	Water	10-300	Thermal conductivity	Chen and Wen (2011)

Particle Type	Base Fluid	Particle Size (nm)	Properties Studied	Author (Year)
Ag	Water	<100	Heat Flux	Parametthanuwat et al. (2011)
Cu Cu	Water Water	60-100 120-200	Thermal conductivity	Saterlie et al. (2011)
Ag Ag Ag	Chloroform Dichloromethane Kerosene	8-12 8-12 8-12	Thermal stability and thermal oxidation stability	Li and Fang (2012)
Al ₂ O ₃ SiO ₂ TiO ₂	Water Water Water	13 12 27	Temperature effect on enhancement of thermal conductivity	Masuda et al. (1993)
Al ₂ O ₃ CuO Al ₂ O ₃ CuO	Water Water Ethylene glycol Ethylene glycol	38.4 23.6 38.4 23.6	Thermal conductivity	Lee et al. (1999)
Al ₂ O ₃ CuO Al ₂ O ₃ CuO Al ₂ O ₃ Al ₂ O ₃	Water Water Ethylene glycol Ethylene glycol Engine oil Pump oil	28 23 28 23 28 28	Thermal conductivity	Wang et al. (1999)
Al ₂ O ₃ Al ₂ O ₃ Al ₂ O ₃ Al ₂ O ₃ Al ₂ O ₃ Al ₂ O ₃ Al ₂ O ₃	Ethylene glycol Ethylene glycol Ethylene glycol Ethylene glycol Water Pump oil Glycerol	15 26 30.2 60.4 60.4 60.4 60.4	Solid crystalline Phase effect Morphology effect pH value effect Base fluid effect	Xie et al. (2002)
Al ₂ O ₃	Water	38	Pool boiling characteristics	Das et al. (2003a)
Al ₂ O ₃ CuO	Water Water	38.4 28.6	Temperature effect on enhancement of thermal conductivity	Das et al. (2003b)
CuO	n-Alkanes	10	Stability	Li and Chang (2004)

Particle Type	Base Fluid	Particle Size (nm)	Properties Studied	Author (Year)
Al ₂ O ₃	Water	42	Convective heat transfer	Wen et al. (2004)
Al ₂ O ₃ Al ₂ O ₃ Al ₂ O ₃	Water Water Water	11 47 150	Temperature effect on enhancement of thermal conductivity	Chon et al. (2005)
SiO ₂ SiO ₂	Water Water	10 20	Ion effect in pool boiling heat transfer	Milanova and Kumar (2005)
TiO ₂ TiO ₂	Water Water	15 10×40	Thermal conductivity	Murshed et al. (2005)
SiO ₂	Water	15-20	Thermal conductivity	Kang et al. (2006a)
CuO	Water	25	pH value effect	Lee et al. (2006)
Al ₂ O ₃ CuO	Water Water	36 29	Temperature effect on enhancement of thermal conductivity	Li et al. (2006)
CuO	Ethylene glycol	30-50	Thermal conductivity enhancement	Liu et al. (2006b)
TiO ₂	Water	34	Dispersant HNO ₃ and NaOH effect	Wen et al. (2006)
CuO	Water	20-80	Microchannel heat sink performance	Chein and Chuang (2007)
Al ₂ O ₃	Water	36	Single phase and two phase heat transfer	Lee and Mudawar (2007)
CuO	Ethylene glycol-water mixture	29	Viscosity	Namburu et al. (2007)
TiO ₂	Water	21	Heat transfer coefficient	Duangthongsuk and Wongwises (2008)
TiO ₂ Al ₂ O ₃	Water Water	15 80	Thermal conductivity	Murshed et al. (2008)

Particle Type	Base Fluid	Particle Size (nm)	Properties Studied	Author (Year)
Al ₂ O ₃	Water	170	Heat transfer coefficient and friction factor	Jung et al. (2009)
CuO	Polyalphaolefin	30-50	Friction reduction properties	Battez et al. (2010)
Al ₂ O ₃ Al ₂ O ₃	Water Ethylene glycol	20 20	Thermal conductivity	Beck et al. (2010)
Al ₂ O ₃ TiO ₂	Water Water	25 10	Heat transfer	Farajollahi et al. (2010)
TiO ₂ CuO	Water Water	21 30-50	Stability	Fedele et al. (2011)
CuO CuO	Water Water	23-37 8-14	Viscosity	Gallego et al. (2011)
CuO	Gear oil	40	Viscosity	Kole and Dey (2011)
Al ₂ O ₃ -Cu	Water	17	Stability, thermal conductivity and viscosity	Suresh et al. (2011)
CuO	Water	20-80	Thermal conductivity	Zhu et al. (2011)
CuO	Oleic acid	1-80	Thermal conductivity, phase change temperature and latent heat	Harikrishnan and Kalaiselvam (2012)
CuO CuO	Water Monoethylene glycol	25 25	Thermal conductivity	Khedkar et al. (2012)
CuO	Water	40-60	Thermal conductivity and viscosity	Priya et al. (2012)
ZnO	Insulated Oil	20	Electrical conductivity	Shen et al. (2012)
CrO ₂	Poly Vinyl Pyrrolidone	25-40	Magnetic properties	Singh et al. (2012)
Fe ₃ O ₄	Heat transfer oil	4-44	Thermal conductivity	Wang et al. (2012)

One step methods, both physical and chemical have been used to synthesize nanofluids of metals like copper, silver, gold, nickel, cobalt and iron. Nanofluids of oxides like those of titanium, copper, aluminium, iron, tin and zinc have also been prepared using single step synthesis. The reported methods are discussed below.

Eastman et al. (2001) studied the anomalously increased effective thermal conductivities of ethylene glycol based nanofluids containing copper nanoparticles. A one step procedure involving the direct condensation of metallic vapor into nanoparticles by contact with a flowing low vapor pressure liquid for producing nanofluids containing metallic particles was used to disperse nano crystalline copper particles into ethylene glycol with little agglomeration. The resultant nanofluid had much higher effective thermal conductivity than either pure ethylene glycol or ethylene glycol containing the same volume fraction of dispersed oxide nanoparticles. The effective thermal conductivity of ethylene glycol was shown to be increased by up to 40 % for a nanofluid consisting of ethylene glycol containing approximately 0.3 volume % copper nanoparticles of mean diameter, 10 nm.

Zhu et al. (2004a) presented a novel one-step method for preparing of copper nanofluids by reducing copper sulfate pentahydrate with sodium hypophosphite in ethylene glycol under microwave irradiation. Non agglomerated and stably suspended copper nanofluids were obtained. The influences of copper sulfate concentration, addition of sodium hypophosphite, and microwave irradiation on the reaction rate and the properties of copper nanofluids were investigated by transmission electron microscopy (TEM), infrared analysis, and sedimentation measurements. It was found to be a fast, efficient one step chemical method to prepare copper nanofluids.

Zhu et al. (2004b) introduced a rapid method for the preparation of copper metal nanoparticles by reducing copper sulfate pentahydrate with sodium hypophosphite in ethylene glycol under microwave irradiation. The influences of the reaction parameters, such as the concentrations of reducing agent and protective polymer, time of microwave

irradiation, on the size and agglomeration of copper nanoparticles were investigated by powder X-ray diffraction (XRD) and TEM. Well dispersed copper nanoparticles with diameter of about 10 nm were obtained.

Bonnemann et al. (2005) prepared copper colloid via reductive stabilization and silver nanofluid by thermal decomposition method. The suspension of the trioctylaluminum stabilized copper colloid was peptized using Korantin SH and CNSL. Fluids with particle sizes <10 nm were obtained with Korantin and 7 nm –15 nm in the case of CNSL. However, the copper colloid was air sensitive. A very straightforward one-step thermal decomposition of silver lactate led to air-stable silver nanofluids. Silver particle formation and air stability were monitored using ultra violet-visible (UV-Vis) spectroscopy. The presence of monodispersed spherical silver nanoparticles in mineral oil medium was confirmed. TEM showed a two-dimensional assembly of the silver particles with a size distribution of $9.5 \text{ nm} \pm 0.7 \text{ nm}$. Fourier transform infra-red (FTIR) analysis revealed information about the interaction between the surfactant and the silver surface.

Cho et al. (2005) prepared nanofluids containing suspended silver particles for enhancing thermal conductivity of fluids. A heat transfer fluid involving the suspension of nanoparticles in the colloidal phase was prepared from silver nitrate, ethylene glycol and poly(acryl-amide-co-acrylic acid). The size and distribution of silver particles were investigated with respect to the different amounts of dispersion stabilizer. In addition different concentrations of silver nanofluid were prepared to investigate the potential improvement in thermal conductivity. The silver particle size became smaller, and the degree of particle distribution became correspondingly narrower, upon increasing the amount of dispersion stabilizer. Typically the average particle size was about 10 nm when the poly(acryl-amide-co-acrylic acid)/silver nitrate ratio was greater than 1. Thermal conductivity improved by 10 %, 16 % and 18 % as the concentration of silver particles in the nanofluids increased to 1000 ppm, 5000 ppm and 10000 ppm, respectively.

Lo et al. (2005a) developed a submerged arc nanosynthesis system for preparing copper based nanofluids with different morphologies and using various dielectric liquids. Pure copper was selected as the electrode as well as the work piece material. Copper was heated and vaporized by arc sparking between two electrodes being immersed in dielectric liquids. The copper aerosol could be condensed to form nanoparticles immediately by the cooling media (dielectric liquids). The nanoparticles then disperse in the dielectric liquids which become metal nanofluids. Various morphological copper based nanoparticles could be synthesized using different dielectric liquids. The effects of experimental parameters and dielectric liquids on the characteristics of final products were investigated.

Lo et al. (2005b) prepared nickel nano magnetic fluid using the developed submerged arc nanoparticle synthesis system (SANSS). Using optimized process parameters, nickel nanoparticles having diameter of 10 nm were fabricated, and these nickel nanoparticles had strong magnetic features. When the surfactant polyvinylpyrrolidone (PVP) - K30 was added to the prepared nanofluid, molecules of the surfactant adhered to the surface of the nanoparticles, enabling the nanoparticles to remain in steady suspension and good dispersion. The nickel nanoparticles fabricated by SANSS had no residual magnetization or coercive force, thus showing super paramagnetism.

Liu et al. (2006a) presented the enhancement of the thermal conductivity of water in the presence of copper using the chemical reduction method. It was the first time that the chemical reduction method for the synthesis of nanofluids containing copper nanoparticles in water was reported. No surfactant was employed as the dispersant. Without the addition of dispersant and surfactant, the thermal conductivity of the produced nanofluids revealed a time-dependent characteristic. The results showed that copper-water nanofluids with low concentration of nanoparticles had noticeably higher thermal conductivities than the water base fluid without copper. For copper nanoparticles at a volume fraction of 0.001 (0.1 volume %), thermal conductivity was enhanced by up to 23.8 %.

Lo et al. (2007) fabricated and characterized silver nanofluid by the SANSS. The silver metal electrodes under the electrical discharge melted and evaporated rapidly and condensed to form the nanoparticles in the lower temperature dielectric liquid and produced the suspended nanoparticle. The results showed that the spherical nanosilver particles were formed in the ethylene glycol and the mean particle size was about 12.5 nm. The silver nanofluid more closely resembled Newtonian fluids.

Phuoc et al. (2007) synthesized silver-deionized water nanofluids using multi-beam laser ablation in liquids. In general, the ablated particles were almost all spherical. For fluence of 0.09 J cm^{-2} and single-beam approach, the mean particle size was about 29 nm. The majority of the particles, however, were in 19 nm - 35 nm range and there were some big ones as large as 50 nm - 60 nm in size. For double-beam approach, the particles were smaller with the average size of about 18 nm and the majority of the particles were in 9 nm - 21 nm range with few big ones as large as 40 nm. Preliminary measurements of the thermal conductivity and viscosity of the produced samples showed that the thermal conductivity increased about 3 % - 5 % and the viscosity increased 3.7 % above the base fluid viscosity even with the particle volume concentration as low as 0.01 %.

Singh and Raykar (2008) applied microwave synthesis to prepare stable silver nanofluids in ethanol by reduction of silver nitrate with PVP, used as stabilizing agent, having silver concentrations of 1 % by volume. The nanofluids were systematically investigated for refractive index, electrical and thermal conductivity, and viscosity for different polymer concentrations. The size of nanoparticles was found to be in the range of 30 nm - 60 nm for two different salt to PVP ratios. For higher concentration of polymer in nanofluid, nanoparticles were 30 nm in size showing increase in thermal conductivity but a decrease in viscosity and refractive index, which was due to the polymer structure around nanoparticles. Thermal conductivity measurements of nanofluids showed substantial increment in the thermal conductivity of nanofluid relative to the base fluid and nonlinear enhancement over the 10 °C – 50 °C temperature range.

Rheology of nanofluids was studied at room temperature showing effect of polymer on viscosity and confirming the Newtonian behavior of nanofluid.

Kim et al. (2009) studied characteristic stability of bare gold-water nanofluids fabricated by pulsed laser ablation in liquids. Gold nanoparticles suspended in water where the suspension was a kind of nanofluid, were produced by pulsed laser ablation in liquids. Under the laser irradiation conditions up to 18 h, the average size of the gold nanoparticles ranged from 7.1 nm to 12.1 nm while their size-distribution tended to become narrower with effects of laser-induced fragmentation. Interestingly, the nanofluid showed an outstanding colloidal stability even after 1 month although no dispersants were used. The thermal conductivity of the gold nanoparticles (0.018 volume %) /water suspension increased by $9.3 \% \pm 5.4 \%$ compared to that of pure water.

Kumar et al. (2009) presented a novel one step method for the preparation of stable, non agglomerated copper nanofluids by reducing copper sulphate pentahydrate with sodium hypophosphite as reducing agent in ethylene glycol as base fluid by means of conventional heating. It was an in situ, one step method which gave high yield of product with less time consumption. The characterization of the nanofluid was done by particle size analyzer, XRD topography, UV-Vis analysis and FTIR spectroscopy followed by the study of thermal conductivity of nanofluid by the transient hot wire method.

Li et al. (2009a) investigated on viscosity of copper-water nanofluids. A procedure for preparing a nanofluid consisting of solid nanoparticles with sizes typically of 1 nm -100 nm suspended in liquid was proposed. The viscosity of copper-water nanofluid was measured using capillary viscometers. The experimental results showed that the temperature and sodium dodecyl benzene sulfonate (SDBS) concentration were the major factors affecting the viscosity of the nano-copper suspensions, while the effect of the mass fraction of copper on the viscosity was not as obvious as that of the temperature and SDBS concentration. The apparent viscosity of the copper nano-

suspensions decreased with the increase in temperature and increased slightly with the increase of the mass fraction of SDBS dispersant, and almost kept invariability with increasing the mass fraction of copper.

Zheng et al. (2010) developed a technique to prepare solvent free gold nanofluids with facile self-assembly. Solvent free gold nanofluids were made in a two step process comprising the grafting of the thiol mercapto undecanoic acid (MUA) onto the gold-nanoparticle surface, followed by self-assembly with a poly ethylene glycol (PEG) - substituted tertiary amine. The surface functionization adds a number of novel properties to the gold nanoparticles, such as conductivity, fluidity, and improved processability. So the solvent free nanofluid was an intelligent nanomaterial due to its ability to flow at low temperatures making it attractive as proton transport, lubricants, battery-cell plasticizers and more.

Tavares and Coulombe (2011) used a dual plasma process for the single-step synthesis of a copper-ethylene glycol nanofluid. They addressed the issue of metallic nanofluid stabilization without the use of traditional surface stabilizing agents such as surfactants. The stability of the suspension was confirmed by UV-Vis absorption spectrometry and electron microscopy. The particles synthesized were also shown to be re-dispersible in aqueous media. Though no heat transfer enhancement was observed due to the low nanoparticle loading, the study demonstrated for the first time that high temperature stable nanofluids containing metal nanoparticles can be synthesized in a single step, without manipulation outside the controlled synthesis environment and without the post addition of surfactants.

Tsai et al. (2011) investigated the effect of suspended nanoparticles in base fluids on the thermal resistance of a disk shaped miniature heat pipe, using gold and carbon nanoparticles, in aqueous solution. Gold nanoparticles were synthesized by citrate reduction from aqueous hydrogen tetrachloroaurate and carbon nanoparticles were prepared by arc discharge between graphite electrodes in reduced pressure of pure

hydrogen gas. An experimental system was set up to measure the thermal resistance of the disk-shaped miniature heat pipe with both nanofluids and deionized water as the working medium. The measured results showed that the thermal resistance of disk shaped miniature heat pipe varies with the charge volume and the type of working medium.

Wang et al. (2011a) fabricated Gold/1-butyl-3-methylimidazolium hexafluoro phosphate nanofluids containing different stabilizing agents by a facile one step chemical reduction method, of which the nanofluids stabilized by CTAB exhibited ultrahigh thermodynamic stability. TEM, UV-Vis absorption, FTIR spectroscopy and X-ray photoelectron spectroscopy (XPS) characterizations were conducted to reveal the stable mechanism. The tribological properties of these ionic liquid based gold nanofluids were investigated. The nanofluids with high stability exhibited much better friction-reduction and anti-wear properties. The thermal conductivity of the stable nanofluids was also measured by a transient hot wire method as a function of temperature. The results indicated that the thermal conductivity of the nanofluid was temperature-dependent and could be attributed to micro-convection caused by the Brownian motion of gold nanoparticles.

Wang et al. (2011b) prepared stable ionic liquid-based nanofluids containing same volume fraction but different sizes or surface states of gold nanoparticles by a one-phase and/or two-phase method and their thermal conductivities were investigated. Five significant experiment parameters, i.e. temperature, dispersion condition, particle size, surface state, and viscosity of base liquid, were evaluated to supply experimental explanations for heat transport mechanisms. The conspicuously temperature dependent and greatly enhanced thermal conductivity under high temperatures and the close relationship between the thermal conductivity enhancements and the viscosity of base liquid indicated that Brownian motion occupies the leading position among various influencing factors like clustering and surface state in the heat transport processes of ionic liquid-based gold nanofluids.

Xiong et al. (2011) synthesized highly stable dispersions of nanosized copper particles using L-ascorbic acid. Particles with average size 2 nm were synthesized by straight forward, cost effective and green method. L-ascorbic acid was utilized both as reducing and capping agent precursor in aqueous medium. The particles were characterized by UV- Vis spectroscopy, TEM and FTIR spectroscopy. The mechanism of L-ascorbic acid on the reduction and stabilization of copper nanoparticles was also discussed.

Lee et al. (2012b) produced aqueous spherical gold nanoparticles using conventional ultrasonic bath. The effects of ultrasonic energy on the size and morphology of gold nanoparticles were investigated. Highly monodispersed spherical gold nanoparticles were successfully synthesized by sodium citrate reduction in a conventional ultrasonic bath, without an additional heater or magnetic stirrer, as evidenced by UV - Vis spectra and TEM. Ultrasonic energy was shown to be a key parameter for producing spherical gold nanoparticles of tunable sizes (20 nm to 50 nm). A proposed scheme for understanding the role of ultrasonic energy in the formation and growth of gold nanoparticles was discussed. The simple single step method demonstrated in their study offered new opportunities in the production of aqueous suspensions of monodispersed spherical gold nanoparticles with a stability of 2 months.

Akoh et al. (1978) prepared ultrafine particles of ferromagnetic metals (Fe, Co and Ni) by the vacuum evaporation onto a running oil substrate. Particles thus obtained were suspended in the oil and their average diameter was about 25 Å. An electron diffraction analysis indicated that the particles were oxidized and the main component was Fe₃O₄, CoO and NiO for Fe, Co and Ni fine particles, respectively. From magnetic measurements in the temperature range between -269 °C and 27 °C, the main magnetic behavior of the fine particles was explained in terms of the super paramagnetism or super antiferromagnetism..

Chang et al. (2004) proposed and developed low pressure control methods for a combined arc submerged nanoparticle synthesis system for TiO₂ nanoparticle fabrication and studied the photocatalytic decomposition of methylene blue on the nanoparticles. The photocatalytic reaction was carried out in a photochemical reactor. Experimental results showed that the rate constant of photocatalytic reaction of TiO₂ nanoparticles for methylene blue is 0.0365 min⁻¹. Experimental results indicate that the TiO₂ nanoparticle fluid possesses excellent photocatalytic activity in photodegradation of methylene blue.

Lo et al. (2005c) optimized the parameters for preparing nanofluid using SANSS using a copper electrode. A suspended copper oxide nanofluid was produced at the current of 8.5 A - 10 A, voltage of 220 V, pulse duration of 12 μs, and dielectric liquid temperature of 2 °C. The CuO nanoparticles were characterized by TEM, FESEM, XRD, selected area electron diffraction (SAED) pattern and electron spectroscopy for chemical analysis (ESCA). The equality volume spherical diameter of the obtained copper oxide particle was 49.1 nm with regular shape and narrow size distribution.

Chang et al. (2007) studied a process optimization using the ultrasonic aided SANSS for preparing TiO₂ nanoparticle suspension, which was an innovative nanoparticle preparation method. They employed some major parameters together with robust design to investigate the optimized parameters, such as peak current, pulse duration, open voltage and amplitude of ultrasonic vibration, for producing TiO₂ nanoparticle suspension. The produced TiO₂ nanoparticle suspension would absorb UV when the wavelength was 300 nm - 380 nm.

Chang and Liu (2007) analyzed the process parameters of an innovative method for preparing anatase type TiO₂ nanofluids. In the arc spray nanofluid synthesis system (ASNSS), a titanium rod, deployed as an electrode in electrical discharge machining, was melted by the submerged arc and vaporized in deionized liquid under a controlled vacuum environment. The vaporized titanium particles were then rapidly quenched by the designed cooling system, thus forming nanocrystalline powders. With a set of designed

process parameters, the developed ASNSS generated the TiO₂ nanofluid with an average particle diameter less than 20 nm and with an improved size distribution and high roundness.

Kao et al. (2007) examined the characteristics of copper-oxide brake nanofluid (CBN) manufactured using the arc-submerged nanoparticle synthesis system. Brake fluids containing copper nanoparticles were developed by melting bulk metal used as the electrode which was submerged in dielectric liquid. Copper was vaporized in brake fluid DOT3, which was used as an insulating liquid, and then rapidly quenched thus nucleating and forming nanocrystalline copper powders. The CBN thus obtained showed higher boiling temperature, higher viscosity and higher conductivity, which were affected by the synthesis parameters such as cooling liquid temperature and processing current.

Chang and Chang (2008) synthesized Al₂O₃ nanofluid with high suspension stability using a modified plasma arc system. The system used high temperature produced by plasma arc system to cause the bulk metal to heat and vaporize. The vaporized metallic gas was inducted into the collection piping by the induction system. At the same time, it mixed thoroughly with the pre-condensed deionized water, and the mixture then underwent a rapid cooling process which helped in grain nucleation and prevented the growth of particle.

Chin et al. (2008) synthesized size selective super paramagnetic nanoparticles in thin fluids under continuous flow conditions. The synthesis was carried out by passing ammonia gas over a thin aqueous film of Fe^{2+/3+} which was introduced through a jet feed close to the centre of a rapidly rotating disc (500 rpm to 2500 rpm). The particle size was controlled with a narrow size distribution over the range of 5 nm to 10 nm. The material was found to have very high saturation magnetizations, in the range of 68 emu g⁻¹ - 78 emu g⁻¹.

Habibzadeh et al. (2009) studied stability and thermal conductivity of nanofluids of tin dioxide synthesized via microwave-induced combustion route. SnO₂ nanofluids

were prepared by dispersing tin dioxide nanoparticles in deionized water as a base fluid. 4 nm – 5 nm tin dioxide crystals were synthesized via chloride solution combustion synthesis (CSCS) using SnCl_4 and sorbitol as a novel precursor and the fuel, respectively. The effects of pH and temperature on the thermal conductivity and on the stability of the nanofluid were investigated. At 80 °C, for the nanofluid prepared by SnO_2 nanoparticles at a weight fraction of 0.024 %, thermal conductivity was enhanced up to about 8.7 %, with an optimal pH= 8.

Nan et al. (2009) developed a novel and facile method for the preparation of stable nanofluid in which ferric chloride hexahydrate and urea were used as reactants without any surfactants. The obtained solid sample was proved to be $\beta\text{-FeOOH}$ by XRD technology and spindle-shaped by TEM technology. The heat capacities of the obtained $\beta\text{-FeOOH}$ particles and the nanofluid were determined by an adiabatic calorimeter. The thermodynamic properties of the obtained $\beta\text{-FeOOH}$ particles and the nanofluid were calculated based on the obtained functions of heat capacity with respect to thermodynamic temperature and the relationships between the thermodynamic properties.

Yu et al. (2009) applied phase-transfer method for preparing stable kerosene based Fe_3O_4 nanofluids. Oleic acid was successfully grafted onto the surface of Fe_3O_4 nanoparticles by chemisorbed mode, which let Fe_3O_4 nanoparticles have good compatibility with kerosene. Pure cubic-phase Fe_3O_4 nanoparticles with an average diameter of 15 nm were obtained. In the temperature range from 10 °C to 60 °C, the thermal conductivities of the nanofluids tracked the thermal conductivities of the base liquid and the enhanced ratios were almost constant for the same loading. The enhancement of the thermal conductivity increased linearly with the volume fraction of Fe_3O_4 nanoparticles and the value was up to 34.0 % for 1.0 volume % nanofluid.

Chen (2010) investigated the effects of process parameters on geometrical features of titanium dioxide nanoparticles synthesized by the SANSS. The experimental results revealed that the electric current for preparing the nanoparticle suspension had

significant impact on the size, distribution and surface sphericity of the nanoparticles synthesized, while other process parameters including pulse duration and temperature of deionized water also had moderate influence on the geometrical properties. With the set of parameters selected through process analysis, TiO₂ nanoparticles having an average particle diameter of 65 nm with a size disparity of 60 nm and particle sphericity of 3.8 % could be synthesized.

Wei et al. (2010) prepared a water-based hematite (α -Fe₂O₃) nanofluid through a simple biomolecule assisted hydrothermal process using a friendly environmental method. The molar heat capacities of the obtained nanofluids, base fluids, and hematite nanoparticles were measured by a high-precision automatic adiabatic calorimeter over the temperature range of 17 °C to 62 °C, respectively. On the basis of the as obtained molar heat capacities, the excess heat capacities of the nanofluids were calculated. These excess heat capacities revealed that the stable hematite nanofluids exhibited unique properties compared with the unstable one.

Nan and Tan (2011) synthesized *n*-butanol-based nanofluid containing nanowire-shaped β -FeOOH by a solvothermal method. The nanofluid was stable for 7 days without any precipitation with 3.0 mM SDBS as stabilizer. Uniform β -FeOOH nanowires with high aspect ratios were fabricated. The heat capacities of the obtained β -FeOOH sample, the base fluid, and the nanofluid were determined by an adiabatic calorimeter. These results were found to be very useful in application for the as produced nanowire-shaped β -FeOOH and the nanofluid in engineering fields.

Zhao and Nan (2011) prepared stable magnetic nanofluids containing Fe₃O₄ nanoparticles coated with polypyrrole (PPy) by using a facile and novel method, through one-pot route. Ferric chloride hexahydrate was applied as the iron source, and the oxidizing agent to produce PPy. Trisodium citrate was used as the reducing reagent to form Fe₃O₄ nanoparticles. The as prepared nanofluid had long-term stability. The Fe₃O₄ nanoparticles in presence of PPy were well dispersed even after 1 month and no

sedimentation was found. The particle sizes of the as-prepared Fe₃O₄ coated PPy were easily controlled from 7 nm to 30 nm by the polymerization reaction of the pyrrole monomers. The steric stabilization and weight of the nanoparticle was found to affect the stability of the nanofluids. The prepared Fe₃O₄ nanoparticles exhibited super paramagnetic behavior.

Kwasny et al. (2012) synthesized two stable nanofluids comprising of mixed valent copper(I,II) oxide clusters (<1 nm) suspended in 1-butyl-3-methylimidazolium acetate, [C₄mim][OAc], and copper(II) oxide nanoparticles (<50 nm) suspended in trioctyl(dodecyl)phosphonium acetate, using a facile one-pot reaction from solutions of copper(II) acetate hydrate in the corresponding ionic liquids. Formation of the nanostructures was studied using ¹³C NMR spectroscopy and differential scanning calorimetry (DSC). From a solution of cupric acetate in 1-ethyl-3-methylimidazolium acetate, [C₂mim][OAc], crystals were obtained that revealed the structure of [C₂mim][Cu₃(OAc)₅(OH)₂(H₂O)]·H₂O, indicating the formation of copper hydroxo-clusters in the course of the reaction. Synthesized nanostructures were studied using TEM and XPS. Physical properties of the prepared ionic liquid nanofluids were examined using infra red and UV-Vis spectroscopy, thermo gravimetric analysis (TGA), DSC and densitometry.

Lee et al. (2012a) prepared ethylene glycol based nanofluid containing ZnO nanoparticles by a one step physical method known as pulsed wire evaporation. The structural properties of the ZnO nanoparticles were studied by XRD method and high-resolution TEM. The thermal conductivity of the ethylene glycol based ZnO nanofluid at a higher concentration exhibited temperature dependency due to the clustering and aggregation of nanoparticles in the fluid. The experimentally measured value of the thermal conductivity was found to be higher than the theoretically calculated value based on the Hamilton–Crosser model. Rheological measurements showed that the nanofluids showed Newtonian behavior. The viscosity increment did not show temperature dependency, and its value increased with the ZnO volume fraction at a fixed temperature.

1.7 SCOPE

Cooling has become one of the top technical challenges faced by hi-tech industries such as microelectronics, transportation, manufacturing and metrology (Kumar et al. 2009). Low thermal conductivity of conventional heat transfer fluids such as water, oil and ethylene glycol is a primary limitation in enhancing the performance and the compactness of many engineering electronic devices. To overcome this drawback, there is a strong motivation to develop advanced heat transfer fluids with substantially higher conductivities to enhance thermal characteristics.

The effort in this direction led to the addition of solid additives to the coolant liquids. But the disadvantages with this method are settling of particles, abrasion, clogging flow channels, eroding pipelines and increase in pressure drop in practical application.

Nanofluids are engineered by suspending nanoparticles with average sizes below 100 nm in traditional heat transfer fluids such as water, oil, and ethylene glycol. A very small amount of guest nanoparticles, when dispersed uniformly and suspended stably in host fluids, can provide dramatic improvements in the thermal properties of host fluids.

Making nanofluids using the two step processes has remained a challenge. It is a step by step method that isolates the preparation of the nanofluid from the preparation of nanoparticles. As a result, agglomeration of nanoparticles may take place in both steps, especially in the process of drying, storage, and transportation of nanoparticles. The agglomeration will not only result in the settlement and clogging of micro channels but also results in the partial dispersion of the nanoparticles, resulting in poor thermal conductivity. So it is necessary to develop one step methods that combine the preparation of nanoparticles with the preparation of nanofluids, so that the limitations of the two step processes are avoided.

Most of the single step methods reported are physical methods involving direct condensation of vaporized copper into nanoparticles by contact with a flowing low vapor pressure liquid, submerged arc nanoparticle synthesis, arc spray nanoparticle synthesis, dual plasma synthesis, pulsed wire evaporation and laser ablation in liquids. The methods have inherent limitations such as only low vapor pressure fluids are compatible with the process, method appears to be cost ineffective, requires expensive experimental setup for the synthesis.

The chemical method involves simultaneous insitu solution phase synthesis of nanoparticles and their dispersion in the base fluid. This method overcomes most of the limitation of the two step methods. One step methods can also reduce production costs. Only a few one step chemical methods have been reported in the literature for the synthesis of copper and cuprous oxide nanofluids. Further, copper being a highly thermal conductive material, copper and cuprous oxide nanofluids are also expected to exhibit appreciable heat transfer capabilities.

In view of the aforesaid facts, an attempt to synthesize copper and cuprous oxide nanofluids by single step chemical method has been made. A study on the thermal conductivities of the nanofluids has been done. The viscosity of the synthesized nanofluids has been studied as viscosity is also as critical as the thermal conductivity in determining the suitability of the liquid as a coolant.

1.8 OBJECTIVES

The objectives of the reported work are as follows:

1. Synthesis of copper and cuprous oxide nanofluids by one step chemical methods.
2. Characterization of the synthesized nanofluids by XRD, EDXA, SAED, TEM, FESEM, FTIR spectroscopy and UV-Vis spectroscopy.
3. Study of the effect of the reaction conditions on the size of the nanoparticles prepared.
4. Study of the stability and thermal conductivity of the prepared nanofluids.
5. Investigation on the effect of particle concentration on the thermal conductivity.

6. Determination of the viscosity of the synthesized nanofluids.
7. Investigation on the effect of particle concentration and temperature on the viscosity.

The contents presented in this thesis have been broadly divided into four chapters with several sections in each chapter. The first chapter titled **Introduction and a Review of the Literature** gives a general introduction to nanotechnology and nanofluids, synthetic methods and various applications of nanofluids. It provides an overview of the literature on synthesis and properties of nanofluids. Scope and objectives of the work has also been included in this chapter.

Chapter 2 titled **Experimental** deals with the materials and methods employed in the present work. The theories underlying the characterization techniques, wherever necessary have been briefly described.

Chapter 3 titled **Results and Discussion** deals with the description of obtained results and their interpretations.

Chapter 4 titled **Summary and Conclusions** outlines the summary of the work presented in the thesis along with important conclusions drawn. Scope for further research has also been included in this chapter.

References used have been listed at the end.



CHAPTER 2

EXPERIMENTAL

Chapter 2 describes the materials and methods employed in this work. It covers the details of experimental work carried out as well as the characterization of the synthesized nanofluids.

2.1 MATERIALS

A brief note on the materials used for the synthesis of copper and cuprous oxide nanofluids has been given below.

2.1.1 Copper Salts

Copper (II) salts are used as reagents for synthesis of various inorganic and organic compounds. Nitrates, sulfates and acetates of copper (II) salts have been used as precursors in the present work.

Copper (II) nitrate is a chemical compound with the formula $\text{Cu}(\text{NO}_3)_2$ that forms blue crystalline solid. Commonly referred to simply as copper nitrate, the anhydrous form is deep blue green crystals with orthorhombic structure. It occurs as five different hydrates: monohydrate, sesquihydrate, hemipentahydrate, trihydrate and hexahydrate; the last two being the most common ones. The hydrates have a rhombohedral crystal structure. The crystals are hygroscopic and sublime in vacuum at $150\text{ }^\circ\text{C} - 200\text{ }^\circ\text{C}$. The trihydrate ($\text{Cu}(\text{NO}_3)_2 \cdot 3\text{H}_2\text{O}$), has a molar mass of 241.60 g mol^{-1} and a density of 2.32 g cm^{-3} . It decomposes at $170\text{ }^\circ\text{C}$ and has a melting point of $114.5\text{ }^\circ\text{C}$. They are very soluble in ethanol, water and ammonia and have a solubility of 137.8 g/100 mL and 1270 g/100 mL at $0\text{ }^\circ\text{C}$ and $100\text{ }^\circ\text{C}$, respectively, in water.

Copper (II) sulfate also known as cupric sulfate is a chemical compound with the chemical formula CuSO_4 . This salt exists as a series of compounds that differ in their degree of hydration. The anhydrous form is a pale green or gray white powder, whereas the pentahydrate ($\text{CuSO}_4 \cdot 5\text{H}_2\text{O}$), the most commonly encountered salt, is bright blue. It is also known as blue vitriol or bluestone and has a triclinic structure. The pentahydrate

has a molar mass of $249.70 \text{ g mol}^{-1}$ and a density of 2.284 g cm^{-3} . It decomposes before melting at $150 \text{ }^\circ\text{C}$, losing two water molecules at $63 \text{ }^\circ\text{C}$, followed by two more at $109 \text{ }^\circ\text{C}$ and the final water molecule at $200 \text{ }^\circ\text{C}$. At $650 \text{ }^\circ\text{C}$, copper (II) sulfate decomposes into copper (II) oxide (CuO) and sulfur trioxide. Copper sulfate exothermically dissolves in water to give the aquo complex $[\text{Cu}(\text{H}_2\text{O})_6]^{2+}$, which has an octahedral molecular geometry and is paramagnetic. The pentahydrate crystals have a solubility of 316 g L^{-1} and 2033 g L^{-1} at $0 \text{ }^\circ\text{C}$ and $100 \text{ }^\circ\text{C}$, respectively, in water.

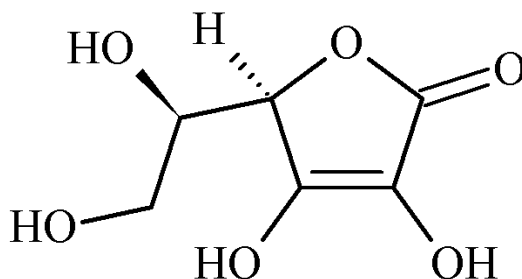
Copper (II) acetate, also referred to as cupric acetate, is the chemical compound with the formula $\text{Cu}(\text{OAc})_2$ where the OAc^- is acetate (CH_3CO_2^-). Anhydrous cupric acetate is a dark green crystalline solid, whereas the hydrated derivative, which contains one molecule of water for each Cu atom, is more bluish green. Copper acetate monohydrate has a molecular formula $\text{Cu}(\text{OAc})_2 \cdot \text{H}_2\text{O}$ and adopts a paddle-wheel structure. The monoclinic crystals have a molar mass of $199.65 \text{ g mol}^{-1}$ and a density of 1.882 g cm^{-3} . Copper (II) acetate has a boiling point of $240 \text{ }^\circ\text{C}$ and it melts at $115 \text{ }^\circ\text{C}$. It has a solubility of $7.2 \text{ g}/100 \text{ mL}$ in cold water and $20 \text{ g}/100 \text{ mL}$ in hot water.

2.1.2 Reducing Agents

A reducing agent, also called a reductant or reducer, is the element or compound in a reduction-oxidation reaction that donates an electron to another species. However, since the reducer loses an electron, it is said to be oxidized. In organic chemistry, reduction more specifically refers to the addition of hydrogen to a molecule, though the aforementioned definition still applies. The size and size distribution of nanofluids vary significantly with the types of reducing agents used in the synthesis. Two different reducing agents, ascorbic acid and glucose, have been employed in the present work.

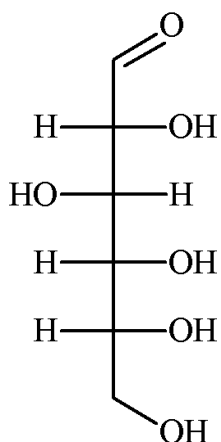
Ascorbic acid is a naturally occurring organic compound with antioxidant properties. It is a white solid, but impure samples can appear yellowish. The molecular formula of the compound is $\text{C}_6\text{H}_8\text{O}_6$ and it has a molar mass of $176.12 \text{ g mol}^{-1}$ and a density of 1.65 g cm^{-3} . It is one form (vitamer) of vitamin C. Ascorbic acid resembles the

sugar from which it is derived, with a ring containing many oxygen functional groups. The molecule exists in equilibrium with two ketone tautomers, which are less stable than the enol form. These forms rapidly interconvert in solutions of ascorbic acid. It has a solubility of 33 g/100 mL in water, yielding mildly acidic solutions. Most importantly, ascorbic acid is a mild reducing agent. It degrades upon exposure to oxygen, converting oxygen to water especially in the presence of metal ions and light. It can be oxidized by one electron to a radical state or doubly oxidized to the stable form called dehydroascorbic acid. The structure of ascorbic acid is given below:

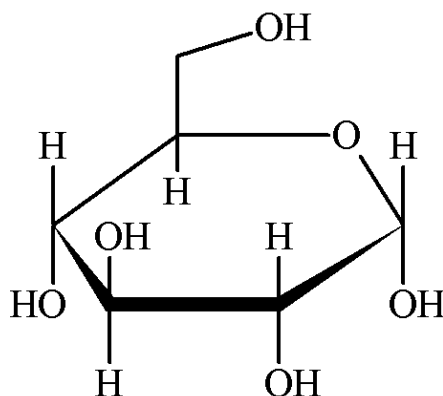


Structure 2.1 Ascorbic acid

Glucose is a simple monosaccharide found in plants. It is also known as D-glucose, dextrose or grape sugar. It is a simple sugar with formula $C_6H_{12}O_6$ or $H-(C=O)-(CHOH)_5-H$, whose five hydroxyl (OH) groups are arranged in a specific way along its six carbon backbone. It is a white powder with molar mass of $180.16 \text{ g mol}^{-1}$ and density of 1.54 g cm^{-3} . It is easily soluble in water and has a solubility of 91 g/100 mL. The open chain form of glucose (Structure 2.2) is thermodynamically unstable and it spontaneously tautomerizes to cyclic forms. In solutions at room temperature, the four cyclic isomers namely α -D-glucopyranose, β -D-glucopyranose, α -D-glucofuranose and β -D-glucofuranose, interconvert over a timescale of hours in a process called mutarotation and the mixture converges to a stable ratio of $\alpha:\beta$ 36:64. Glucose is an aldose with an aldehyde group in its open chain form. Due to the presence of free hemiacetal group it is classified under reducing sugars. The structure of α -D-glucopyranose is as shown in structure 2.3.



Structure 2.2 D-Glucose: Open chain form



Structure 2.3 α -D-glucopyranose

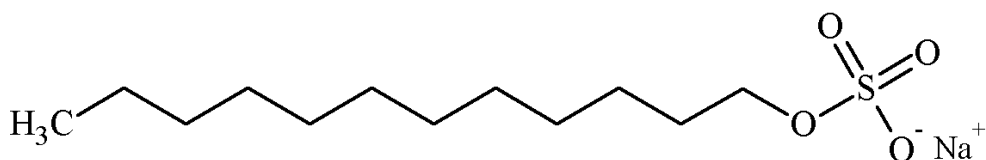
2.1.3 Stabilizing Agents

The long term stability of nanofluids is a key issue for both scientific and practical application. For the fabrication of nanoparticles, small size is not the only requirement. The processing conditions need to be controlled in such a way that the resulting particles have uniform size distribution, crystallinity, chemical composition and microstructure. It should overcome the huge surface energy, a result of enormous surface area or large surface to volume ratio. For this purpose surfactants or polymer stabilizers can be used.

Surfactants are compounds that lower the surface tension of a liquid, the interfacial tension between two liquids or that between a liquid and a solid. When the concentration of the surfactants exceeds a critical level, they self assemble in such a way, as to form micelles. During synthesis of nanoparticles using micellar route, the reactions proceed among the reactants that are available only inside the micelle and the particle stops growing when the reactants are consumed. Most commonly used surfactants are classified according to polar head group. A non-ionic surfactant has no charge groups in its head. The head of an ionic surfactant carries a net charge. If the charge is negative, the surfactant is more specifically called anionic and if the charge is positive, it is called

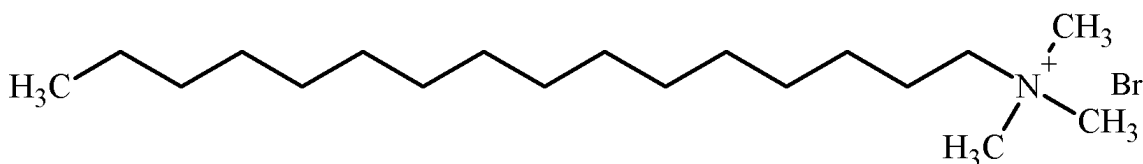
cationic. One of each kind of ionic surfactant has been used in the synthesis to provide nanofluid the required stability.

Sodium lauryl sulfate (SLS) also called as sodium dodecyl sulfate (SDS or NaDS) is an anionic surfactant with the formula $C_{12}H_{25}SO_4Na$. The salt consists of an anionic organosulfate consisting of a 12 carbon tail attached to a sulphate group, giving the material the amphiphilic properties required of a detergent. The solids are white or cream colored with molar mass of $288.372 \text{ g mol}^{-1}$ and a density of 1.01 g cm^{-3} . It has a melting point of $206 \text{ }^\circ\text{C}$. The critical micelle concentration (CMC) in pure water at $25 \text{ }^\circ\text{C}$ is 0.0082 M and the aggregation number at this concentration is usually considered to be about 62. The micelle ionization fraction (α) is around 0.3 (or 30 %). The structure of SLS is given below:



Structure 2.4 Sodium lauryl sulfate

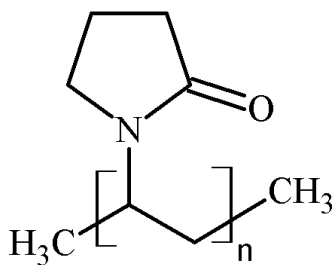
Cetyl trimethyl ammonium bromide (CTAB) also called as cetrimonium bromide or hexadecyltrimethylammonium bromide is a cationic surfactant with formula $C_{19}H_{42}BrN$. The white powder has a molar mass of $364.45 \text{ g mol}^{-1}$. It decomposes during melting around $237 \text{ }^\circ\text{C}$ - $243 \text{ }^\circ\text{C}$. At $30 \text{ }^\circ\text{C}$ it forms micelles in aqueous solutions with aggregation number 75 - 120 (average ~ 95) and degree of ionization α (fractional charge) 0.2 - 0.1 (from low to high concentration)



Structure 2.5 Cetyl trimethyl ammonium bromide

Polymer stabilizers are widely used in synthesis of nanoparticles. They are introduced primarily to form a monolayer on the surface of nanoparticles so as to prevent their agglomeration. Their presence during the formation of nanoparticles can have various influences on the growth process of nanoparticles. Interaction between the surface of a solid particle and polymer stabilizer may vary significantly depending on the surface chemistry of the solid, the polymer, solvent and temperature. A strong adsorption of polymer stabilizers would occupy the growth sites and thus reduce the growth rate of nanoparticles. A full coverage of polymer stabilizer would also hinder the diffusion of growth species from surrounding solution to the surface of growing particle. PVP is a well known polymer stabilizer and has been used in the current work.

PVP also called polyvidone or povidone, is a water soluble polymer made from the monomer *N*-vinylpyrrolidone. When dry it is a light flaky white to light yellow powder, which readily absorbs up to 40% of its weight of atmospheric water. It has a molar mass of $2,500 \text{ g mol}^{-1} - 2,50,00,000 \text{ g mol}^{-1}$ and a density of 1.2 g cm^{-3} . Its glass transition temperature is around $150 \text{ }^\circ\text{C} - 180 \text{ }^\circ\text{C}$. In solution it has excellent wetting properties and readily forms films.



Structure 2.6 Poly vinyl pyrrolidone

2.2 SYNTHESIS OF NANOFLUIDS

All the chemicals used in the investigation were of analytical grade and were used without any further purification. Standard solutions of copper nitrate trihydrate (0.1 M), copper sulfate pentahydrate (0.1 M), copper acetate monohydrate (0.25 M), SLS (0.1 M),

CTAB (0.1 M), PVP (0.1 M) and ascorbic acid (2 M) were prepared by dissolving required amount in water or ethylene glycol as required. The solutions were diluted as per the requirement. Deionized water was used for preparing aqueous solutions. Onida Power convection 20, microwave oven equipped with 800 watt microwave power was used for carrying out microwave assisted reactions.

2.2.1 Synthesis of Copper Nanofluids

Copper nanofluids were prepared from copper nitrate trihydrate, copper sulfate pentahydrate and copper acetate monohydrate using ascorbic acid in the presence of SLS, CTAB and PVP. Copper nanofluids were also synthesized using glucose as reducing agent from copper nitrate tri hydrate and copper sulfate pentahydrate in the presence of SLS as stabilizing agent.

2.2.1.1 Synthesis of copper nanofluids in the presence of SLS

➤ Synthesis of nanofluids using copper nitrate and ascorbic acid

30 mL of 0.1 M aqueous solution of copper nitrate trihydrate was stirred for 15 minutes with 50 mL solution of 0.01 M SLS in water. 30 mL 0.5 M solution of ascorbic acid in ethylene glycol was added and stirred at 65 °C. When the color changed from blue to golden brown the solution was cooled to obtain copper nanofluid. Similar reactions were carried out at varying concentration of ascorbic acid, SLS and dilution.

Microwave assisted reactions were also carried out at 50 % power for 4 minutes. The reactions were also carried out by varying the concentration of reducing agent, irradiation duration and power.

➤ Synthesis of nanofluids using copper nitrate and glucose

30 mL 0.1 M aqueous solution of copper nitrate trihydrate was made alkaline by adding ammonium hydroxide till the color became deep blue. Later the solution was

stirred with 30 mL of 0.01 M solution of SLS in ethylene glycol. After 15 minutes 3 g of glucose was added and stirred at 75 °C till the color changed to golden yellow. At this point sulphuric acid was added. When the color became brown the solution was cooled to get copper nanofluid. The synthesis was repeated by varying the concentration of reducing agent, SLS and dilution.

The reduction was also carried out under microwave irradiation. The solution was subjected to microwave irradiation for 5 minutes at 50 % power. The synthesis was also repeated at different reactant ratio, power and irradiation duration.

➤ *Synthesis of nanofluids using copper sulphate and ascorbic acid*

In a typical experiment, 15 mL of aqueous solution of 0.1 M copper sulfate pentahydrate was mixed with 50 mL of aqueous solution of 0.01 M SLS and stirred for 15 minutes. Then, 30 mL of 0.5 M ascorbic acid solution in ethylene glycol was added. Further the stirring was continued at 60 °C. The color change during the process was from blue to golden brown. After being cooled to room temperature naturally, copper nano fluid was obtained. The synthesis was also carried out by varying concentration of ascorbic acid, SLS and dilutions.

In order to investigate the effect of microwave radiation the same reaction was subjected to microwave irradiation at 50 % power for 3 minutes. Experiments were also carried by varying the ratio of the reactants, microwave power and irradiation duration.

➤ *Synthesis of nanofluids using copper sulphate and glucose*

In a typical procedure, 20 mL of 0.1 M aqueous solution of copper sulphate pentahydrate was made sufficiently alkaline by adding ammonium hydroxide. 20 mL of aqueous solution of 0.01 M SLS was added and stirred for 15 minutes. Then 3 g of glucose was added and stirred at 70 °C. During heating the color changed from blue to greenish to golden yellow. At this point the pH was brought down to 3 by the addition of

sulphuric acid. The heating was continued till the color changed to reddish brown color. On cooling, copper nanofluid was obtained. The synthesis was also carried out at varying amounts of glucose, SLS and various dilutions.

Similar types of reactions were carried out by subjecting the mixtures to microwave radiation. The solution was irradiated for 5 minutes with 50 % power. Synthesis was also repeated at varying ratio of reactants, irradiation duration and power of microwave.

➤ *Synthesis of nanofluids using copper acetate and ascorbic acid*

15 mL aqueous solution of 0.25 M copper acetate monohydrate was vigorously stirred with 50 mL 0.01 M aqueous solution of SLS. Then 30 mL solution of 0.5 M ascorbic acid in ethylene glycol was added. The reaction mixture was stirred at 80 °C till the color changed from blue to golden brown. The solution was cooled to get copper nanofluid. The synthesis was also repeated by varying the ratio of reactants, SLS and dilution.

The same procedure was used in microwave reactions. The reaction mixture was subjected to microwave irradiation for 3 minutes at 50 % power. Reactions were also carried out by varying the concentration of reducing agent, irradiation duration and power.

2.2.1.2 Synthesis of copper nanofluids in the presence of CTAB

➤ *Synthesis of nanofluids using copper nitrate and ascorbic acid*

10 mL of 0.01 M aqueous solution of CTAB was added to 20 mL of 0.1 M aqueous solution of copper nitrate trihydrate and stirred for 15 minutes. Then 30 mL of 0.5 M solution of ascorbic acid in ethylene glycol was added and stirred at room temperature. When the green colored solution obtained a yellowish tinge two drops of dilute sulfuric acid was added and the mixture was stirred further at 60 °C. When the

color completely changed to reddish brown the solution was cooled to obtain the nanofluid. Similar reactions were carried out at various dilutions and varying reactant ratios and varying amount of CTAB.

Microwave assisted reactions were carried out at 50 % power for 3 minutes. The reactions were also carried out at varying concentration of reducing agent, irradiation duration and power.

➤ ***Synthesis of nanofluids using copper sulfate and ascorbic acid***

20 mL of 0.1 M aqueous solution of copper sulphate pentahydrate was vigorously stirred with 10 mL of 0.01 M CTAB solution in water. After 15 minutes of stirring 30 mL of 0.5 M solution of ascorbic acid in ethylene glycol was added and stirring was continued at room temperature. Immediately the color changed to bluish green and then to green. At this point two drops of dilute sulfuric acid was added and the mixture was heated at 70 °C with stirring. When the color changed to reddish orange the solution is allowed to cool to room temperature to obtain copper nanofluid. The synthesis was also carried out by varying the concentration of ascorbic acid, CTAB and at various dilutions.

In order to investigate the effect of microwave radiation the reaction was also subjected to microwave irradiation at 50 % power for 4 minutes. Experiments were also carried out by varying the ratio of the reactants, microwave power and irradiation duration.

➤ ***Synthesis of nanofluids using copper acetate and ascorbic acid***

20 mL aqueous solution of 0.25 M copper acetate monohydrate was stirred vigorously with 10 mL 0.01 M aqueous solution of CTAB. Then 30 mL solution of 0.5 M ascorbic acid in ethylene glycol was added to the mixture and stirring was continued at room temperature. Later when there was a color change to greenish yellow two drops of sulfuric acid was added and the reaction mixture was stirred at 70 °C till the color

changed to golden orange. When the solution was cooled to room temperature naturally, copper nanofluid was obtained. The synthesis was also repeated by varying the ratio of reactants, concentration of CTAB and dilution.

A similar procedure was used in microwave reaction. The reaction mixture was subjected to microwave irradiation for 4 minutes at 50 % power. Reactions were also carried out by varying the concentration of reducing agent, irradiation duration and power.

2.2.1.3 Synthesis of copper nanofluids in the presence of PVP

➤ Synthesis of nanofluids using copper nitrate and ascorbic acid

In the preparation of copper nano fluids, 5mL of 0.01 M solution of PVP in ethylene glycol was added to 30 mL of 0.1 M aqueous solution of copper nitrate trihydrate. To this 45 mL of water was added and stirred for 15 minutes. Then 30 mL, 0.5 M solution of ascorbic acid in ethylene glycol was added and stirred at 70 °C. When the color changed from blue to reddish brown the solution was cooled to obtain copper nanofluid. Similar reactions were carried out at varying concentration of ascorbic acid, PVP and dilution.

Microwave assisted reactions were also carried out at 50 % power for 4 minutes. The reactions were also carried out at varying concentration of reducing agent, irradiation duration and power.

➤ Synthesis of nanofluids using copper sulfate and ascorbic acid

In a typical experiment, 15 mL of aqueous solution of 0.1 M copper sulfate pentahydrate was mixed with 5 mL of solution of 0.01 M PVP in ethylene glycol and 45 mL water and stirred for 15 minutes. Then 30 mL of 0.5 M ascorbic acid solution in ethylene glycol was added. Further the stirring was continued at 75 °C. The color change during the process was from blue to brownish red. After being cooled to room

temperature naturally, copper nano fluid was obtained. The synthesis was also carried out at varying concentrations of ascorbic acid, PVP and various dilutions.

In order to investigate the effect of microwave radiation the same reaction was subjected to microwave irradiation at 50 % power for 5 minutes. Experiments were also carried out by varying the ratio of the reactants, microwave power and irradiation duration.

➤ *Synthesis of nanofluids using copper acetate and ascorbic acid*

15 mL aqueous solution of 0.25 M copper acetate monohydrate was vigorously stirred with 5 mL 0.01 M solution of PVP in ethylene glycol and 45 mL of water. Then 30 mL solution of 0.5 M ascorbic acid in ethylene glycol was added. The reaction mixture was stirred at 80 °C till the color changed from blue to golden brown. The solution was cooled to get copper nanofluid. The synthesis was also repeated by varying the ratio of reactants, PVP and dilution.

The same procedure was used in microwave reactions. The reaction mixture was subjected to microwave irradiation for 4 minutes at 50 % power. Reactions were also carried out by varying the concentration of reducing agent, irradiation duration and power.

2.2.2 Synthesis of Cuprous Oxide Nanofluids

Cuprous oxide nanofluids were prepared using glucose as reducing agent from copper nitrate tri hydrate and copper sulfate pentahydrate in the presence of CTAB and PVP and copper acetate mono hydrate in the presence of SLS, CTAB and PVP as stabilizing agents.

2.2.2.1 Synthesis of cuprous oxide nanofluids in the presence of SLS using copper acetate and glucose

In a typical synthesis, to 20 mL 0.25 M aqueous solution of copper acetate monohydrate, ammonium hydroxide was added till it became dark blue in colour. It was then stirred with 10 mL solution of 0.01 M SLS in water for 15 minutes. Then 2.5 g of glucose was added and stirred at 75 °C. When the color changed from blue to golden yellow sulphuric acid was added to neutralize the initially added base and heating was continued for some time. Finally brown colored nanofluid was obtained on cooling. Synthesis was also carried out by varying the concentrations of reactants and dilution of the reaction mixture.

Similar reactions were carried out in microwave oven. The solutions were subjected to 50 % microwave irradiation for 7 minutes. The reactions were carried out by varying the duration of irradiation and power of microwave irradiation.

2.2.2.2 Synthesis of cuprous oxide nanofluids in the presence of CTAB

➤ Synthesis of nanofluids using copper nitrate and glucose

10 mL of 0.01 M aqueous solution of CTAB was added to 20 mL of 0.1 M aqueous solution of copper nitrate trihydrate and stirred at room temperature for 15 minutes. Then 2 g of glucose was added and stirring was continued till the glucose dissolved completely. The reaction mixture was heated with stirring at 70 °C. When the turbidity appeared, 1 mL of dilute sulfuric acid and 30 mL of ethylene glycol were added. The color of the solution changed to reddish brown after sometime. This was cooled to get cuprous oxide nanofluid. The synthesis was repeated by varying the concentration of reducing agent, CTAB and dilution.

The reduction was also carried out under microwave irradiation. The solution was subjected to microwave irradiation for 4 minutes at 50 % power. The synthesis was also repeated at different reactant ratio, power and irradiation duration.

➤ *Synthesis of nanofluids using copper sulfate and glucose*

In a typical synthesis, to 20 mL of 0.1 M aqueous solution of copper sulphate pentahydrate, 10 mL of 0.01 M aqueous solution of CTAB was added and stirred for 15 minutes. Later 2.5 g of glucose was added. On complete dissolution, the solution was heated to 75 °C with stirring. 1 mL of sulfuric acid was then added to dissolve the appeared turbidity and in addition 30 mL of ethylene glycol was added to the reaction mixture. When the mixture turned reddish orange, it was cooled to room temperature to get cuprous oxide nanofluid. The synthesis was also carried out at varying amounts of glucose, CTAB and various dilutions.

Similar type of reactions was carried out by subjecting the mixtures to microwave radiation. The solution was irradiated for 5 minutes with 50 % power. Synthesis was also repeated at varying ratio of reactants, irradiation duration and power of microwave.

➤ *Synthesis of nanofluids using copper acetate and glucose*

10 mL of solution of 0.01 M CTAB in water was added to 20 mL of 0.25 M aqueous solution of copper acetate monohydrate and stirred for 15 minutes. Later 2.5 g of glucose was added and stirring was continued. After the dissolution of glucose the reaction mixture was subjected to heating at 75 °C. When the turbidity appeared 1 mL of dilute sulfuric acid and 30 ml of ethylene glycol were added and heating was continued. The golden brown solution was cooled to obtain the nanofluid. Synthesis was also carried out by varying the reagent concentrations and dilutions.

Similar reactions were carried out in microwave oven. The solutions were subjected to 50 % microwave irradiation for 5 minutes. The reactions were carried out at different irradiation duration, power and varying amounts of glucose.

2.2.2.3 Synthesis of cuprous oxide nanofluids in the presence of PVP

➤ Synthesis of nanofluids using copper nitrate and glucose

30 mL 0.1 M solution of copper nitrate trihydrate in ethylene glycol was made alkaline by adding ammonium hydroxide till the color became deep blue. To this 5 mL solution of 0.01 M PVP in ethylene glycol was added. This mixture was diluted with 35 mL water and stirred for 15 minutes. After that 3 g of glucose was added and stirred at 75 °C till the color changed to golden yellow. At this point sulfuric acid was added. When the color became magenta the solution was cooled to get cuprous oxide nanofluid. The synthesis was repeated by varying the concentration of reducing agent, PVP and dilution.

The reduction was also carried out under microwave irradiation. The solution was subjected to microwave irradiation for 5 minutes at 50 % power. The synthesis was also repeated at different reactant ratio, power and irradiation duration.

➤ Synthesis of nanofluids using copper sulfate and glucose

25 mL of 0.1 M solution of copper sulfate pentahydrate in ethylene glycol was made sufficiently alkaline by adding ammonium hydroxide. Further 5 mL of ethylene glycol solution of 0.01 M PVP was added along with 30 mL of water and stirred for 15 minutes. Then 3 g of glucose was added and stirred at 70 °C. During heating the color changed from blue to pale yellow. At this point the pH was brought down to 3 by the addition of sulfuric acid. The heating was continued till the color changed to reddish brown color. On cooling cuprous oxide nanofluid was obtained. The synthesis was also carried out at varying amounts of glucose, PVP and various dilutions.

Similar types of reactions were carried out by subjecting the mixtures to microwave irradiation. The solution was irradiated for 3 minutes with 50 % power. Synthesis was also repeated at varying ratio of reactants, irradiation duration and power of microwave.

➤ *Synthesis of nanofluids using copper acetate and glucose*

In a typical experiment, to 15 mL 0.25 M solution of copper acetate monohydrate in ethylene glycol, ammonium hydroxide was added till it became dark blue in colour. It was then stirred with 5 mL solution of 0.01 M PVP in ethylene glycol and 20 mL of water for 15 minutes. Then 2.5 g of glucose was added and stirred at 80 °C. When the color changed from blue to reddish yellow, sulfuric acid was added to neutralize the initially added base and heating was continued for some time. Finally brownish red colored cuprous oxide nanofluid was obtained. Synthesis was also carried out by varying the reagent concentrations.

Similar reactions were carried out in microwave oven. The solutions were subjected to 50 % microwave irradiation for 3 minutes. The reactions were carried out at different irradiation duration, power and varying amounts of glucose.

2.3 CHARACTERIZATION

The prepared nanofluids were characterized by XRD technique, TEM, FESEM, EDXA, FTIR spectroscopy and UV-Vis spectroscopy. Thermal conductivity and viscosity measurements were also carried out.

2.3.1 XRD Studies

The powder XRD method is very important and useful in qualitative phase analysis because every crystalline material has its own characteristic powder pattern: indeed, the method is often called the powder finger print method. There are two main factors which determine powder patterns: the size and shape of the unit cell and the atomic number and position of various atoms in the cell. Thus, two materials may have the same crystal structure but almost certainly they have quite distinct powder patterns.

XRD can be used for particle size measurement. If the average crystal size in a powder is below a certain limit (~ 2000 Å diameter), additional broadening of the

diffracted X-ray beams occurs. From measurement of this extra broadening an average particle size may be obtained. In the absence of extra broadening due to small particle size, powder lines or peaks have a finite breadth for several reasons: the radiation is not absolutely monochromatic, the $K\alpha$ line has an intrinsic breadth due to the Heisenberg uncertainty principle and the focusing geometry of the instrument may not be perfect for a variety of reasons.

The commonly accepted formula for the particle size broadening is the Scherrer formula:

$$D = \frac{K\lambda}{B\cos\theta} \quad (2.1)$$

where D is the thickness of the crystal (in Å), K is the shape factor, λ the X-ray wavelength and θ the Bragg angle. The line broadening, B , is measured from the extra peak width at half the peak height and is obtained from the Warren formula:

$$B^2 = B_M^2 - B_S^2 \quad (2.2)$$

where B_M is the measured peak width in radians at half peak height and B_S is the corresponding width of a peak of a standard material, mixed in with the sample, whose particle size is considerably greater than 2000 Å and which has a diffraction peak near to the relevant peak of the sample.

Nanofluid was diluted with absolute ethanol and centrifuged for one hour. The nanoparticles were then given repeated wash with water and ethanol. Finally the particles were dried at 80 °C. X-ray diffraction patterns of the nanoparticles were taken on a JEOL X-ray Diffractometer (Model DX GE 2P) using Ni filtered Cu K_α radiation ($\lambda = 1.54178$ Å) with an operating voltage of 30 kV. The scan rate was set at 0.06 °/s in the 2θ range 25 °- 85 °.

2.3.2 TEM Analysis

The formation of nanoparticles is best studied by TEM, which gives two types of information in routine examination, firstly, the particle size distribution. The second type of information is the crystallinity of a sample, obtained through electron diffraction or nano diffraction. More detailed information on particle shape; phase transitions, two- and three-dimensional ordering, in-situ nano measurements, and evaluation of other properties are possible using TEM.

The transmission electron microscope images of the nano fluids and selected area electron diffraction pattern of the nanoparticles were recorded on a Philips CM200 transmission electron microscope operating with an accelerating voltage of 20-200 kV with a resolution of 2.4 Å. The samples for TEM were prepared by sonicating the nanofluid and later placing it on carbon coated copper grid for analysis.

2.3.3 FESEM Analysis

FESEM is an extremely versatile technique capable of providing structural information over a wide range of magnification. It is used to image the sample surface by scanning it with a high-energy beam of electrons in a raster scan pattern. The electrons interact with the atoms that make up the sample producing signals that contain information about the sample's surface topography and composition. It is also used to determine the size of the sample.

The field emission scanning electron microscopy images were taken on a Supra 40VP FESEM having a resolution upto 2 nm. Energy dispersive X-ray analysis was carried out on a JEOL JSM 6380LA model Analytical Scanning Electron Microscope.

2.3.4 FTIR and UV-Vis Spectroscopic Analysis

FTIR spectroscopy is used to identify the ingredients of the reaction solution. Copper is an inorganic species, which shows characteristic absorption that can be identified qualitatively by UV-Vis spectroscopy.

FTIR spectra were taken using Nicolet Avatar 330 FTIR spectrometer. UV-Vis spectra of the nanofluids were obtained using Ocean optics, inc SD2000 fibre optic spectrometer at room temperature.

2.3.5 Thermal Conductivity Measurements

Thermal conductivity measurement using thermal property analyzer is basically a transient line heat source method. Typically a probe for this measurement consists of a needle with a heater and temperature sensor inside. A current is passed through the heater and the temperature of the probe is monitored over time. An analysis of the probe temperature is used to determine thermal conductivity. An ideal sensor would have a very small diameter and a length perhaps 100 times its diameter. It would be in intimate contact with the surrounding material and would measure the temperature of the material during heating and cooling. Ideally the temperature and composition of the material being measured would not change during the measurement.

The thermal conductivity of the as such prepared nanofluid as well as at various particle weight fractions were measured using KD2 pro thermal property analyzer. The KS-1 sensor was oriented vertically in the sample and the measurements were recorded at low power mode with read time of 1 min. To eliminate forced convection, the fluid sample and the sensor were kept absolutely still during the measurement. Measurements were done at 30 °C with different particle weight fractions by diluting the nanofluid with a mixture of water and ethylene glycol in 1:1 ratio.

2.3.6 Viscosity Measurements

Viscosity is one of the key properties of nanofluids. Rheological behavior is an important attribute in application of nanofluids. In order to investigate the rheological behavior, measurements are done to verify whether nanofluid behaves like a Newtonian fluid or non-Newtonian fluid. The equation governing Newtonian behavior of a fluid is given by

$$\tau = \mu\dot{\gamma} \quad (2.3)$$

where τ is shear stress, μ is the coefficient of viscosity and $\dot{\gamma}$ is the shear strain. The linear relation between shear stress and shear rate demonstrates Newtonian behavior. The non-Newtonian fluid behavior and shear rate dependent viscosity require consideration in engineering design of the processing and applications of nanofluids. The study of the rheological behavior of a nanofluid helps to understand the structure of nanofluid.

The viscosity of the nanofluids was measured using Brookfield LV DV III ultra rheometer. The measurements were carried out at different particle concentrations by subjecting the fluid to serial dilution and at different temperature.



CHAPTER 3

RESULTS AND DISCUSSION

Chapter 3 deals with the results and discussions pertaining to the investigation. It gives the description of the obtained results and their interpretations.

3.1 COPPER NANOFUIDS

➤ *Results of XRD, EDX and SAED analysis*

The phase structure and the purity of the products have been examined by X ray diffraction studies. The powder XRD pattern of the copper nanoparticles obtained by the reduction of copper nitrate, copper sulfate and copper acetate precursors using ascorbic acid in the presence of CTAB are shown in Fig. 3.1, Fig. 3.2 and Fig. 3.3, respectively. The diffraction peaks could be indexed to the face centered cubic Cu [JCPDS Card No. 04-0838, $a = 3.6150 \text{ \AA}$, Space group: Fm3m (225)] corresponding to (111), (200) and (220) planes, respectively. The average size of the particle has been calculated using Scherrer's formula (West 1989). No peaks of impurities such as those of cuprous or cupric oxide were detected, suggesting the high purity of the products.

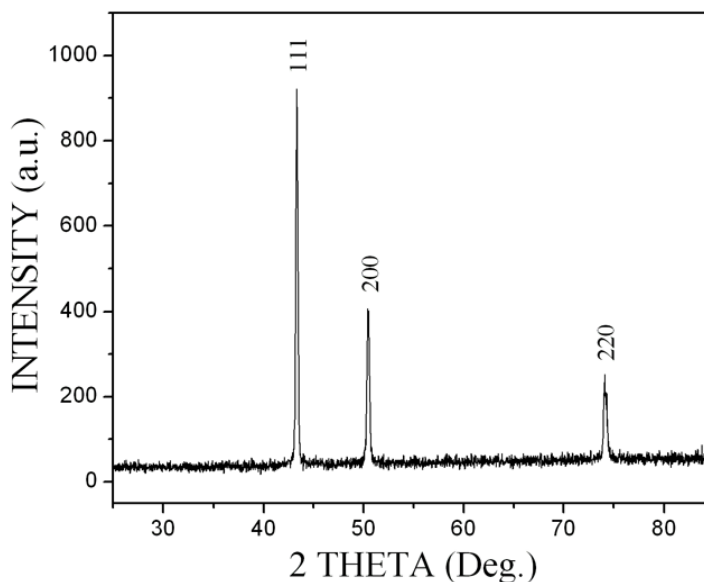


Fig. 3.1 Powder XRD pattern of copper nanoparticles prepared by the reduction of copper nitrate by ascorbic acid in the presence of CTAB

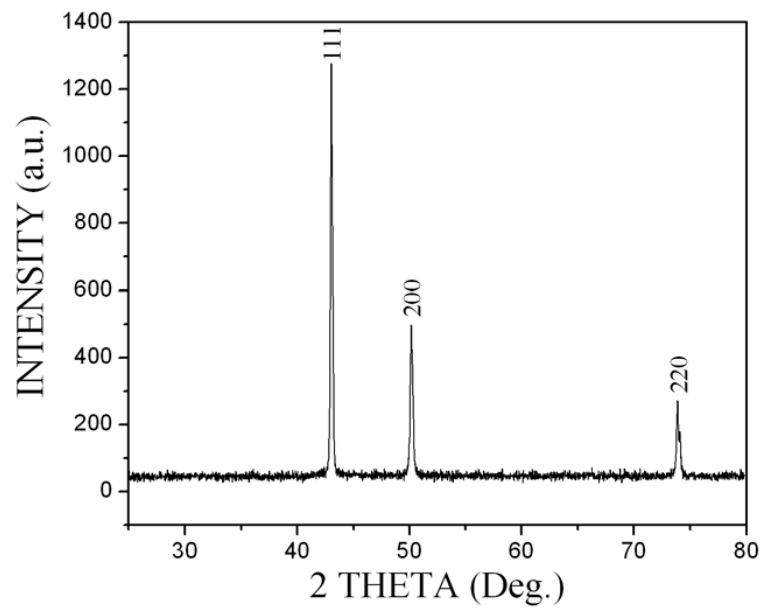


Fig. 3.2 Powder XRD pattern of copper nanoparticles prepared by the reduction of copper sulfate by ascorbic acid in the presence of CTAB

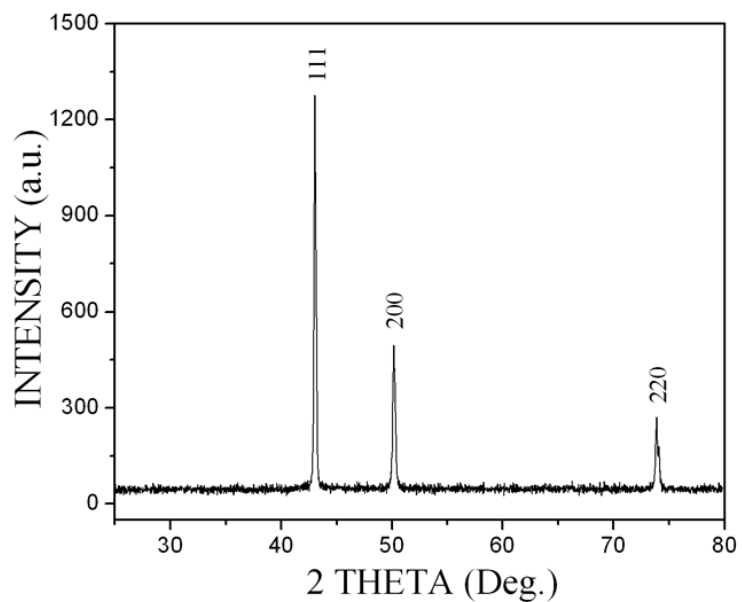


Fig. 3.3 Powder XRD pattern of copper nanoparticles prepared by the reduction of copper acetate by ascorbic acid in the presence of CTAB

The chemical composition and purity of the products has also been examined using EDXA. EDX spectra of the copper nanoparticles obtained by the reduction of copper nitrate, copper sulfate and copper acetate precursors using ascorbic acid in the presence of CTAB are shown in the Fig. 3.4, Fig. 3.5 and Fig. 3.6, respectively. Only copper is detected in the spectrum indicating that there is no contamination.

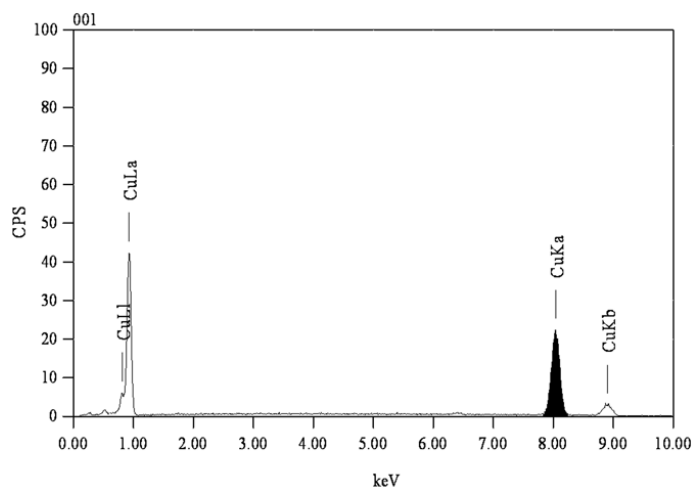


Fig. 3.4 EDX spectrum of copper nanoparticles prepared by the reduction of copper nitrate by ascorbic acid in the presence of CTAB

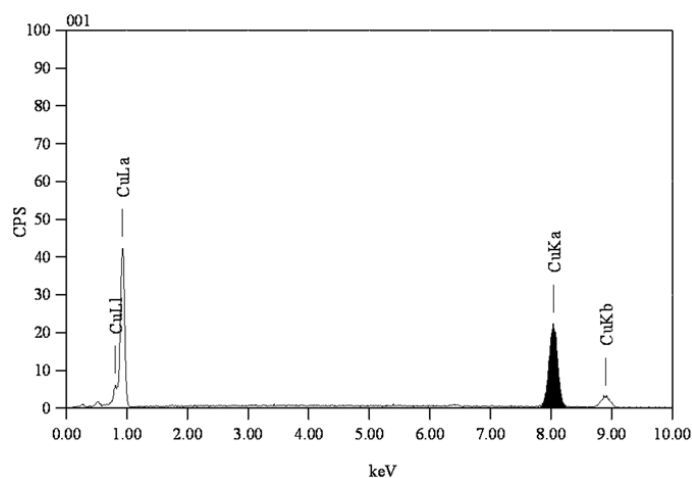


Fig. 3.5 EDX spectrum of copper nanoparticles prepared by the reduction of copper sulfate by ascorbic acid in the presence of CTAB

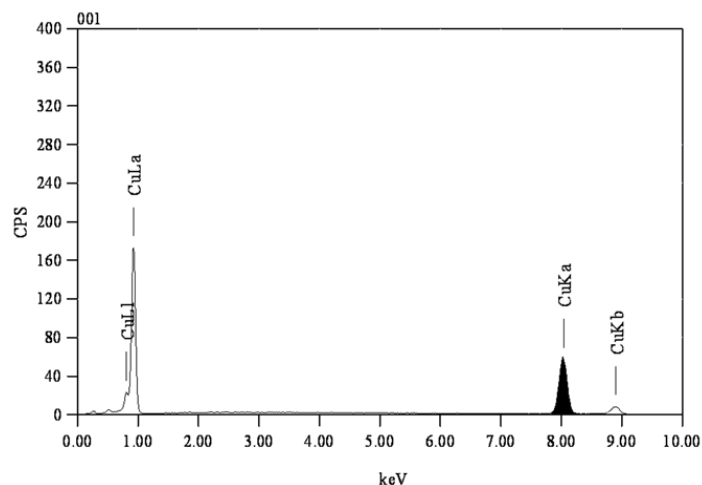


Fig. 3.6 EDX spectrum of copper nanoparticles prepared by the reduction of copper acetate by ascorbic acid in the presence of CTAB

The SAED pattern of copper nanoparticles obtained by the reduction of copper nitrate, copper sulfate and copper acetate precursors using ascorbic acid in the presence of CTAB are shown in the Fig. 3.7, Fig. 3.8 and Fig. 3.9, respectively.

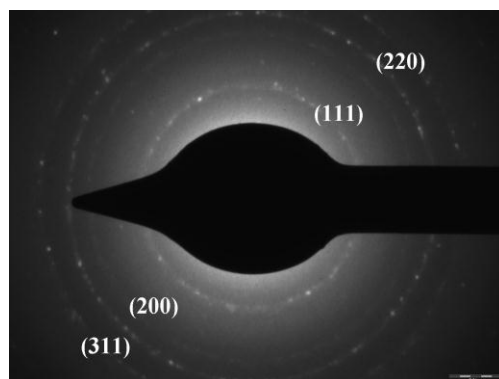


Fig. 3.7 SAED pattern of copper nanoparticles prepared by the reduction of copper nitrate by ascorbic acid in the presence of CTAB

The SAED pattern of the nanoparticles show four fringes with 2.09 Å, 1.81 Å, 1.28 Å and 1.09 Å as the plane distances which can be related to (111), (200), (220) and (311) planes, respectively, of face centered cubic copper.

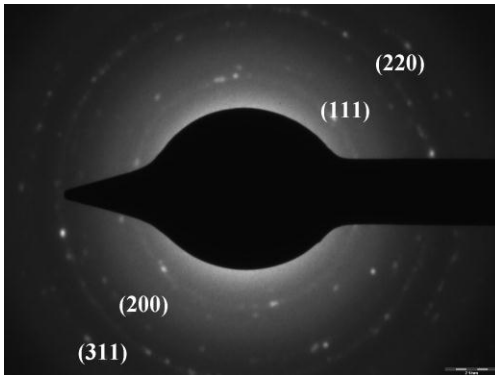


Fig. 3.8 SAED pattern of copper nanoparticles prepared by the reduction of copper sulfate by ascorbic acid in the presence of CTAB

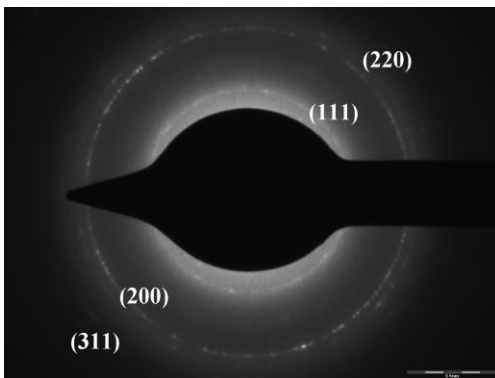


Fig. 3.9 SAED pattern of copper nanoparticles prepared by the reduction of copper acetate by ascorbic acid in the presence of CTAB

➤ *Results of FTIR and UV-Vis spectroscopic analysis*

Though different reducing agents are used to reduce cupric (Cu^{2+}) ions of the salts to form copper nanoparticles, there is a probability of ethylene glycol itself acting as a reducing agent. In order to ascertain the fact, whether ethylene glycol acts as a reducing agent in the process of nanofluid preparation, the FTIR spectra of the pure ethylene glycol and the nanofluid (containing mixture of water and ethylene glycol as base fluid) were compared. The FTIR spectra of copper nanofluid obtained by the reduction of copper nitrate (B), copper sulfate (C) and copper acetate (D) precursors using ascorbic

acid in the presence of CTAB each stacked with pure ethylene glycol (A) are shown in Fig. 3.10, Fig. 3.11 and Fig. 3.12, respectively.

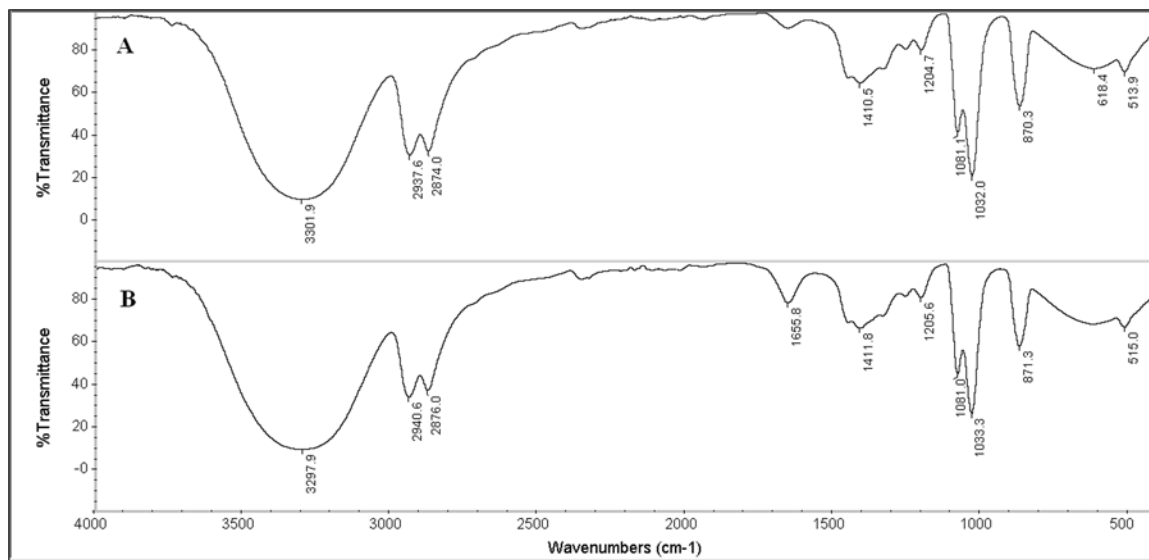


Fig. 3.10 FTIR spectra of (A) ethylene glycol and (B) copper nanofluid prepared by the reduction of copper nitrate by ascorbic acid in the presence of CTAB

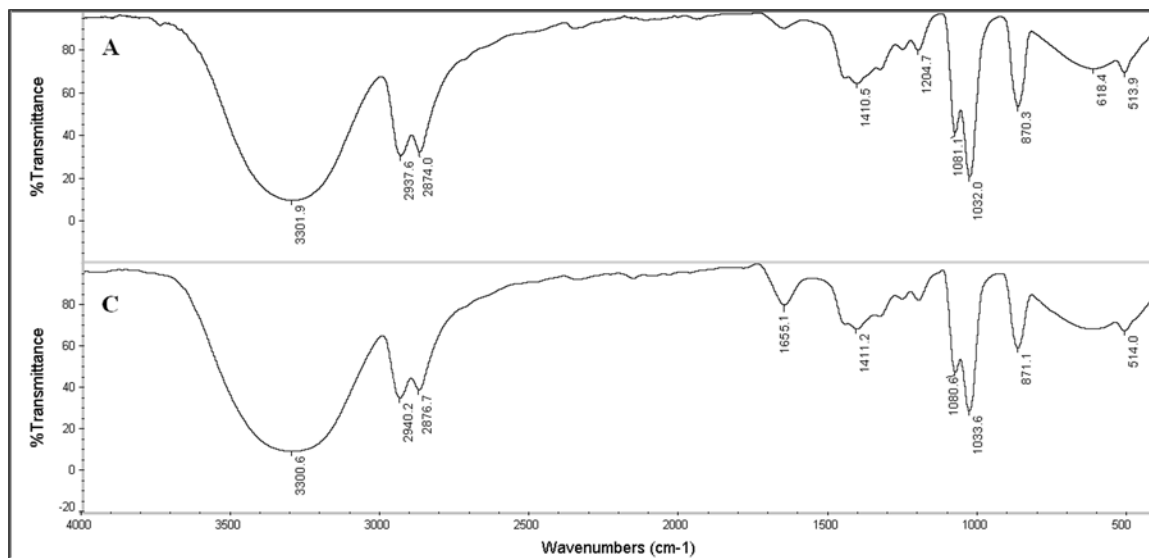


Fig. 3.11 FTIR spectra of (A) ethylene glycol and (C) copper nanofluid prepared by the reduction of copper sulfate by ascorbic acid in the presence of CTAB

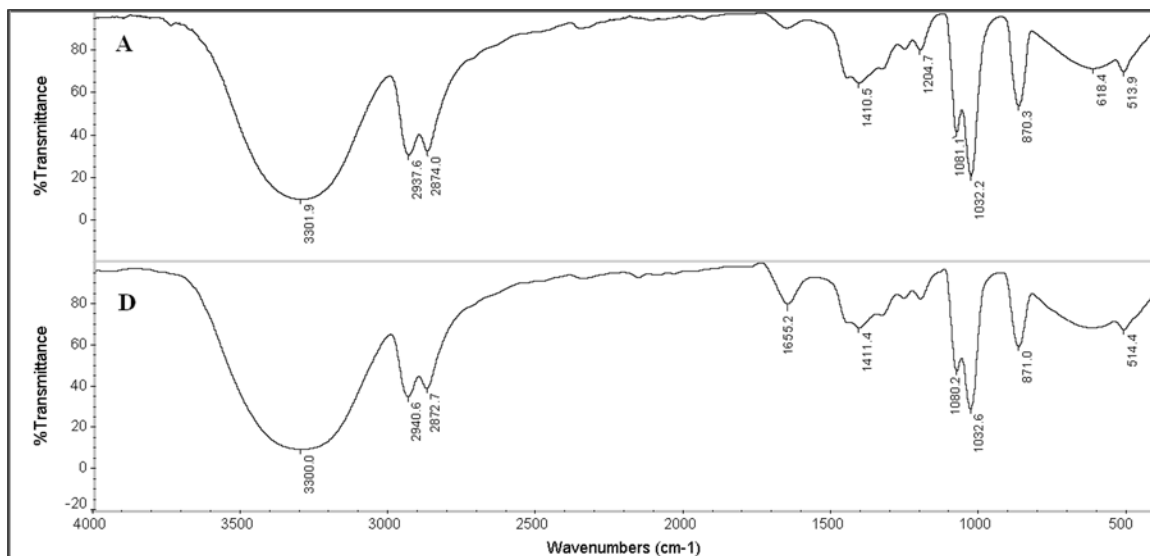


Fig. 3.12 FTIR spectra of (A) ethylene glycol and (D) copper nanofluid prepared by the reduction of copper acetate by ascorbic acid in the presence of CTAB

It is seen that the two spectra resemble each other indicating that the ethylene glycol is not oxidized. It suggests that ascorbic acid and glucose used in the process are the ones acting as reducing agents and not ethylene glycol. This method preserves the advantages of the polyol process and aqueous chemical reduction method as well.

Fig. 3.13, Fig. 3.14 and Fig. 3.15 show the UV-Vis spectra of copper nanofluid obtained by the reduction of copper nitrate, copper sulfate and copper acetate precursors using ascorbic acid in the presence of CTAB, respectively. The absorption peaks at 560 nm, 551 nm and 576 nm in the Fig. 3.13, Fig. 3.14 and Fig. 3.15, respectively indicate the presence of copper nanoparticles (Bicer et al. 2010).

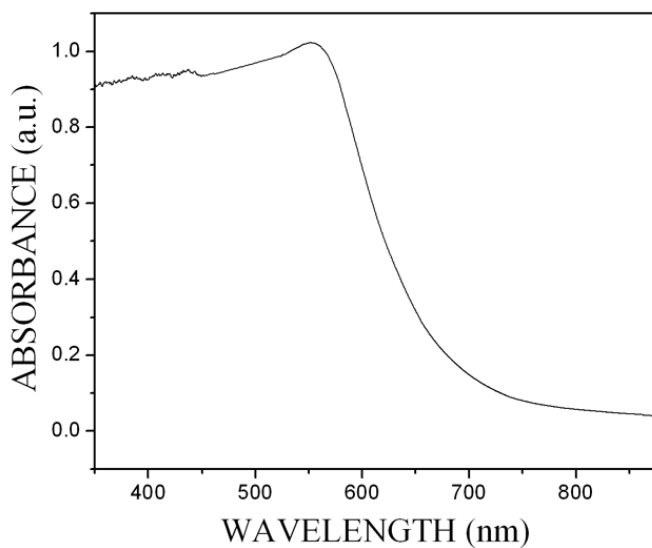


Fig. 3.13 UV-Vis spectrum of copper nanofluid prepared by the reduction of copper nitrate by ascorbic acid in the presence of CTAB

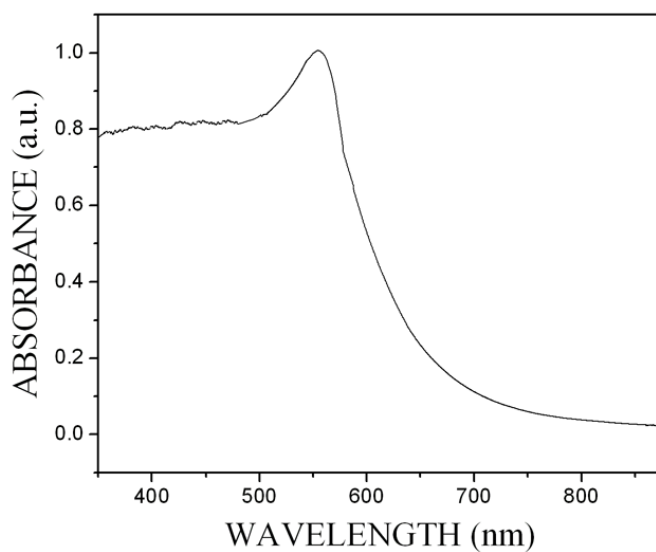


Fig. 3.14 UV-Vis spectrum of copper nanofluid prepared by the reduction of copper sulfate by ascorbic acid in the presence of CTAB

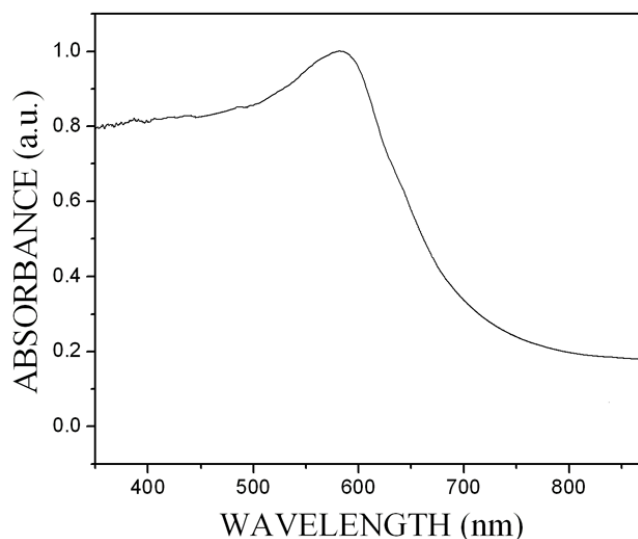


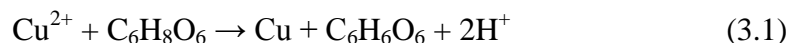
Fig. 3.15 UV-Vis spectrum of copper nanofluid prepared by the reduction of copper acetate by ascorbic acid in the presence of CTAB

3.1.1 Copper Nanofluids Synthesized in the Presence of SLS

3.1.1.1 Nanofluids synthesized using copper nitrate and ascorbic acid

➤ *Results of variation in reaction parameters*

Effect of pH: The effect of pH of the reaction medium on the size of the copper nanoparticles was studied by varying the pH of the reaction mixture. The variation in the pH of the reaction mixture showed a significant effect on the size of copper nanoparticles. With the decrease in the pH value, the size of the copper particle was found to be increasing. When the pH of the reaction mixture was brought down from 7 to 3 by the addition of sulphuric acid, the size of the particles increased from 22 nm to 39 nm. This trend is attributed to the decrease in the reducing power of ascorbic acid (Wu 2007). The chemical reaction between Cu^{2+} ions and ascorbic acid is represented by the equation (3.1).



Also, the electrode potential for the redox equilibrium of ascorbic acid as represented in equation (3.2), is given by the equation (3.3).



$$E = E^\circ - 0.059 \text{ pH, at 298 K} \quad (3.3)$$

It is evident from the equation (3.3) that the electrode potential increases as the pH decreases. Therefore the tendency to undergo oxidation decreases and the reducing power of ascorbic acid decreases as the pH decreases. This results in slower reaction between copper nitrate and ascorbic acid, which in turn results in the formation of smaller number of copper atoms in the initial stages of the reactions. Then initially formed particles act as nuclei for further growth of the particles. This results in the growth of the fewer particles into a larger size. As the pH is increased, the reducing power of ascorbic acid increases, which in turn increases the reaction rate between Cu^{2+} and ascorbic acid, and results in more number of particles with smaller sizes. This is schematically given in Fig. 3.16.

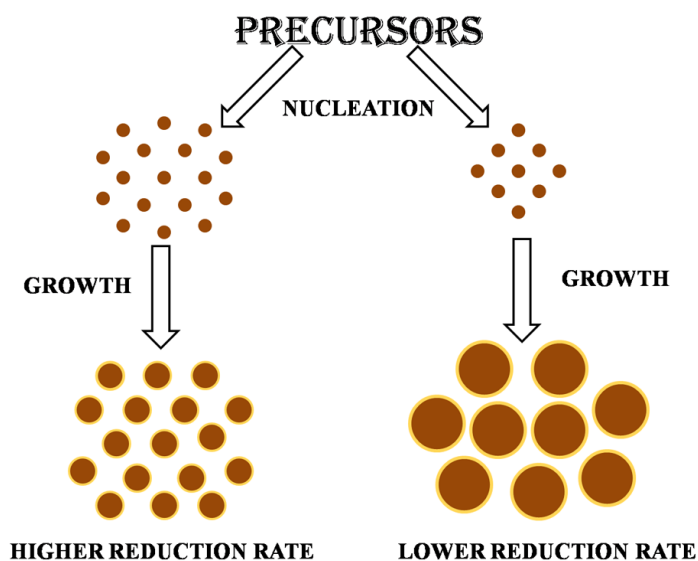


Fig. 3.16 Schematic representation of influence of rate of reduction on the sizes of the particles formed

Effect of ratio of reactants: One of the factors influencing the size of the nanoparticles is the ratio of reactants (Zhu et al. 2004b). The effect of ratio of reactants on the particle size was studied by varying the molar ratio of ascorbic acid to copper nitrate from 5 to 20. It was observed that whenever the molar ratio of ascorbic acid to copper nitrate was less than 5 the reaction did not go for completion. Hence always molar ratio of more than 5 was maintained. It was found that the particle size increased from 22 nm to 32 nm under thermal conditions and decreased from 35 nm to 18 nm under microwave irradiation, when the ratio was changed from 5 to 20. The observation under thermal conditions could be attributed to the decrease in the pH of the reaction mixture as the ascorbic acid content is increased. As discussed in the previous section, decrease in the pH of the reaction medium decreases the reducing power of ascorbic acid, which in turn results in slower rate of nucleation and formation of fewer numbers of bigger particles. Thus, when the ascorbic acid content in the mixture is increased, the size of the particles increases.

Microwave heating rate is faster than conventional heating methods; and accelerates the nucleation of copper particles (Zhu et al. 2004b). This results in the formation of more number of nuclei, and therefore, more particles with smaller sizes. Also, the intense friction and collisions of the particles created by the microwave irradiation suppresses the ready growth of the copper particles and results in smaller particles. With increase in concentration of ascorbic acid the number of collision increases and this factor dominates over the pH effect. Hence the opposite trend is seen.

Effect of dilution: Dilution of the reaction mixture with water decreases the overall concentration of the reactants in the reaction mixture, which has the bearing on the reaction rate and the particle size as well. Reactions were carried out by diluting the reaction mixture with different volumes of water. It was found that the particle size increased with dilution. Dilution with 50 mL water resulted in increase in size to 32 nm from 22 nm without dilution. It further increased to 39 nm for 75 mL dilution. For 100 mL dilution the particle size was 21 nm with reaction proceeding very slowly. The

observations can be explained by the influence of reaction rate on the nucleation. At a low overall concentration, on dilution of the reaction mixture, the reduction of copper nitrate by ascorbic acid takes place slowly and only a few nuclei of copper are formed in the early period of the reaction. Since the rate of the reaction is slow, the subsequently formed copper atoms get deposited on the already existing nuclei rather than forming new nuclei. As a result of the rate of nucleation being slower than the rate of particle growth, fewer numbers of particles with bigger size are obtained.

Effect of addition of SLS: The effect of SLS on the size of the copper nanoparticles as well as stability was studied by varying the concentration of SLS. The results are tabulated in the Table 3.1.

Table 3.1 Effect of concentration of SLS on the size of copper particles prepared by the reduction of copper nitrate by ascorbic acid

Effective concentration of SLS in the reaction mixture (mM)	Particle Size (nm)
0	58
4.5	22
22.7	27
45.5	36

It was observed that the addition of SLS as a surfactant decreases the size of the copper nanoparticles. The results suggest that the addition of SLS as a surfactant efficiently restricts the growth of the copper particles. This could be attributed to the capping effect of SLS in controlling the size of copper particles. It was further observed that when the concentration of the SLS in the reaction mixture was increased, the particle size increased to some extent. These observations can be explained by the model suggested for similar observations on the effect of polyacrilamide on size of cuprous oxide nanoparticles (Lee et al. 2009).

The copper nanoparticles are formed by the aggregation of primary nanoparticles and are stabilized by the surfactant, SLS. As the concentration of SLS increases, in the presence of more number of SLS molecules, it can act not only as a stabilizing agent but also as a cross linking agent by binding to the surface of the primary nanoparticles. The SLS bound to the primary particle can link to the adjacent particles forming dimers, trimers, etc., of the primary particles. The aggregation of particles now takes place by the combination of multi-mers resulting in bigger particle size. Therefore, the aggregation process predominates over surface stabilization process, resulting in the formation of larger copper nanoparticles. The same is illustrated in Fig. 3.17.

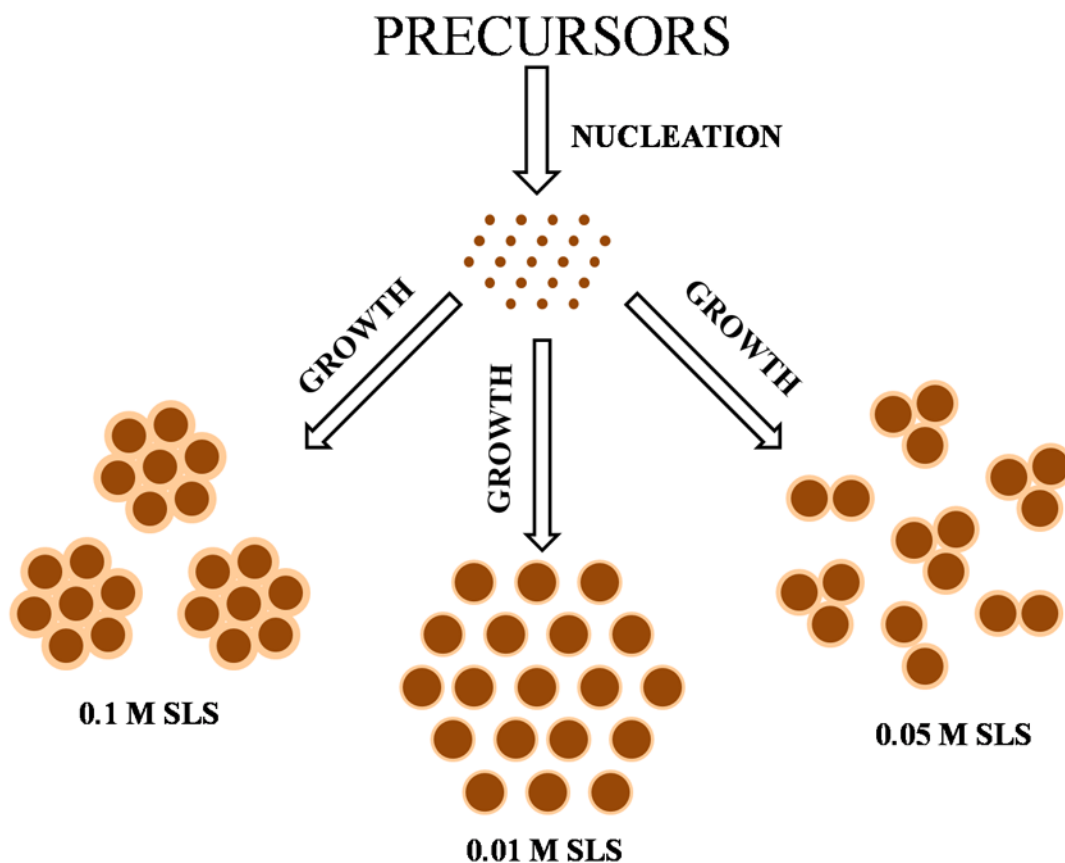


Fig. 3.17 Schematic representation of influence of concentration of SLS on the sizes of the particles formed

The utility of the nanofluid for any application is dependent on its stability. When prepared in the absence of SLS the nano fluid was unstable and the particles began to settle down. The samples of nanofluid prepared in the presence of SLS under different conditions were stable for several weeks at room temperature under stationary conditions; and even the least stable fluid was stable up to 5 weeks.

The stability of the as prepared copper nanofluid was found to be better than the one achieved by the two step method where in stability was only for one week in the case of copper - transformer oil system and 30 h for copper - water system (Xuan et al. 2000). In the case of one step chemical method the copper nanofluid stayed stable for duration of 3 weeks (Kumar et al. 2009). The stability of the nanofluid in the presence of SLS is attributed to two factors. One of the factors is the smaller sizes of the particles, which facilitate their better dispersity in the medium and the second factor is that the addition of SLS prevents the agglomeration of the metal nanoparticles.

Effect of power of microwave radiation and irradiation duration: The effect of power of microwave radiation and irradiation duration was studied by carrying out the reaction between copper nitrate and ascorbic acid at different power of microwave for different time periods. At 30 % microwave irradiation for 4 minutes the reaction was incomplete with size of the resulting particle being 42 nm. When the power of microwave radiation was increased to 50 %, the reaction proceeded to completion. When the power of microwave radiation was increased from 50 % to 70 % the particle size decreased from 35 nm to 22 nm, for 4 minutes of irradiation duration. The decrease in particle size with increase in power of microwave radiation is attributed to the formation of large number of small particles due to rapid nucleation, as the rate of the reaction is increased with microwave power.

The effect of microwave irradiation duration on the formation of nanoparticles in the reaction medium was also investigated. For 50 % irradiation power the size of the particles formed was 46 nm for 6 minutes irradiation duration and 58 nm for 8 minute

irradiation duration. The results are consistent with the results reported in the literature (Zhu et al. 2004b). The continued interaction of the particles might be the cause for the growth of the particles, resulting in the increase in particle size.

TEM has been used to investigate the morphology as well as size of the copper nanoparticles. The sizes obtained from the TEM match well with those obtained from XRD. Fig. 3.18 (A) shows the TEM image of the copper nanofluid prepared under microwave irradiation. The TEM images show elongated copper nanoparticles as compared with those prepared under thermal conditions (Fig. 3.18B). Under microwave irradiations, the rate of formation of copper nanoparticles is high and therefore particles do not get sufficient time to orient themselves on the growing particles. This leads to uneven growth of particles on all directions, which could be the reason for the formation of elongated particles.

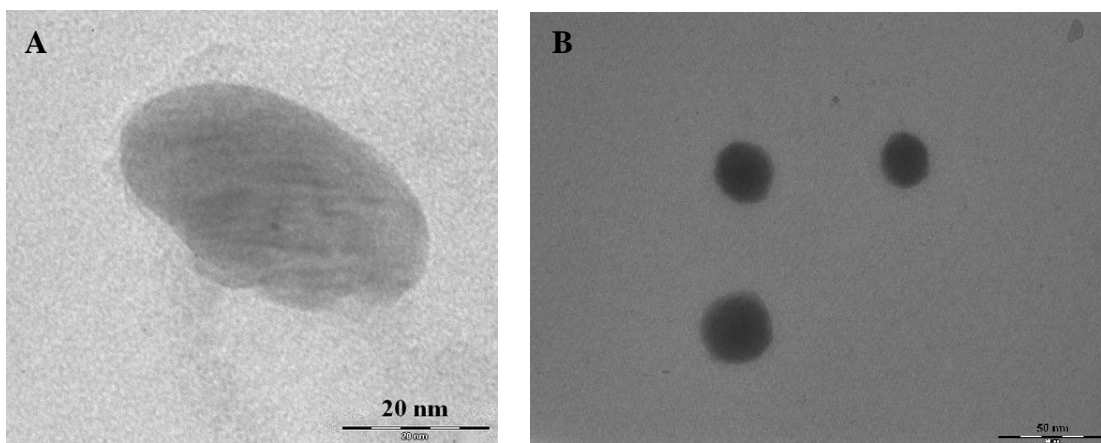


Fig. 3.18 TEM image of copper nanofluid prepared by the reduction of copper nitrate by ascorbic acid in the presence of SLS (A) under microwave irradiation and (B) by conventional heating

➤ *Results of thermal conductivity measurements*

The thermal conductivity of the as synthesized nanofluid was found to be $1.04 \text{ W m}^{-1} \text{ K}^{-1}$ when the weight fraction of copper nanoparticles was 0.167 %, significantly

higher than the reported value of $0.279 \text{ W m}^{-1} \text{ K}^{-1}$ for copper nanofluid (0.1 %) prepared using sodium hypophosphite (Zhu et al. 2004a), $0.6 \text{ W m}^{-1} \text{ K}^{-1}$ for copper nanofluid reported by Kumar et al. (2009) and $0.259 \text{ W m}^{-1} \text{ K}^{-1}$ for copper nanofluid (0.5 %) prepared by single step physical method of direct evaporation technique (Eastman et al. 2001). The variation of thermal conductivity ratio (K_{eff}/K_f) with nanoparticle weight fraction is as shown in Fig. 3.19. K_{eff} is the thermal conductivity of the nanofluid while K_f is that of the base fluid alone. The ratio of water and ethylene glycol was maintained 1:1 during the measurements. Similar trend was observed for different ratios of the base fluids, indicating that the trend is independent of medium composition.

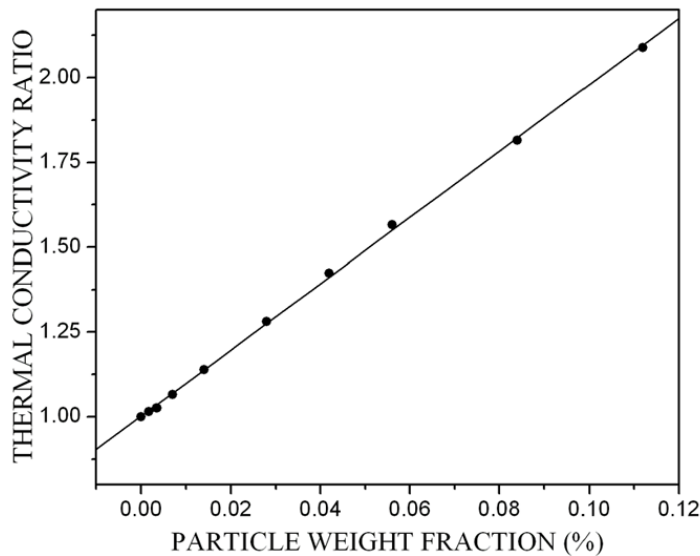


Fig. 3.19 Variation of thermal conductivity ratio with particle weight fraction for copper nanofluid prepared by the reduction of copper nitrate by ascorbic acid in the presence of SLS

It was observed that with the increase in the particle concentration the thermal conductivity of the nanofluid increased. The increase in thermal conductivity could be attributed to the higher conductivity of copper, its nano size and uniform distribution of the particles in the fluid (Chopkar et al. 2006; Murshed et al. 2008). The free Brownian

motions of the particles could have also facilitated higher thermal conductivity (Singh 2008; Wang et al. 2011b).

➤ **Results of viscosity measurements**

The variation of shear stress with shear rate at 30 °C for a particle loading of 0.167 % is as shown in Fig. 3.20. The linear relation between the shear stress and shear rate demonstrates the Newtonian behavior of the nanofluid.

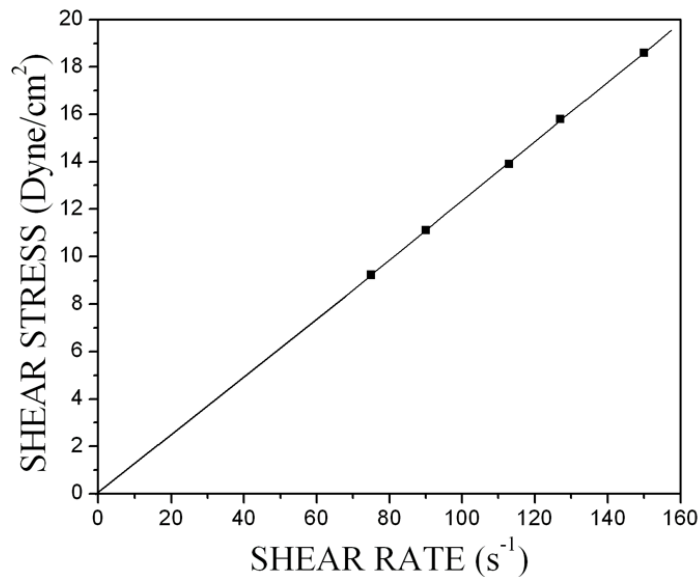


Fig. 3.20 Shear stress verses shear rate for copper nanofluid prepared by the reduction of copper nitrate by ascorbic acid in the presence of SLS

Viscosity as a function of shear rate for 0.167 % particle loading at different temperatures (Fig. 3.21) demonstrates that viscosity is independent of shear rate (Yu et al. 2009b). The results for other particle concentrations are similar.

The viscosity of the nanofluids was measured at different particle weight fractions at 30 °C and the changes in relative viscosity (n_{eff}/n_f) of the nanofluid with particle weight fraction are shown in Fig. 3.22. n_{eff} is the viscosity of the nanofluid while n_f is that

of the base fluid. It is seen from Fig. 3.22 that the relative viscosity increases with the increase in particle concentration.

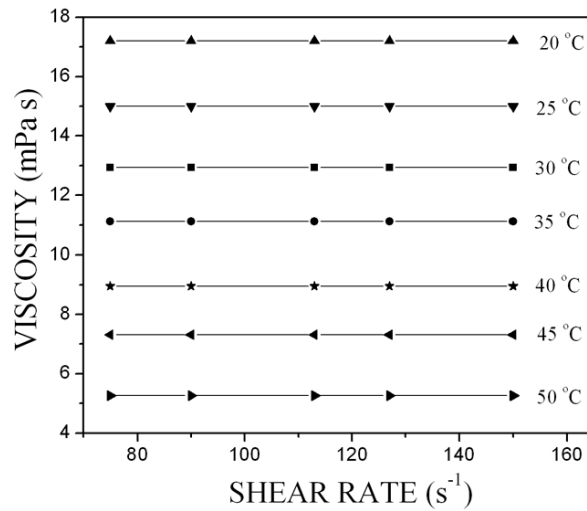


Fig. 3.21 Viscosity as a function of shear rate at different temperatures for copper nanofluid prepared by the reduction of copper nitrate by ascorbic acid in the presence of SLS

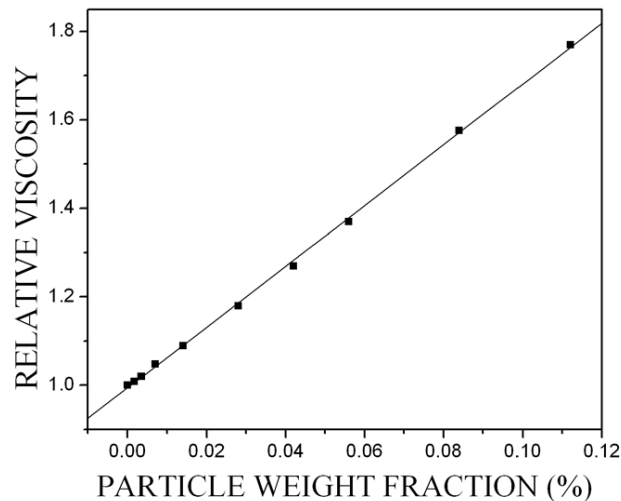


Fig.3.22 Variation of relative viscosity with particle weight fraction for copper nanofluid prepared by the reduction of copper nitrate by ascorbic acid in the presence of SLS

The effect of temperature on the viscosity of the nanofluid was studied (Fig. 3.23) and was seen that the viscosity decreases with the increase in temperature of the fluid. The trend is similar to the one reported by Li et al. (2011).

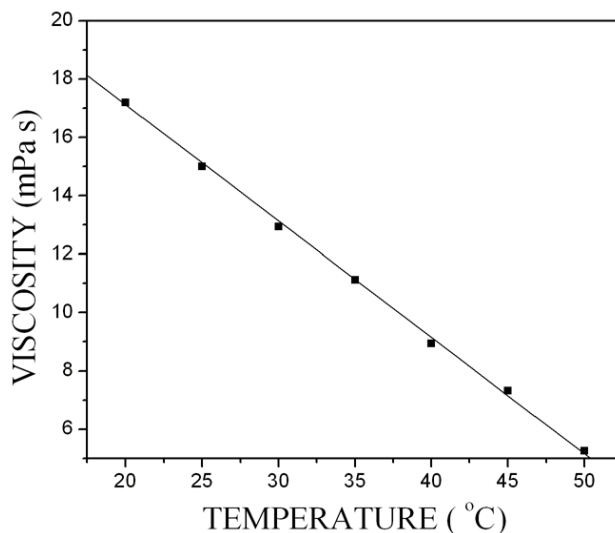
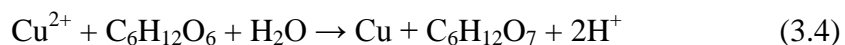


Fig. 3.23 Viscosity as a function of temperature for copper nanofluid prepared by the reduction of copper nitrate by ascorbic acid in the presence of SLS

3.1.1.2 Nanofluids synthesized using copper nitrate and glucose

➤ Results of variation in reaction parameters

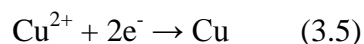
Effect of ratio of reactants: The synthesis was carried out by varying the molar ratio of glucose to copper nitrate. It was observed that whenever the molar ratio of glucose to copper nitrate was less than 5.5 the reaction did not go for completion. Hence always the molar ratio of more than 5.5 was maintained. The increase in molar ratio from 5.5 to 18.5 resulted in particles having sizes decreasing from 36 nm to 17 nm in thermal conditions and 28 nm to 16 nm in microwave conditions respectively. Glucose reduces copper ions as shown in equation (3.4).



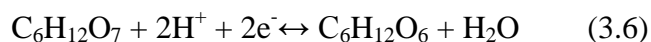
According to this equation the rate and the amount of electrons supplied to copper ions is determined by the concentration of glucose. At lower concentration of reducing agent, the reduction rate of copper precursor is slow and consequently only a few nuclei are formed at the nucleation step. The precipitating copper atoms at the later period of the reactions are mostly involved in particle growth by collision with already generated nuclei rather than formation of new particles. This leads to the formation of larger sized particles. With the increase in the concentration of reducing agent, reduction rate is enhanced, leading to the formation of smaller particles. At higher reduction rate the number of precipitating metallic clusters increases steeply and hence more number of nuclei is formed during the nucleation period. Eventually the size of the particles decreases because the amount of solute available for particle growth per growing particle decreases with increasing number of nuclei (Park et al. 2007).

Effect of addition of ammonia: It was observed that when the reaction between copper nitrate and glucose was carried out in neutral condition, the reaction took place very fast and the product separated out as a brown suspension. Since the Cu^{2+} ions exist as free ions, the overall concentrations of the reactants are higher. When the reaction was carried out in the presence of ammonia, copper nanofluid was obtained.

The standard half cell potential for the reduction of copper ion is 0.34 V.



The standard half cell potential for the redox equilibrium of glucose is 0.050 V.



The overall standard state cell potential for the reaction given in equation (3.4) is 0.29 V and hence the reaction as represented in the equation (3.4) is feasible. However the reaction is not run under standard state conditions. It takes place in a solution to which aqueous ammonia has been added. Most of the copper ion is therefore present as

$[\text{Cu}(\text{NH}_3)_4]^{2+}$ complex ion. The half cell potential for the reduction of this complex is considerably smaller than that for the reduction of Cu^{2+} ion. This leads to a significant decrease in the overall cell potential for the reaction because the complex ion is a much weaker oxidizing agent than the Cu^{2+} ion.

The fact that the reaction is run in an aqueous ammonia solution has an effect on the electrode potential of the glucose system also, because a pair of H^+ ions is involved in the redox equilibrium as shown in equation (3.6). The half cell potential for the reaction given in equation (3.6) therefore depends on the pH of the solution. Since two H^+ ions are given off when glucose is oxidized, the reaction quotient for this reaction depends on the square of H^+ ion concentration. A change in solution pH from standard state conditions to pH of 11, therefore results in a decrease of half cell potential for this reaction as per equation (3.7)

$$E_{Gl} = E_{Gl}^{\circ} - \frac{2.303RT}{2F} \log \frac{[\text{C}_6\text{H}_{12}\text{O}_6]}{[\text{C}_6\text{H}_{12}\text{O}_7][\text{H}^+]^2} \quad (3.7)$$

The decrease in the half cell potential results in the increase in the reducing strength of glucose. The increase in the reducing strength of glucose when the reaction is run at pH 11 more than compensates for the decrease in oxidizing strength of Cu^{2+} in the presence of ammonia. Therefore the overall cell potential for the reduction of copper ions to copper metal is actually more favorable in aqueous ammonia than under standard state conditions.

Ammonia is added whenever glucose is used as reducing agent along with stabilizing agents such as SLS and PVP, for the above said reasons. However ammonia is not used, with glucose in the presence of CTAB. This is because the use of ammonia disturbs the pH condition required for the proper functioning of CTAB.

Effect of dilution: It was observed that the particle size decreased with the increase in the extent of dilution from 0 to 100 mL of water. The particles yielded had 36 nm, 35 nm, 26

nm and 21 nm size for 0, 50 mL, 75 mL and 100 mL dilution respectively. For 100 mL dilution the reaction proceeded very slowly due to the decrease in effective concentration of the reacting species. With the increase in the dilution the proximity between the precipitating metal atoms decreases and hence the collision between them is reduced preventing the particle growth and hence resulting in smaller size of the nanoparticles formed.

Effect of addition of SLS: The concentration of the surfactant SLS, also played a role in controlling the size of the particle as well as stability of the nanofluid. The effect on size of the particle with increase in surfactant concentration is as shown in Table 3.2.

Table 3.2 Effect of concentration of SLS on the size of copper particles prepared by the reduction of copper nitrate by glucose

Effective concentration of SLS in the reaction mixture (mM)	Particle Size (nm)
0	58
5	36
25	28
50	19

The results clearly indicate that SLS acts as a capping agent and hence restricts the growth of the particles. As the SLS concentration increases, the particle size decreases. This indicates that in this case SLS does not facilitate the aggregation of particles by the formation of multi-mers as observed in the case of reduction by ascorbic acid. Sedimentation measurements showed that the nanofluid was stable up to 3 weeks at room temperature under stationary state.

Effect of power of microwave radiation and irradiation duration: When the reaction mixture was irradiated at 30 % power microwave for 5 minutes and at 50 % power for duration of 2.5 minutes the reactions were incomplete and size of the particles obtained

were 20 nm. As power was increased (50 % to 70 % to 90 %) for 5 minutes irradiation duration the particle size was found to decrease (28 nm, 25 nm to 19 nm). With the increase in irradiation duration at 50 % power the size increased as shown in Table 3.3. The observed trend is identical to the results mentioned in the case of reduction using ascorbic acid.

Table 3.3 Effect of irradiation duration on the size of copper particles prepared by the reduction of copper nitrate by glucose in the presence of SLS

Irradiation duration (min)	Particle Size (nm)
2.5	20
5	28
7.5	32
10	35

Fig. 3.24 shows a typical TEM image (A) and FESEM image (B) of the prepared nanoparticles. The images reveal that the particles are somewhat spherical in shape. The sizes obtained from the XRD results match well with that of the TEM and FESEM results.

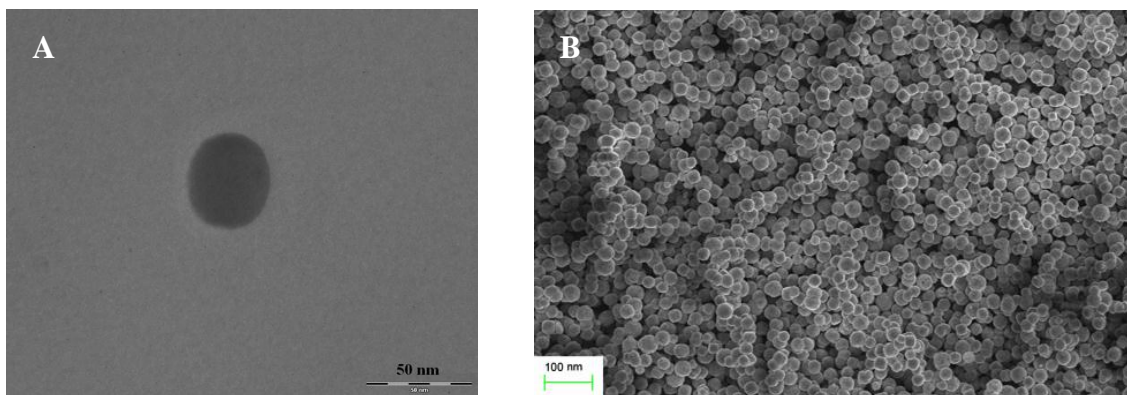


Fig. 3.24 (A) TEM image and (B) FESEM image of copper nanoparticles prepared by the reduction of copper nitrate by glucose in the presence of SLS

➤ **Results of thermal conductivity and viscosity measurements**

The thermal conductivity of the as synthesized nanofluid was found to be $0.834 \text{ W m}^{-1} \text{ K}^{-1}$ when the weight fraction of copper nanoparticles was 0.299 %. The variation of thermal conductivity ratio with nanoparticle weight fraction is as shown in Fig. 3.25. The thermal conductivity of the nanofluid increased linearly with the increase in the particle concentration. Maximum thermal conductivity of $0.968 \text{ W m}^{-1} \text{ K}^{-1}$ was observed at a particle weight fraction of 0.15 % after this the thermal conductivity showed a gradual decrease. The increase in thermal conductivity with the increase in particle weight fraction may be due to the increase in amount of stably dispersed copper nanoparticles which basically have high thermal conductivity. The free Brownian motion of the copper particles may have also facilitated higher thermal conductivity (Singh 2008; Wang et al. 2011b). But after certain level of particle loading, due to higher number of particles per unit volume the movements of particles are hindered and hence there will be restriction of Brownian motion of the particles. This might have led to the gradual decrease in thermal conductivity with increase in particle weight fraction after 0.15 %.

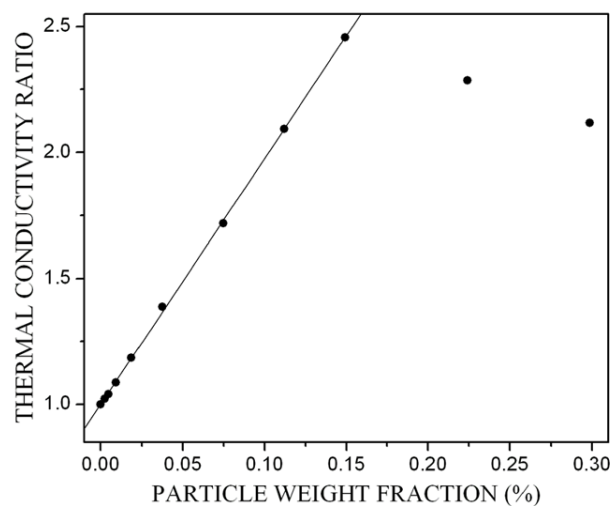


Fig. 3.25 Variation of thermal conductivity ratio with particle weight fraction for copper nanofluid prepared by the reduction of copper nitrate by glucose in the presence of SLS

The viscosity measurements of the nanofluid showed trends similar to that of the nanofluid prepared by the reduction of copper nitrate by ascorbic acid. Fig. 3.26 demonstrates the Newtonian behavior of the copper nanofluid and the variation of viscosity with particle loading and temperature.

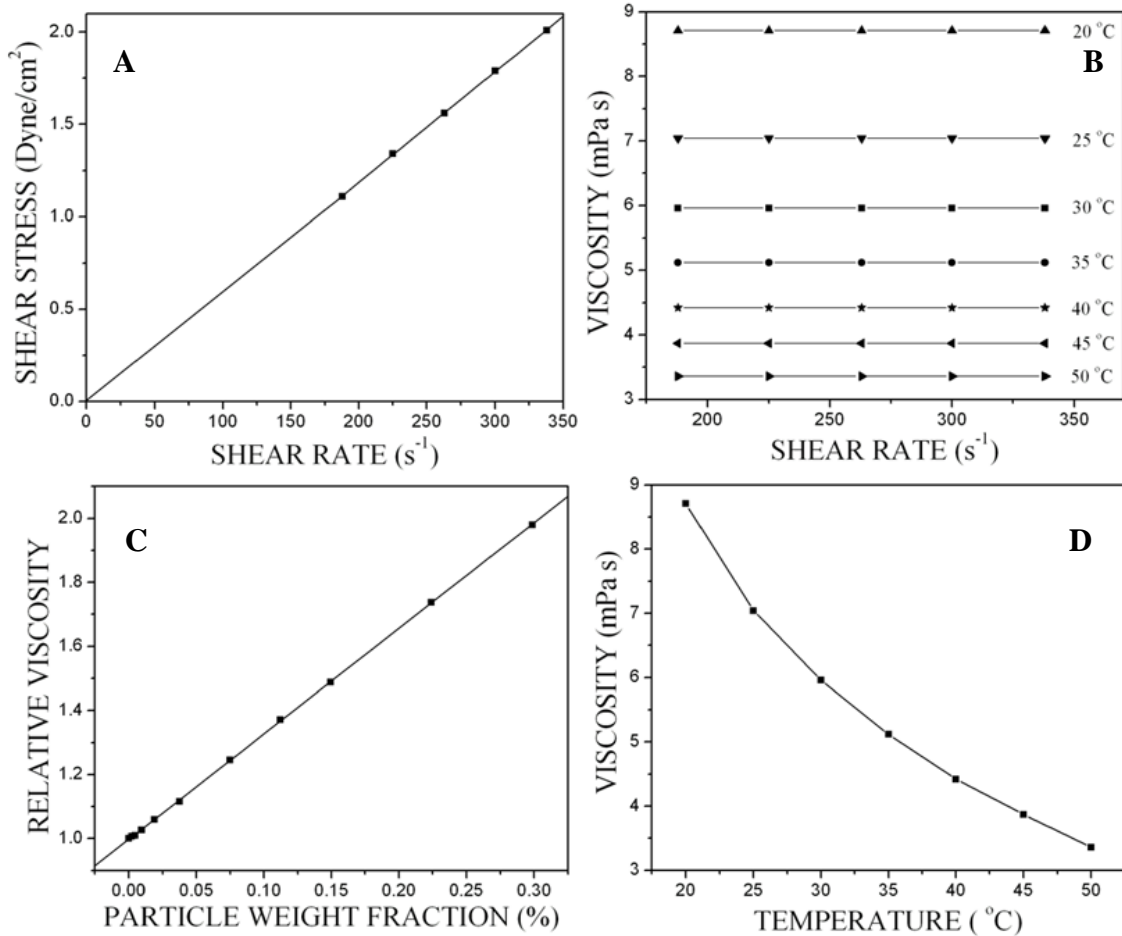


Fig. 3.26 Viscosity measurements of copper nanofluid prepared by the reduction of copper nitrate by glucose in the presence of SLS. (A) Shear stress verses shear rate; (B) Viscosity as a function of shear rate at different temperatures; (C) Variation of relative viscosity with particle weight fraction; (D) Viscosity as a function of temperature

3.1.1.3 Nanofluids synthesized using copper sulphate and ascorbic acid

➤ *Results of variation in reaction parameters*

Effect of pH, ratio of reactants and dilution: In the case of reduction of copper sulfate using ascorbic acid it was observed that pH of the reaction mixture did not play a role in determining the size of the particles formed. When sulfuric acid was added to bring down the pH of the reaction mixture to 3, the size of the particles remained the same as at higher pH.

Synthesis was carried out at different concentrations of ascorbic acid. It was observed that whenever the molar ratio of ascorbic acid to copper sulfate was less than 10 the reaction did not go for completion. Hence always molar ratio of more than 10 was maintained. Under thermal conditions the size decreased from 29 nm to 26nm to 24 nm with the increase in molar ratio of ascorbic acid to copper sulphate from 10 to 20 to 40 and under microwave irradiation it decreased from 32 nm to 29 nm to 26 nm. The decrease in size of the particles with increase in the concentration of ascorbic acid is due to the increase in rate of nucleation similar to the reduction of copper nitrate by glucose.

The reaction mixture was diluted with 50 mL, 100 mL, 150 mL and 200 mL of water. The size of the copper particles decreased from 29 nm which was obtained without dilution to 18 nm for 200 mL dilution. The variation in size is as shown in Table 3.4.

Table 3.4 Effect of dilution on the size of copper particles prepared by the reduction of copper sulfate by ascorbic acid in the presence of SLS

Dilution (mL)	Particle Size (nm)
0	29
50	25
100	22
150	19
200	18

The observed decrease in size of the particles is because of decrease in collision of the particles leading to lesser agglomeration and growth of the initially formed nuclei. The trend is similar to that in the case of reduction of copper nitrate by glucose.

Effect of addition of SLS: To prepare stable copper nanofluids 0.01 M SLS was added. The concentration of SLS was changed to see its effect on the size of particles. The results are summarized in Table 3.5.

Table 3.5 Effect of concentration of SLS on the size of copper particles prepared by the reduction of copper sulfate by ascorbic acid

Effective concentration of SLS in the reaction mixture (mM)	Particle size (nm)
0	54
5.26	29
26.3	33
52.6	40

The observed trend in the size is similar to that in the case of nanofluids prepared by reducing copper nitrate with ascorbic acid. Sedimentation measurements were used to evaluate the stabilization of nanofluids. In the absence of SLS the solution was not stable. In the presence of SLS, nanofluids were found to be stable up to 3 weeks in stationary state at room temperature. This indicates that the addition of SLS helps in achieving the required fluid stability by keeping the particles suspended and by preventing the growth and agglomeration of the particles.

Effect of power of microwave radiation and irradiation duration: In order to study the effect of power of microwave radiation on the size of the particles the solution was subjected to varying power for duration of 3 minutes. At 30 % power the size obtained was 29 nm but the power was not sufficient for the reaction to complete. At 50 %, 70 % and 90 % power the particle size was 32 nm, 28 nm and 20 nm, respectively. The

microwave radiation causes intense friction and collision of molecules thereby increasing the nucleation rate and reducing the growth of particles.

When the irradiation duration was increased from 3 minutes to 7 minutes at 50 % power the size of the particles decreased from 32 nm to 28 nm as shown in the Table 3.6. The longer duration of irradiation could have caused the reduction in size because of disintegration of the particles under prolonged turbulent conditions.

Table 3.6 Effect of irradiation duration on the size of copper particles prepared by the reduction of copper sulfate by ascorbic acid in the presence of SLS

Irradiation duration (min)	Particle size (nm)
3	32
5	30
7	28

TEM and FESEM have been used to investigate the morphology as well as size of the particles. Fig. 3.27 shows a typical TEM image (A) and FESEM image (B) of the obtained product.

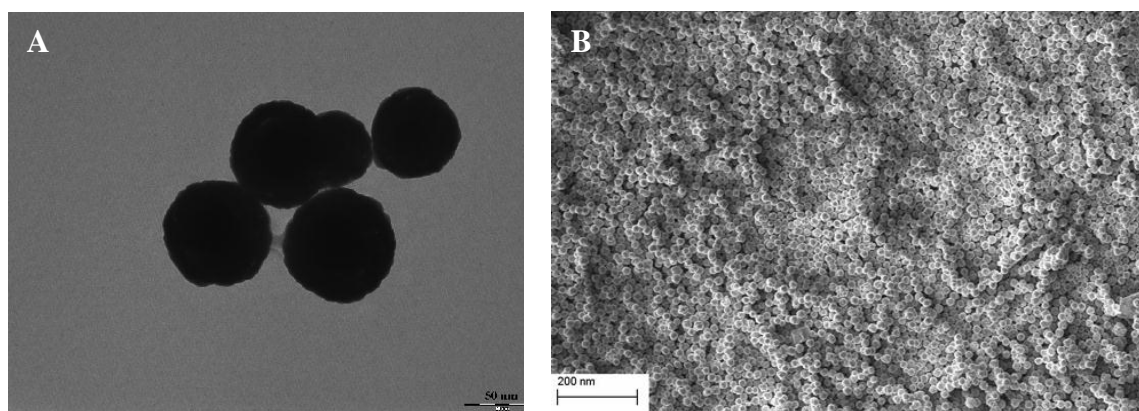


Fig. 3.27 (A) TEM image and (B) FESEM image of copper nanoparticles prepared by the reduction of copper sulfate by ascorbic acid in the presence of SLS

The images reveal that the particles are somewhat spherical in nature. The sizes obtained from the XRD results match well with that of the TEM and FESEM results.

➤ ***Results of thermal conductivity and viscosity measurements***

The thermal conductivity of the as synthesized nanofluid was found to be $0.912 \text{ W m}^{-1} \text{ K}^{-1}$ when the weight fraction of copper nanoparticles was 0.097 %. The variation of thermal conductivity ratio with nanoparticle weight fraction is as shown in Fig. 3.28. The trend is similar to that in the case of nanofluids synthesized using copper nitrate precursor and ascorbic acid.

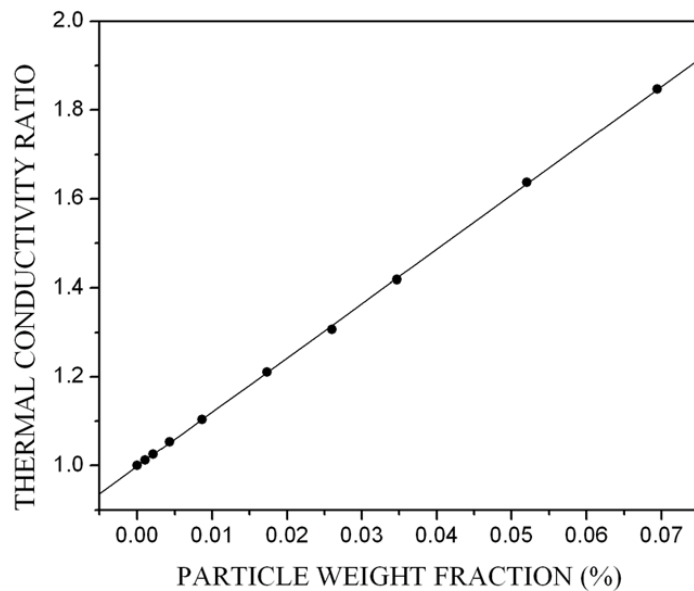


Fig. 3.28 Variation of thermal conductivity ratio with particle weight fraction for copper nanofluid prepared by the reduction of copper sulfate by ascorbic acid in the presence of SLS

The viscosity measurements of the nanofluid showed trends similar to that of nanofluid prepared by reduction of copper nitrate by ascorbic acid. Fig. 3.29 demonstrates the Newtonian behavior of the copper nanofluid and the variation of viscosity with particle weight fraction and temperature.

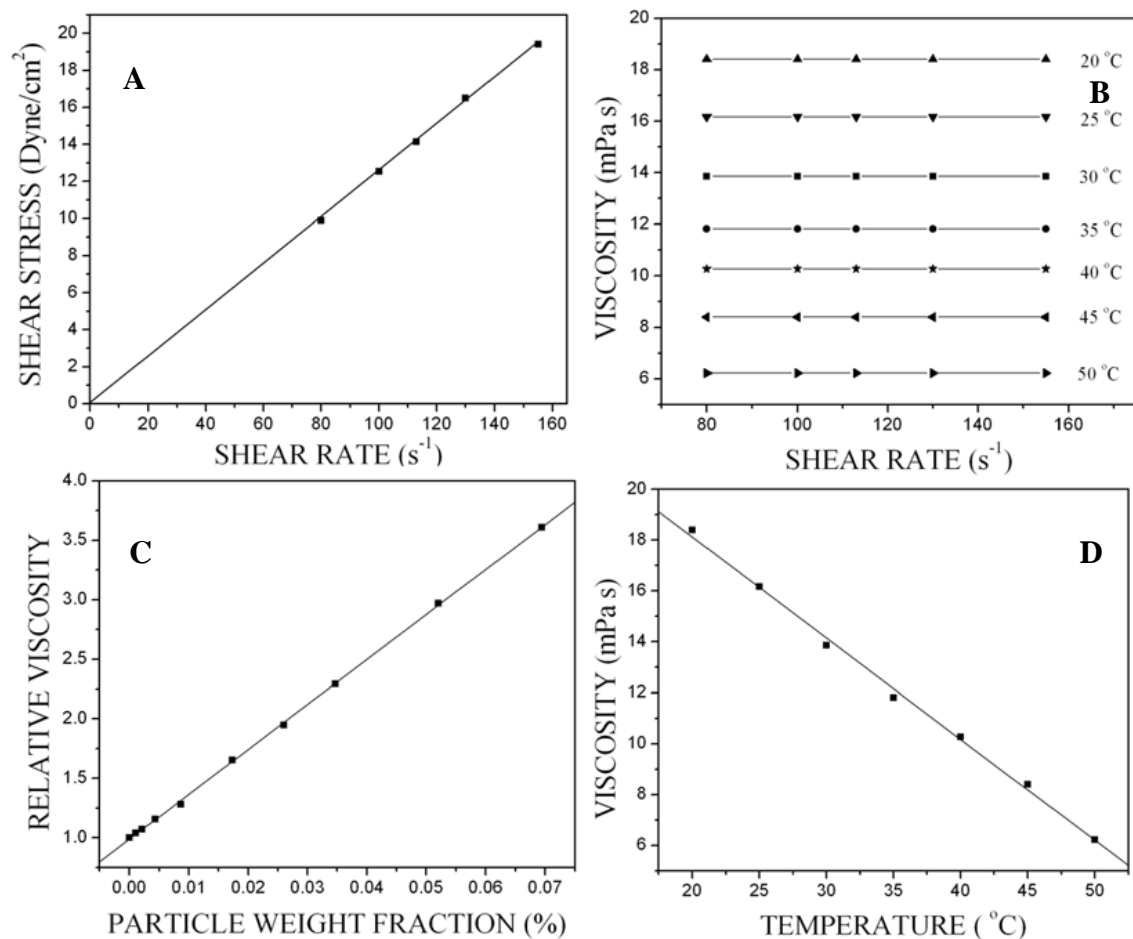


Fig. 3.29 Viscosity measurements of copper nanofluid prepared by the reduction of copper sulfate by ascorbic acid in the presence of SLS. (A) Shear stress verses shear rate; (B) Viscosity as a function of shear rate at different temperatures; (C) Variation of relative viscosity with particle weight fraction; (D) Viscosity as a function of temperature

3.1.1.4 Nanofluids synthesized using copper sulphate and glucose

➤ Results of variation in reaction parameters

Effect of ratio of reactants: The effect of amount of glucose added on the size of copper particles have been studied both under thermal and microwave conditions. It was

observed that whenever the molar ratio of glucose to copper sulfate was less than 4.2 the reaction did not go for completion. Hence always molar ratio of more than 4.2 was maintained. The results are as shown in the Table 3.7.

Table 3.7 Effect of ratio of reactants on the size of copper particles prepared by the reduction of copper sulfate by glucose in the presence of SLS

Molar ratio of glucose to copper sulphate	Particle Size (nm)	
	Thermal	Microwave
4.2	38	40
8.3	32	33
13.8	27	24

The results indicate that the size of the particle decreases with the increase in the concentration of glucose. This is because of the increase in the nucleation rate leading to formation of smaller particles similar to the case of reduction of copper nitrate precursor by glucose.

Effect of dilution: The reaction mixtures were diluted with varying amount of water. It was seen that with dilution the size of the particle decreased. The particle size ranged between 32 nm for zero dilution to 21 nm for 50 mL dilution. It further decreased to 16 nm for 100 mL dilution. The observed trend goes hand in hand with the trend observed for dilution in the case of nanofluids synthesized by the reduction of copper sulfate using ascorbic acid.

Effect of addition of SLS: The effect of surfactant concentration on the particle size is as shown in the results, summarized in Table 3.8. It was observed that the addition of SLS as a surfactant decreases the size of the copper nanoparticles. This could be attributed to the capping effect of SLS resulting in restriction on the growth of particles and controlling the size of copper particles.

Surfactant also provided the required stability to the fluid. In the absence of surfactant the fluid was highly unstable. The fluid was found to be stable for a minimum period of 6 weeks at room temperature under stationary conditions.

Table 3.8 Effect of concentration of SLS on the size of copper particles prepared by the reduction of copper sulfate by glucose

Effective concentration of SLS in the reaction mixture (mM)	Particle Size (nm)
0	48
5	32
25	27
50	23

Effect of power of microwave radiation and irradiation duration: The reaction was carried out at varying power of microwave radiation and irradiation duration. Irradiation for 5 minutes with 30 % power yielded particles of 13 nm but the reaction was not complete. At 50 % power the reaction proceeded towards completion. For 50 %, 70 % and 90 % power the size of the particles were 33 nm, 28 nm and 19 nm respectively.

The irradiation duration also had an effect on size as well as progress of reaction. For 2.5 minutes irradiation duration the particles formed had a size of 30 nm but the reaction was incomplete. For 5 minutes, 7.5 minutes and 10 minutes irradiation duration the sizes obtained were 33 nm, 28 nm and 17 nm, respectively. The observed trend is identical to the trend observed in the case of reduction of copper sulfate using ascorbic acid.

Typical TEM image (A) and FESEM image (B) are shown in Fig. 3.30. The particles are of irregular shape. The sizes obtained from the XRD results match well with that of the TEM and FESEM results.

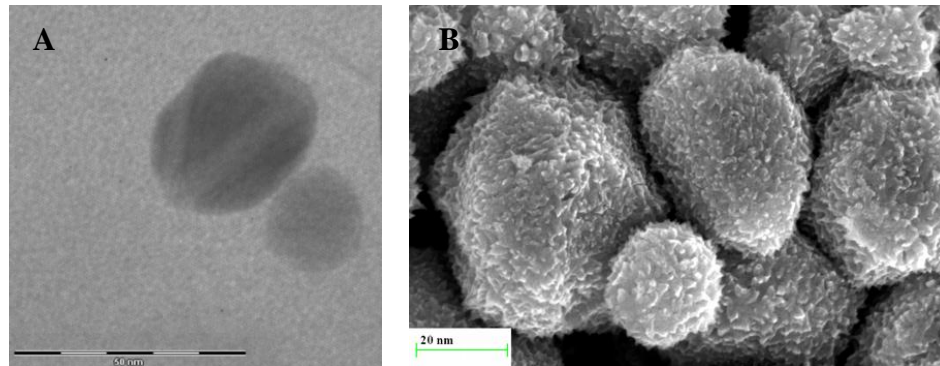


Fig. 3.30 (A) TEM image and (B) FESEM image of copper nanoparticles prepared by the reduction of copper sulfate by glucose in the presence of SLS

➤ *Results of thermal conductivity and viscosity measurements*

The thermal conductivity of the as synthesized nanofluid was found to be $0.812 \text{ W m}^{-1} \text{ K}^{-1}$ when the weight fraction of copper nanoparticles was 0.3 %. The variation of thermal conductivity ratio with nanoparticle weight fraction is as shown in Fig. 3.31.

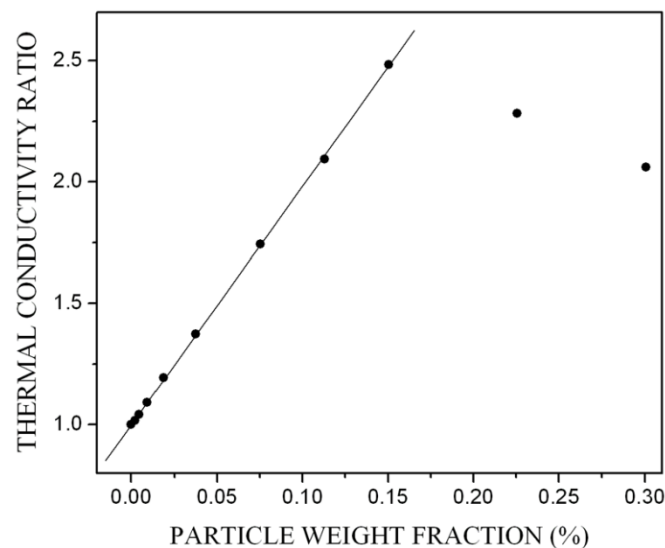


Fig. 3.31 Variation of thermal conductivity ratio with particle weight fraction for copper nanofluid prepared by the reduction of copper sulfate by glucose in the presence of SLS

With the increase in the weight fraction up to 0.15 %, the thermal conductivity increases and shows a maximum conductivity of $0.979 \text{ W m}^{-1} \text{ K}^{-1}$. On further increasing the nanoparticle weight fraction, the thermal conductivity decreased. The trend is similar to that in the case of nanofluids synthesized using copper nitrate precursor and glucose.

The viscosity measurements of the nanofluid showed trends similar to that of nanofluid prepared by the reduction of copper nitrate by ascorbic acid. Fig. 3.32 demonstrates the Newtonian behavior of the copper nanofluid and the variation of viscosity with particle loading and temperature.

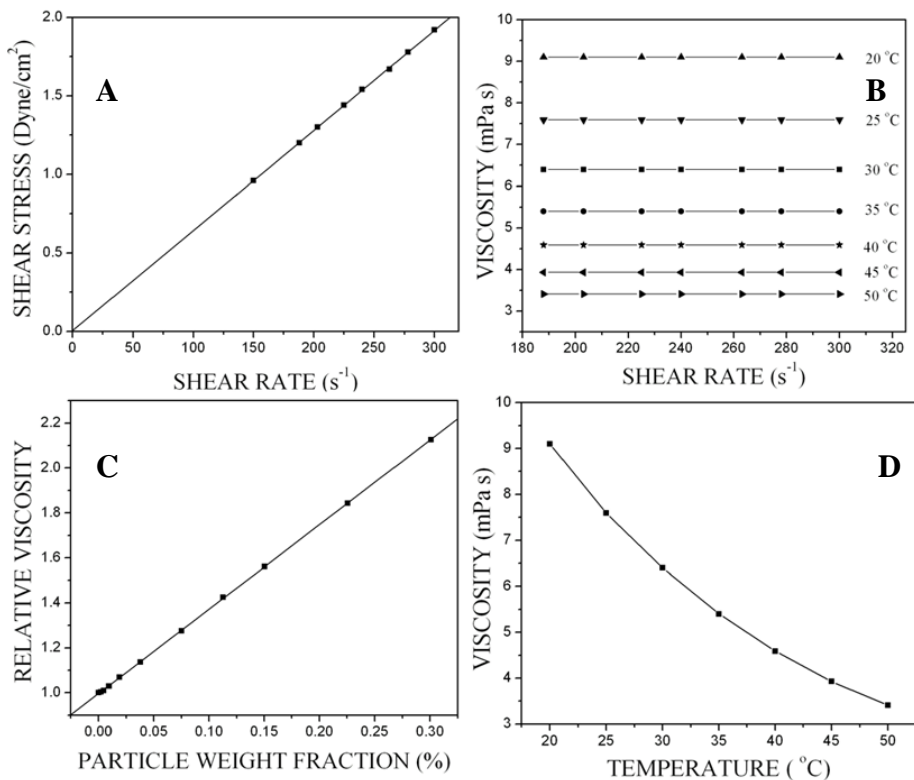


Fig. 3.32 Viscosity measurements of copper nanofluid prepared by the reduction of copper sulfate by glucose in the presence of SLS. (A) Shear stress verses shear rate; (B) Viscosity as a function of shear rate at different temperatures; (C) Variation of relative viscosity with particle weight fraction; (D) Viscosity as a function of temperature

3.1.1.5 Nanofluids synthesized using copper acetate and ascorbic acid

➤ Results of variation in reaction parameters

Effect of pH: To study the effect of pH of the reaction mixture, sulfuric acid was added during reduction. When the pH of the reaction mixture was brought down from 7 to 3 the size of the particles increased from 13 nm to 29 nm. The observations are similar to the ones observed for the reduction of copper nitrate; due to the decrease in the reduction power of ascorbic acid with the decrease in pH, the size of the resulting particles increases.

Effect of ratio of reactants and dilution: The synthesis of copper nanofluids was carried out in thermal as well as microwave conditions at different concentrations of ascorbic acid. It was observed that whenever the molar ratio of ascorbic acid to copper acetate was less than 4 the reaction did not go for completion. Hence always molar ratio of more than 4 was maintained.

During conventional heating size increased from 13 nm to 24 nm to 27 nm as the molar ratio of ascorbic acid to copper acetate was increased from 4 to 8 to 16, respectively, whereas during irradiation with microwave, the particle size decreased from 33 nm to 21 nm to 17 nm. The trend is similar to that observed in case of copper nitrate reduction using ascorbic acid.

Dilution of the reaction mixture with water had an effective impact over the size of particles and the results are listed in Table 3.9. The decrease in the size of particles with the increase in dilution is due to the decrease in overall concentration of solution leading to fewer collisions of precipitating atoms and thus reduction in the growth of the particles.

Table 3.9 Effect of dilution on the size of copper particles prepared by the reduction of copper acetate by ascorbic acid in the presence of SLS

Dilution (mL)	Particle Size (nm)
0	13
50	11
100	8
150	6
200	5

Effect of addition of SLS: The reaction was carried out in the absence of SLS and in presence of varying concentration of SLS. The effect of SLS concentration is evident from the results in Table 3.10.

Table 3.10 Effect of concentration of SLS on the size of copper particles prepared by the reduction of copper acetate by ascorbic acid

Effective concentration of SLS in the reaction mixture (mM)	Particle Size (nm)
0	43
5.26	13
26.3	28
52.6	36

The effect of SLS on the particle size is similar to that in the case of nanofluids prepared using copper nitrate and ascorbic acid. SLS also acts as a stabilizing agent for the resulting fluid. The nanofluid was stable up to 8 weeks under stationary state at room temperature.

Effect of power of microwave radiation and irradiation duration: The reaction mixture was subjected to varying power of microwave radiation for duration of 3 minutes. At 30 % power the size of the particle obtained was 36 nm. But the reaction was not complete. The solution retained a bluish green tinge. When the power was increased from 50 % to 70 % to 90 % the size of the particle decreased from 33 nm to 28 nm to 19 nm, respectively.

With the increase in irradiation duration from 3 minutes to 10 minutes the size of the particle decreased from 33 nm to 9 nm. The observed trend is similar to the one observed in the case of reduction of copper sulfate using ascorbic acid.

A typical TEM image of the copper nanofluid at 200 mL dilution is as shown in the Fig. 3.33. The shape of the particles is somewhat irregular. The sizes obtained from the XRD results match well with that of the TEM results.

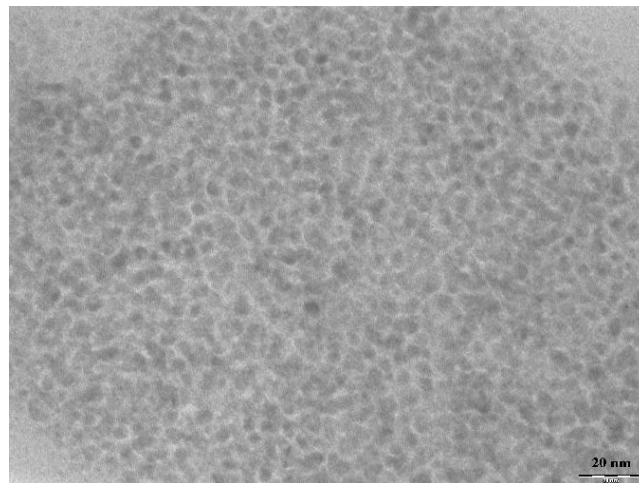


Fig. 3.33 TEM image of copper nanofluid prepared by the reduction of copper acetate by ascorbic acid in the presence of SLS

➤ **Results of thermal conductivity and viscosity measurements**

The thermal conductivity of the as synthesized nanofluid was found to be $1.68 \text{ W m}^{-1} \text{ K}^{-1}$ when the weight fraction of copper nanoparticles was 0.242 %. The variation of thermal conductivity ratio with nanoparticle weight fraction is as shown in Fig. 3.34. It is seen that with the increase in particle weight fraction the thermal conductivity increased.

The thermal conductivity increased to $1.92 \text{ W m}^{-1} \text{ K}^{-1}$ when the particle weight fraction was 0.13 %. Further increase in the particle concentration decreased the thermal conductivity gradually. The trend is similar to that in the case of nanofluids synthesized using copper nitrate and glucose.

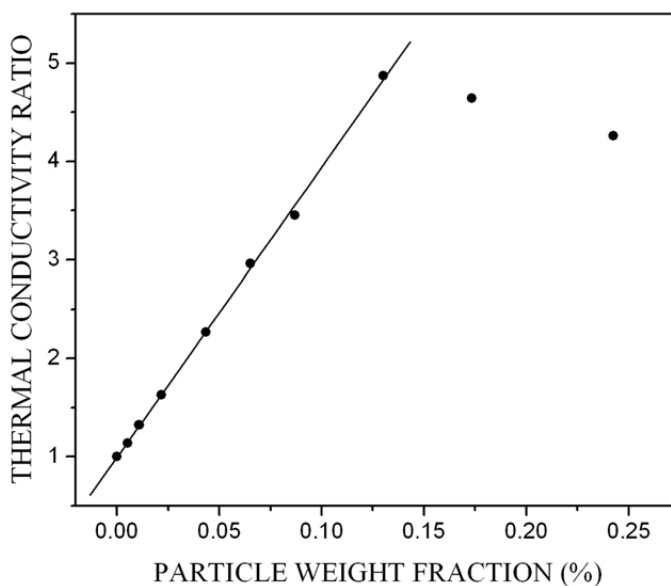


Fig. 3.38 Variation of thermal conductivity ratio with particle weight fraction for copper nanofluid prepared by the reduction of copper acetate by ascorbic acid in the presence of SLS

Fig. 3.35 indicates the Newtonian behavior of the copper nanofluid and the variation of viscosity with particle weight fraction and temperature. The viscosity

measurements of the nanofluid showed trends similar to that of nanofluid prepared by the reduction of copper nitrate by ascorbic acid.

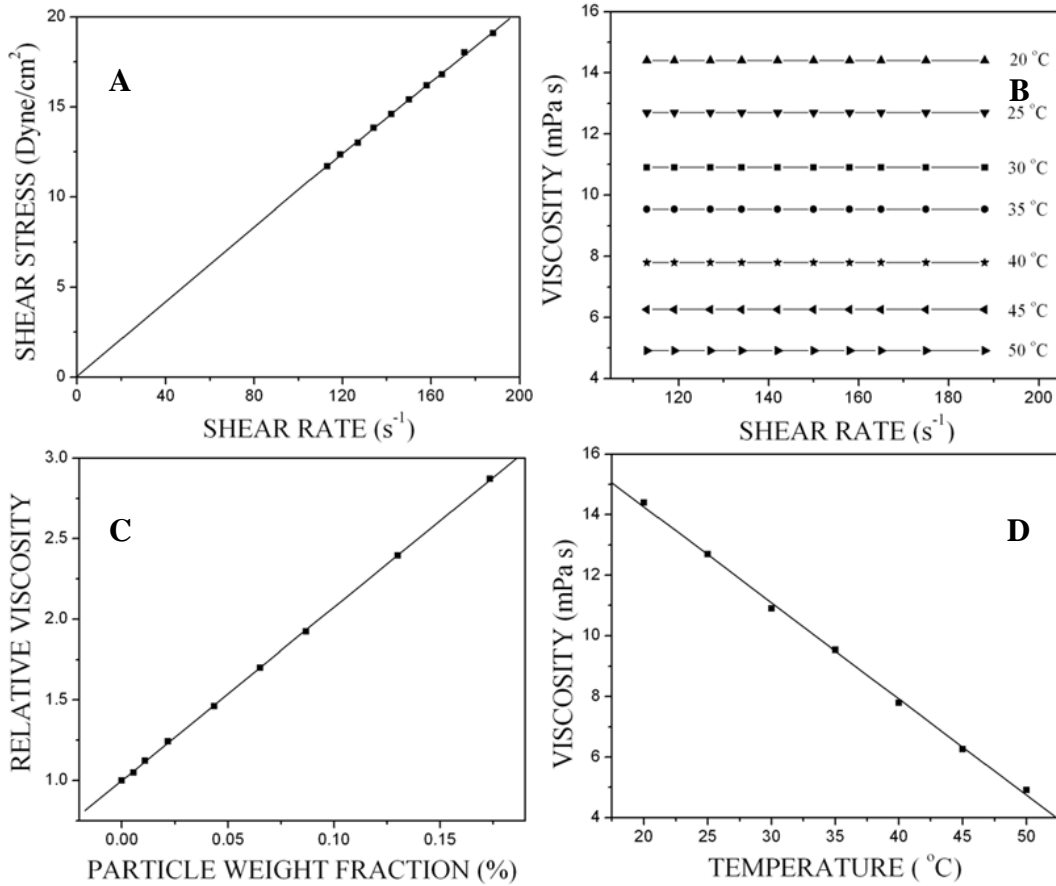


Fig. 3.35 Viscosity measurements of copper nanofluid prepared by the reduction of copper acetate by ascorbic acid in the presence of SLS. (A) Shear stress verses shear rate; (B) Viscosity as a function of shear rate at different temperatures; (C) Variation of relative viscosity with particle weight fraction; (D) Viscosity as a function of temperature

3.1.2 Copper Nanofluids Synthesized in the Presence of CTAB

3.1.2.1 Nanofluids synthesized using copper nitrate and ascorbic acid

➤ Results of variation in reaction parameters

Effect of ratio of reactants: The effect of ratio of reactants on the particle size was studied by varying the molar ratio of ascorbic acid to copper nitrate from 7.5 to 30. It was observed that whenever the molar ratio of ascorbic acid to copper nitrate was less than 7.5 the reaction did not go for completion. Hence always molar ratio of more than 7.5 was maintained. It was found that the particle size decreased from 59 nm to 47 nm under thermal conditions and decreased from 57 nm to 46 nm under microwave irradiation, when the ratio was changed from 7.5 to 30, respectively.

The reduction of cupric ion by ascorbic acid is as shown in equation (3.1). The amount of electrons supplied to cupric ions during reduction is determined by the concentration of reducing agent both in thermal as well as microwave reactions. At lower concentration of reducing agent, the reduction rate of copper precursor is slow and consequently only a few nuclei are formed at the nucleation step, which eventually grow during the growth phase. This leads to the formation of larger sized particles.

With increase in concentration of reducing agent, reduction rate is enhanced, hence more number of nuclei is formed during the nucleation period. With increasing number of nuclei formed, the size of the growing particle decreases because the amount of solute available for particle growth decreases (Park et al. 2007).

Effect of dilution: To study the effect of dilution reactions were carried out by diluting the reaction mixture with different volumes of water. It was found that the particle size decreased with the increase in dilution as shown in Table 3.11. With the increase in dilution, the reaction proceeded very slowly due to the decrease in effective concentration of the reacting species.

The observations can be explained as follows, with the increase in the overall dilution the proximity between the precipitating metal atoms decreases and hence the collision between them is reduced preventing the particle growth and hence resulting in smaller size of the nanoparticles formed.

Table 3.11 Effect of dilution on the size of copper particles prepared by the reduction of copper nitrate by ascorbic acid in the presence of CTAB

Dilution (mL)	Particle Size (nm)
0	59
50	54
100	50
150	48
200	43

Effect of addition of CTAB: The effect of CTAB on the size of the copper nanoparticles as well as stability was studied by varying the concentration of CTAB. The results are tabulated in the Table 3.12.

Table 3.12 Effect of concentration of CTAB on the size of copper particles prepared by the reduction of copper nitrate by ascorbic acid

Effective concentration of CTAB in the reaction mixture (mM)	Particle Size (nm)
0	87
1.67	59
8.33	52
16.67	45

It is seen from the Table that the addition of CTAB decreases the size of the copper particles and the particle size decreases with the increase in the concentration of CTAB. The results suggest that CTAB efficiently restricts their growth which could be attributed to the capping effect of CTAB.

When prepared in the absence of CTAB the nano fluid was unstable and the particles began to settle down. The nanofluid prepared in presence of CTAB was stable up to 6 months. The stability of the nanofluid in the presence of CTAB is attributed to the smaller sizes of the particles, which facilitate their better dispersity in the medium and the fact that addition of CTAB prevents the agglomeration of the nanoparticles.

Effect of power of microwave radiation and irradiation duration: At 30 % microwave power for 3 minutes the reaction was incomplete with size of the resulting particle being 42 nm. When the power was increased to 50 %, the reaction proceeded to completion. When the power of microwave radiation was increased from 50 % to 70 % to 90 % the particle size decreased from 57 nm to 54 nm to 49 nm, respectively. The decrease in particle size with increase in power of microwave radiation is attributed to the formation of large number of small particles due to rapid nucleation.

The effect of microwave irradiation duration on the formation of nanoparticles in the reaction medium was also investigated. The sizes of the particles formed for irradiation duration of 3 minutes, 5 minutes and 7 minutes were 57 nm, 63 nm and 67 nm, respectively. The trend is similar as in the case of SLS for the same precursors. The continued interaction of the particles might be the cause for the growth of the particles, resulting in the increase in particle size.

It may be noted here that when sulfuric acid was used for bringing down the pH of the medium in the presence of CTAB during initial stages of the reaction, the reaction did not proceed. Hence pH variation was not done when CTAB was used as stabilizing agent.

TEM and FESEM have been used to investigate the morphology as well as size of the sample. Fig. 3.36 shows the high magnification TEM image (A) and the FESEM image (B) of the copper nanoparticles. The particles are star shaped. The sizes obtained from the XRD results match well with that of the TEM and FESEM results.

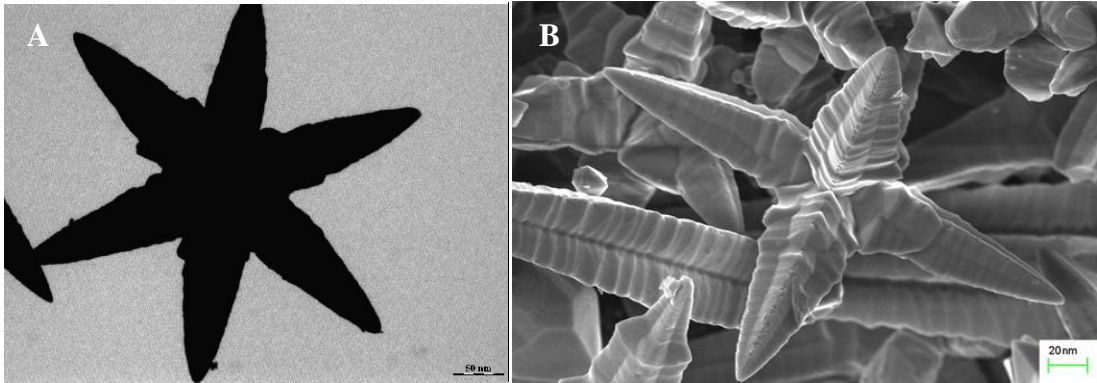


Fig. 3.36 (A) TEM image and (B) FESEM image of copper nanoparticles prepared by the reduction of copper nitrate by ascorbic acid in the presence of CTAB

➤ *Results of thermal conductivity and viscosity measurements*

The thermal conductivity of the as synthesized nanofluid was found to be $4.695 \text{ W m}^{-1} \text{ K}^{-1}$ when the weight fraction of copper nanoparticles was 0.200 %.

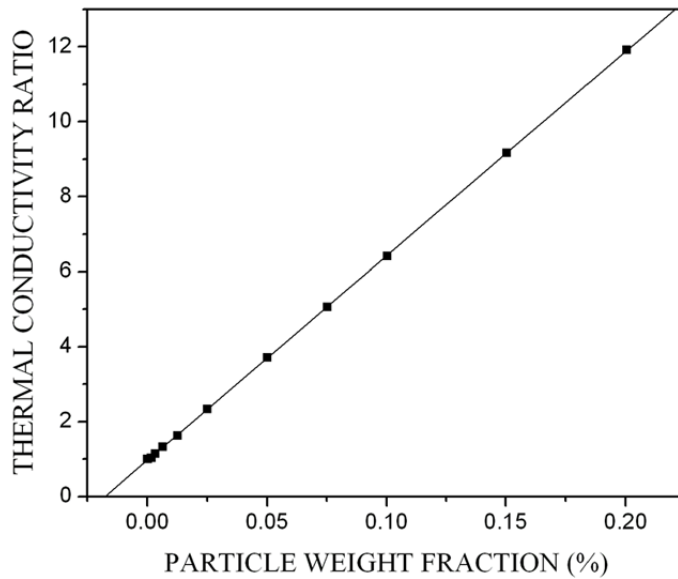


Fig. 3.37 Variation of thermal conductivity ratio with particle weight fraction for copper nanofluid prepared by the reduction of copper nitrate by ascorbic acid in the presence of CTAB

The variation of thermal conductivity ratio with nanoparticle weight fraction is as shown in Fig. 3.37. The trend is similar to that in the case of nanofluids synthesized using same precursors in the presence of SLS.

The viscosity measurements of the nanofluid showed trends similar to that of nanofluid prepared by reduction of copper nitrate by ascorbic acid in the presence of SLS. Fig. 3.38 demonstrates the Newtonian behavior of the copper nanofluid and the variation of viscosity with particle weight fraction and temperature.

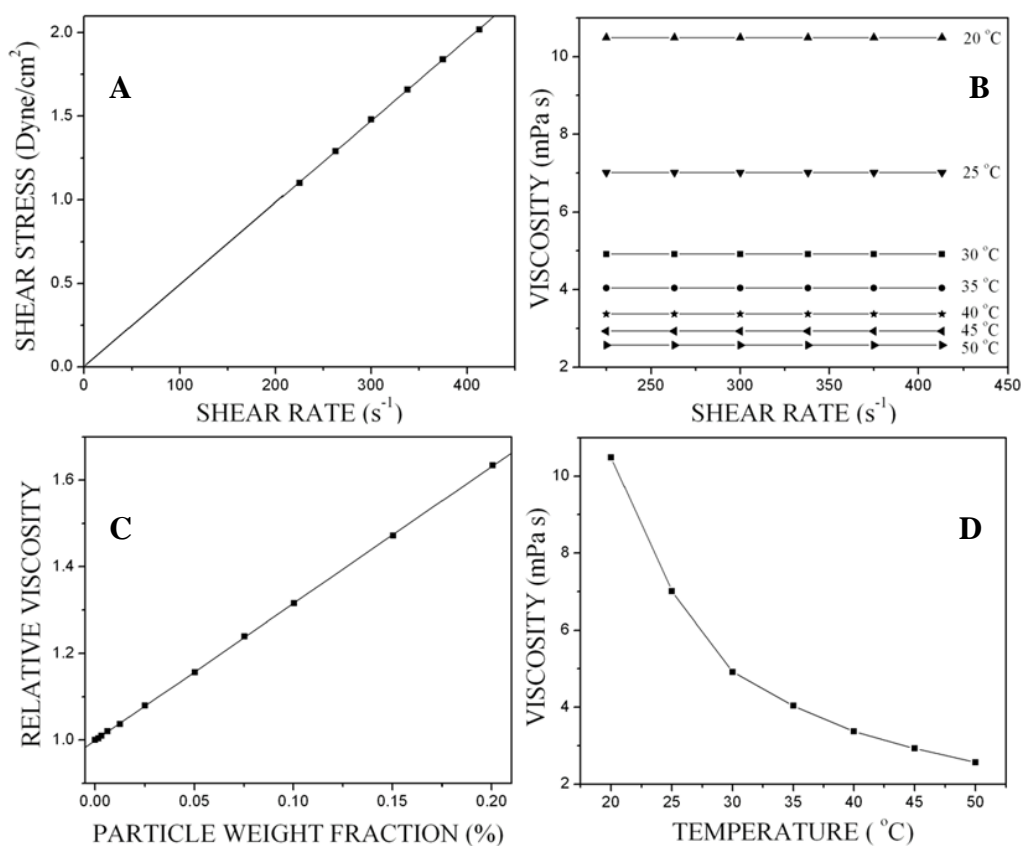


Fig. 3.43 Viscosity measurements of copper nanofluid prepared by the reduction of copper nitrate by ascorbic acid in the presence of CTAB. (A) Shear stress verses shear rate; (B) Viscosity as a function of shear rate at different temperatures; (C) Variation of relative viscosity with particle weight fraction; (D) Viscosity as a function of temperature

3.1.2.2 Nanofluids synthesized using copper sulfate and ascorbic acid

➤ *Results of variation in reaction parameters*

Effect of ratio of reactants and dilution: Synthesis was carried out at different concentrations of ascorbic acid. It was observed that whenever the molar ratio of ascorbic acid to copper sulfate was less than 7.5 the reaction did not go for completion. Hence always molar ratio of more than 7.5 was maintained. In thermal conditions the size decreased from 52 nm to 38 nm with the increase in the molar ratio of ascorbic acid to copper sulfate from 7.5 to 30 and under microwave irradiation it decreased from 49 nm to 36 nm, respectively. The reduction of copper ion by ascorbic acid is as shown in equation (3.1). The decrease in size of the particles with increase in the concentration of ascorbic acid is due to the increase in the rate of nucleation similar to the reduction of copper nitrate by ascorbic acid mentioned above.

It was found that the particle size decreased with dilution. Dilution with 50 mL water resulted in decrease in the size of the particles from 52 nm to 48 nm. It further decreased to 43 nm and 39 nm for 100 mL and 150 mL dilution, respectively. For 200 mL dilution the particle size was 34 nm with reaction proceeding very slowly. The observations are similar to the ones in the case of reduction of copper nitrate discussed in the earlier section.

Effect of addition of CTAB: The effect of CTAB on the stability of the nanofluids and also on the size of the particle formed was studied by adding different concentrations of CTAB to the reaction mixture. The results are summarized Table 3.13. The observed decreasing trend in the size is similar to that observed in the case of copper nanofluids prepared by the reduction of copper nitrate with ascorbic acid in the presence of CTAB. Sedimentation measurements were used to evaluate the stabilization of nanofluids. In the absence of CTAB the solution was not stable. In the presence of CTAB, nanofluids were found to be stable up to 6 months in stationary state at room temperature. This indicates

that CTAB helps in achieving required fluid stability by keeping the particles suspended and by preventing the growth and agglomeration of the particles.

Table 3.13 Effect of concentration of CTAB on the size of copper particles prepared by the reduction of copper sulfate by ascorbic acid

Effective concentration of CTAB in the reaction mixture (mM)	Particle size (nm)
0	71
1.67	52
8.33	45
16.67	40

Effect of power of microwave radiation and irradiation duration: In order to study the effect of power of microwave radiation on the size of the particles the solution was subjected to varying power for duration of 4 minutes. At 30 % power the size obtained was 32 nm but the power was not sufficient for the reaction to complete. At 50 %, 70 % and 90 % power the particle size was 49 nm, 42 nm and 37 nm, respectively. The trend is attributed to the fact that microwave irradiation causes intense friction and collision of molecules thereby increasing the nucleation rate and reducing the growth of particles.

Microwave irradiation for duration of 4 minutes was sufficient for the completion of reaction and yielded particles of size 49 nm. When the irradiation duration was increased from 6 minutes to 8 minutes at 50 % power the size of the particles increased from 53 nm to 58 nm. The trend is similar to the one observed in ascorbic acid reduction of copper nitrate in the presence of CTAB.

Fig. 3.39 shows typical TEM image (A) and FESEM image (B) of the copper nanoparticles. The images reveal that the particles are star like in nature. These particles appear to be brittle as is evident from the broken arms of the star shaped particles found in TEM investigation. The image of the broken arms of the star shaped particles is shown

in inset of Fig. 3.39 (A). The sizes obtained from the XRD results match well with that of the TEM and FESEM results.

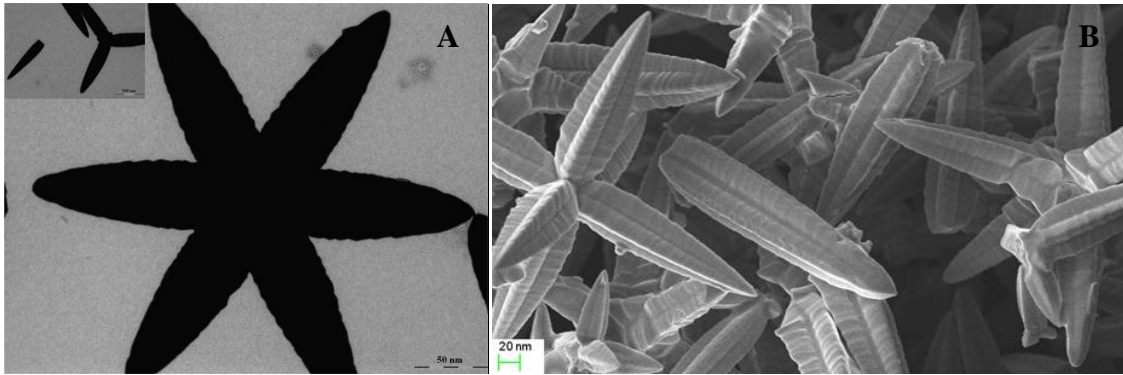


Fig. 3.39 (A) TEM image and (B) FESEM image of copper nanoparticles prepared by the reduction of copper sulfate by ascorbic acid in the presence of CTAB

➤ *Results of thermal conductivity and viscosity measurements*

The thermal conductivity of the as synthesized nanofluid was found to be $4.727 \text{ W m}^{-1} \text{ K}^{-1}$ when the weight fraction of copper nanoparticles was 0.200 %.

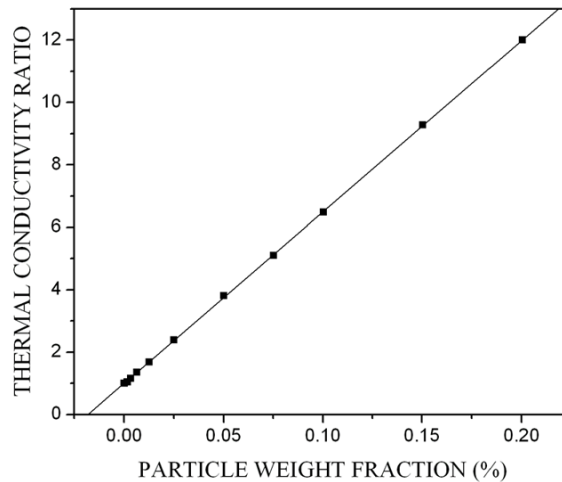


Fig. 3.40 Variation of thermal conductivity ratio with particle weight fraction for copper nanofluid prepared by the reduction of copper sulfate by ascorbic acid in the presence of CTAB

The variation of thermal conductivity ratio with the nanoparticle weight fraction is as shown in Fig. 3.40. The trend is similar to that observed in the case of nanofluids synthesized using copper nitrate in the presence of CTAB.

The viscosity measurements of the nanofluid showed trends similar to that of the nanofluid prepared in the presence of SLS. Fig. 3.41 demonstrates the Newtonian behavior of the copper nanofluid and the variation of viscosity with particle loading and temperature.

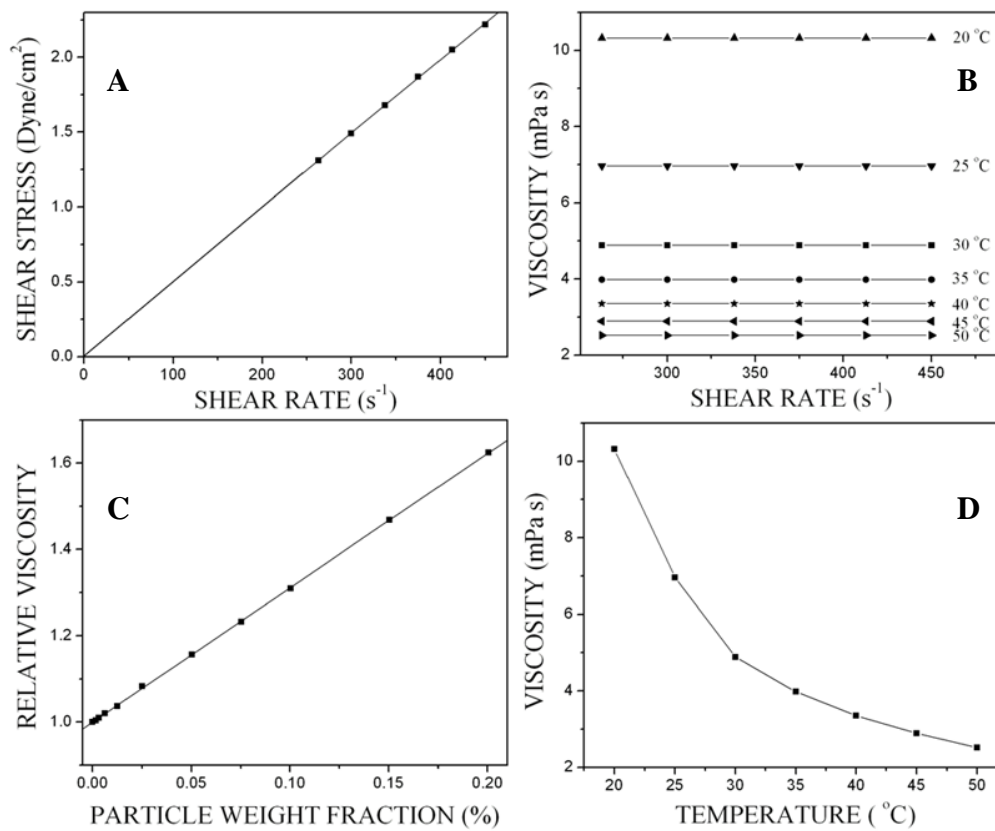


Fig. 3.41 Viscosity measurements of copper nanofluid prepared by the reduction of copper sulfate by ascorbic acid in the presence of CTAB. (A) Shear stress verses shear rate; (B) Viscosity as a function of shear rate at different temperatures; (C) Variation of relative viscosity with particle weight fraction; (D) Viscosity as a function of temperature

3.1.2.3 Nanofluids synthesized using copper acetate and ascorbic acid

➤ *Results of variation in reaction parameters*

Effect of ratio of reactants and dilution: The synthesis of copper nanofluids was carried out in thermal as well as microwave conditions at different concentrations of ascorbic acid. It was observed that whenever the molar ratio of ascorbic acid to copper acetate was less than 3 the reaction did not go for completion. Hence always molar ratio of more than 3 was maintained. During conventional heating the nanoparticle size decreased from 74 nm to 61 nm as the molar ratio of ascorbic acid to copper acetate was increased from 3 to 12, respectively and on irradiation with microwave, the particle size decreased from 69 nm to 59 nm, respectively. The trend is similar to that observed in the case of copper nitrate and copper sulfate reduction in the presence of CTAB.

Dilution of the reaction mixture with water had an effective impact over the size of particles as shown in the Table 3.14.

Table 3.14 Effect of dilution on the size of copper particles prepared by the reduction of copper acetate by ascorbic acid in the presence of CTAB

Dilution (mL)	Particle Size (nm)
0	74
50	68
100	61
150	56
200	49

The decrease in the size of the particles with the increase in dilution is due to the decrease in overall concentration of the solution as mentioned in the earlier sections.

Effect of addition of CTAB: The reaction was carried out in the absence of CTAB and in the presence of varying concentration of CTAB. The results on the effect of concentration of CTAB on the particle size are listed in Table 3.15

Table 3.15 Effect of concentration of CTAB on the size of copper particles prepared by the reduction of copper acetate by ascorbic acid

Effective concentration of CTAB in the reaction mixture (mM)	Particle Size (nm)
0	96
1.67	74
8.33	68
16.67	62

The effect of CTAB on particle size is similar to the ones observed in the case of nanofluids prepared using copper nitrate and ascorbic acid. CTAB also stabilized the resulting fluid. The fluid was stable up to 4 months under stationary state at room temperature.

Effect of power of microwave radiation and irradiation duration: The reaction mixture was subjected to varying microwave powers for duration of 4 minutes. At 30 % power the size of the particle obtained was 44 nm. But the reaction was not complete. When the power was increased from 50 % to 70 % to 90 % the size of the particle decreased from 69 nm to 63 nm to 58 nm. With the increase in irradiation duration from 4 minutes to 6 minutes to 8 minutes the size of the particle increased from 69 nm to 73 nm to 76 nm. The observed trend is similar to the ones mentioned in the earlier sections.

A typical TEM image (A) and FESEM image (B) of the copper nanoparticles are as shown in the Fig. 3.42. The particles are star shaped. The sizes obtained from the XRD results match well with that of the TEM and FESEM results.

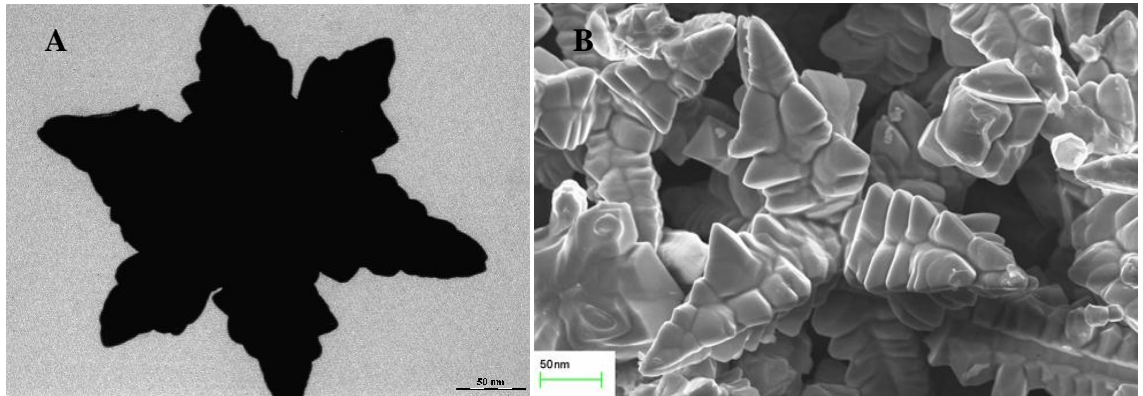


Fig. 3.42 (A) TEM image and (B) FESEM image of copper nanoparticles prepared by the reduction of copper acetate by ascorbic acid in the presence of CTAB

➤ *Results of thermal conductivity and viscosity measurements*

The thermal conductivity of the as synthesized nanofluid was found to be $1.671 \text{ W m}^{-1} \text{ K}^{-1}$ when the weight fraction of copper nanoparticles was 0.501 %. The variation of thermal conductivity ratio with nanoparticle weight fraction is as shown in Fig. 3.43.

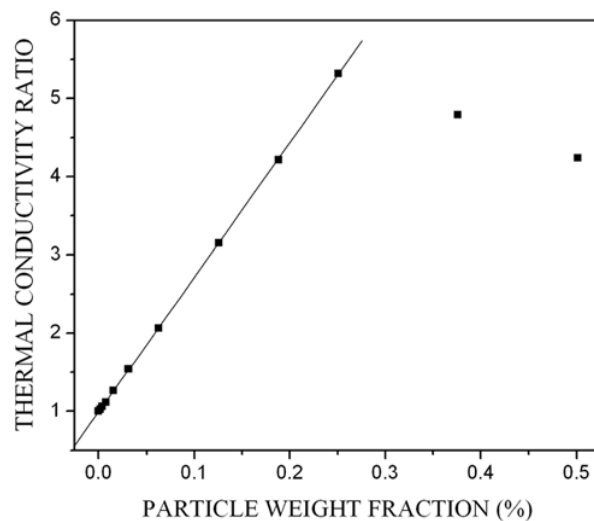


Fig. 3.43 Variation of thermal conductivity ratio with particle weight fraction for copper nanofluid prepared by the reduction of copper acetate by ascorbic acid in the presence of CTAB

It was found that thermal conductivity increased with the increase in particle weight fraction. Maximum thermal conductivity was found to be $2.097 \text{ W m}^{-1} \text{ K}^{-1}$ at a particle loading of 0.251 % and there after it showed a gradual decrease. The trend is similar to that in the case of nanofluids synthesized using copper nitrate precursor and glucose in the presence of SLS.

The viscosity measurements of the nanofluid showed trends similar to that of nanofluid prepared in the presence of SLS. Fig. 3.44 demonstrates the Newtonian behavior of the copper nanofluid and the variation of viscosity with particle weight fraction and temperature.

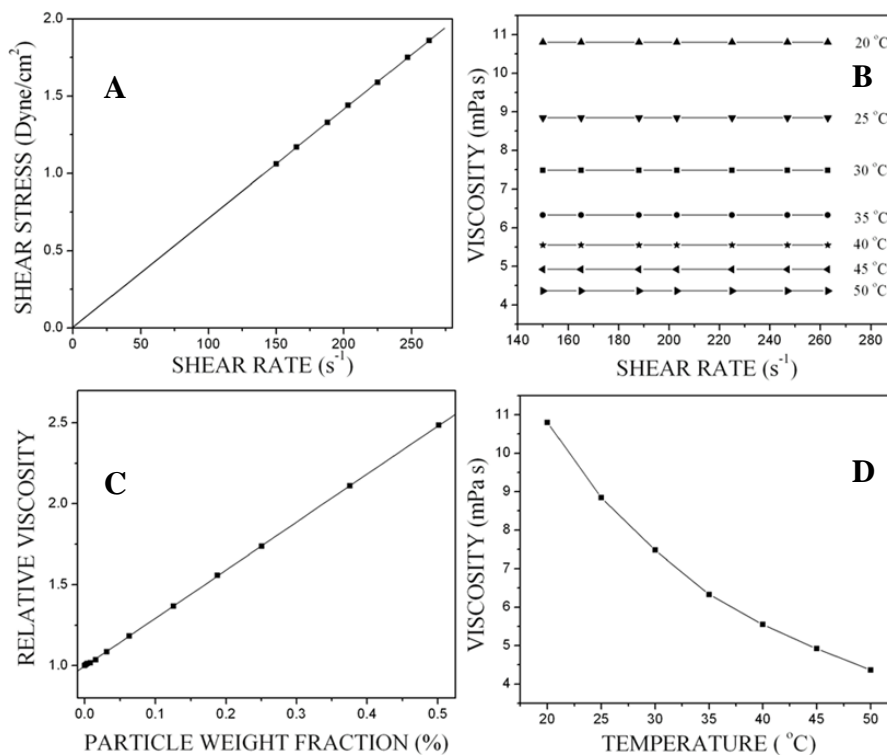


Fig. 3.44 Viscosity measurements of copper nanofluid prepared by the reduction of copper acetate by ascorbic acid in the presence of CTAB. (A) Shear stress verses shear rate; (B) Viscosity as a function of shear rate at different temperatures; (C) Variation of relative viscosity with particle weight fraction; (D) Viscosity as a function of temperature

3.1.3 Copper Nanofluids Synthesized in the Presence of PVP

3.1.3.1 Nanofluids synthesized using copper nitrate and ascorbic acid

➤ *Results of variation in reaction parameters*

Effect of pH: The effect of the pH of the reaction mixture on size of the particle formed was studied. When the pH of the reaction mixture was brought down from 7 to 3 by the addition of sulfuric acid, the size of the particles increased from 32 nm to 56 nm. With the decrease in the pH value, the size of the copper particle was found to be increasing. This trend is attributed to the decrease in the reducing power of ascorbic acid similar to the case of reduction of copper nitrate in the presence of SLS.

Effect of ratio of reactants: The molar ratio of ascorbic acid to copper nitrate was varied from 5 to 20 to study its effect on particle size. It was observed that whenever the molar ratio of ascorbic acid to copper nitrate was less than 5 the reaction did not go for completion. Hence always molar ratio of more than 5 was maintained. It was found that the particle size increased from 32 nm to 49 nm under thermal conditions and decreased from 33 nm to 19 nm under microwave irradiation, when the ratio was changed from 5 to 20, respectively. The particle sizes were 36 nm and 41 nm under thermal conditions and 29 nm and 24 nm under microwave reactions, when the molar ratios were 10 and 15, respectively. The observations can be explained as in the case of ascorbic acid reduction of copper nitrate in the presence of SLS.

Due to the decrease in pH of the solution with the increase in the ascorbic acid content, the reduction power of ascorbic acid decreases and hence the particle size increases in thermal conditions. While in the case of microwave reactions the increased number of collisions due to increase in reducing agent concentration dominates over the pH effect and hence particle size decreases.

Effect of dilution: Reactions were carried out by diluting the reaction mixture with different volumes of water. It was found that the particle size decreased with the increase in dilution. In addition to the initially added 45 mL of water, 55 mL, 105 mL and 155 mL of water was further added. The particles yielded had 32 nm, 26 nm, 22 nm and 19 nm size for 45 mL, 100 mL, 150 mL and 200 mL total dilution, respectively. The observed trend is similar to the ones obtained in the presence of CTAB.

Effect of addition of PVP: The effect of PVP on the size of the copper nanoparticles as well as on the stability was studied by varying the concentration of PVP. The results of particle size variation are tabulated in Table 3.16.

Table 3.16 Effect of concentration of PVP on the size of copper particles prepared by the reduction of copper nitrate by ascorbic acid

Effective concentration of PVP in the reaction mixture (mM)	Particle Size (nm)
0	60
0.45	32
2.27	21
4.55	16

The results in the Table indicate that the addition of PVP decreases the size of the copper particle by the capping action. When prepared in the absence of PVP the nano fluid was unstable and the particles began to settle down but in the presence of PVP even the least stable fluid was stable up to 6 weeks as revealed by the sedimentation measurements. This stability is attributed to the smaller size of the particles and their non agglomerated nature resulting in better dispersion.

Effect of power of microwave radiation and irradiation duration: At 30 % microwave power, for 4 minutes irradiation duration the reaction was incomplete with size of the resulting particle being 25 nm. When the power was increased to 50 %, the reaction

proceeded to completion. When the power of microwave was increased from 50 % to 70 % to 90% the particle size decreased from 33 nm to 28 nm to 21 nm, respectively. The decrease in particle size with increase in the power of microwave radiation is attributed to the formation of large number of small particles due to rapid nucleation.

The effect of microwave irradiation duration on the formation of nanoparticles in the reaction medium was also investigated. For irradiation duration of 4 minutes, the particle size was found to be 33 nm. The particle size increased from 37 nm to 48 nm when the irradiation duration was increased from 7 minutes to 10 minutes, respectively. The observed trend is similar to that observed in the presence of CTAB.

Fig. 3.45 shows the TEM image (A) and the high magnification FESEM image (B) of the copper nanoparticles. The particles are octahedral in shape. The sizes obtained from the XRD results match well with that of the TEM and FESEM results.

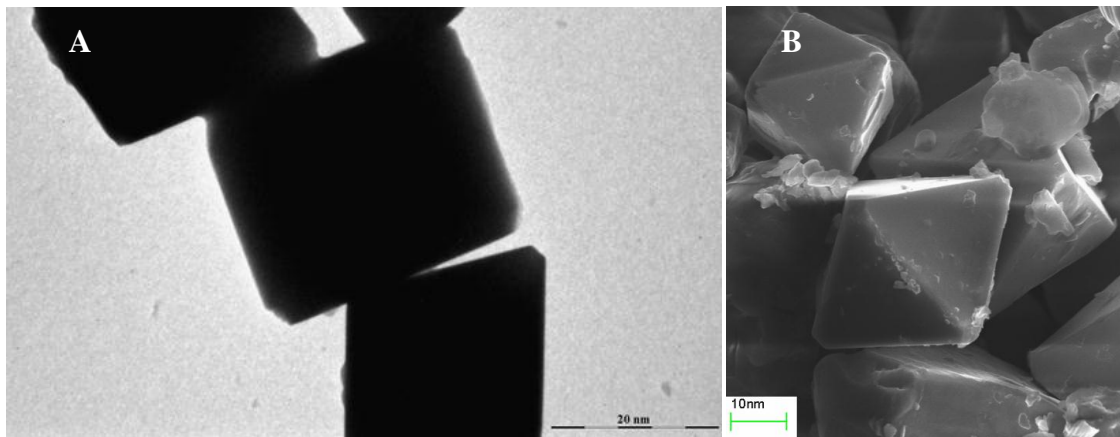


Fig. 3.45 (A) TEM image and (B) FESEM image of copper nanoparticles prepared by the reduction of copper nitrate by ascorbic acid in the presence of PVP

➤ *Results of thermal conductivity and viscosity measurements*

The thermal conductivity of the as synthesized nanofluid was found to be $1.774 \text{ W m}^{-1} \text{ K}^{-1}$ when the weight fraction of copper nanoparticles was 0.167 %. The variation

of thermal conductivity ratio with nanoparticle weight fraction is as shown in Fig. 3.46. The trend is similar to that in the case of nanofluids synthesized using similar precursors in presence of SLS.

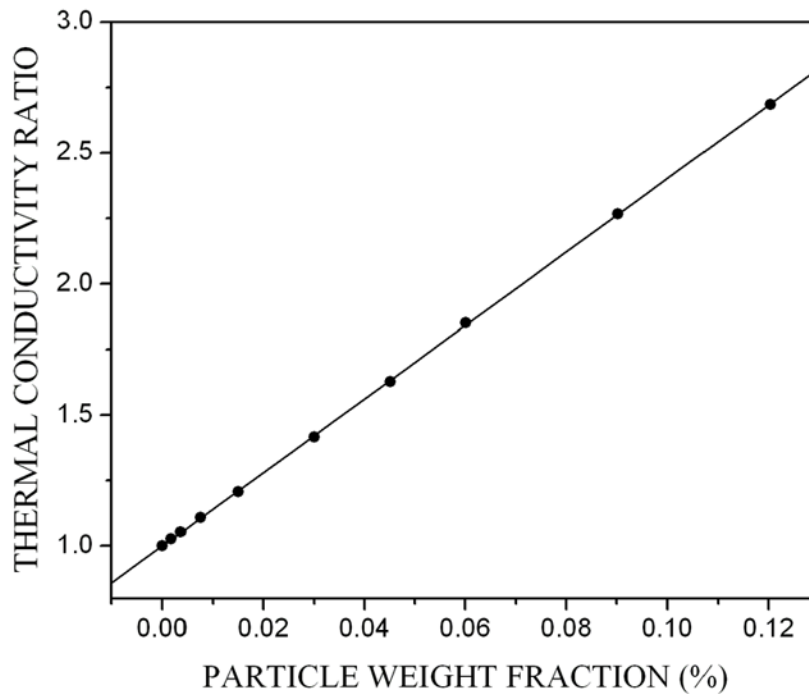


Fig. 3.46 Variation of thermal conductivity ratio with particle weight fraction for copper nanofluid prepared by the reduction of copper nitrate by ascorbic acid in the presence of PVP

The viscosity measurements of the nanofluid showed trends similar to that of nanofluid prepared in the presence of CTAB. Fig. 3.47 demonstrates the Newtonian behavior of the copper nanofluid and the variation of viscosity with particle loading and temperature.

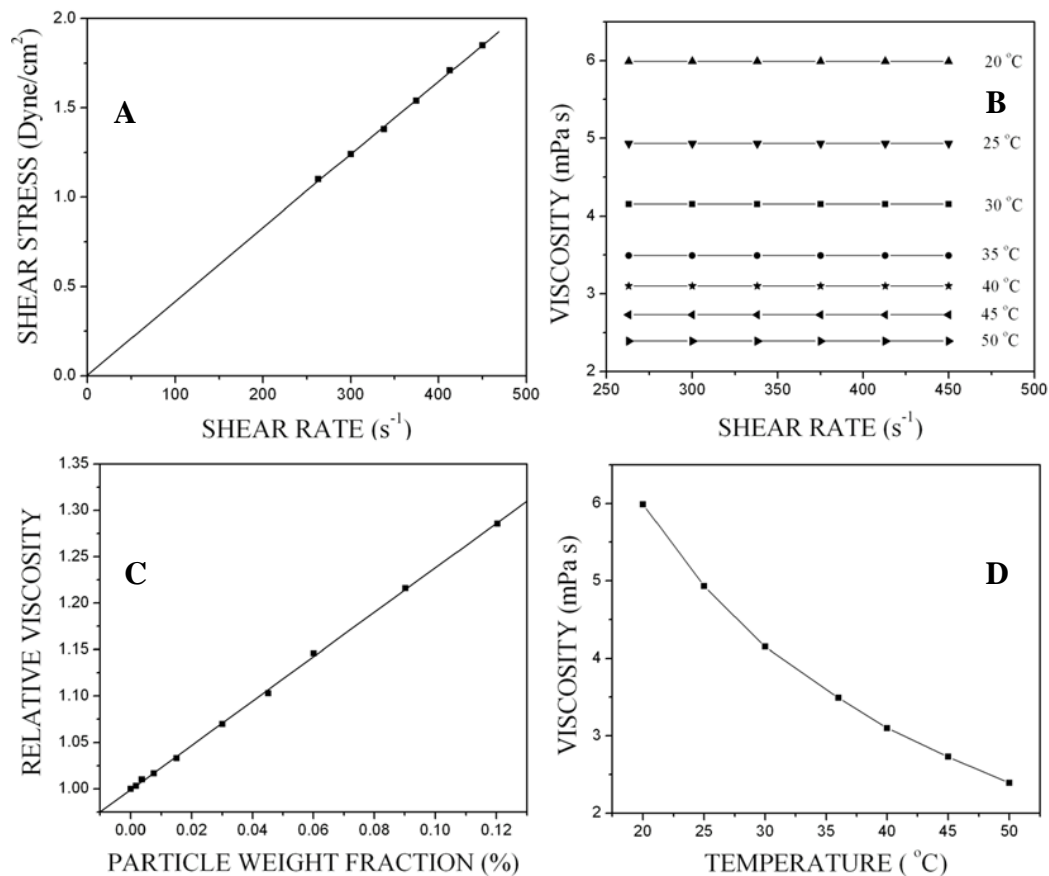


Fig. 3.47 Viscosity measurements of copper nanofluid prepared by the reduction of copper nitrate by ascorbic acid in the presence of PVP. (A) Shear stress verses shear rate; (B) Viscosity as a function of shear rate at different temperatures; (C) Variation of relative viscosity with particle weight fraction; (D) Viscosity as a function of temperature

3.1.3.2 Nanofluids synthesized using copper sulfate and ascorbic acid

➤ Results of variation in reaction parameters

Effect of pH, ratio of reactants and dilution: In the case of reduction of copper sulfate using ascorbic acid it was observed that pH of the reaction mixture did not play a role in

determining the size of the particles formed. When sulfuric acid was added to bring down the pH of the reaction mixture to 3, the size of the particles remained the same as in the absence of sulfuric acid.

Synthesis was carried out at different concentrations of ascorbic acid. It was observed that whenever the molar ratio of ascorbic acid to copper sulfate was less than 10 the reaction did not go for completion. Hence always molar ratio of more than 10 was maintained. Under thermal conditions the size decreased from 70 nm to 62 nm to 57 nm to 48 nm with increase in molar ratio of ascorbic acid to copper sulfate from 10 to 20 to 30 to 40 and under microwave irradiation it decreased from 64 nm to 59 nm to 46 nm to 39 nm, respectively. The reduction of copper ion by ascorbic acid is as shown in equation (3.1). The decrease in size of the particles with the increase in the concentration of ascorbic acid is due to the increase in the rate of nucleation as explained in the reduction of copper sulfate by ascorbic acid in the presence of CTAB.

It was found that the particle size increased with dilution. Dilution with 100 mL water resulted in the increase in size to 76 nm from 70 nm which was for 45 mL dilution. It further increased to 81 nm for 150 mL dilution. For 200 mL dilution the particle size was 83 nm with reaction proceeding very slowly. The observations can be explained by the influence of reaction rate on the nucleation.

At a low overall concentration, on dilution of the reaction mixture, the reduction of copper sulfate by ascorbic acid takes place slowly and only a few nuclei of copper are formed in the early period of the reaction. Since the rate of the reaction is slow, the subsequently formed copper atoms get deposited on the already existing nuclei rather than forming new nuclei. As a result of the rate of nucleation being slower than the rate of particle growth, fewer numbers of particles with bigger size are obtained.

Effect of addition of PVP: The results of effect of PVP concentration on the size of particles are tabulated in Table 3.17.

Table 3.17 Effect of concentration of PVP on the size of copper particles prepared by the reduction of copper sulfate by ascorbic acid

Effective concentration of PVP in the reaction mixture (mM)	Particle size (nm)
0	73
0.53	70
2.63	58
5.26	45

The observed decreasing trend in the size with the increase in the concentration of PVP is similar to that observed in the case of copper nitrate precursor discussed earlier. Sedimentation measurements revealed that the nanofluids were stable up to 3 weeks in stationary state at room temperature in the presence of PVP. In the absence of PVP the fluid was not stable.

Effect of power of microwave radiation and irradiation duration: In order to study the effect of power of microwave radiation on the size of the particles the solution was subjected to varying power for duration of 5 minutes. At 30 % power the size obtained was 44 nm but the power was not sufficient for the reaction to complete. At 50 %, 70 % and 90 % power the particle size was 64 nm, 58 nm and 52 nm, respectively. The microwave irradiation causes intense friction and collision of molecules thereby increasing the nucleation rate and reducing the growth of particles.

Microwave irradiation for duration of 3 minutes at 50 % power was insufficient for the completion of reaction and yielded particles of size 56 nm. When the irradiation duration was increased from 5 minutes to 7 minutes to 10 minutes at 50 % power the size of the particles increased from 64 nm to 68 nm to 74 nm respectively. The trend is similar to the one in reduction of copper nitrate by ascorbic acid in the presence of PVP.

Fig. 3.48 shows typical TEM image (A) and FESEM image (B) of the copper nanoparticles. The images reveal that the particles are hexagonal disc shaped. The sizes obtained from the XRD results match well with that of the TEM and FESEM results.

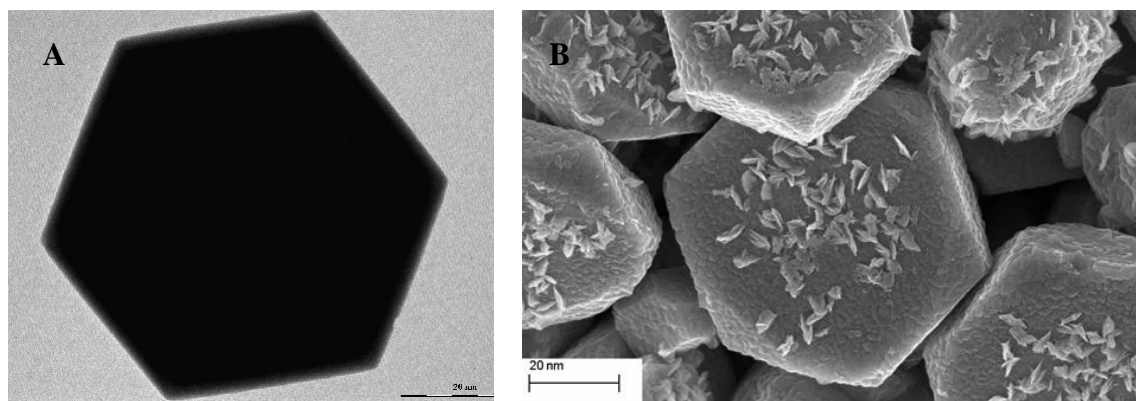


Fig. 3.48 (A) TEM image and (B) FESEM image of copper nanoparticles prepared by the reduction of copper sulfate by ascorbic acid in the presence of PVP

➤ *Results of thermal conductivity and viscosity measurements*

The thermal conductivity of the as synthesized nanofluid was found to be $0.827 \text{ W m}^{-1} \text{ K}^{-1}$ when the weight fraction of copper nanoparticles was 0.096 %. The variation of thermal conductivity ratio with nanoparticle weight fraction is as shown in Fig. 3.49. The trend is similar to that in case of nanofluids synthesized using same precursors in the presence of CTAB.

The viscosity measurements of the nanofluid showed trends similar to that of nanofluid prepared in the presence of CTAB. Fig. 3.50 demonstrates the Newtonian behavior of the copper nanofluid and the variation of viscosity with particle loading and temperature.

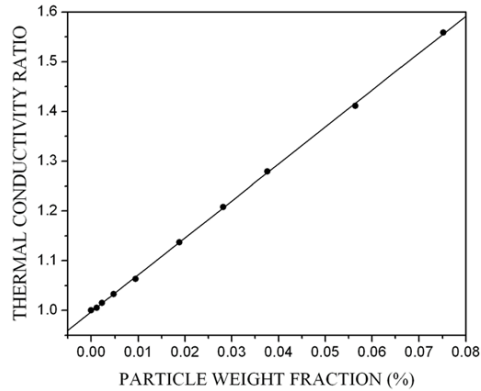


Fig. 3.58 Variation of thermal conductivity ratio with particle weight fraction for copper nanofluid prepared by the reduction of copper sulfate by ascorbic acid in the presence of PVP

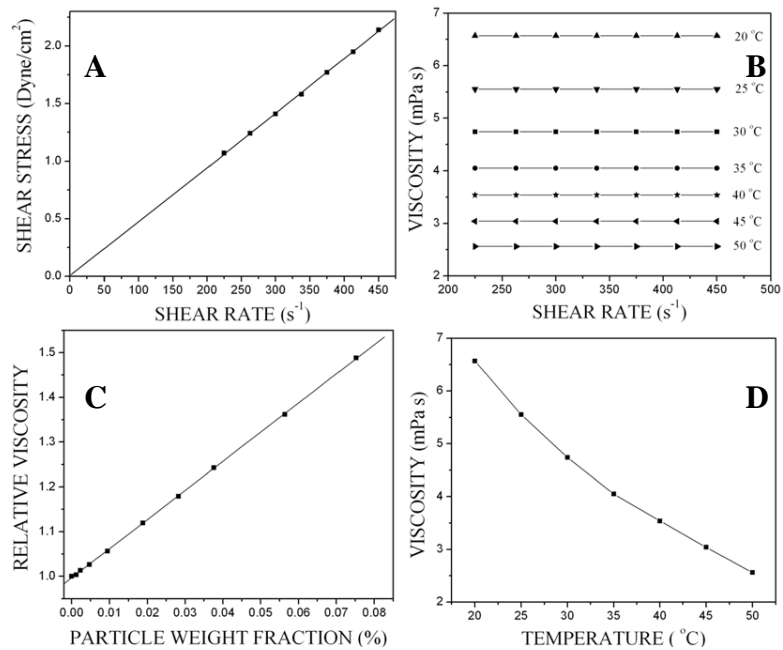


Fig. 3.59 Viscosity measurements of copper nanofluid prepared by the reduction of copper sulfate by ascorbic acid in the presence of PVP. (A) Shear stress verses shear rate; (B) Viscosity as a function of shear rate at different temperatures; (C) Variation of relative viscosity with particle weight fraction; (D) Viscosity as a function of temperature

3.1.3.3 Nanofluids synthesized using copper acetate and ascorbic acid

➤ *Results of variation in reaction parameters*

Effect of pH: To study the effect of pH of the reaction mixture, sulfuric acid was added during reduction. When the pH of the reaction mixture was brought down from 7 to 3 the size of the particles increased from 39 nm to 67 nm. The observations are similar to the ones for the reduction of copper acetate using ascorbic acid in presence of SLS; i.e. due to the decrease in reduction power of ascorbic acid with the decrease in the pH, the size of the particles increases.

Effect of ratio of reactants and dilution: The synthesis of copper nanofluids was carried out in thermal as well as microwave conditions at different concentrations of ascorbic acid. It was observed that whenever the molar ratio of ascorbic acid to copper acetate was less than 4 the reaction did not go for completion. Hence always molar ratio of more than 4 was maintained.

During conventional heating size increased from 39 nm to 44 nm to 49 nm to 56 nm as the molar ratio of ascorbic acid to copper acetate was increased from 4 to 8 to 12 to 16, respectively. During irradiation with microwave average particle size decreased from 42 nm to 38 nm to 33 nm to 27 nm, respectively. The trend is similar to that observed in case of copper acetate in the presence of SLS.

Dilution of the reaction mixture with water had an effective impact over the size of particles and the results are summarized in Table 3.18. The decrease in the size of particles with the increase in dilution is due to the decrease in overall concentration of solution leading to fewer collisions of precipitating atoms and thus reduction in the growth of the particles similar to the one observed in the presence of CTAB.

Table 3.18 Effect of dilution on the size of copper particles prepared by the reduction of copper acetate by ascorbic acid in the presence of PVP

Dilution (mL)	Particle Size (nm)
45	39
100	36
150	29
200	25
250	22

Effect of addition of PVP: The reaction was carried out in the absence of PVP and in the presence of varying concentration of PVP. The effect of concentration of PVP on the particle size are indicated in the results tabulated in Table 3.19

Table 3.19 Effect of concentration of PVP on the size of copper particles prepared by the reduction of copper acetate by ascorbic acid

Effective concentration of PVP in the reaction mixture (mM)	Particle Size (nm)
0	43
0.53	39
2.63	26
5.26	22

The effect of PVP on particle size is similar to that observed in the case of nanofluids prepared using copper sulfate discussed in the earlier section. PVP also stabilizes the resulting fluid. The fluid was stable up to 5 weeks under stationary state at room temperature.

Effect of power of microwave radiation and irradiation duration: The reaction mixture was subjected to varying powers for duration of 4 minutes. At 30 % power the size of the particle obtained was 37 nm. But the reaction was not complete. When the power was increased from 50 % to 70 % to 90 % the size of the particle decreased from 42 nm to 35 nm to 29 nm, respectively.

With increase in irradiation duration from 4 minutes to 7 minutes to 10 minutes the size of the particle increased from 42 nm to 46 nm to 53 nm, respectively. The observed trend is similar to the one mentioned in the case of ascorbic acid reduction of copper sulfate.

A typical TEM image (A) and FESEM image (B) of the copper nanoparticles are shown in the Fig. 3.51. The particles are jumbled sphere shaped. The sizes obtained from the XRD results match well with that of the TEM and FESEM results.

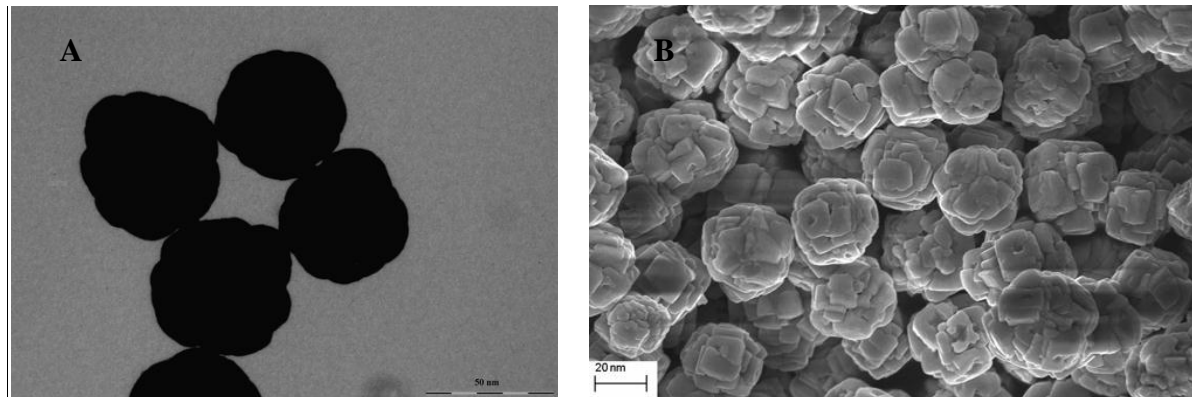


Fig. 3.52 (A) TEM image and (B) FESEM image of copper nanoparticles prepared by the reduction of copper acetate by ascorbic acid in the presence of PVP

➤ *Results of thermal conductivity and viscosity measurements*

The thermal conductivity of the as synthesized nanofluid was found to be $1.072 \text{ W m}^{-1} \text{ K}^{-1}$ when the weight fraction of copper nanoparticles was 0.241 %. The variation of thermal conductivity ratio with nanoparticle weight fraction is as shown in Fig. 3.52.

It was found that thermal conductivity increased with the increase in particle weight fraction. Maximum thermal conductivity was found to be $1.268 \text{ W m}^{-1} \text{ K}^{-1}$ at particle loading of 0.188 % and there after it showed a gradual decrease. The trend is similar to that in case of nanofluids synthesized using copper acetate in presence of CTAB.

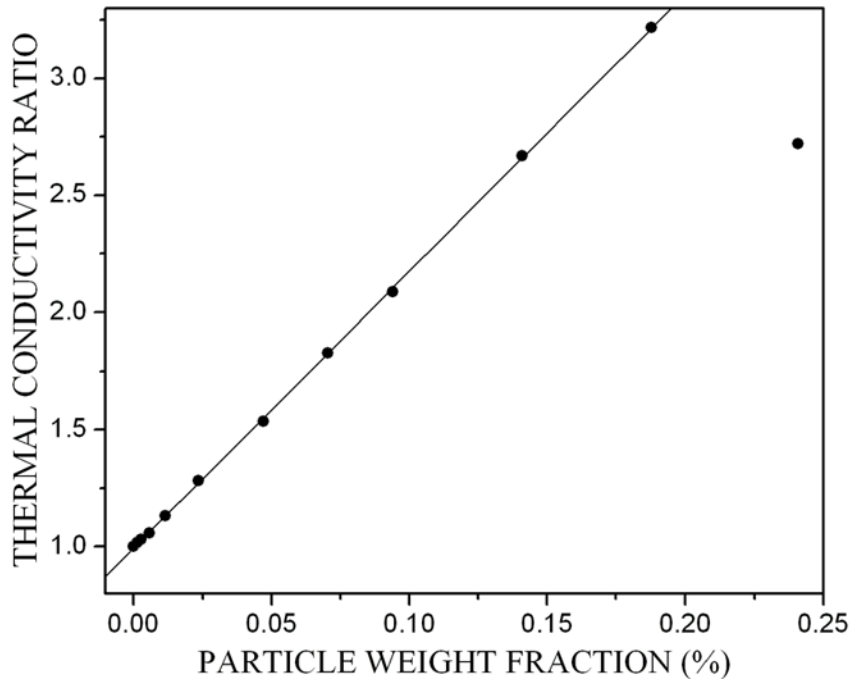


Fig. 3.52 Variation of thermal conductivity ratio with particle weight fraction for copper nanofluid prepared by the reduction of copper acetate by ascorbic acid in the presence of PVP

The viscosity measurements of the nanofluid showed trends similar to that of nanofluid prepared in presence of CTAB. Fig. 3.53 demonstrates the Newtonian behavior of the copper nanofluid and the variation of viscosity with particle weight fraction and temperature.

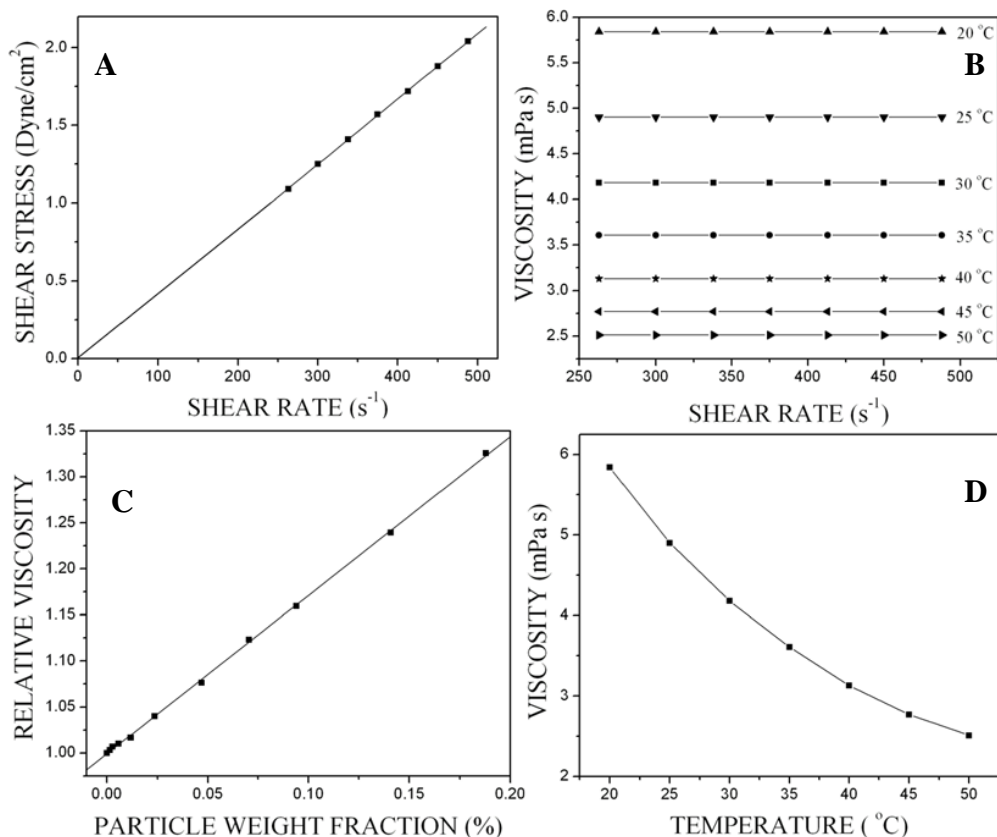


Fig. 3.53 Viscosity measurements of copper nanofluid prepared by the reduction of copper acetate by ascorbic acid in the presence of PVP. (A) Shear stress verses shear rate; (B) Viscosity as a function of shear rate at different temperatures; (C) Variation of relative viscosity with particle weight fraction; (D) Viscosity as a function of temperature

3.2 CUPROUS OXIDE NANOFLUIDS

➤ *Results of XRD, EDX and SAED analysis*

The XRD pattern of the cuprous oxide nanoparticles prepared by the reduction of copper nitrate, copper sulfate and copper acetate precursors using glucose in the presence of CTAB are shown in Fig. 3.54, Fig. 3.55 and Fig. 3.56, respectively.

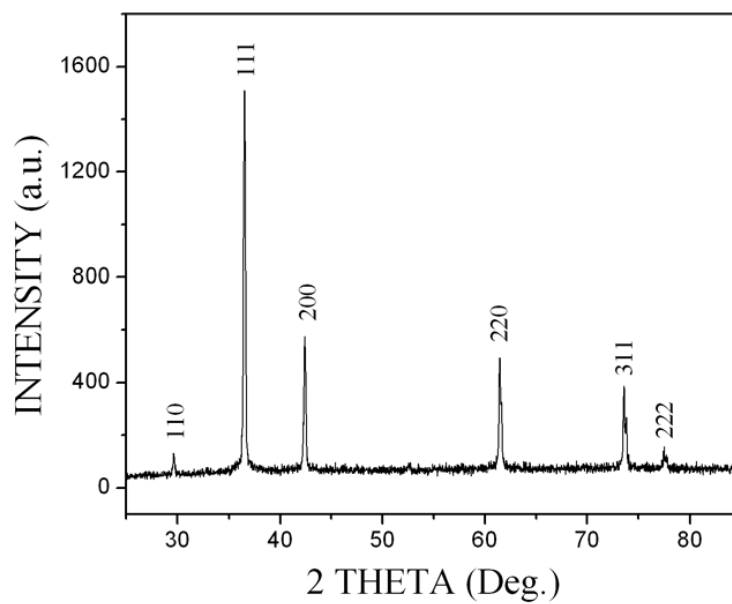


Fig. 3.54 Powder XRD pattern of cuprous oxide nanoparticles prepared by the reduction of copper nitrate by glucose in the presence of CTAB

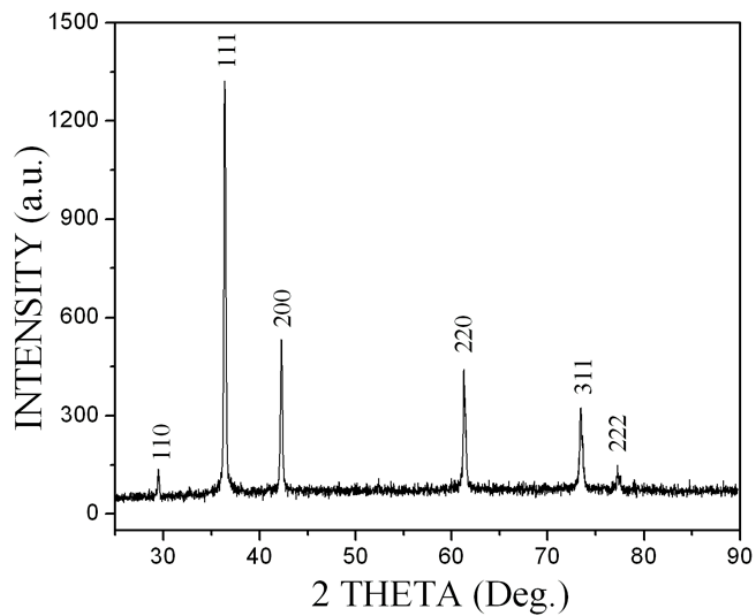


Fig. 3.55 Powder XRD pattern of cuprous oxide nanoparticles prepared by the reduction of copper sulfate by glucose in the presence of CTAB

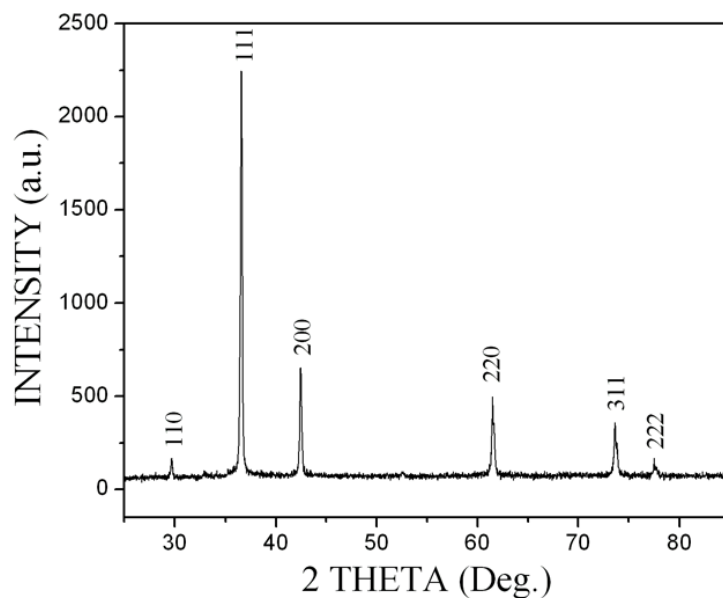


Fig. 3.56 Powder XRD pattern of cuprous oxide nanoparticles prepared by the reduction of copper acetate by glucose in the presence of CTAB

All the peaks could be indexed to standard cubic structure of Cu_2O [JCPDS Card No. 05-0667, $a = 4.2696 \text{ \AA}$, Space group: $\text{Pn}3\text{m} (224)$]. The peaks correspond to (110), (111), (200), (220), (311) and (222) planes, respectively. None of the peaks could be indexed to copper or cupric oxide indicating that the products are highly pure.

Fig. 3.57, Fig. 3.58 and Fig. 3.59 display the EDX spectra of cuprous oxide nanoparticles synthesized by the reduction of copper nitrate, copper sulfate and copper acetate precursors using glucose in the presence of CTAB, respectively. It reveals copper and oxygen as the only detectable elements, indicating that the sample is without any contamination. Their atomic ratio is close to 2:1 confirming that the nanoparticles are of Cu_2O .

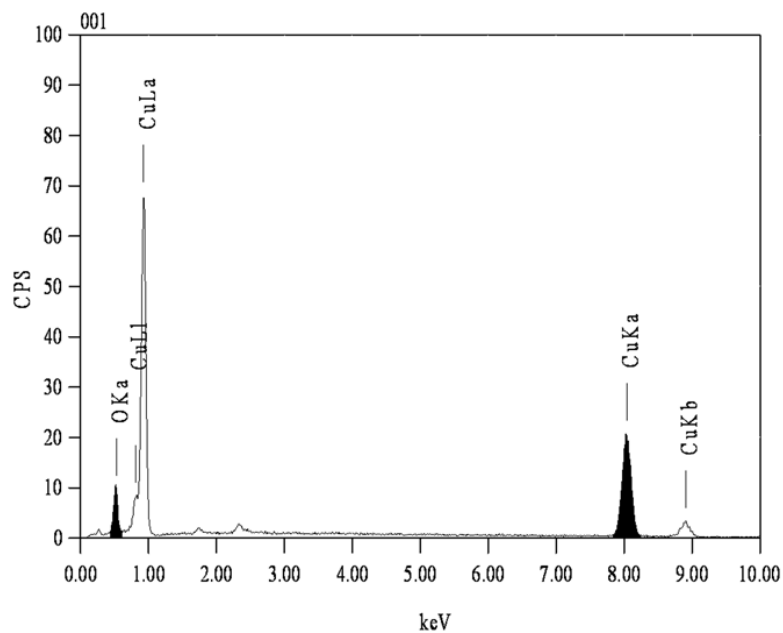


Fig. 3.57 EDX spectrum of cuprous oxide nanoparticles prepared by the reduction of copper nitrate by glucose in the presence of CTAB

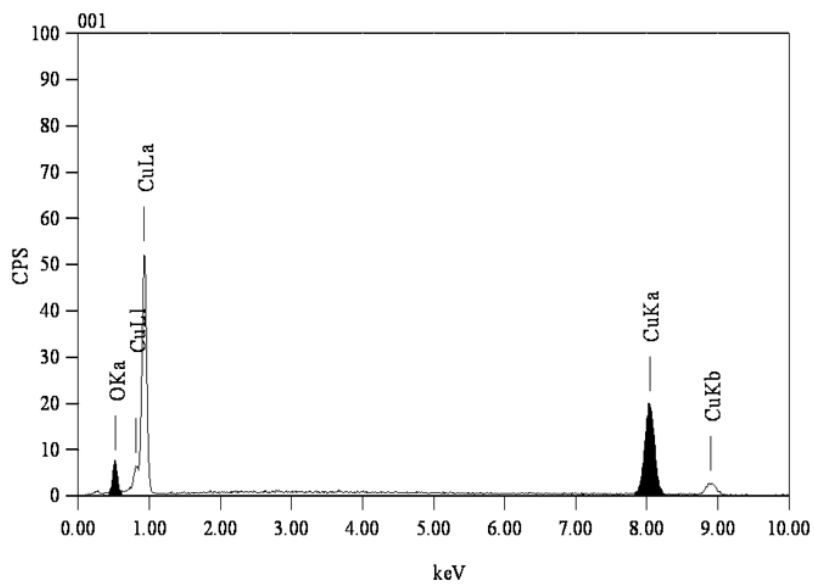


Fig. 3.58 EDX spectrum of cuprous oxide nanoparticles prepared by the reduction of copper sulfate by glucose in the presence of CTAB

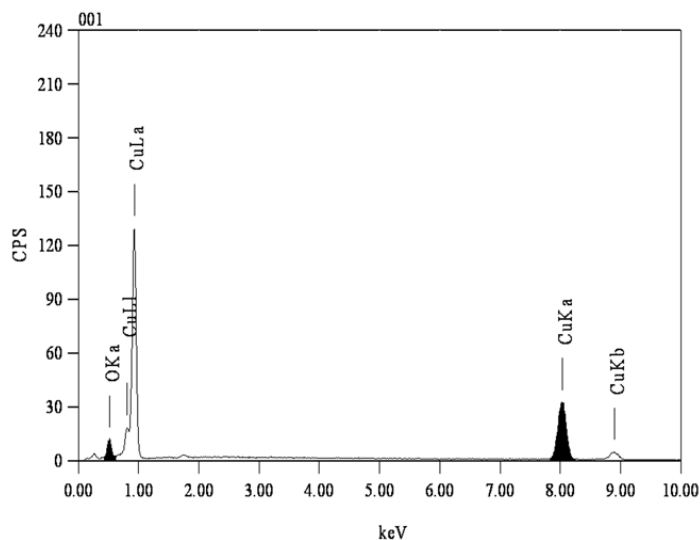


Fig. 3.59 EDX spectrum of cuprous oxide nanoparticles prepared by the reduction of copper acetate by glucose in the presence of CTAB

The SAED pattern of cuprous oxide nanoparticles obtained by the reduction of copper nitrate, copper sulfate and copper acetate precursors using glucose in the presence of CTAB are shown in Fig. 3.60, Fig. 3.61 and Fig. 3.62, respectively. Six rings corresponds to (110), (111), (200), (220), (311) and (222) planes with distances 3.02 Å, 2.465 Å, 2.135 Å, 1.51 Å, 1.287 Å and 1.23 Å, respectively. These data matches well with the standard data for cubic phase Cu₂O.

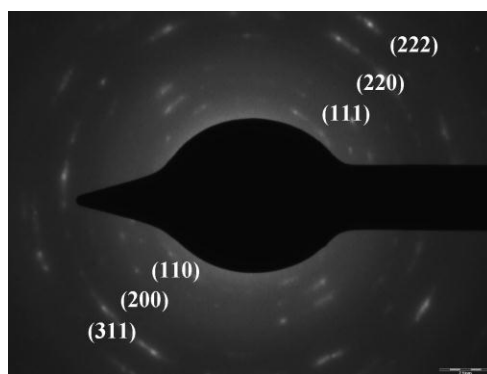


Fig. 3.60 SAED pattern of cuprous oxide nanoparticles prepared by the reduction of copper nitrate by glucose in the presence of CTAB

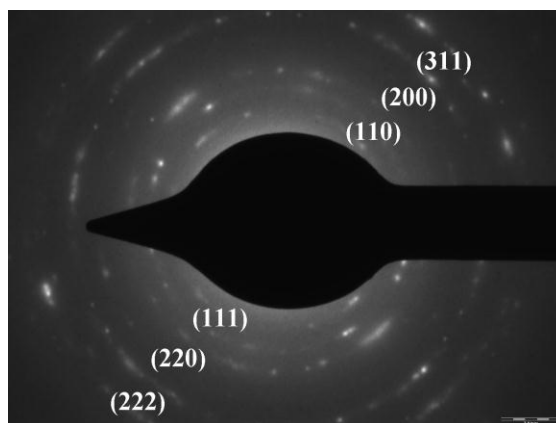


Fig. 3.61 SAED pattern of cuprous oxide nanoparticles prepared by the reduction of copper sulfate by glucose in the presence of CTAB

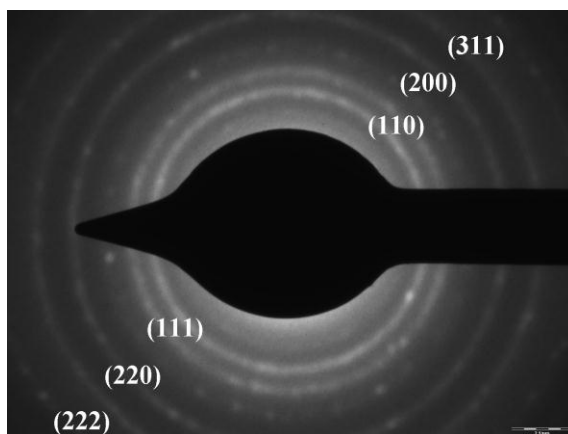


Fig. 3.62 SAED pattern of cuprous oxide nanoparticles prepared by the reduction of copper acetate by glucose in the presence of CTAB

➤ *Results of FTIR and UV-Vis spectroscopic analysis*

The FTIR spectra of cuprous oxide nanofluid prepared by the reduction of copper nitrate (E), copper sulfate (F) and copper acetate (G) precursors using glucose in the presence of CTAB each stacked with pure ethylene glycol (A) are shown in Fig. 3.63, Fig. 3.64 and Fig. 3.65, respectively. It is seen that the two spectra resemble indicating

that the ethylene glycol is not oxidized. It suggests that the reducing agent used in the reaction i.e. glucose is the one acting as reducing agent and not ethylene glycol.

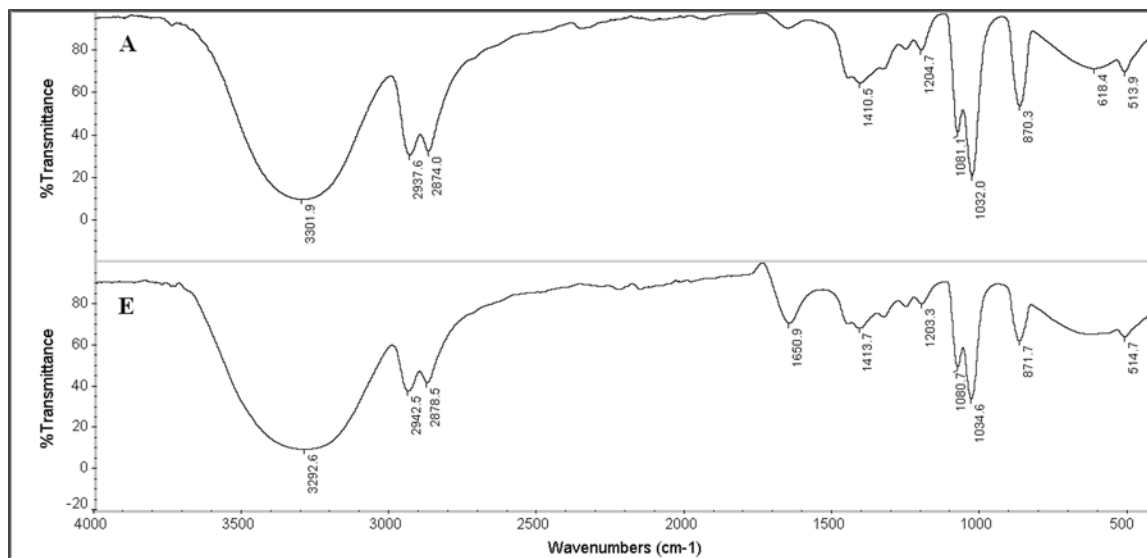


Fig. 3.73 FTIR spectra of (A) ethylene glycol and (E) cuprous oxide nanofluid prepared by the reduction of copper nitrate by glucose in the presence of CTAB

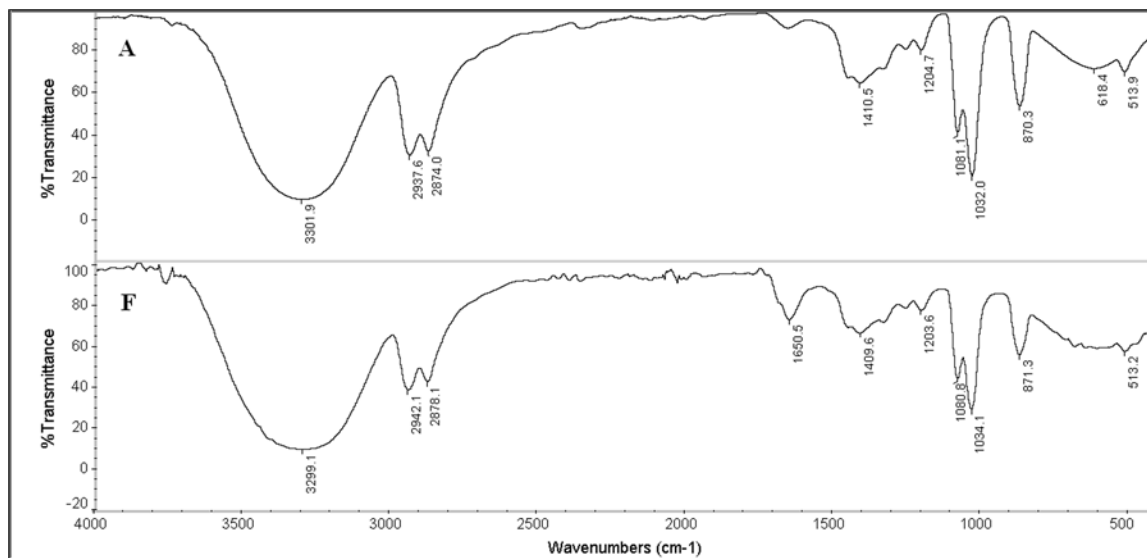


Fig. 3.74 FTIR spectra of (A) ethylene glycol and (F) cuprous oxide nanofluid prepared by the reduction of copper sulfate by glucose in the presence of CTAB

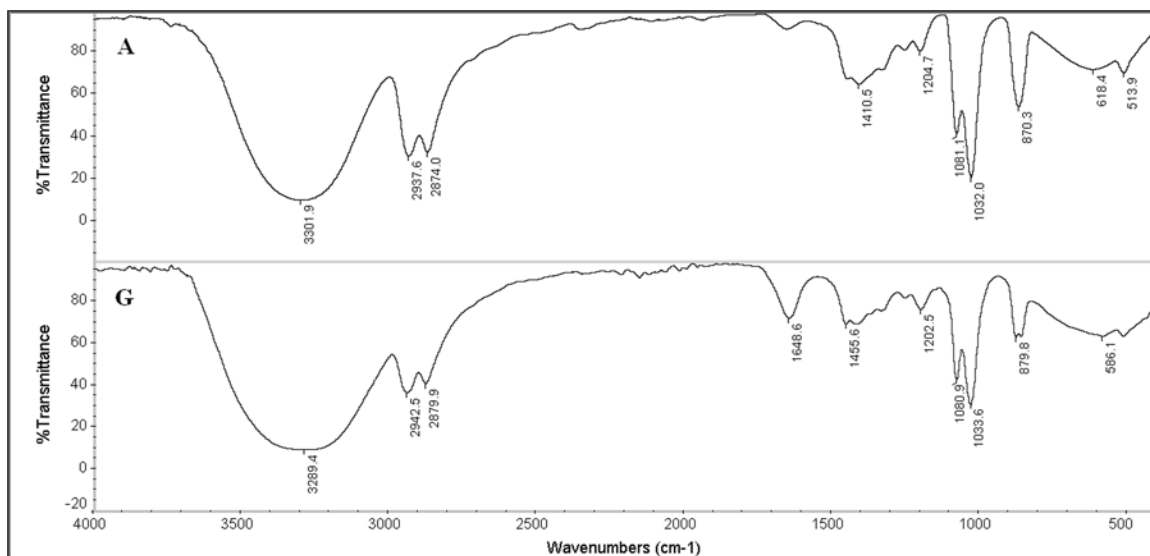


Fig. 3.65 FTIR spectra of (A) ethylene glycol and (G) cuprous oxide nanofluid prepared by the reduction of copper acetate by glucose in the presence of CTAB

UV-Vis spectra of cuprous oxide nanofluid synthesized by the reduction of copper nitrate, copper sulfate and copper acetate precursors using glucose in the presence of CTAB are shown in Fig. 3.66, Fig. 3.67 and Fig. 3.68, respectively.

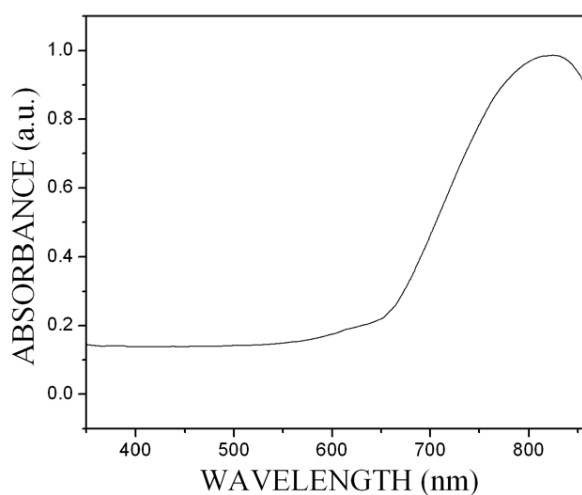


Fig. 3.76 UV-Vis spectrum of cuprous oxide nanofluid prepared by the reduction of copper nitrate by glucose in the presence of CTAB

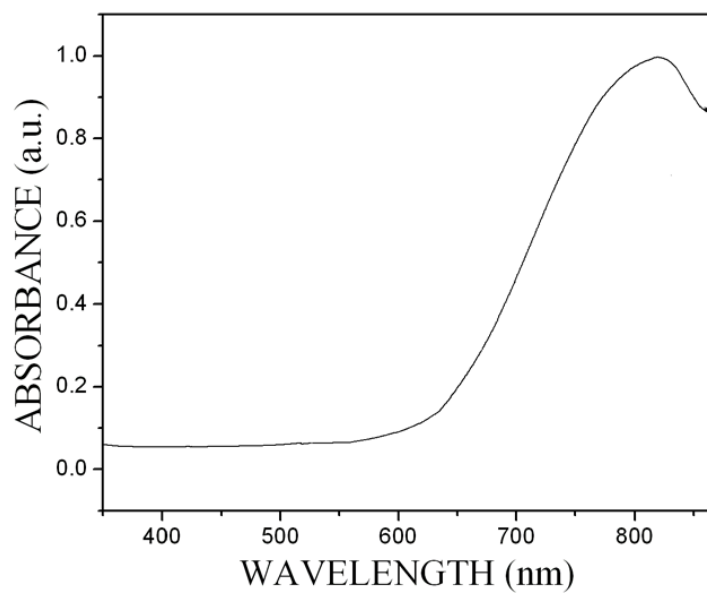


Fig. 3.67 UV-Vis spectrum of cuprous oxide nanofluid prepared by the reduction of copper sulfate by glucose in the presence of CTAB

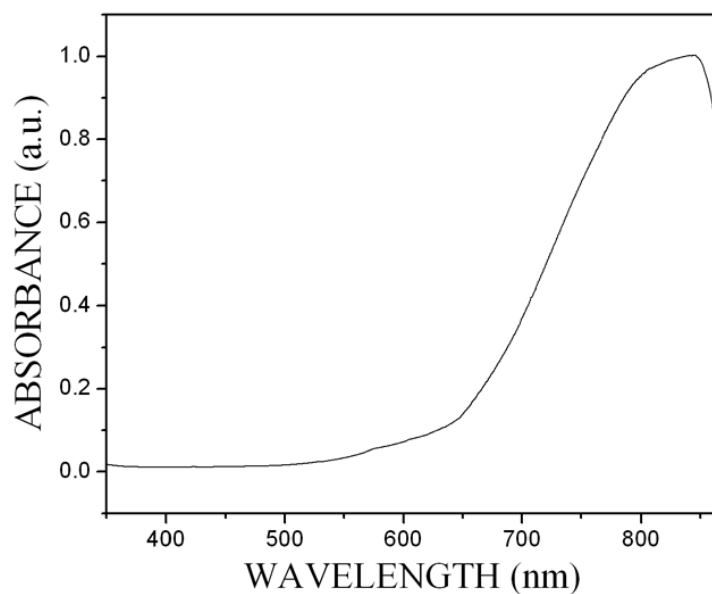


Fig. 3.68 UV-Vis spectrum of cuprous oxide nanofluid prepared by the reduction of copper acetate by glucose in the presence of CTAB

Peak at 830 nm, 820 nm and 845 nm in the Fig. 3.66, Fig. 3.67 and Fig. 3.68, respectively indicate the presence of cuprous oxide nanoparticles.

3.2.1 Cuprous Oxide Nanofluids Synthesized in the Presence of SLS Using Copper Acetate and Glucose

➤ *Results of variation in reaction parameters*

Effect of ratio of reactants: Synthesis of nanofluids was carried out with different amount of glucose and the effect of concentration of glucose on the size of cuprous oxide particle was studied. It was observed that the particle size increased with the increase in the amount of glucose added. It was also observed that whenever the molar ratio of glucose to copper acetate was less than 2.8 the reaction did not go for completion. Hence always molar ratio of more than 2.8 was maintained. The sizes of the particle obtained were 32 nm, 36 nm, 44 nm and 49 nm for glucose to copper acetate ratio of 2.8, 5.6, 8.9 and 11.1, respectively. It was observed that at lower concentration of glucose the particles of smaller size were formed. However at higher concentration the tiny nuclei formed, readily collided with each other giving particles of larger size (Chang et al. 2011).

Effect of addition of ammonia: Glucose reduces copper ions as shown in Equation (3.8).



The standard half cell potential for the reduction of Cu^{2+} to Cu^+ (equation 3.9) is 0.16 V.



The standard half cell potential for the redox equilibrium of glucose, given in equation (3.6) is 0.050 V.

The overall standard state cell potential for the reaction given in equation (3.8) is positive and hence the reaction as represented in equation (3.8) is feasible. Since the

reaction is carried out in the presence of ammonia most of the copper ion is, therefore, present as $[\text{Cu}(\text{NH}_3)_4]^{2+}$ complex ion. The half cell potential for the reduction of this complex is considerably smaller than that for the reduction of Cu^{2+} ion to Cu^+ . This leads to a significant decrease in the overall cell potential for the reaction because the complex ion is a much weaker oxidizing agent than the Cu^{2+} ion.

Due to the involvement of a pair of H^+ ions in the reaction, the presence of ammonia alters the electrode potential of the glucose redox system (equation 3.6). The half cell potential for the reaction given in equation (3.6) therefore depends on the pH of the solution. As two H^+ ions are given off when glucose is oxidized, the reaction quotient for this reaction depends on the square of H^+ ion concentration. A change in solution pH from standard state conditions to pH of 11, therefore results in a decrease of half cell potential for this reaction as per equation (3.7). This results in the increase in the reducing strength of glucose. The increase in the reducing strength of glucose under this condition more than makes up for the decrease in oxidizing strength of Cu^{2+} in the presence of ammonia and therefore the reaction is more propitious.

Effect of dilution: Varying amount of water was used to dilute the reaction mixtures. It was observed that with dilution the size of the particle decreased. The particle size ranged between 32 nm to 13 nm for zero dilution to 200 mL dilution. The particle sizes were 29 nm and 24 nm for 50 mL and 100 mL dilution, respectively. The observed trend can be attributed to the fact that with the increase in the dilution the overall concentration of the species decreases, the proximity between the precipitating metal oxide molecules decreases and hence the collision between them is reduced. This prevents the particle growth and hence resulting in smaller size of the cuprous oxide nanoparticles formed.

Effect of addition of SLS: The effect of surfactant concentration on the particle size and stability was studied. In the absence of the surfactant, the particles of 52 nm size were obtained. When the effective concentration of the SLS was increased the particle size decreased as shown in Table 3.20. This decrease in size could be attributed to the capping

effect of SLS resulting in restriction on the growth of particles and controlling the size of cuprous oxide particles. With the increase in the concentration of SLS the capping action increases and hence size of the particles decreases.

Table 3.20 Effect of concentration of SLS on the size of cuprous oxide particles prepared by the reduction of copper acetate by glucose

Effective concentration of SLS in the reaction mixture (mM)	Particle Size (nm)
0	52
3.3	32
16.7	26
33.3	17

SLS not only showed an effect on the size of particles but also endowed the nanofluid with required stability. In the absence of surfactant the fluid was highly unstable and the particles started settling quickly. Addition of surfactant prevents the agglomeration of particles and their settlement in the medium. This facilitates uniform distribution of the particles in the medium. Sedimentation measurements showed that in the presence of surfactant, the fluid was stable for a minimum period of 3 months at room temperature under stationary conditions. Such high stability can be accredited to the small size and uniform distribution of the formed particles.

Effect of power of microwave radiation and irradiation duration: The reaction between copper acetate and glucose in the presence of SLS was also carried out under microwave irradiation at varying power and irradiation duration. The reaction was incomplete for 7 minutes irradiation at 30 % power and yielded particles of 30 nm. At 50 % power microwave irradiation the reaction proceeded to completion and resulted in the formation of particles with size of 60 nm and 10 nm. For 70 % power the particles of size 70 nm were formed.

The duration of irradiation also had a significant effect on the size as well as the progress of the reaction. The power was set to 50 % and the duration of irradiation was varied. For duration of 5 minutes, particles formed had a size of 45 nm but the reaction was incomplete. When the duration was increased to 7 minutes particles with two different sizes were formed. A second nucleation event resulted in the formation of new particles with size around 10 nm and the particles formed during the first nucleation showed growth up to 60 nm. When the irradiation duration was extended up to 10 minutes the particles grew bigger due to Ostwald ripening and attained a size of 75 nm. As the duration of the irradiation increases the temperature of the reaction mixture increases resulting in increase in the solubility of the particles which promotes Ostwald ripening (Cao 2003). The relatively larger particles grow at the expense of smaller particles. The result is the elimination of smaller particles, and thus the size distribution of nanoparticles becomes narrower. When the temperature is increased the concentration of solid in the base fluid falls below the equilibrium solubility of small nanoparticles and the small particles dissolve into the solvent. As the dissolution of nanoparticle proceeds, the nanoparticle becomes smaller and has higher solubility. Once a nanoparticle starts dissolving into the basefluid, the dissolution process stops only when the nanoparticle is dissolved completely. On the other hand the concentration of solid in base fluid is still higher than the equilibrium solubility of larger particles and thus these particles would continue to grow. Such a growth process would stop when the concentration of solid in the base fluid equals the equilibrium solubility of these relatively large nanoparticles. Therefore the smaller particles observed when the irradiation duration was 7 minutes disappeared when the irradiation duration was increased to 10 minutes.

A typical TEM image of the nanofluid synthesized by the reduction of copper acetate using glucose under thermal conditions is shown in Fig. 3.69. Fig. 3.70 shows the FESEM images of the cuprous oxide particles formed at 50 % irradiation for 7 minutes (A) and 10 minutes (B). The sizes obtained from the XRD results match well with that of the TEM and FESEM results.

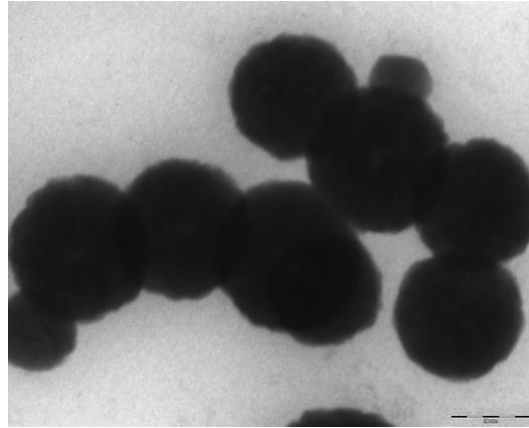


Fig. 3.69 TEM image of cuprous oxide nanofluid prepared by conventional heating by the reduction of copper acetate by glucose in the presence of SLS

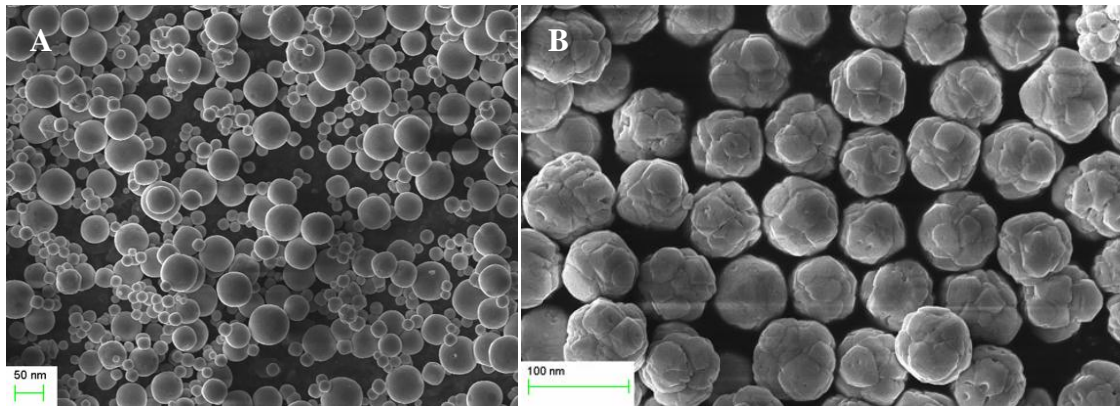


Fig. 3.70 FESEM image of cuprous oxide nanoparticles prepared by (A) 7 minutes and (B) 10 minutes microwave irradiation by the reduction of copper acetate by glucose in the presence of SLS

➤ *Results of thermal conductivity measurement*

The cuprous oxide nanofluid showed a thermal conductivity of $2.127 \text{ W m}^{-1} \text{ K}^{-1}$ for particle weight fraction of 1.5 %. The thermal conductivity of the nanofluid increased linearly with the increase in particle weight fraction. A maximum thermal conductivity of $2.948 \text{ W m}^{-1} \text{ K}^{-1}$ was observed at 0.282 % particle weight fraction. There after it showed a

gradual decrease in conductivity. The enhancement of the conductivity of the base fluid with the increase in particle weight fraction could be attributed to the higher conductivity and uniform dispersal of cuprous oxide nanoparticles. Fig. 3.71 shows the variation of thermal conductivity ratio with particle weight fraction. Same trend was seen for different ratios of base fluids showing the independency of fluid composition. The thermal conductivity ratio of 7.48 of the synthesized nanofluid is found to be significantly higher than the value of 1.24 reported by Wei et al. (2009).

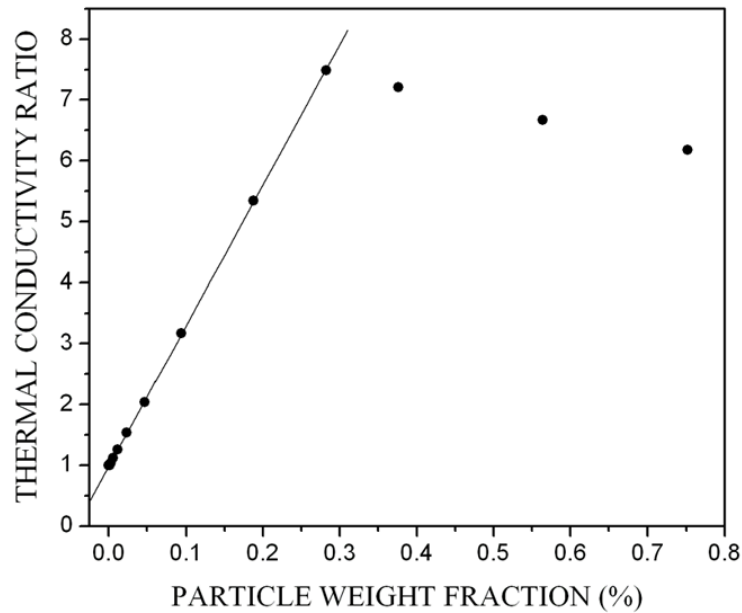


Fig. 3.71 Variation of thermal conductivity ratio with particle weight fraction for cuprous oxide nanofluid prepared by the reduction of copper acetate by glucose in the presence of SLS

➤ *Results of viscosity measurement*

The viscosity measurements of the nanofluid showed trends similar to that of copper nanofluids discussed in the earlier sections. Fig. 3.72 demonstrates the Newtonian behavior of the cuprous oxide nanofluid and the variation of viscosity with particle weight fraction and temperature.

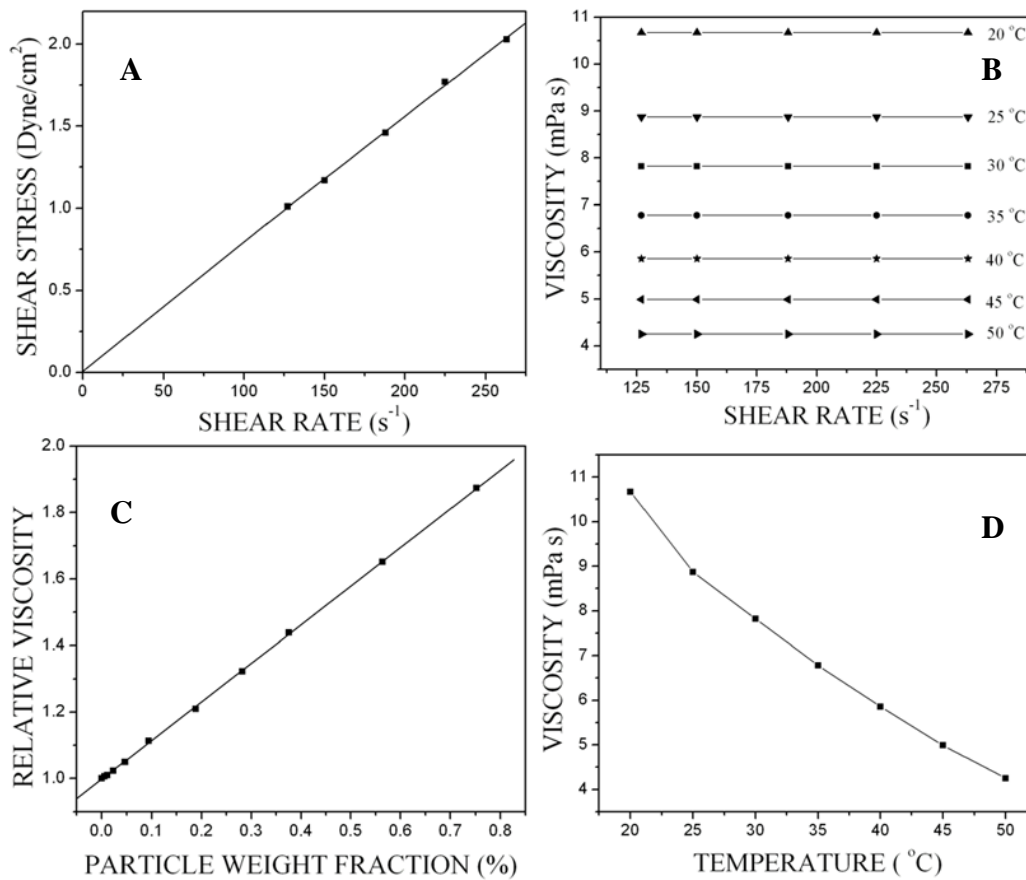


Fig. 3.72 Viscosity measurements of cuprous oxide nanofluid prepared by the reduction of copper acetate by glucose in the presence of SLS. (A) Shear stress verses shear rate; (B) Viscosity as a function of shear rate at different temperatures; (C) Variation of relative viscosity with particle weight fraction; (D) Viscosity as a function of temperature

3.2.2 Cuprous Oxide Nanofluids Synthesized in the Presence of CTAB

3.2.2.1 Nanofluids synthesized using copper nitrate and glucose

➤ *Results of variation in reaction parameters*

Effect of ratio of reactants: The synthesis was carried out by varying the molar ratio of glucose to copper nitrate. It was observed that whenever the molar ratio of glucose to

copper nitrate was less than 5.55 the reaction did not go for completion. Hence always molar ratio of more than 5.55 was maintained. The increase in molar ratio from 5.55 to 22.20 resulted in particles having sizes decreasing from 52 nm to 41 nm in thermal conditions and 48 nm to 38 nm in microwave conditions, respectively. The sizes of the particles obtained were 46 nm and 43 nm during conventional heating and during microwave heating, respectively, for molar ratio of 11.10.

Reduction of cupric ions to cuprous oxide is as shown in equation (3.7). The amount of electrons supplied to copper ions during reduction is determined by concentration of glucose. At lower concentration of reducing agent, the reduction rate of copper precursor is slow and consequently only a few nuclei are formed at the nucleation step. Precipitated cuprous oxide molecules at the later period of the reactions are mostly involved in particle growth by collision with the already generated nuclei rather than formation of new particles. This leads to the formation of larger sized particles. With increase in concentration of reducing agent, reduction rate is enhanced, leading to the formation of smaller particles. At higher reduction rate the number of precipitating cuprous oxide clusters increases steeply and hence more number of nuclei is formed during the nucleation period. Eventually the size of the particles decreases because the amount of solute available for particle growth per growing particle decreases with the increasing number of nuclei (Park et al. 2007).

Effect of dilution: The reaction mixture was diluted with 50 mL, 100 mL, 150 mL and 200 mL of water. The particle size decreased with the increase in the amount of dilution. Without dilution of the reaction mixture the particle size was found to be 52 nm. The particles yielded had 49 nm, 45 nm, 40 nm and 36 nm size for 50 mL, 100 mL, 150 mL, and 200 mL dilution, respectively. For 200 mL dilution the reaction proceeded very slowly due to the decrease in effective concentration of the reacting species. The observed decrease in the size of the particles is because of the decrease in collision of the particles leading to lesser agglomeration and decreased growth of the initially formed nuclei.

Effect of addition of CTAB: Concentration of CTAB also played a role in controlling the size of the particle as well as stability of the nanofluid. The results indicating the effect on the size of the particle with the increase in CTAB concentration are summarized in Table 3.21. The results clearly indicate that CTAB acts as a capping agent and hence restricts the growth of the particles. As the CTAB concentration increases, the particle size decreases. Sedimentation measurements showed that the nanofluid was stable up to 6 months at room temperature under stationary state.

Table 3.21 Effect of concentration of CTAB on the size of cuprous oxide particles prepared by the reduction of copper nitrate by glucose

Effective concentration of CTAB in the reaction mixture (mM)	Particle Size (nm)
0	69
1.67	52
8.33	46
16.67	38

Effect of power of microwave radiation and irradiation duration: For 30 % power microwave irradiation for 4 minutes the reaction was incomplete and size of the particles obtained was 34 nm. As power was increased (50 % to 70 % to 90 %) for 4 minutes irradiation duration the particle size was found to decrease (48 nm, 44 nm to 39 nm). With the increase in irradiation duration at 50 % power the size increased as 53 nm and 57 nm for 6 minutes and 8 minutes, respectively. The observed trend is identical to the results mentioned in the case of reduction of copper nitrate into copper using ascorbic acid in the presence of CTAB.

Fig. 3.73 shows FESEM images of the cuprous oxide nanoparticles separated from the as prepared nanofluid at low magnification (A) and high magnification (B). The

images reveal that the particles are flower like. The sizes obtained from the XRD results match well with that of the FESEM results.

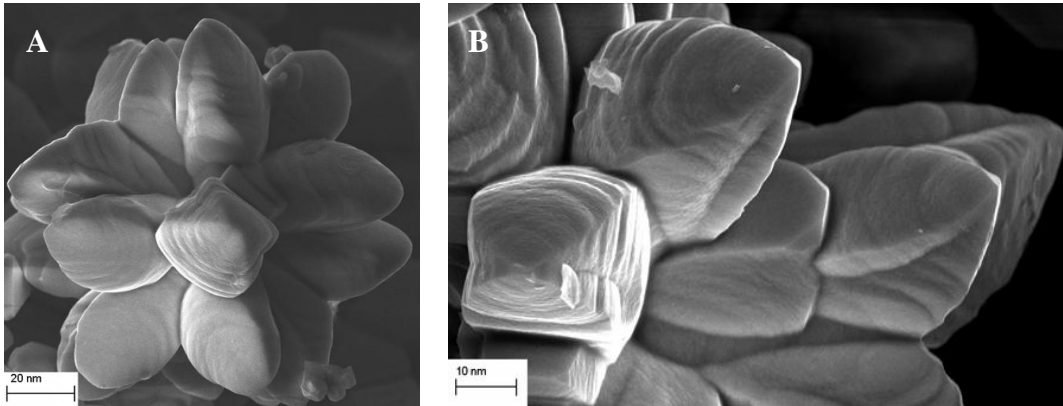


Fig. 3.73 (A) Low magnification and (B) high magnification FESEM images of cuprous oxide nanoparticles prepared by the reduction of copper nitrate by glucose in the presence of CTAB

➤ *Results of thermal conductivity and viscosity measurements*

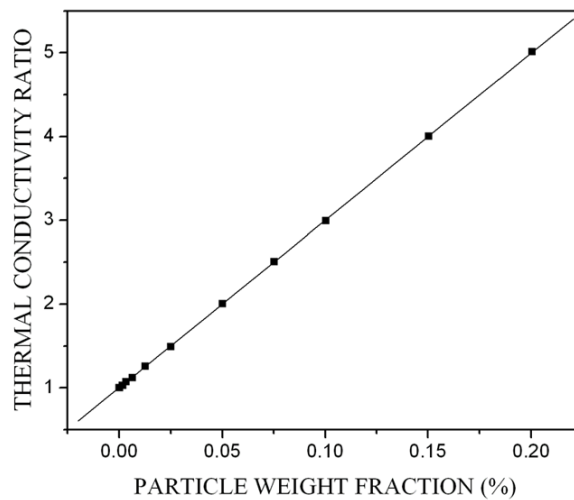


Fig. 3.74 Variation of thermal conductivity ratio with particle weight fraction for cuprous oxide nanofluid prepared by the reduction of copper nitrate by glucose in the presence of CTAB

The cuprous oxide nanofluid showed a thermal conductivity of $1.975 \text{ W m}^{-1} \text{ K}^{-1}$ for particle weight fraction of 0.200 %. The thermal conductivity of the nanofluid increased linearly with increase in particle weight fraction which could be attributed to the higher conductivity and uniform dispersal of nanoparticles. Fig. 3.74 shows the variation of thermal conductivity ratio with particle weight fraction. The trend is similar to that of nanofluid prepared by the reduction of copper nitrate using ascorbic acid in presence of CTAB.

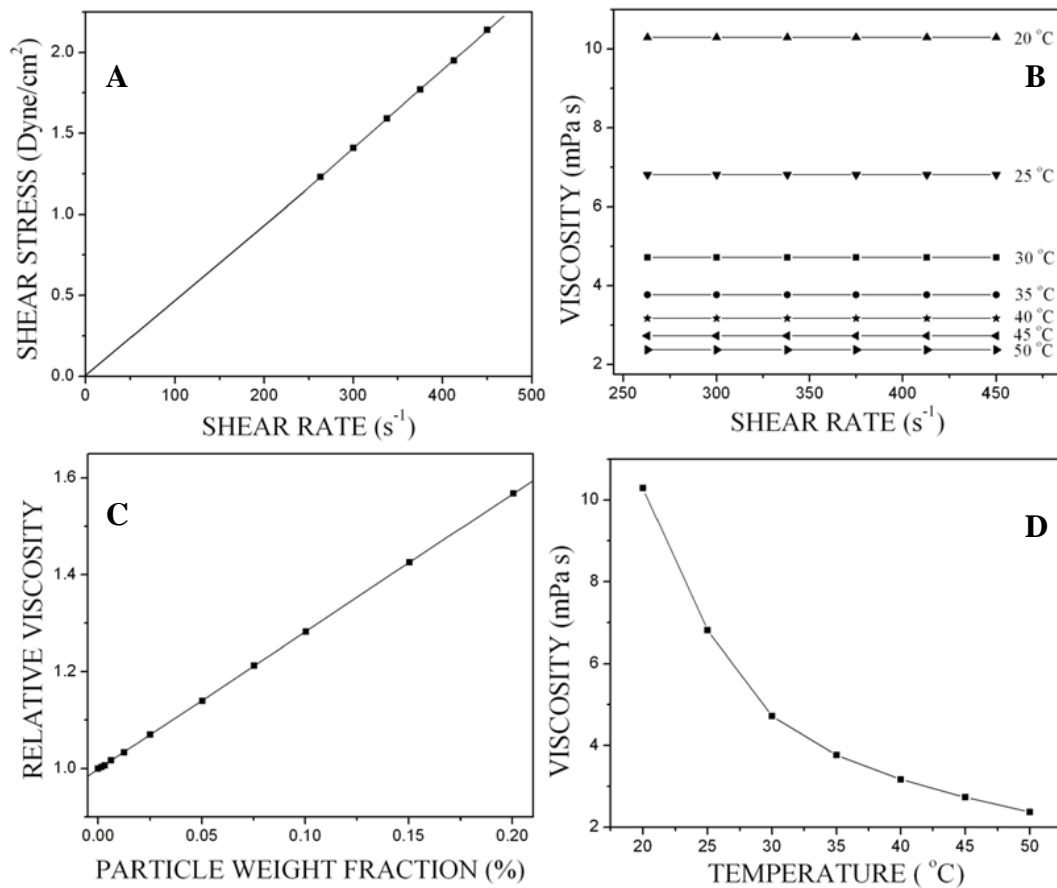


Fig. 3.75 Viscosity measurements of cuprous oxide nanofluid prepared by the reduction of copper nitrate by glucose in the presence of CTAB. (A) Shear stress verses shear rate; (B) Viscosity as a function of shear rate at different temperatures; (C) Variation of relative viscosity with particle weight fraction; (D) Viscosity as a function of temperature

The viscosity measurements of the nanofluid showed trends similar to that of copper nanofluids reported in earlier sections. Fig. 3.75 demonstrates the Newtonian behavior of the cuprous oxide nanofluid and the variation of viscosity with particle loading and temperature.

3.2.2.2 Nanofluids synthesized using copper sulfate and glucose

➤ *Results of variation in reaction parameters*

Effect of ratio of reactants: The effect of amount of glucose added on the size of the cuprous oxide nanoparticles was studied both under thermal and microwave conditions. It was also observed that whenever the molar ratio of glucose to copper sulfate was less than 6.94 the reaction did not go for completion. Hence always molar ratio of more than 6.94 was maintained. The results are as summarized in Table 3.22

The results indicate that the size of the particles decrease with the increase in the concentration of glucose. This is because of the increase in the nucleation rate leading to formation of smaller particles as in the case of copper nitrate precursor mentioned in the earlier section.

Table 3.22 Effect of ratio of reactants on the size of cuprous oxide particles prepared by the reduction of copper sulfate by glucose in the presence of CTAB

Molar ratio of glucose to copper sulfate	Particle Size (nm)	
	Thermal	Microwave
6.94	42	39
13.88	36	34
27.75	28	27

Effect of dilution: The reaction mixtures were diluted with varying amount of water. It was seen that with dilution the size of the particles decreased. The results of variation in

particle size are given in Table 3.23. The observed trend goes hand in hand with the trend observed for dilution in the case discussed in earlier section.

Table 3.23 Effect of dilution on the size of cuprous oxide particles prepared by the reduction of copper sulfate by glucose in the presence of CTAB

Dilution (mL)	Particle Size (nm)
0	42
50	39
100	35
150	29
200	25

Effect of addition of CTAB: The results pertaining to the effect of CTAB concentration on the size of the cuprous oxide particle are listed in Table 3.24. From the Table 3.24 it is seen that the addition of CTAB decreases the size of the cuprous oxide nanoparticles and also, as the concentration of CTAB increases, the particle size decreases. This could be attributed to the capping effect of CTAB resulting in restriction on the growth of particles and controlling the size of the formed particles.

Table 3.24 Effect of concentration of CTAB on the size of cuprous oxide particles prepared by the reduction of copper sulfate by glucose

Effective concentration of CTAB in the reaction mixture (mM)	Particle Size (nm)
0	56
1.67	42
8.33	35
16.67	29

The addition of CTAB provided the required stability to the fluid. In its absence the fluid was highly unstable. The fluid was stable for a minimum period of 6 months at room temperature under stationary conditions with the addition of CTAB.

Effect of power of microwave radiation and irradiation duration: The reaction was carried out at varying power of microwave radiation and irradiation duration. Irradiation for 5 minutes with 30 % power yielded particles of 24 nm but the reaction was not complete. At 50 % power microwave irradiation the reaction proceeded towards completion. For 50 %, 70 % and 90 % power for 5 minutes irradiation duration the size of the particles were 39 nm, 33 nm and 28 nm, respectively.

The irradiation duration also had an effect on the size as well as on the progress of the reaction. For 7 minutes and 10 minutes irradiation at 50 % power the size calculated were 46 nm and 50 nm, respectively. The observed trend is identical to the trend discussed in the case of reduction of copper nitrate in earlier section.

Typical low magnification (A) and high magnification (B) FESEM images of flower like cuprous oxide nanoparticles are shown in Fig. 3.76.

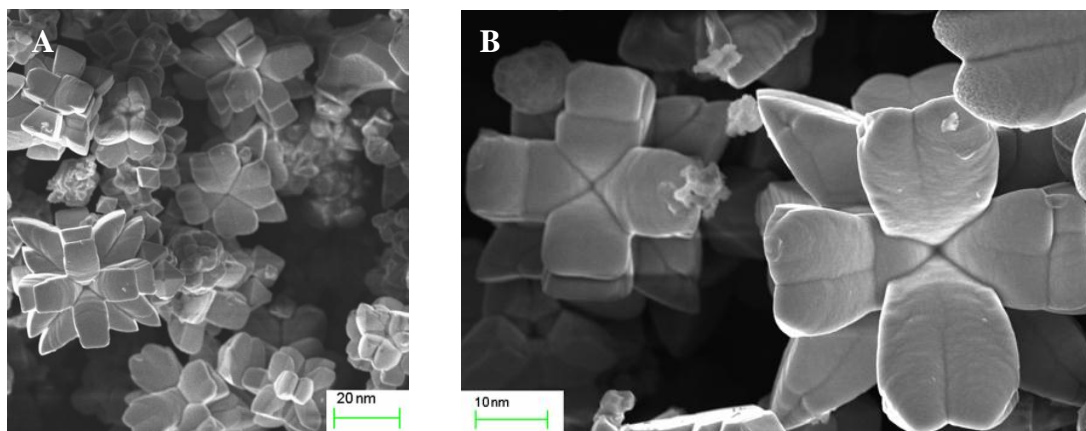


Fig. 3.76 (A) Low magnification and (B) high magnification FESEM images of cuprous oxide nanoparticles prepared by the reduction of copper sulfate by glucose in the presence of CTAB

The sizes obtained from the XRD results match well with that of the FESEM results.

➤ ***Results of thermal conductivity and viscosity measurements***

The cuprous oxide nanofluid showed a thermal conductivity of $1.653 \text{ W m}^{-1} \text{ K}^{-1}$ for particle weight fraction of 0.200 %. Fig. 3.77 shows the variation of thermal conductivity ratio with particle weight fraction. It is seen that the thermal conductivity of the nanofluid increases linearly with the increase in particle weight fraction. The trend is similar as in the cases discussed in the earlier sections.

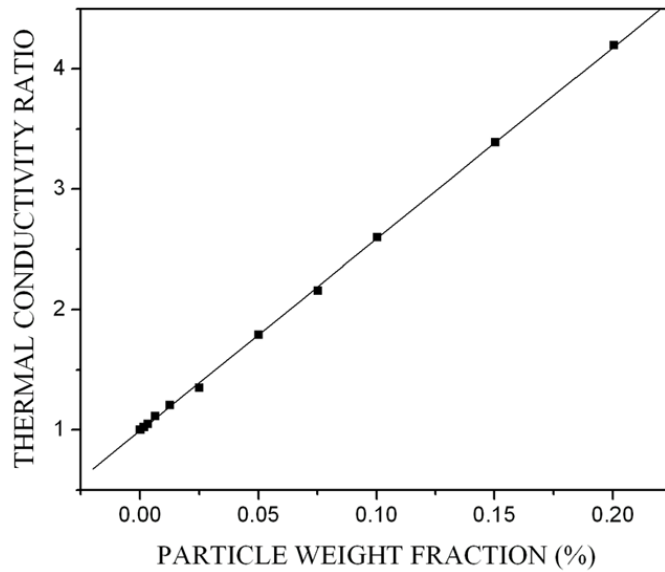


Fig. 3.77 Variation of thermal conductivity ratio with particle weight fraction for cuprous oxide nanofluid prepared by the reduction of copper sulfate by glucose in the presence of CTAB

The viscosity measurements of the nanofluid showed trends similar to that of copper nanofluids discussed in the earlier sections. Fig. 3.78 demonstrates the Newtonian behavior of the cuprous oxide nanofluid and the variation of viscosity with particle weight fraction and temperature.

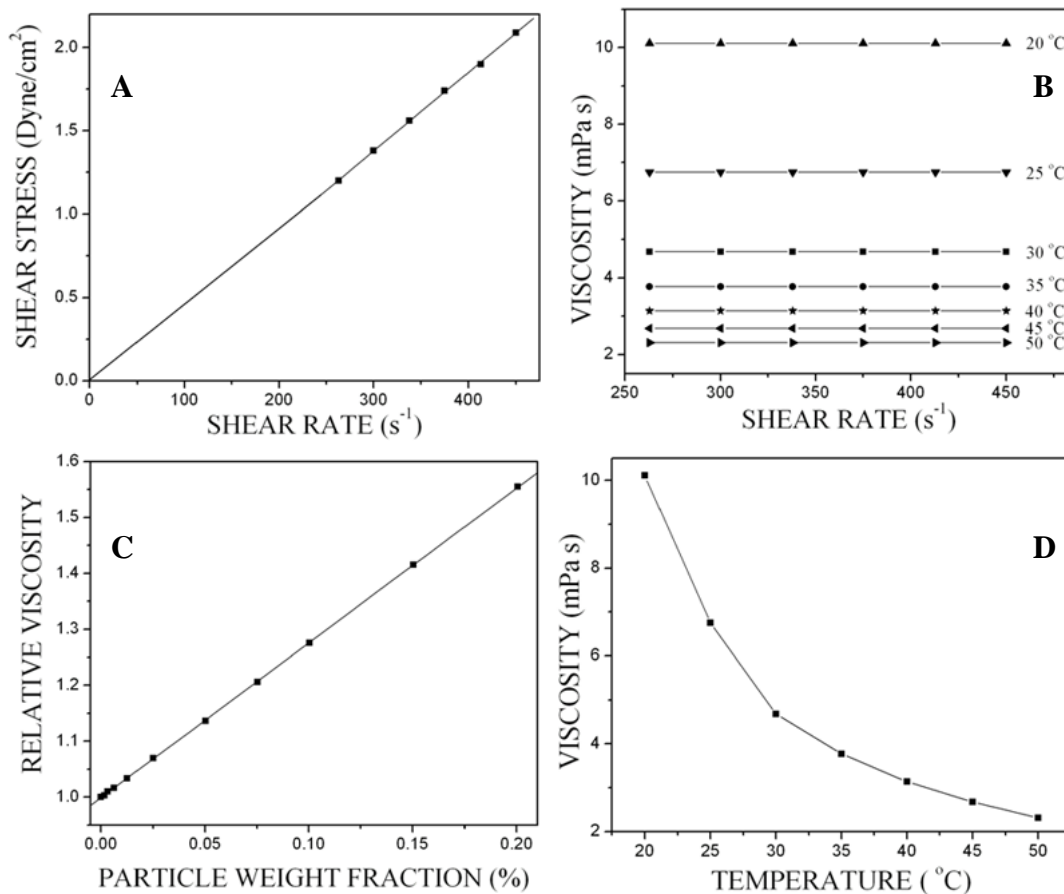


Fig. 3.78 Viscosity measurements of cuprous oxide nanofluid prepared by the reduction of copper sulfate by glucose in the presence of CTAB. (A) Shear stress verses shear rate; (B) Viscosity as a function of shear rate at different temperatures; (C) Variation of relative viscosity with particle weight fraction; (D) Viscosity as a function of temperature

3.2.2.3 Nanofluids synthesized using copper acetate and glucose

➤ Results of variation in reaction parameters

Effect of ratio of reactants: Synthesis of nanofluids was carried out with different amount of glucose and the effect of varying concentration of glucose on the size in both thermal as well as microwave conditions was studied. It was observed that the size of the cuprous

oxide particle decreased with the increase in the amount of glucose added. It was also observed that whenever the molar ratio of glucose to copper acetate was less than 2.77 the reaction did not go for completion. Hence always molar ratio of more than 2.77 was maintained. When the molar ratio of glucose to copper acetate was increased from 2.77 to 5.55 to 11.10 the size of the particles decreased from 74 nm to 69 nm to 63 nm, under conventional heating and 70 nm to 66 nm to 61 nm, under microwave irradiation. The observed trend is similar to that in the case of reduction of copper sulfate in the presence of CTAB mentioned in the earlier section.

Effect of dilution: The reaction mixture was diluted with varying volumes of water. It was found that with the increase in dilution there was decrease in the size of the particle due to the decrease in collision among the particles leading to retarded growth of particles as in the case discussed in the earlier sections. The results are given in Table 3.25

Table 3.25 Effect of dilution on the size of cuprous oxide particles prepared by the reduction of copper acetate by glucose in the presence of CTAB

Dilution (mL)	Particle Size (nm)
0	74
50	68
100	64
150	58
200	53

Effect of addition of CTAB: CTAB was added to provide stability to the nanofluid. The nanofluid was stable for more than 4 months at room temperature under stationary conditions. Concentration of surfactant also played an important role in controlling the size of the particle apart from enhancing the stability of the nanofluid. The results pertaining to the effect of concentration of CTAB on the size of the particle are tabulated in Table 3.26.

Table 3.26 Effect of concentration of CTAB on the size of cuprous oxide particles prepared by the reduction of copper acetate by glucose

Effective concentration of CTAB in the reaction mixture (mM)	Particle Size (nm)
0	92
1.67	74
8.33	69
16.67	63

The results clearly indicate that CTAB acts as a capping agent and hence restricts the growth of the particles.

Effect of power of microwave radiation and irradiation duration: It was found that at 30 % power for 5 minutes irradiation the particles obtained had a size of 49 nm but the reaction was incomplete. With increase in power of microwave radiation from 50% to 70 % to 90 % for 5 minutes duration the reaction proceeded to completion and the size of the particles decreased from 70 nm to 68 nm to 62 nm. The irradiation duration also was varied and its effect on particle size was studied. With the increase in duration of irradiation from 7 minutes to 10 minutes the particle size increased from 75 nm to 79 nm. The continued interaction of the particles for longer duration might be the cause for the growth of the particles, resulting in the increase in particle size.

FESEM images of cuprous oxide nanoparticles synthesized under microwave irradiation (A) and thermal conditions (B) are given in Fig. 3.79. The particles have whorled leaf like morphology. Since microwave reactions take place rapidly, time may not be sufficient enough for finer growth of the vein like or ridge like structures on the leaf surface. In thermal conditions ample time available may be facilitating such smooth and natural like structures in the formed particles. The sizes obtained from the XRD results match well with that of the FESEM results.

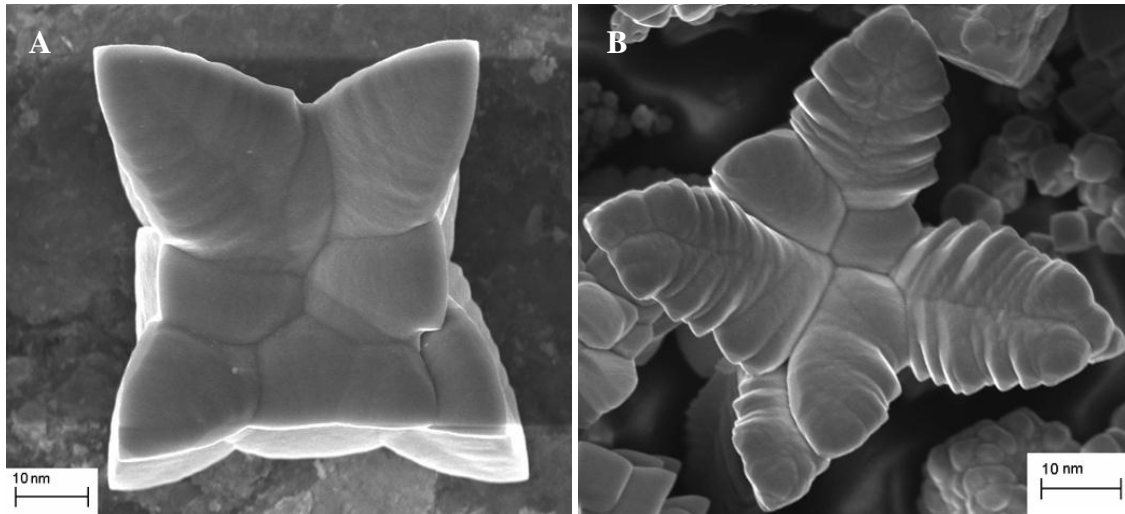


Fig. 3.79 FESEM image of cuprous oxide nanoparticles prepared by the reduction of copper acetate by glucose in the presence of CTAB (A) under microwave irradiation and (B) by conventional heating

➤ *Results of thermal conductivity and viscosity measurements*

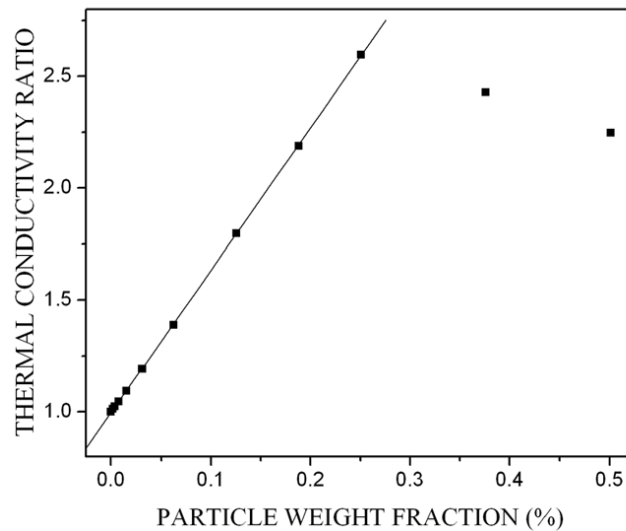


Fig. 3.80 Variation of thermal conductivity ratio with particle weight fraction for cuprous oxide nanofluid prepared by the reduction of copper acetate by glucose in the presence of CTAB

The nanofluid showed a thermal conductivity of $0.885 \text{ W m}^{-1} \text{ K}^{-1}$ for particle weight fraction of 0.501 %. The thermal conductivity of the nanofluid increased linearly with the increase in particle weight fraction. A maximum thermal conductivity of $1.023 \text{ W m}^{-1} \text{ K}^{-1}$ was observed at 0.251 % particle weight fraction. There after it showed a gradual decrease in conductivity. Figure 3.80 shows the variation of thermal conductivity ratio with particle weight fraction. The observed trend is similar as in case of cuprous oxide nanofluids prepared by reduction of copper acetate by glucose in the presence of SLS.

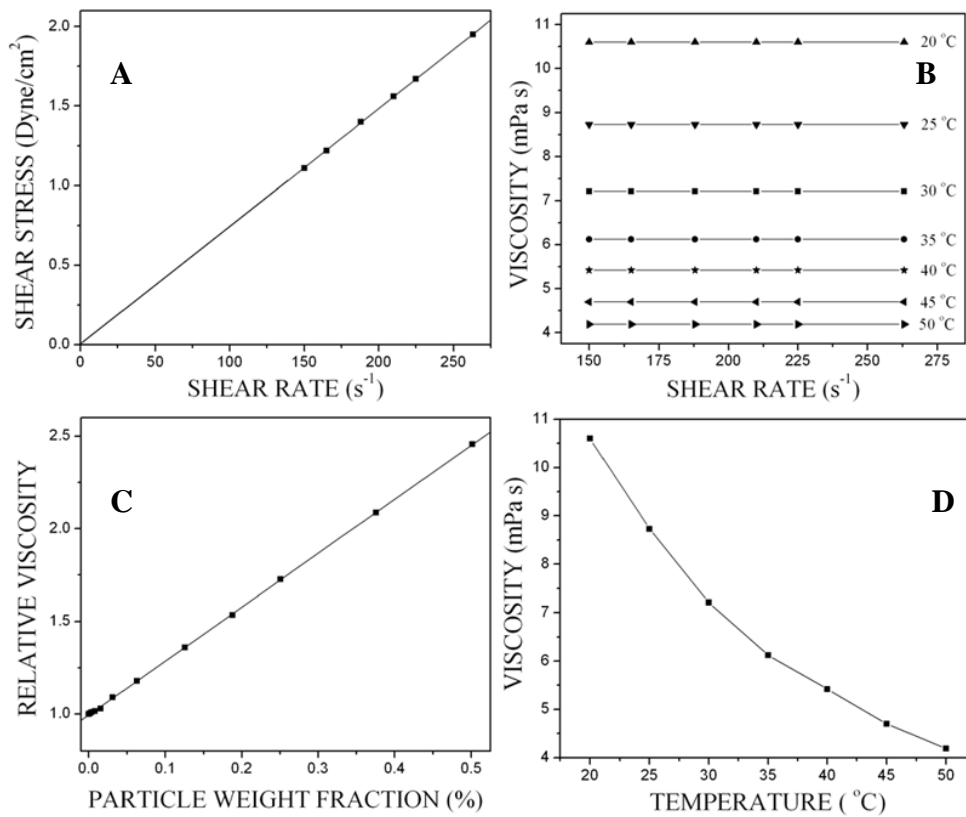


Fig. 3.81 Viscosity measurements of cuprous oxide nanofluid prepared by the reduction of copper acetate by glucose in the presence of CTAB. (A) Shear stress verses shear rate; (B) Viscosity as a function of shear rate at different temperatures; (C) Variation of relative viscosity with particle weight fraction; (D) Viscosity as a function of temperature

The viscosity measurements of the nanofluid showed trends similar to that of copper nanofluids discussed in earlier sections. Fig. 3.81 demonstrates the Newtonian behavior of the cuprous oxide nanofluid and the variation of viscosity with particle loading and temperature.

3.2.3 Cuprous Oxide Nanofluids Synthesized in the Presence of PVP

3.2.3.1 Nanofluids synthesized using copper nitrate and glucose

➤ *Results of variation in reaction parameters*

Effect of ratio of reactants: The synthesis was carried out by varying the molar ratio of glucose to copper nitrate. It was also observed that whenever the molar ratio of glucose to copper nitrate was less than 5.55 the reaction did not go for completion. Hence always molar ratio of more than 5.55 was maintained. The increase in molar ratio from 5.55 to 18.5 resulted in particles having sizes decreasing from 26 nm to 10 nm in thermal conditions and 28 nm to 9 nm in microwave conditions respectively. The size of the particles obtained were 23 nm and 17 nm during conventional heating and 26 nm and 19 nm during microwave heating, for molar ratio of 9.25 and 12.95, respectively. The observed trend is similar to the one observed for the same precursors in presence of CTAB.

Effect of dilution: The reaction mixture was diluted with 35 mL, 100 mL, 150 mL, 200 mL and 250 mL of water. The particle size decreased with the increase in amount of dilution. The particles yielded had 26 nm, 18 nm, 13 nm, 9 nm and 5 nm size for 35 mL, 100 mL, 150 mL, 200 mL and 250 mL dilution, respectively. For 250 mL dilution the reaction proceeded very slowly due to decrease in effective concentration of the reacting species. The observed decrease in size of the particles is because of the decrease in collision of the particles leading to lesser agglomeration and growth of the initially formed nuclei.

Effect of addition of PVP: Concentration of polymer also played a role in controlling the size of the particle as well as stability of the nanofluid. The results indicating the effect of concentration of PVP on the size of the particle are summarized in Table 3.27

Table 3.27 Effect of concentration of PVP on the size of cuprous oxide particles prepared by the reduction of copper nitrate by glucose

Effective concentration of PVP in the reaction mixture (mM)	Particle Size (nm)
0	48
0.71	26
3.57	19
7.14	14

The results clearly indicate that PVP acts as a capping agent and hence restricts the growth of the particles. As the PVP concentration increases, the particle size decreases. Sedimentation measurements showed that the nanofluid was stable up to 9 weeks at room temperature under stationary state.

Effect of power of microwave radiation and irradiation duration: When the reaction mixture was subjected to 30 % power microwave irradiation for 5 minutes the reaction was incomplete and size of the particles obtained was 24 nm. As power was increased (50 % to 70 % to 90 %) for 5 minutes irradiation duration the reaction proceeded to completion and the particle size was found to decrease (28 nm, 23 nm to 17 nm).

For 50 % irradiation for 3 minutes the incomplete reaction led to the formation of particles with size 20 nm. With increase in irradiation duration at 50 % power the size increased as 28 nm, 31 nm and 36 nm for 5 minutes, 7 minutes and 10 minutes respectively. The observed trend is identical to the results mentioned in the case of cuprous oxide nanofluids in the presence of CTAB.

Fig. 3.82 shows the low magnification TEM image (A) and high magnification FESEM image (B) of the cuprous oxide nanoparticles. The images reveal that the particles are somewhat cuboctahedral in shape. The sizes obtained from the XRD results match well with that of the TEM and FESEM results.

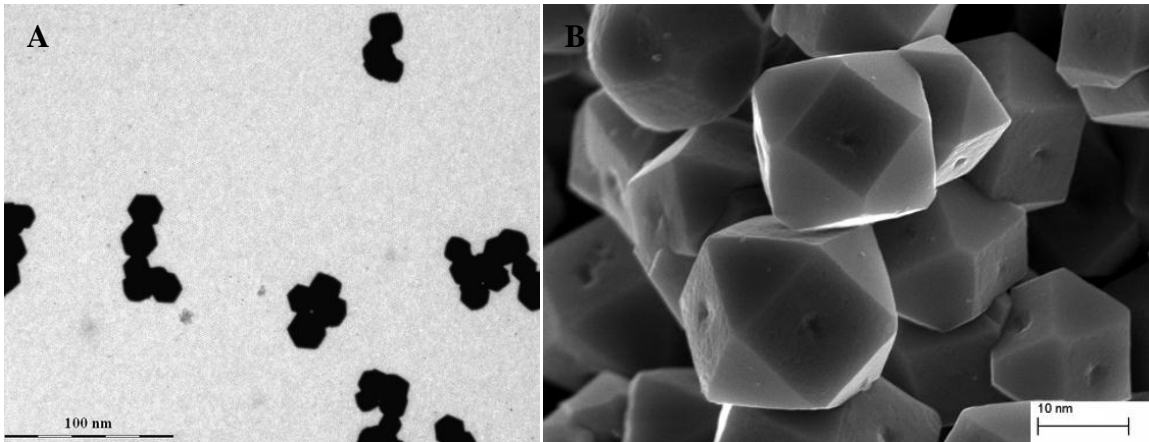


Fig. 3.82 (A) TEM image and (B) FESEM image of cuprous oxide nanoparticles prepared by the reduction of copper nitrate by glucose in the presence of PVP

➤ *Results of thermal conductivity and viscosity measurements*

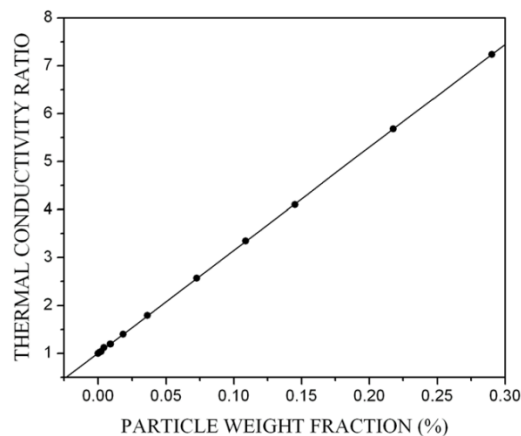


Fig. 3.83 Variation of thermal conductivity ratio with particle weight fraction for cuprous oxide nanofluid prepared by the reduction of copper nitrate by glucose in the presence of PVP

The cuprous oxide nanofluid showed a thermal conductivity of $2.852 \text{ W m}^{-1} \text{ K}^{-1}$ for particle weight fraction of 0.290 %. The thermal conductivity of the nanofluid increased linearly with the increase in particle weight fraction which could be attributed to the higher conductivity and uniform dispersal of nanoparticles. Fig. 3.83 shows the variation of thermal conductivity ratio with particle weight fraction. The trend is similar to that of cuprous oxide nanofluids prepared using same precursors in the presence of CTAB.

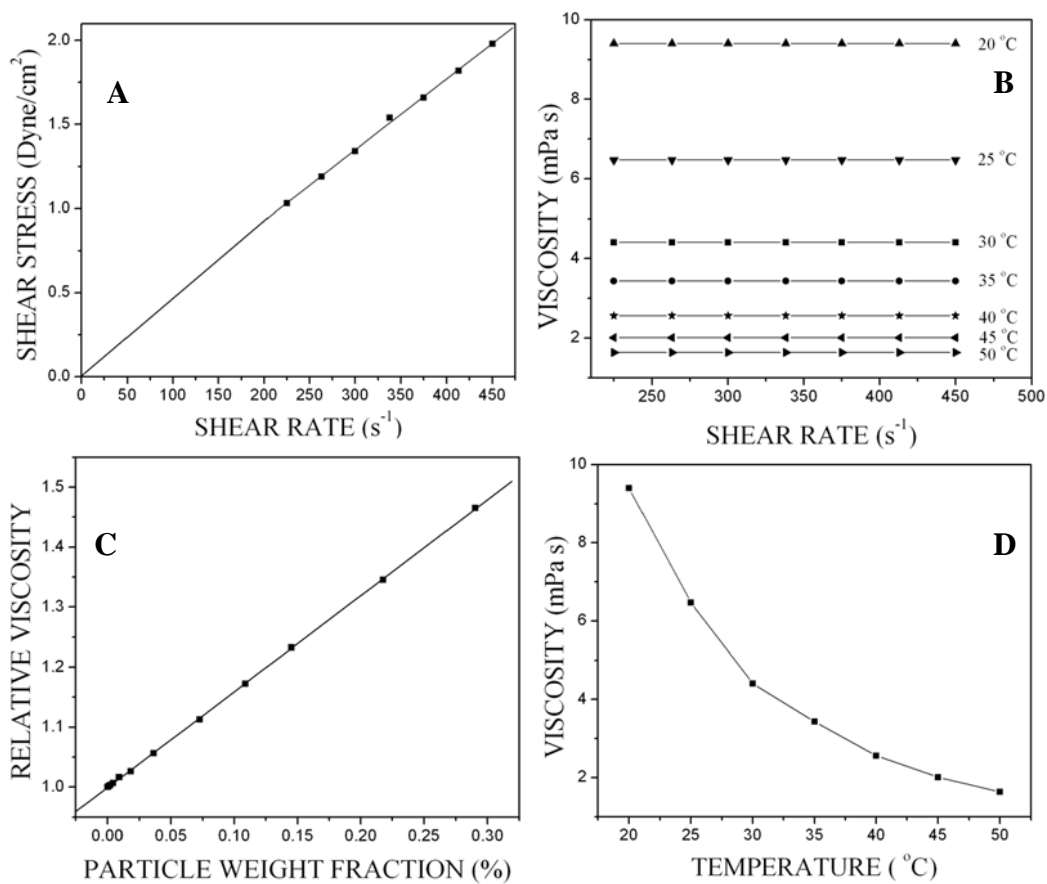


Fig. 3.84 Viscosity measurements of cuprous oxide nanofluid prepared by the reduction of copper nitrate by glucose in the presence of PVP. (A) Shear stress verses shear rate; (B) Viscosity as a function of shear rate at different temperatures; (C) Variation of relative viscosity with particle weight fraction; (D) Viscosity as a function of temperature

The viscosity measurements of the nanofluid showed trends similar to that of copper nanofluids discussed in the earlier sections. Fig. 3.84 demonstrates the Newtonian behavior of the cuprous oxide nanofluid and the variation of viscosity with particle loading and temperature.

3.2.3.2 Nanofluids synthesized using copper sulfate and glucose

➤ *Results of variation in reaction parameters*

Effect of ratio of reactants: The effect of amount of glucose added on the size of the cuprous oxide nanoparticle was studied both under thermal and microwave conditions. It was observed that whenever the molar ratio of glucose to copper sulfate was less than 6.66 the reaction did not go for completion. Hence always molar ratio of more than 6.66 was maintained. The results are as tabulated in Table 3.28

Table 3.28 Effect of ratio of reactants on the size of cuprous oxide particles prepared by the reduction of copper sulfate by glucose in the presence of PVP

Molar ratio of glucose to copper sulfate	Particle Size (nm)	
	Thermal	Microwave
6.66	24	25
11.10	22	22
15.54	19	18
22.20	14	11

The results indicate that the size of the particles decrease with the increase in concentration of glucose which is because of the increase in the nucleation rate leading to formation of smaller particles as discussed in the earlier sections.

Effect of dilution: The reaction mixtures were diluted with varying amount of water. It was seen that with dilution the size of the particle decreased. The results of variation in

particle size with dilution are given in Table 3.29. The observed trend is similar to the one discussed in the earlier sections.

Table 3.29 Effect of dilution on the size of cuprous oxide particles prepared by the reduction of copper sulfate by glucose in the presence of PVP

Dilution (mL)	Particle Size (nm)
30	24
100	17
150	12
200	8
250	4

Effect of addition of PVP: The results pertaining to the effect of polymer concentration on the size of cuprous oxide particle are summarized in Table 3.30. It is clear from the Table that the addition of PVP decreases the size of the cuprous oxide nanoparticles. As the concentration of PVP increases, the size of the particle decreases. This could be attributed to the capping effect of PVP resulting in restriction on the growth of the particles and controlling the size of the formed particles.

Table 3.30 Effect of concentration of PVP on the size of cuprous oxide particles prepared by the reduction of copper sulfate by glucose

Effective concentration of PVP in the reaction mixture (mM)	Particle Size (nm)
0	56
0.83	24
4.17	16
8.33	12

PVP also provided the required stability to the fluid. In its absence the fluid was highly unstable. The fluid was stable for a minimum period of 9 weeks at room temperature under stationary conditions in the presence of PVP.

Effect of power of microwave radiation and irradiation duration: The reaction was carried out at varying microwave power and irradiation duration. Irradiation for 3 minutes with 30 % power yielded particles of 21 nm but the reaction was not complete. At 50 % irradiation power the reaction proceeded towards completion. For 50 %, 70 % and 90 % power the size of the particles were 25 nm, 16 nm and 8 nm, respectively.

The irradiation duration also had an effect on the size as well as on the progress of the reaction. For 5 minutes, 7 minutes and 10 minutes irradiation the sizes of the particles obtained were 29 nm, 33 nm and 38 nm, respectively. The observed trend is identical to the trend mentioned in the earlier sections.

Typical TEM image (A) and low magnification FESEM image (B) of cuprous oxide nanoparticles are shown in Fig. 3.85.

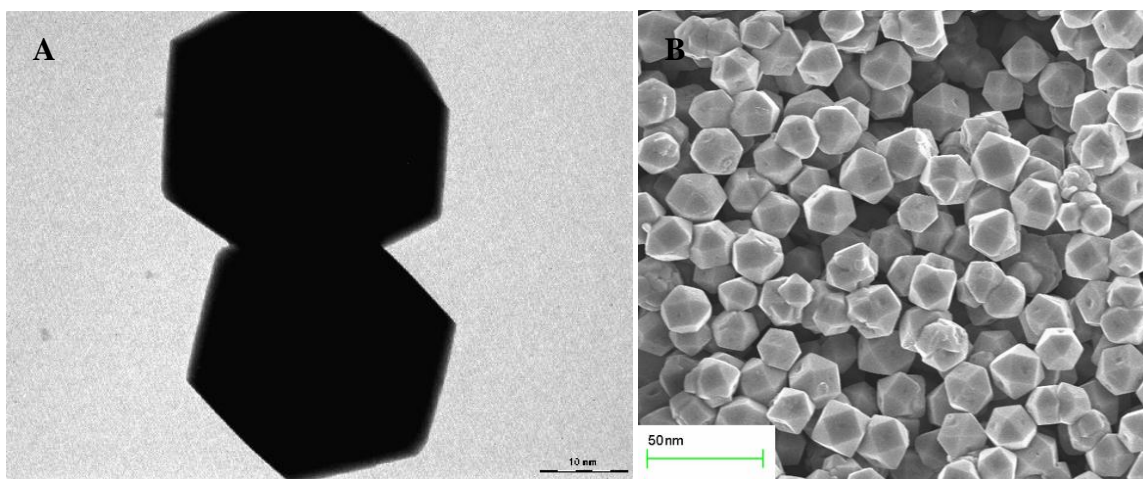


Fig. 3.85 (A) TEM image and (B) FESEM image of cuprous oxide nanoparticles prepared by the reduction of copper sulfate by glucose in the presence of PVP

The particles are somewhat cuboctahedral in shape. The sizes obtained from the XRD results match well with that of the TEM and FESEM results.

➤ ***Results of thermal conductivity and viscosity measurements***

The cuprous oxide nanofluid showed a thermal conductivity of $2.876 \text{ W m}^{-1} \text{ K}^{-1}$ for particle weight fraction of 0.282 %. Fig. 3.86 shows the variation of thermal conductivity ratio with particle weight fraction. It is seen from the Fig. 3.86 that the thermal conductivity of the nanofluid increases linearly with the increase in particle weight fraction. The trend is similar as discussed in the earlier sections.

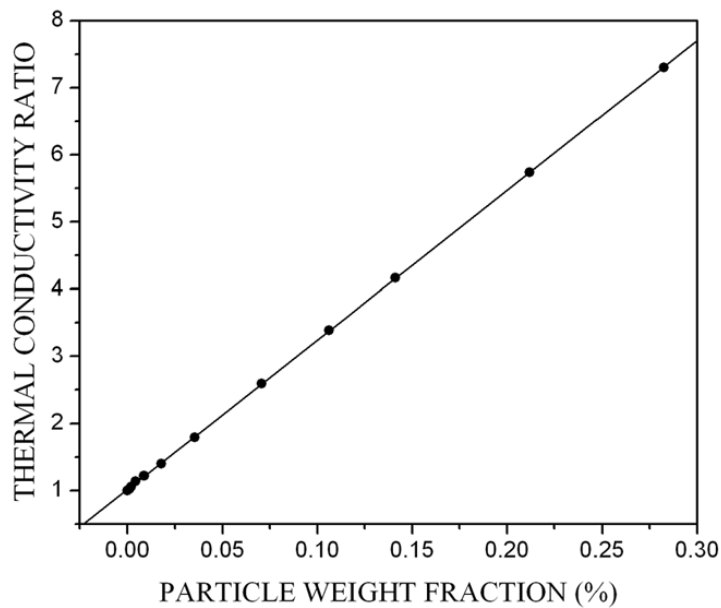


Fig. 3.86 Variation of thermal conductivity ratio with particle weight fraction for cuprous oxide nanofluid prepared by the reduction of copper sulfate by glucose in the presence of PVP

The viscosity measurements of the nanofluid showed trends similar to that of copper nanofluids discussed in the earlier sections. Fig. 3.87 demonstrates the Newtonian

behavior of the cuprous oxide nanofluid and the variation of viscosity with particle weight fraction and temperature.

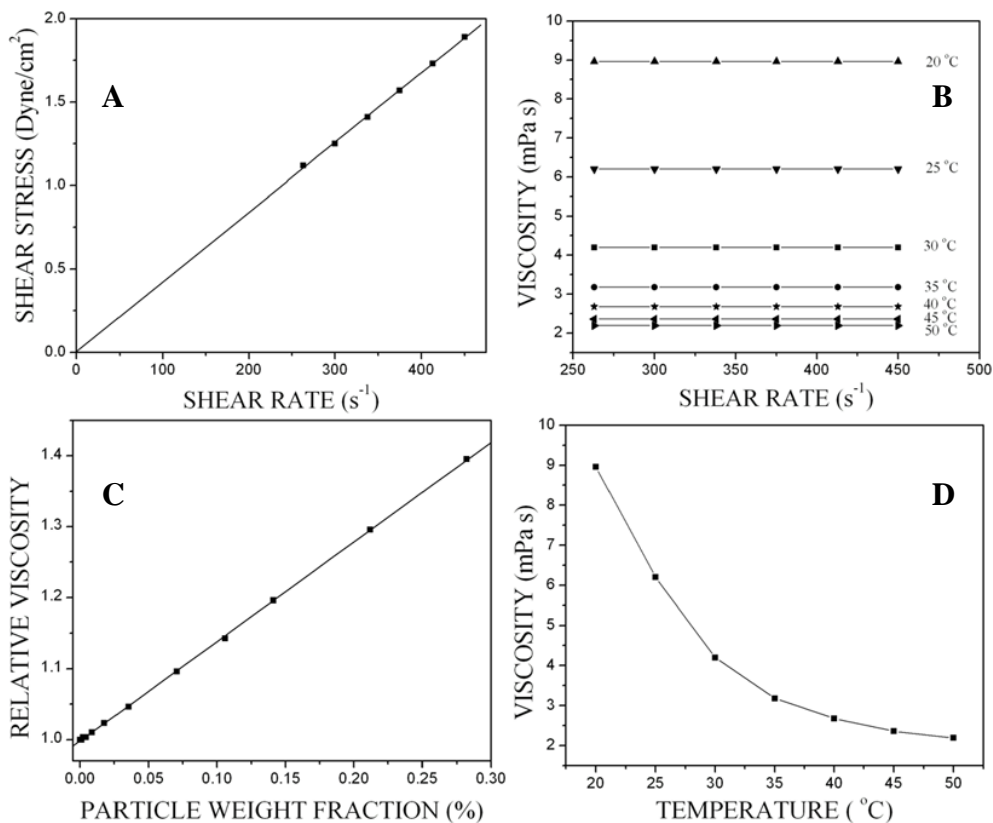


Fig. 3.87 Viscosity measurements of cuprous oxide nanofluid prepared by the reduction of copper sulfate by glucose in the presence of PVP. (A) Shear stress verses shear rate; (B) Viscosity as a function of shear rate at different temperatures; (C) Variation of relative viscosity with particle weight fraction; (D) Viscosity as a function of temperature

3.2.3.3 Nanofluids synthesized using copper acetate and glucose

➤ Results of variation in reaction parameters

Effect of ratio of reactants: Synthesis of nanofluids was carried out with different amount of glucose and the effect on the size in both thermal as well as microwave conditions was

studied. It was observed that the cuprous oxide particle size decreased with the increase in the amount of glucose added. It was also observed that whenever the molar ratio of glucose to copper acetate was less than 3.7 the reaction did not go for completion. Hence always molar ratio of more than 3.7 was maintained. When the molar ratio of glucose to copper acetate was increased from 3.7 to 7.4 to 10.36 to 14.8 the size of the particles decreased from 45 nm to 38 nm to 32 nm to 27 nm under conventional heating and 41 nm to 35 nm to 31 nm to 26 nm under microwave irradiation, respectively. The observed trend is similar to that in the case of reduction of copper sulfate by glucose in the presence of PVP.

Effect of dilution: The reaction mixture was diluted with varying volumes of water to study the effect of dilution. It was found that with the increase in dilution there was decrease in the size of the particle due to the decrease in collision among the particles leading to retarded growth of particles. The results are given in Table 3.31

Table 3.31 Effect of dilution on the size of cuprous oxide particles prepared by the reduction of copper acetate by glucose in the presence of PVP

Dilution (mL)	Particle Size (nm)
20	45
50	42
100	39
150	34
200	29
250	24
300	19

Effect of addition of PVP: PVP was added to provide stability to the nanofluid. The nanofluid was stable for more than 4 weeks at room temperature under stationary conditions. Concentration of polymer also played an important role in controlling the size

of the particle apart from enhancing the stability of the nanofluid. The results pertaining to the effect of concentration of PVP on the size of the particles are as shown in Table 3.32. The results clearly indicate that PVP acts as a capping agent and hence restricts the growth of the particles.

Table 3.32 Effect of concentration of PVP on the size of cuprous oxide particles prepared by the reduction of copper acetate by glucose

Effective concentration of PVP in the reaction mixture (mM)	Particle Size (nm)
0	58
1.25	45
6.25	36
12.5	29

Effect of power microwave radiation and irradiation duration: It was found that when the reaction mixture was subjected to microwave irradiation at 30 % power for 3 minutes the particles obtained had a size of 36 nm but the reaction was incomplete. With increase in power of microwave radiation from 50% to 70 % to 90 % for 3 minutes duration the reaction proceeded to completion and the size of the particles decreased from 41 nm to 37 nm to 24 nm, respectively.

The irradiation duration also was varied and its effect on particle size was studied. At 50 % power irradiation for 5 minutes obtained particles had a size of 44 nm. With the increase in duration of irradiation from 7 minutes to 10 minutes the particle size increased from 48 nm to 53 nm. The continued interaction of the particles for longer duration might be the cause for the growth of the particles, resulting in the increase in the particle size.

TEM image (A) and FESEM image (B) of the cuprous oxide nanoparticles are shown in Fig. 3.88. The particles are mixture of somewhat truncated cube shaped and spherical structures. High magnification image of a single truncated cube shaped particle

is given as inset in Fig. 3.88 (B). The sizes obtained from the XRD results match well with that of the TEM and FESEM results.

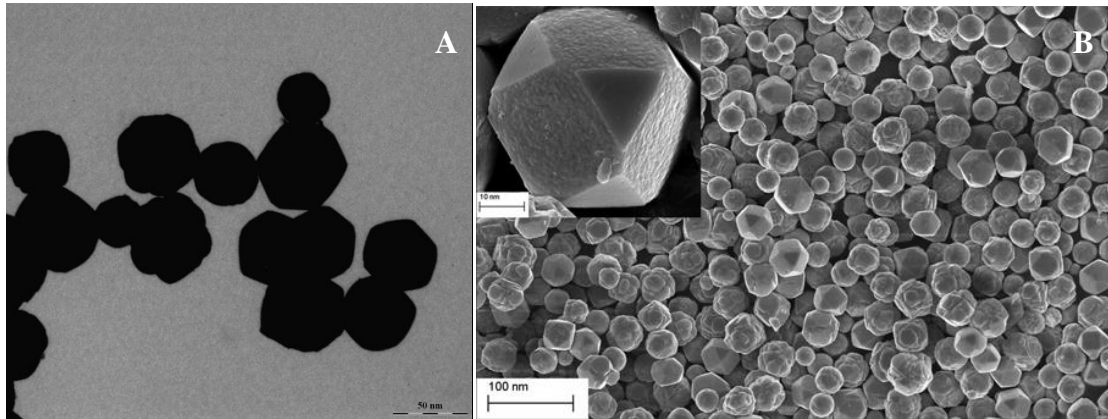


Fig. 3.88 (A) TEM image and (B) FESEM image of cuprous oxide nanoparticles prepared by the reduction of copper acetate by glucose in the presence of PVP

➤ *Results of thermal conductivity and viscosity measurements*

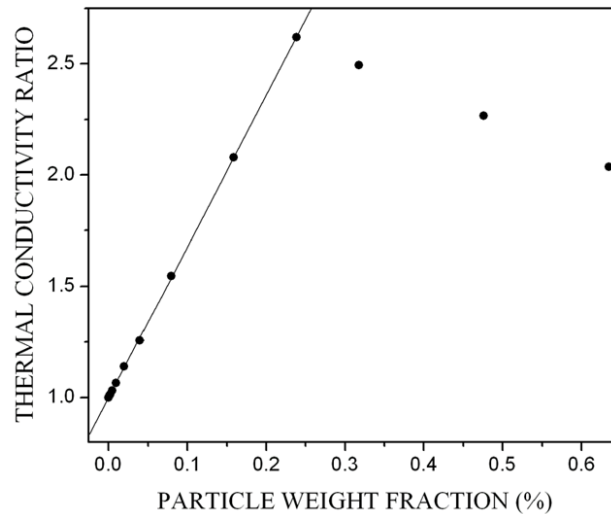


Fig. 3.106 Variation of thermal conductivity ratio with particle weight fraction for cuprous oxide nanofluid prepared by the reduction of copper acetate by glucose in the presence of PVP

The thermal conductivity of the nanofluid increased linearly with the increase in particle weight fraction. A maximum thermal conductivity of $1.032 \text{ W m}^{-1} \text{ K}^{-1}$ was observed at 0.238 % particle weight fraction. There after it showed a gradual decrease in conductivity. Fig. 3.89 shows the variation of thermal conductivity ratio with particle weight fraction. The observed trend is similar as in case of cuprous oxide nanofluids prepared by reduction of copper acetate by glucose in the presence of CTAB.

The viscosity measurements of the nanofluid showed trends similar to that of copper nanofluids discussed in the earlier sections. Fig. 3.90 demonstrates the Newtonian behavior of the cuprous oxide nanofluid and the variation of viscosity with particle loading and temperature.

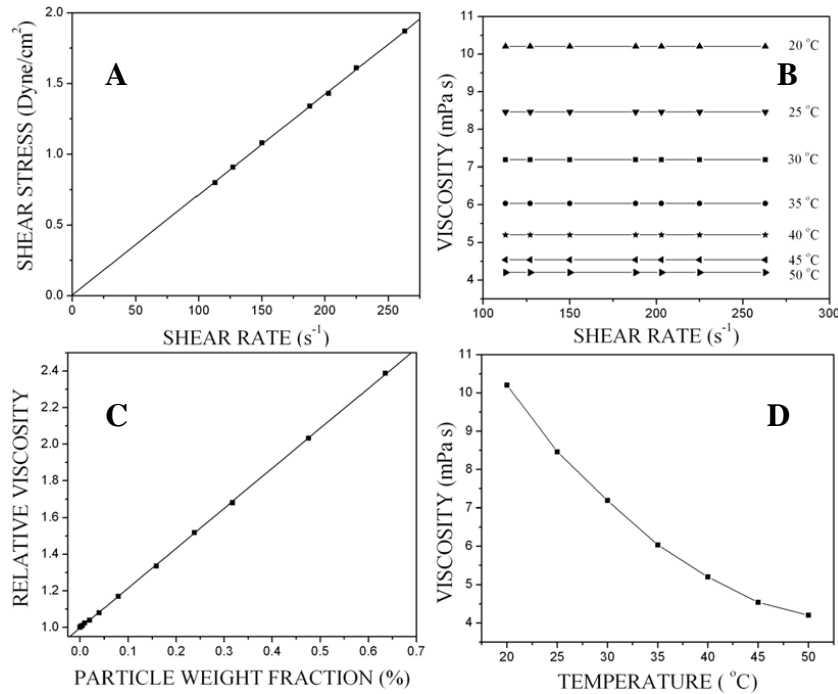


Fig. 3.90 Viscosity measurements of cuprous oxide nanofluid prepared by the reduction of copper acetate by glucose in the presence of PVP. A. Shear stress verses shear rate; B. Viscosity as a function of shear rate at different temperatures; C. Variation of relative viscosity with particle weight fraction; D. Viscosity as a function of temperature

Table 3.33 Comparison of particle sizes and thermal conductivities of synthesized nanofluids

Precursor Copper Salt	Reducing Agent	Stabilizing Agent	Nanofluid	Particle Size		Particle Weight Fraction (%)	Maximum Thermal Conductivity ($\text{W m}^{-1} \text{K}^{-1}$)
				Thermal (nm)	Microwave (nm)		
Nitrate	Ascorbic acid	SLS	Copper	22	35	0.1669	1.04
Sulfate	Ascorbic acid	SLS	Copper	29	32	0.0969	0.912
Acetate	Ascorbic acid	SLS	Copper	13	33	0.1301	1.92
Nitrate	Ascorbic acid	CTAB	Copper	59	57	0.2005	4.695
Sulfate	Ascorbic acid	CTAB	Copper	52	49	0.2005	4.727
Acetate	Ascorbic acid	CTAB	Copper	74	69	0.2506	2.097
Nitrate	Ascorbic acid	PVP	Copper	32	33	0.1672	1.774
Sulfate	Ascorbic acid	PVP	Copper	70	64	0.0963	0.827
Acetate	Ascorbic acid	PVP	Copper	39	42	0.1879	1.268
Nitrate	Glucose	SLS	Copper	36	28	0.1493	0.968
Sulfate	Glucose	SLS	Copper	38	40	0.1503	0.979
Acetate	Glucose	SLS	Cuprous oxide	32	60&10	0.2819	2.948
Nitrate	Glucose	CTAB	Cuprous oxide	52	48	0.2005	1.975
Sulfate	Glucose	CTAB	Cuprous oxide	42	39	0.2005	1.653
Acetate	Glucose	CTAB	Cuprous oxide	74	70	0.2506	1.023
Nitrate	Glucose	PVP	Cuprous oxide	26	28	0.2902	2.852
Sulfate	Glucose	PVP	Cuprous oxide	24	25	0.2823	2.876
Acetate	Glucose	PVP	Cuprous oxide	45	41	0.2381	1.032



CHAPTER 4

SUMMARY AND CONCLUSIONS

Chapter 4 outlines the summary of the work presented in the thesis along with the conclusions pertaining to the research work. Scope for further work also has been included in this chapter.

4.1 SUMMARY

The work presented in this report has been broadly divided into four chapters with several sections in each chapter. The first chapter titled **Introduction and a Review of the Literature** covers a general introduction, literature review on nanofluids, scope and objectives of the work. The second chapter titled **Experimental** deals with the materials and methods employed in the present work. The third chapter titled **Results and Discussion** deals with the results and their interpretations.

Copper and cuprous oxide nanofluids have been prepared using copper nitrate, copper sulfate and copper acetate by one step solution phase method. Ascorbic acid and glucose were used as reducing agents in the presence of SLS, CTAB and PVP. The synthesized nanofluids were characterized using XRD, EDXA, SAED, TEM, FESEM, FTIR spectroscopy and UV-Vis spectroscopy. The effect of reaction conditions like ratio of reactants, dilution, pH, power of microwave radiation, irradiation duration on the size of the particles formed have been studied. Sedimentation measurements have been made to investigate the stability of the fluid. Thermal conductivity and viscosity measurements have also been carried out. The findings have been briefed below.

- Reduction using ascorbic acid led to the formation of copper nanofluids in the presence of SLS, CTAB and PVP.
- Cuprous oxide nanofluids were obtained when glucose was used as reducing agent in the presence of CTAB and PVP.
- Synthesis using glucose as reducing agent in the presence of SLS led to the formation of copper nanofluids except where copper acetate was used as precursor where cuprous oxide nanofluid was obtained.
- The results obtained from various analyses were in agreement with each other.

- The particle sizes were found to be well within nano range varying between 4 nm to 96 nm under different conditions employed during synthesis.
- In the presence of SLS and PVP when nitrates and acetates were reduced by ascorbic acid, decrease in pH of the reaction mixture led to the increase in size of the particles formed.
- The particle size was found to decrease with the increase in the molar ratio of reducing agent to salt in microwave reactions.
- Synthesis in thermal conditions led to the decrease in particle size with the increase in concentration of reductant in general, except where pH of the reaction mixture played a role and also in the case of glucose reduction of copper acetate in the presence of SLS, where the particle size increased.
- In general particle size decreased with the increase in dilution except in the case of ascorbic acid reduction of copper nitrate and copper sulphate in the presence of SLS and PVP, respectively.
- The stabilizing agents added in general led to the decrease in size of the particles, except in the case where ascorbic acid was used as reductant in the presence of SLS where particle size increased with the increase in surfactant concentration after the initial decrease.
- With the increase in power of microwave irradiated the particle size in general decreased except in the case of reduction of acetate precursor with glucose in the presence of SLS.
- The particle size increased in general when the irradiation duration was increased except in the presence of SLS in the case of sulfate precursor and when acetate salt was reduced by ascorbic acid.
- Copper nanofluids synthesized by reducing copper sulfate by ascorbic acid in the presence of SLS and PVP and by reducing copper nitrate using glucose in the presence of SLS were least stable, with stability period of 3 weeks.
- Maximum stability of 6 months was achieved in the case of copper and cuprous oxide nanofluids prepared in the presence of CTAB using nitrate and sulfate precursors.

- The least thermal conductivity was found to be $0.812 \text{ W m}^{-1} \text{ K}^{-1}$ for copper nanofluids (0.3 %) synthesized by reducing copper sulfate using glucose in the presence of SLS.
- The highest thermal conductivity was found to be $4.727 \text{ W m}^{-1} \text{ K}^{-1}$ for copper nanofluids (0.2 %) synthesized by reducing copper sulfate using ascorbic acid in the presence of CTAB.
- The least and highest thermal conductivity was found to be $0.802 \text{ W m}^{-1} \text{ K}^{-1}$ (0.635 %) and $2.876 \text{ W m}^{-1} \text{ K}^{-1}$ (0.282 %) for cuprous oxide nanofluids synthesized in the presence of PVP by reducing copper acetate and copper sulfate, respectively, using glucose.
- The thermal conductivity of the nanofluids increased with the increase in particle weight fraction.
- The nanofluids were found to be Newtonian in nature.
- The viscosity of the fluids increased with the increase in particle weight fraction and decreased with the increase in temperature.

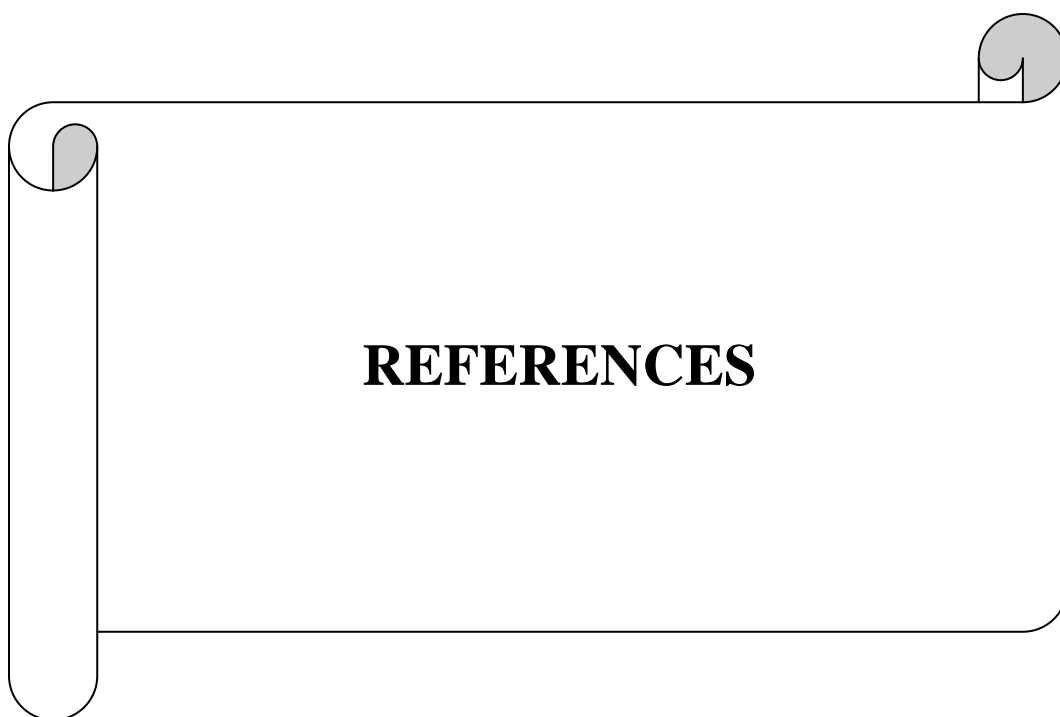
4.2 CONCLUSIONS

- Copper nanofluids can be prepared by the reduction of copper nitrate, copper sulfate and copper acetate using ascorbic acid as reducing agent in the presence of SLS, CTAB and PVP. Copper nanofluids can also be prepared by the reduction of copper nitrate and copper sulfate using glucose in the presence of SLS.
- Cuprous oxide nanofluids can be prepared by the reduction of copper nitrate, copper sulfate and copper acetate using glucose as reducing agent in the presence of CTAB and PVP. Cuprous oxide nanofluids can also be prepared by the reduction of copper acetate using glucose as reducing agent in the presence of SLS.
- The copper nanofluids synthesized under different conditions were stable from a minimum period of 3 weeks to a maximum period of 6 months.
- Stability period from least of 4 weeks to a maximum of 6 months was achievable for cuprous oxide nanofluids.
- All the nanofluids showed enhanced thermal conductivity.

- Among all the nanofluids synthesized, copper nanofluid showed a maximum thermal conductivity of $4.727 \text{ W m}^{-1} \text{ K}^{-1}$ and that of cuprous oxide nanofluid was $2.876 \text{ W m}^{-1} \text{ K}^{-1}$
- The method employed is fast, simple, low cost and extendible.

4.3 SCOPE FOR FURTHER WORK

1. Synthesis of copper and cuprous oxide nanofluids by one step chemical methods using other copper salts and reducing agents.
2. Synthesis of copper and cuprous oxide nanofluids in the presence of various other stabilizing agents.
3. Synthesis of other metal and metal oxide nanofluids by one step chemical methods.
4. Application of the as synthesized nanofluids for real world devices.



REFERENCES

REFERENCES:

Akoh, H., Tsukasaki, Y., Yatsuya, S. and Tasaki, A. (1978). "Magnetic properties of ferromagnetic ultrafine particles prepared by vacuum evaporation on running oil substrate." *J. Cryst. Growth*, 45, 495 – 500.

Anwar, K., Han, T. and Kim, S.M. (2011). "Reversible sealing techniques for microdevice applications." *Sens. Actuators, B.*, 153, 301 – 311.

Battez, A.H., Viesca, J.L., Gonzalez, R., Blanco, D., Asedegbega, E. and Osorio, A. (2010). "Friction reduction properties of a CuO nanolubricant used as lubricant for a NiCrBSi coating." *Wear*, 268, 325 – 328.

Beck, M.P., Yuan, Y, Warriar, P. and Teja, A.S. (2010). "The thermal conductivity of alumina nanofluids in water, ethylene glycol and ethylene glycol - water mixtures." *J. Nanopart. Res.*, 12, 1469 – 1477.

Bicer, M. and Sisman, I. (2010). "Controlled synthesis of copper nano/microstructures using ascorbic acid in aqueous CTAB solution." *Powder Technol.*, 198, 279 – 284.

Bonnemann, H., Botha, S.S., Bladergroen, B. and Linkov V. M. (2005). "Monodisperse copper and silver nanocolloids suitable for heat-conductive fluids." *Appl. Organometal. Chem.*, 19, 768 – 773.

Cao, G. (2003). "Nanostructures and nanomaterials - Synthesis, properties and applications." Imperial college press, London.

Chang, H., Tsung, T.T., Lin, H.M. and Lin, C.K. (2004). "Photocatalytic activity of TiO₂ nanoparticle fluid prepared by combined ASNSS." *China Part.*, 2(4), 171 – 173.

Chang, H., Tsung, T.T., Chen, L.C., Yang, Y.C., Lin, H.M., Lin, C.K. and Jwo, C.S. (2005). "Nanoparticle suspension preparation using the arc spray nanoparticle synthesis

system combined with ultrasonic vibration and rotation electrode.” *Int. J. Adv. Manuf. Technol.* 26, 552 – 558.

Chang, H., Jwo, C.S., Lo, C.H., Kao, M.J. and Pai, S.H. (2007). “A study of process optimization using the combined submerged arc nanoparticle synthesis system for preparing TiO₂ nanoparticle suspension.” *J. Alloys Compd.*, 434 - 435, 668 – 671.

Chang, H. and Liu, M.K. (2007). “Fabrication and process analysis of anatase type TiO₂ nanofluid by an arc spray nanofluid synthesis system.” *J. Cryst. Growth*, 304, 244 – 252.

Chang, H. and Chang, Y.C. (2008). “Fabrication of Al₂O₃ nanofluid by a plasma arc nanoparticles synthesis system.” *J. Mater. Process. Technol.*, 207, 193 – 199.

Chang, M.H., Liu, H.S. and Tai, C.Y. (2011). “Preparation of copper oxide nanoparticles and its applications in nanofluid.” *Powder Technol.*, 207, 378 – 386.

Chein, R. and Chuang, J. (2007). “Experimental microchannel heat sink performance studies using nanofluids.” *Int. J. Therm. Sci.*, 46, 57 – 66.

Chen, L.C. (2010). “Preparation of TiO₂ nanoparticles by submerged arc nanoparticle synthesis system.” *J. Alloys Compd.*, 495(2), 476 – 480.

Chen, H.J. and Wen, D. (2011). “Ultrasonic aided fabrication of gold nanofluids.” *Nanoscale Res. Lett.*, 6, 198 – 198-8.

Chin, S.F., Iyer, S.K, Raston, C.L. and Saunders, M. (2008). “Size selective synthesis of superparamagnetic nanoparticles in thin fluids under continuous flow conditions.” *Adv. Funct. Mater.*, 18(6), 922 – 927.

Cho, T., Baek, I., Lee, J. and Park, S. (2005). “Preparation of nanofluids containing suspended silver particles for enhancing fluid thermal conductivity of fluids.” *J. Ind. Eng. Chem.*, 11(3), 400 – 406.

Choi, C., Yoo, H.S. and Oh, J.M. (2008). "Preparation and heat transfer properties of nanoparticle in transformer oil dispersions as advanced energy efficient coolants." *Curr. Appl. Phys.*, 8, 710 – 712.

Chopkar, M., Das, P.K. and Manna, I. (2006). "Synthesis and characterization of a nanofluid for advanced heat transfer applications." *Scr. Mater.*, 55, 549 – 552.

Dadgostar, N., Ferdous, S. and Henneke, D. (2010). "Colloidal synthesis of copper nanoparticles in a two-phase liquid - liquid system." *Mater. Lett.*, 64, 45 – 48.

Das, S.K., Putra, N. and Roetzel, W. (2003a). "Pool boiling characteristics of nanofluids." *Int. J. Heat Mass Transfer*, 46, 851 – 862.

Das, S.K., Putra, N., Thiesen, P. and Roetzel, W. (2003b). "Temperature dependence of thermal conductivity enhancement for nanofluids." *J. Heat Transfer*, 125, 567 – 574.

Das, S.K., Choi, S.U.S., Yu, W. and Pradeep, T. (2008). "Nanofluids - science and technology." John wiley & sons, inc., New Jersey.

Duangthongsuk, W. and Wongwises, S. (2008). "Effect of thermophysical properties models on the predicting of the convective heat transfer coefficient for low concentration nanofluid." *Int. Commun. Heat Mass Transfer*, 35, 1320 – 1326.

Eastman, J.A., Choi, S.U.S., Li, S., Yu, W. and Thompson, L.J. (2001). "Anomalously increased effective thermal conductivities of ethylene glycol based nanofluids containing copper nanoparticles." *Appl. Phys. Lett.*, 78, 718 – 720.

Farajollahi, B., Etemad, S.G. and Hojjat, M. (2010). "Heat transfer of nanofluids in a shell and tube heat exchanger." *Int. J. Heat Mass Transfer*, 53, 12 – 17.

Fedele, L., Colla, L., Bobbo, S., Barison, S. and Agresti, F. (2011). “Experimental stability analysis of different water based nanofluids.” *Nanoscale Res. Lett.*, 6, 300 – 300-8.

Gallego, M.J.P., Casanova, C., Legido, J.L. and Pineiro, M.M. (2011). “CuO in water nanofluid: Influence of particle size and polydispersity on volumetric behaviour and viscosity.” *Fluid Phase Equilib.*, 300, 188 – 196.

Habibzadeh, S., Beydokhty, A.K., Khodadadi, A.A., Omanovic, S. and Niassar, M.S. (2009). “Stability and thermal conductivity of nanofluids of tin dioxide synthesized via microwave-induced combustion route.” *Chem. Eng. J.*, 11, 7 – 15.

Harikrishnan, S. and Kalaiselvam, S. (2012). “Preparation and thermal characteristics of CuO-oleic acid nanofluids as a phase change material.” *Thermochim. Acta*, 533, 46 – 55.

Hong, T.K., Yang, H.S. and Choi, C.J. (2005). “Study of enhanced thermal conductivity of Fe nanofluids.” *J. Appl. Phys.*, 97, 064311 – 064311-4.

Hong, K.S., Hong, T.K. and Yang, H.S. (2006). “Thermal conductivity of Fe nanofluids depending on the cluster size of nanoparticles.” *Appl. Phys. Lett.*, 88, 031901 – 031901-3.

Jana, N.R., Wang, Z.L., Sau, T.K. and Pal, T. (2000). “Seed-mediated growth method to prepare cubic copper nanoparticles.” *Curr. Sci.*, 79, 1367 – 1370.

Jordan, A., Scholz, R., Wust, P., Fahling, H. and Felix R. (1999). “Magnetic fluid hyperthermia (MFH): cancer treatment with ac magnetic field induced excitation of biocompatible superparamagnetic nanoparticles.” *J. Magn. Magn. Mater.*, 201(1-3), 413 – 419.

Jung, J.Y., Oh, H.S. and Kwak, H.Y. (2009). “Forced convective heat transfer of nanofluids in microchannels.” *Int. J. Heat Mass Transfer*, 52, 466 – 472.

Kang, H.U., Kim, S.H. and Oh, J.M. (2006a). "Estimation of thermal conductivity of nanofluid using experimental effective particle volume." *Exp. Heat Transfer*, 19, 181 – 191.

Kang, S.W., Wei, W.C., Tsai, S.H. and Yang, S.Y. (2006b). "Experimental investigation of silver nano-fluid on heat pipe thermal performance." *Appl. Therm. Eng.*, 26, 2377 – 2382.

Kao, M. J., Lo, C.H., Tsung, T.T., Wu Y.Y., Jwo, C.S. and Lin H.M. (2007). "Copper-oxide brake nanofluid manufactured using arc-submerged nanoparticle synthesis system." *J. Alloys Compd.*, 434 - 435, 672 – 674.

Kebllinski, P., Eastman, J.A. and Cahill, D.G. (2005). "Nanofluids for thermal transport." *Mater. Today*, 8(6), 36 – 44.

Khedkar, R.S., Sonawane, S.S. and Wasewar, K.L. (2012). "Influence of CuO nanoparticles in enhancing the thermal conductivity of water and monoethylene glycol based nanofluids." *Int. Commun. Heat Mass Transfer*, 39(5), 665 – 669.

Kim, Y.S., Nakatsuka, K., Fujita, T. and Atarashi, T. (1999). "Application of hydrophilic magnetic fluid to oil seal." *J. Magn. Magn. Mater.*, 201(1-3), 361 – 363.

Kim, Y.S. and Kim, Y.H. (2003). "Application of ferro-cobalt magnetic fluid for oil sealing." *J. Magn. Magn. Mater.*, 267, 105 – 110.

Kim, H.J., Bang, I.C. and Onoe, J. (2009). "Characteristic stability of bare Au-water nanofluids fabricated by pulsed laser ablation in liquids." *Opt. Lasers Eng.*, 47, 532 – 538.

Kole, M. and Dey, T.K. (2011). "Effect of aggregation on the viscosity of copper oxide-gear oil nanofluids." *Int. J. Therm. Sci.*, 50(9), 1741 – 1747.

Kumar, S.A., Meenakshi, K.S., Narashimhan, B.R.V., Srikanth, S. and Arthanareeswaran, G. (2009). "Synthesis and characterization of copper nanofluid by a novel one-step method." *Mater. Chem. Phys.*, 113, 57 – 62.

Kwasny, M.S., Chancelier, L., Ng, S., Manyar, H.G., Hardacre, C. and Nockemann, P. (2012). "Facile in situ synthesis of nanofluids based on ionic liquids and copper oxide clusters and nanoparticles." *Dalton Trans.*, 41, 219 – 227.

Lee, S. and Choi, S.U.S. (1996). "Application of metallic nanoparticle suspensions in advanced cooling systems." *Am. Soc. Mech. Eng. Mater. Div.*, 72, 227 – 234.

Lee, J. and Mudawar, I. (2007). "Assessment of the effectiveness of nanofluids for single-phase and two-phase heat transfer in micro-channels." *Int. J. Heat Mass Transfer*, 50, 452 – 463.

Lee, W., Piao, L., Park, C.H, Lim, Y.S., Do, Y.R., Yoon, S. and Kim, S.H. (2009). "Facile synthesis and size control of spherical aggregates composed of Cu₂O nanoparticles." *J. Colloid Interface Sci.*, 342, 198 – 201.

Lee, G.J., Kim, C.K., Lee, M.K., Rhee, C.K., Kim, S. and Kim, C. (2012a). "Thermal conductivity enhancement of ZnO nanofluid using a one-step physical method." *Thermochim. Acta*, 542, 24 – 27.

Lee, J.H., Choi, S.U.S., Jang, S.P. and Lee, S.Y. (2012b). "Production of aqueous spherical gold nanoparticles using conventional ultrasonic bath." *Nanoscale Res. Lett.*, 7, 420 – 420-7.

Li, C.C. and Chang, M. H. (2004). "Colloidal stability of CuO nanoparticles in alkanes via oleate modifications." *Mater. Lett.*, 58, 3903 – 3907.

- Li, D., Xu, H., He, X. and Lan, H. (2005). "Mechanism of magnetic liquid flowing in the magnetic liquid seal gap of reciprocating shaft." *J. Magn. Magn. Mater.*, 289, 407 – 410.
- Li, X., Zhu, D. and Wang, X. (2007). "Evaluation on dispersion behavior of the aqueous copper nano-suspensions." *J. Colloid Interface Sci.*, 310, 456 – 463.
- Li, X.F., Zhu, D.S., Wang, X.J., Wang, N., Gao, J.W. and Li, H. (2008). "Thermal conductivity enhancement dependent pH and chemical surfactant for Cu-H₂O nanofluids." *Thermochim. Acta*, 469, 98 – 103.
- Li, X., Dongsheng, Z. and Xianju, W. (2009a). "Experimental investigation on viscosity of Cu-H₂O nanofluids." *J. Wuhan University Technol. Mater. Sci. Ed.*, 24(1), 48 – 52.
- Li, Y., Zhou, J., Tung, S., Schneider, E. and Xi, S. (2009b). "A review on development of nanofluid preparation and characterization." *Powder Technol.*, 196, 89 – 101.
- Li, D., Hong, B., Fang, W., Guo, Y. and Lin, R. (2010). "Preparation of well dispersed silver nanoparticles for oil based nanofluids." *Ind. Eng. Chem. Res.*, 49(4), 1697 – 1702.
- Li, D., Xie, W. and Fang, W. (2011). "Preparation and properties of copper oil based nanofluids." *Nanoscale Res. Lett.*, 6, 373 – 373-6.
- Li, D. and Fang, W. (2012). "Preparation and stability of silver/kerosene nanofluids." *Nanoscale Res. Lett.*, 7, 362 – 362-6.
- Lin, Y.H., Kang, S.W. and Chen, H.L. (2008). "Effect of silver nano-fluid on pulsating heat pipe thermal performance." *Appl. Therm. Eng.*, 28, 1312 – 1317.
- Liu, M.S., Lin, M.C.C., Tsai, C.Y. and Wang, C.C. (2006a). "Enhancement of thermal conductivity with Cu for nanofluids using chemical reduction method." *Int. J. Heat Mass Transfer*, 49, 3028 – 3033.

- Liu, M.S., Lin, M.C.C., Huang, I.T. and Wang, C.C. (2006b). "Enhancement of thermal conductivity with CuO for nanofluids." *Chem. Eng. Technol.*, 29(1), 72 – 77.
- Lo, C.H., Tsung, T.T. and Chen, L.C. (2005a). "Shape-controlled synthesis of Cu-based nanofluid using submerged arc nanoparticle synthesis system (SANSS)." *J. Cryst. Growth*, 277, 636 – 642.
- Lo, C.H., Tsung, T.T. and Chen, L.C. (2005b). "Ni nanomagnetic fluid prepared by Submerged Arc Nano Synthesis System (SANSS)." *JSME Int. J., Ser. B.*, 48(4), 750 – 755.
- Lo, C.H., Tsung, T.T. Chen, L.C., Su, C.H. and Lin, H.M. (2005c). "Fabrication of copper oxide nanofluid using Submerged Arc Nanoparticle Synthesis System (SANSS)." *J. Nanopart. Res.*, 7, 313 – 320.
- Lo, C.H., Tsung, T.T. and Lin, H.M. (2007). "Preparation of silver nanofluid by the submerged arc nanoparticle synthesis system (SANSS)." *J. Alloys Compd.*, 434-435, 659 – 662.
- Lu, L., Lv, L.C. and Liu, Z.H. (2011a). "Application of Cu-water and Cu-ethanol nanofluids in a small flat capillary pumped loop." *Thermochim. Acta*, 512, 98 – 104.
- Lu, L., Liu, Z.H. and Xiao, H.S. (2011b). "Thermal performance of an open thermosyphon using nanofluids for high-temperature evacuated tubular solar collectors Part 1: Indoor experiment." *Sol. Energy*, 85, 379 – 387.
- Manna, I. (2009). "Synthesis, characterization and application of nanofluid - an overview." *J. Indian Inst. Sci.*, 89(1), 21 – 33.
- Milanova, D. and Kumar, R. (2005). "Role of ions in pool boiling heat transfer of pure and silica nanofluids." *Appl. Phys. Lett.*, 87, 233107 – 233107-3.

- Mitamura, Y., Arioka, S., Sakota, D., Sekine, K. and Azegami, M. (2008). "Application of a magnetic fluid seal to rotary blood pumps." *J. Phys. Condens. Matter.*, 20, 204 – 208.
- Murshed, S.M.S., Leong, K.C. and Yang, C. (2005). "Enhanced thermal conductivity of TiO₂ - water based nanofluids." *Int. J. Therm. Sci.*, 44, 367 – 373.
- Murshed, S.M.S., Leong, K.C. and Yang, C. (2008). "Investigations of thermal conductivity and viscosity of nanofluid." *Int. J. Therm. Sci.*, 47, 560 – 568.
- Murshed, S.M.S., Leong, K.C. and Yang C. (2009). "A combined model for the effective thermal conductivity of nanofluids." *Appl. Therm. Eng.*, 29, 2477 – 2483.
- Namburu, P.K., Kulkarni, D.P., Misra, D. and Das, D.K. (2007). "Viscosity of copper oxide nanoparticles dispersed in ethylene glycol and water mixture." *Exp. Therm. Fluid Sci.*, 32, 397 – 402.
- Nan, Z., Zhang, P., Yu, A., Wei, C., Shi, Q. and Tan, Z. (2009). "Novel synthesis of β -FeOOH nanofluid and determination of its heat capacity by an adiabatic calorimeter." *Chin. J. Chem.*, 27, 1249 – 1253.
- Nan, Z. and Tan, Z. (2011). "Thermodynamic Studies of a Nanowire-shaped β -FeOOH nanofluid produced by a solvothermal route." *J. Chem. Eng. Data.*, 56(4), 915 – 919.
- Ochonski, W. (1989). "Dynamic sealing with magnetic fluids." *Wear*, 130(1), 261 – 268.
- Parametthanuwat, T., Rittidech, S., Pattiya, A., Ding, Y. and Witharana, S. (2011). "Application of silver nanofluid containing oleic acid surfactant in a thermosyphon economizer." *Nanoscale Res. Lett.*, 6, 315 – 315-10.

Park, B. K., Jeong, S., Kim, D., Moon, J., Lim, S. and Kim, J. S. (2007). “Synthesis and size control of monodisperse copper nanoparticles by polyol method.” *J. Colloid Interface Sci.*, 311, 417 – 424.

Peng, D.X., Chen, C.H., Kang, Y., Chang, Y.P. and Chang, S.Y. (2010). “Size effects of SiO₂ nanoparticles as oil additives on tribology of lubricant.” *Ind. Lubr. Tribol.*, 62(2), 111 – 120.

Phuoc, T.X., Soong, Y. and Chyu, M.K. (2007). “Synthesis of Ag-deionized water nanofluids using multi-beam laser ablation in liquids.” *Opt. Lasers Eng.*, 45, 1099 – 1106.

Prasher, R., Song, D. and Wang, J. (2006). “Measurements of nanofluid viscosity and its implications for thermal applications.” *Appl. Phys. Lett.*, 89, 133108 – 133108-3.

Priya, K.R., Suganthi, K.S. and Rajan, K.S. (2012). “Transport properties of ultra low concentration CuO-water nanofluids containing non spherical nanoparticles.” *Int. J. Heat Mass Transfer*, 55(17-18), 4734 – 4743.

Putnam, S.A., Cahill, D.G., Braun, P.V., Ge, Z. and Shimmin, R.G. (2006). “Thermal conductivity of nanoparticle suspensions.” *J. Appl. Phys.*, 99, 084308 – 084308-6.

Riehl, R.R. and Santos, N. (2012). “Water-copper nanofluid application in an open loop pulsating heat pipe.” *Appl. Therm. Eng.*, 42, 6 – 10.

Rosensweig (1987). “Magnetic fluids.” *Annu. Rev. Fluid Mech.*, 19, 437 – 461.

Saidur, R., Leong, K.Y. and Mohammad, H.A. (2011). “A review on applications and challenges of nanofluids.” *Renewable Sustainable Energy Rev.*, 15, 1646 – 1668.

Samal, S., Satpati, B. and Chaira, D. (2010). “Production and dispersion stability of ultrafine Al-Cu alloy powder in base fluid.” *J. Alloys Compd.*, 504S, S389 – S394.

- Santra, A.K., Sen, S. and Chakraborty, N. (2008). "Study of heat transfer augmentation in a differentially heated square cavity using copper - water nanofluid." *Int. J. Therm. Sci.*, 47, 1113 – 1122.
- Santra, A.K., Sen, S. and Chakraborty, N. (2009). "Study of heat transfer due to laminar flow of copper - water nanofluid through two isothermally heated parallel plates." *Int. J. Therm. Sci.*, 48, 391 – 400.
- Saterlie, M., Sahin, H., Kavlicoglu, B., Liu, Y. and Graeve, O. (2011). "Particle size effects in the thermal conductivity enhancement of copper based nanofluids." *Nanoscale Res. Lett.*, 6, 217 – 217-7.
- Sharifi, I., Shokrollahi, H. and Amiri, S. (2012). "Ferrite based magnetic nanofluids used in hyperthermia applications." *J. Magn. Magn. Mater.*, 324, 903 – 915.
- Shen, L.P., Wang, H., Dong, M., Ma, Z.C. and Wang, H.B. (2012). "Solvothermal synthesis and electrical conductivity model for the zinc oxide-insulated oil nanofluid." *Phys. Lett. A*, 376, 1053 – 1057.
- Singh, A.K. (2008). "Thermal conductivity of nanofluids." *Defence Sci. J.*, 58(5), 600 – 607.
- Singh, A.K. and Raykar, V.S. (2008). "Microwave synthesis of silver nanofluids with polyvinylpyrrolidone (PVP) and their transport properties." *Colloid Polym Sci.*, 286, 1667 – 1673.
- Singh, M., Sinha, I., Premkumar, M., Singh, A.K. and Mandal, R.K. (2010). "Structural and surface Plasmon behavior of Cu nanoparticles using different stabilizers." *Colloid Surf. A.*, 359, 88 – 94.

Singh, D.K., Pandey, D.K., Yadav, R.R. and Singh, D. (2012). "Characterization of CrO₂ poly vinyl pyrrolidone magnetic nanofluid." *J. Magn. Magn. Mater.*, 324(22), 3662 – 3667.

Suresh, S., Venkataraj, K.P., Selvakumar, K.P. and Chandrasekar, M. (2011). "Synthesis of Al₂O₃ – Cu/ water hybrid nanofluids using two step method and its thermophysical properties." *Colloids Surf., A Physicochem. Eng. Aspects*, 388, 41 – 48.

Tamjid, E. and Guenther, B.H. (2010). "Rheology and colloidal structure of silver nanoparticles dispersed in diethylene glycol." *Powder Technol.*, 197, 49 – 53.

Tavares, J. and Coulombe, S. (2011). "Dual plasma synthesis and characterization of a stable copper - ethylene glycol nanofluid." *Powder Technol.*, 210, 132 – 142.

Tsai, C.Y., Chien, H.T., Ding, P.P., Chan, B., Luh, T.Y. and Chen, P.H. (2004). "Effect of structural character of gold nanoparticles in nanofluid on heat pipe thermal performance." *Mater. Lett.*, 58, 1461 – 1465.

Tsai, T.H., Chien, H.T. and Chen, P.H. (2011). "Improvement on thermal performance of a disk shaped miniature heat pipe with nanofluid." *Nanoscale Res. Lett.*, 6, 590 – 590-7.

Tzeng, S.C., Lin, C.W. and Huang, K.D. (2005). "Heat transfer enhancement of nanofluids in rotary blade coupling of four-wheel-drive vehicles." *Acta Mech.*, 179(1-2), 11 – 23.

Vekas, L., Bica, D. and Avdeev, M.V. (2007). "Magnetic nanoparticles and concentrated magnetic nanofluids: Synthesis, properties and some applications." *China Part.*, 5, 43 – 49.

Wang, H., Xu, J.Z., Zhu, J.J. and Chen, H.Y. (2002). "Preparation of CuO nanoparticles by microwave irradiation." *J. Cryst. Growth*, 244, 88 – 94.

Wang, X.Q. and Mujumdar, A.S. (2008a). "A review on nanofluids - part I: theoretical and numerical investigations." *Braz. J. Chem. Eng.*, 25(4), 613 – 630.

Wang, X.Q. and Mujumdar, A.S. (2008b). "A review on nanofluids - part II: experiments and applications." *Braz. J. Chem. Eng.*, 25(4), 631 – 648.

Wang, B., Wang, X., Lou, W. and Hao, J. (2011a). "Gold - ionic liquid nanofluids with preferably tribological properties and thermal conductivities." *Nanoscale Res. Lett.*, 6, 259 – 259-10.

Wang, B., Wang, X., Lou, W. and Hao, J. (2011b). "Ionic liquid based stable nanofluids containing gold nanoparticles." *J. Colloid Interface Sci.*, 362(1), 5 – 14.

Wang, B., Wang, B., Wei, P., Wang, X. and Lou, W. (2012). "Controlled synthesis and size dependent thermal conductivity of Fe₃O₄ magnetic nanofluids." *Dalton Trans.*, 41, 896 – 899.

Wei, X., Zhu, H., Kong, T. and Wang, W. (2009). "Synthesis and thermal conductivity of Cu₂O nanofluids." *Int. J. Heat Mass Transfer*, 52, 4371 – 4374.

Wei, C., Nan, Z., Wang, X. and Tan, Z. (2010). "Investigation on thermodynamic properties of a water based hematite nanofluid." *J. Chem. Eng. Data.*, 55(7), 2524 – 2528.

West, A.R. (1989). "Solid State Chemistry and its Applications." John Wiley and Sons, Singapore, 173 – 175.

Wu, S. (2007). "Preparation of fine copper powder using ascorbic acid as reducing agent and its application in MLCC." *Mater. Lett.*, 61, 1125 – 1129.

Xie, H., Wang, J., Xi, T., Liu, Y., Ai, F. and Wu, Q. (2002). "Thermal conductivity enhancement of suspensions containing nanosized alumina particles." *J. Appl. Phys.*, 91(7), 4568 – 4572.

Xiong, J., Wang, Y., Xue, Q. and Wu, X. (2011). "Synthesis of highly stable dispersions of nanosized copper particles using L-ascorbic acid." *Green Chem.*, 13, 900 – 904.

Xuan, Y. and Li, Q. (2000). "Heat transfer enhancement of nanofluids." *Int. J. Heat Fluid Flow*, 21, 58 – 64.

Yang, B. and Han, Z.H. (2006). "Thermal conductivity enhancement in water-in-FC72 nanoemulsion fluids." *Appl. Phys. Lett.*, 88, 261914 – 261914-3.

Yang, Z., Sun, S., Kong, C., Song, X. and Ding, B. (2010). "Designated- tailoring on {100} facets of Cu₂O nanostructures: from octahedral to its different truncated forms." *J. Nanomater.*, 10, 710584 – 710584-11.

Yeshchenko, O.A., Dmitruk, I.M., Dmytruk, A.M. and Alexeenko, A.A. (2007). "Influence of annealing conditions on size and optical properties of copper nanoparticles embedded in silica matrix." *Mater. Sci. Eng., B*, 137, 247 – 254.

Yu, W., Xie, H., Chen, L. and Li, Y. (2009a). "Enhancement of thermal conductivity of kerosene-based Fe₃O₄ nanofluids prepared via phase-transfer method." *Colloids Surf., A Physicochem. Eng. Aspects*, 11, 44 – 52.

Yu, W., Xie, H., Chen, L. and Li, Y. (2009b). "Investigation of thermal conductivity and viscosity of ethylene glycol based ZnO nanofluid." *Thermochim. Acta*, 491, 92 – 96.

Yu, W., Xie, H., Chen, L. and Li, Y. (2010). "Investigation on the thermal transport properties of ethylene glycol-based nanofluids containing copper nanoparticles." *Powder Technol.*, 197, 218 – 221.

Zhao, B. and Nan, Z. (2011). "Preparation of stable magnetic nanofluids containing Fe₃O₄@PPy nanoparticles by a one pot route." *Nanoscale Res. Lett.*, 6, 230 – 230-8.

Zhang, Z., Xue, Q. and Zhang, J. (1997). "Synthesis, structure and lubricating properties of dialkyldithiophosphate-modified Mo-S compound nanoclusters." *Wear*, 209(1-2), 8 – 12.

Zhang, L., Jiang, Y., Ding, Y., Povey, M. and York, D. (2007). "Investigation into the antibacterial behavior of suspensions of ZnO nanoparticles (ZnO nanofluids)." *J. Nanopart. Res.*, 9, 479 – 489.

Zhang, L., Ding, Y., Povey, M. and York, D. (2008). "ZnO nanofluids - a potential antibacterial agent." *Prog. Nat. Sci.*, 18, 939 – 944.

Zhang, Y., Gu, S., Yan, B. and Ren, J. (2012). "Solvent free ionic molybdenum disulphide (MoS₂) nanofluids." *J. Mater. Chem.*, 22, 14843 – 14846.

Zheng, Y., Zhang, J., Lan, L., Yu, P., Rodriguez, R., Herrera, R., Wang, D. and Giannelis, E.P. (2010). "Preparation of solvent-free gold nanofluids with facile self-assembly technique." *ChemPhysChem.*, 11, 61 – 64.

Zhu, H., Lin, Y. and Yin, Y. (2004a). "A novel one-step chemical method for preparation of copper nanofluids." *J. Colloid Interface Sci.*, 277, 100 – 103.

Zhu, H., Zhang, C. and Yin, Y. (2004b). "Rapid synthesis of copper nanoparticles by sodium hypophosphite reduction in ethylene glycol under microwave irradiation." *J. Cryst. Growth*, 270, 722 – 728.

Zhu, H., Han, D., Meng, Z., Wu, D. and Zhang, C. (2011). "Preparation and thermal conductivity of CuO nanofluid via a wet chemical method." *Nanoscale Res. Lett.*, 6, 181 – 181-6.

BIODATA

Name: SANDHYA SHENOY U

Register number: 090718CY09F03

Date of birth: 3 JANUARY 1987

Email id: sandhyashenoy347@gmail.com

Phone: 9611099854

Address: #39/1 SHRI SKANDA,

1ST CROSS, RAM RAO LAYOUT, KATHRIGUPPE,

BSK III STAGE, BANGALORE – 560085

Education:

M.Sc. Details

DISCIPLINE	INSTITUTION	YEAR	CGPA
CHEMISTRY	NATIONAL INSTITUTE OF TECHNOLOGY KARNATAKA, SURATHKAL	2009	10

LIST OF PUBLICATIONS

Journal papers

➤ Shenoy, S.U. and Shetty, N.A. (2012). “Synthesis of copper nanofluids using ascorbic acid reduction method via one step solution phase approach.” *J. ASTM Int.*, 9(5), JAI104416.

➤ Shenoy, S.U. and Shetty, N.A. (2012). “Simple glucose reduction route for one step synthesis of copper nanofluids.” *Appl. Nanosci.*, DOI 10.1007/s13204-012-0169-6.

➤ Shenoy, S.U. and Shetty, N.A. (2013). “A simple solution phase synthesis of copper nanofluids using single step glucose reduction method.” *Synth. React. Inorg. Met. -Org. Nanomet. Chem.*, 43(3), 343 – 348.

- Shenoy, S.U. and Shetty, N.A. (2013). “Copper nanofluids: A facile synthetic approach.” *J. Nanoeng. Nanomanuf.*, 3, 64 – 69.
- Shenoy, S.U. and Shetty, N.A. (2013). “A facile one step solution route to synthesize cuprous oxide nanofluid.” *Nanomater. Nanotechol.*, 3, 5:2013.

Conference papers

- Shenoy, S.U. and Shetty, N.A. (2011). “A facile ascorbic acid reduction method for solution phase single step synthesis of copper nanofluids.” National Symposium on Chemistry and Humanity, July 11-12, MIT, Manipal.
- Shenoy, S.U. and Shetty, N.A. (2013). “Direct synthesis of copper nanofluids containing hexagonal disc shaped particles.” International Conference on Recent Trends in Material Science and Technology, January 17-19, NITK, Surathkal.